Title: A Study into the Biological Activity and Therapeutic Potential of Molecular Hydrogen and Oxyhydrogen Gases.

Author: Grace Russell
Word Count: Main Body – 39,256

A thesis submitted in partial fulfilment of the requirements of the University of the West of England, Bristol for the degree of Doctor of Philosophy in the School of Applied Sciences. This research programme was part-funded by and carried out in collaboration with Water Fuel Engineering. UK.

School of Applied Sciences, University of the West of England, Bristol

Submission: July 2024

ABSTRACT

Molecular hydrogen (H_2) and oxyhydrogen (66% H_2/ 33% O_2) gases can remediate the effects of numerous diseases in adults. By acting as an anti-inflammatory and antioxidative agent, it is reported that H_2 administration can improve recovery through mitigating the hyperinflammatory response and reducing oxidative stress.

As the precise mechanisms of H_2 activity are currently undefined, the lack of primary target identification, coupled with difficulties regarding administration methods (*e.g.,* dosage and dosage frequencies, and long-term effects of treatments), there is a requirement for H_2 research to evidence whether it should, and how it can reasonably and effectively, be incorporated into healthcare.

To better understand the molecular mechanism(s) behind the activity of H_2, and to ascertain whether H_2 can be utilised as an effective nutraceutical, this treatise investigates the modality of action, and effects of H_2, using a range of bioinformatical, theoretical and empirical approaches. The question of how H_2 may reach distal somatic sites, and the subsequent cellular effects are also discussed.

Before using oxyhydrogen gas to assess the effects of H_2 on immortalised B-lymphocytes, nematodes and seeds; the gas-purity, flow-rate, and infusion limits of the HydroVitality™ alkaline water electrolyser were evaluated. Exposing cells to dissolved oxyhydrogen gas in cell media identified a trend of replicative inhibition of TK6-malignant cells with a single infusion. Further analysis detailed a significant increase in DNA in the Sub G1 phase, indicating increased apoptosis. Additionally, evidence described in this thesis identifies a possible evolutionary relationship between subunits of Complex 1 (mitochondria) and hydrogenase enzymes of ancient archaeal and bacterial species.

In conclusion, this study encompasses a range of theories incorporating the evolutionary requirement of H_2, how H_2 may interact at a molecular level in plants and humans, and the effect of H_2 administration on malignant cells, by providing novel experimental protocols and innovative theories into the biological activity of H_2.

Table of Contents:

Contents

Chapter 1: An Introduction to Molecular Hydrogen (H_2) and its Potential for Use as an Effective and Versatile Medical Compound.

1.1 Therapeutic Gases

Therapeutic and medical gases are defined as gaseous products, created and packaged specifically for use within healthcare settings. Examples of commonly utilised medical gases include Oxygen (O_2), medical air (containing 78% Nitrogen (N_2), 21% Oxygen, 0.9% Argon (A), and 0.1% mainly comprising of a mixture of Carbon dioxide (CO_2), Helium (He), Hydrogen (H_2), Methane (CH_4) and Ozone (O_3)). Nitrogen and Carbon (C) gas compounds (*e.g.,* Nitrous oxide (N_2O) and Carbon monoxide (CO)) are also utilised as treatments providing dose-dependent anaesthetic and anti-inflammatory benefits, accordingly (Müller, 2015, Ryter, 2020). The requirement for these gases in healthcare has led to complex delivery assemblies being constructed within hospitals, designed specifically for the distribution of multiple gas lines into numerous facilities including operating theatres, recovery areas, and wards (Salah, Osman, and Hosny, 2018). Medical gases are frequently utilised as anaesthetic, diagnostic and therapeutic agents during hospital care (Rosewarne, 2005), and are often prescribed as at-home treatments for chronically ill patients (Saleem *et al.,* 2023).

Although studies into the beneficial effects of molecular hydrogen treatments and therapies in mammalian physiology are relatively well established, more recently, research has expanded from molecular hydrogen to oxyhydrogen (an admixture of 66% H_2 and 33% O_2 gases), as potential therapeutics, both gases (H_2 and oxyhydrogen) are considered in this treatise. Hydrogen

Hydrogen (H) is the first element of the periodic table and constitutes approximately 75% of the universe's elemental mass. It is the lightest (Weight: 1.00784g/mol) atomic particle known. Nonetheless, as Earth's gravity is unable to retain atomic hydrogen gas, it is instead found combined with other elements, commonly forming molecules such as water (H_2O) and hydrocarbon (organic) compounds (Coppola *et al.,* 2011). Under natural conditions, hydrogen gas is found consisting of two atoms, formulating the diatomic molecule H_2 (Molecular weight: 2.016g/mol) (Di Lullo, Oni and Kumar, 2021). As a result of its neutral charge, non-polarity and low molecular weight, H_2 gas is highly diffusible in biological systems, negotiating passage through the blood/brain, placental and testes barriers, lipid membranes, cytosolic fluid and into cellular compartments including organelles relatively unobstructed (Barancik *et al.,* 2020). This property of H_2 is favourable as conventional antioxidant lack these abilities and are therefore likely to be therapeutically less effective (Ichihara *et al.,* 2015).

Endogenously, H_2 is produced by fermentation of carbohydrate nutriments by intestinal

microorganisms such as *Clostridia* and *Coliform* (*e.g., Escherichia coli*) species of bacteria, where H_2 formation results primarily from oxidation of pyruvate, formate or reduced pyridine nucleotides (*i.e.,* nicotinamide adenine dinucleotide/flavin adenine dinucleotide (NADH/FADH), accordingly) (McKay, Holbrook and Eastwood, 1982). Consequently, H_2 can influence acid-based, or redox, chemistry within the cell. *Per contra*, endogenous H_2 is not found in sufficient quantities to be therapeutically advantageous and medicinal application of H_2 is administered largely by three alternative methods: Inhalation of H_2 gas, H_2 dissolved in water (Hydrogen-rich water: HRW), or by saline/hydrogen intravenous infusion (Hydrogen-rich saline: HRS) (reviewed by Russell *et al.,* 2021).

H_2 is classified as a 'generally regarded as safe' (GRAS) product by the Food and Drug Administration (2014) and is regarded as a food supplement (E949) under part C group I of regulation 1129/2011 in the European Union (EU Commissions Regulation, 2011) and U.K (Food Standards Agency, 2018). Furthermore, inhalation of H_2 gas is mooted as a biologically safe and noninvasive process, which has been used for the prevention of high-pressure nervous syndrome in deep-sea divers for many years with no documented adverse effects (ZetterstrÖm, 1948).

1.1.1. A Brief History of H_2 as a Medical Gas

Adapted from the publication 'Molecular Hydrogen as Medicine: An Assessment of Administration Methods' (Russell *et al.,* 2021)

Since its discovery by Henry Cavendish in the mid-late 18th century (1766), hydrogen has been demonstrated to be well tolerated as a medical gas, first in animals, and then in humans (Hancock and LeBaron, 2023). Much of the initial research into these newly discovered gases was conducted in the late 1700s with such eminent scientists as Antoine-Laurent Lavoisier, Carl Wilhelm Scheele and Joseph Priestly (Figure 1.1).

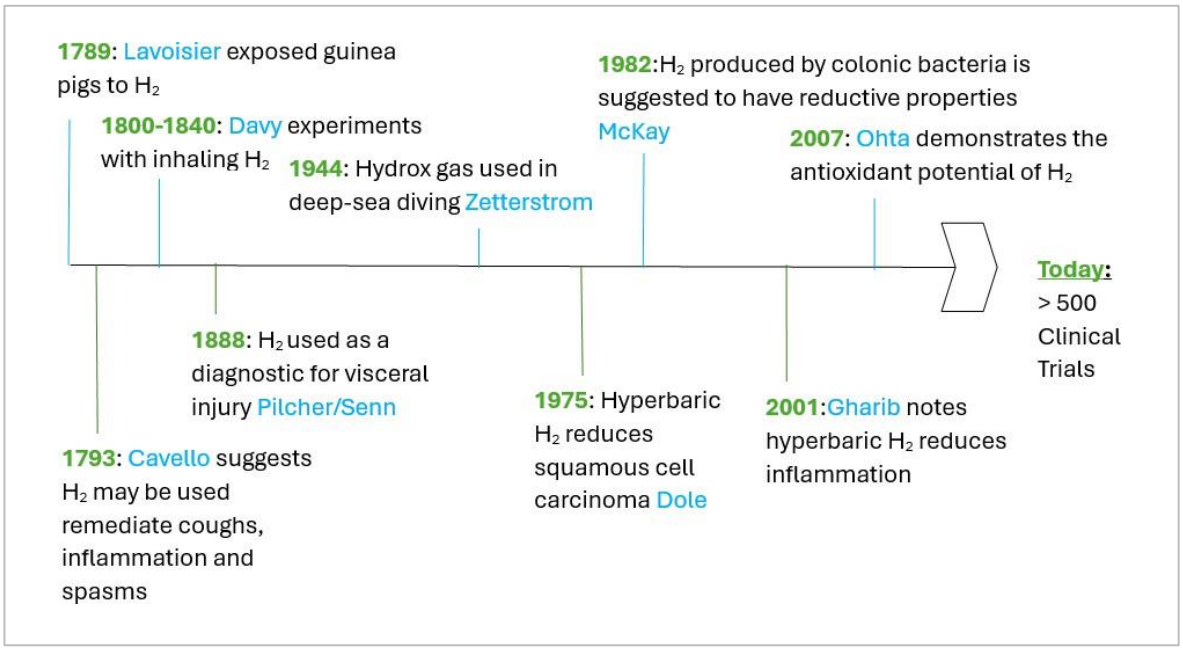

Figure 1.1 Timeline of hydrogen research. Linear chart depicting the major discoveries regarding hydrogen and its medical applications.

In the 1940s Arne ZetterstrÖm was credited with creating Hydrox gas, a combination of hydrogen and oxygen (96% and 4%, respectively) that allowed deep-sea divers to traverse depths of up to 500 meters, by preventing decompression sickness (ZetterstrÖm, 1948). The hydrogen-oxygen mixture can be compressed into cylinders as the low concentration of oxygen rendered the composition nonexplosive, a factor that made this method of hydrogen delivery useful for exploration, industrial use and submarine rescues.

Despite the popularity and demonstrated efficacy of hydrogen as an inhalation treatment, further advances in medical research were not put forward until 1975 when Dole and colleagues realized hyperbaric administration (95% H_2/8 atm) for periods of 10-14 days could reduce squamous-cell carcinoma in murine models of disease (Dole, Wilson and Fife, 1975). Even though this discovery was revolutionary, medical hydrogen research again subsided, and it would be another two decades before a key article in this field was published (Shirahata *et al.,* 1997), where hydrogen, created from the electrolysis of water, was shown to protect deoxyribose nucleic acid (DNA) from oxidative damage. Once again, however, research into medical hydrogen lapsed and was not fully revived until 2007 when Ohsawa's laboratory in the Department of Biochemistry and Cell Biology, Nippon Medical School, Japan, reported an antioxidant effect of H_2 in a rodent model of ischemia-reperfusion injury (Fukuda *et al.,* 2007; Ohsawa *et al.,* 2007). Since, this discovery there has been renewed interest in the effects of H_2 as a medical gas, and research into this promising area of medicine is developing rapidly. Nearly two decades later, it is now increasingly well-documented that H2 has potent cellular protective effects in plants (reviewed by Russell, Zulfiqar and Hancock, 2020; Hancock, Russell and Stratakos, 2022), animals (Tsubone et al., 2013; Yamazaki et al., 2015; Sobue et al., 2017; Ji, Zheng and Yao, 2019) and humans (Senn, 1888; ZetterstrÖm, 1948; Ostojic, 2015; Ge et al., 2017; Ono et al., 2017; Nogueira et al., 2021), and in this regard, H_2 has potential both as prophylactic and remedial therapy.

1.2.2 H_2 as an Antioxidant

Arguably, it is the oxidation status of the cell that is the most basic cellular process that becomes disrupted during illness or injury. As modern humans, we are exposed to oxidants in our daily lives, from lifestyle choices such as intake of alcohol and processed foods, to chemicals and preservatives, smoking, and vehicle emissions (Sharifi-Rad *et al.,* 2020).

Reactive oxygen and reactive nitrogen species (ROS/RNS, respectively) are able to affect fundamental processes including genetic transcription and mitochondrial activity through the modification of essential proteins and protective membranes. Such molecules are chemically

unstable having strong affinities for hydrogen atoms. Antioxidants can counteract the effects of damaging oxygen and nitrogen reactive species, nevertheless, antioxidants such as ascorbic acid (vitamin C), although effective in the short-term, can accumulate in the body leading to adverse effects including digestive distress, and improper kidney or liver function, if taken in large doses(Doseděl et al., 2021). As H_2 is highly diffusible, such accumulation is not known to occur, with excesses being exhaled (Hammer et al., 2022), thus H_2 therapies may prove to be of greater therapeutic value than conventional nutraceuticals. Enquiries into the effects of H_2 have described a cytoprotective action specifically around the mitochondria. Here H_2 has been demonstrated to effectively reduce levels of ROS/RNS (*i.e.,* the hydroxyl radical ($^{\bullet}OH$) and peroxynitrite ($ONOO^-$)) (Ohsawa *et al.,* 2007; Ohta, 2012; LeBaron *et al.,* 2019a; Ishibashi, 2019; Ohta, 2021). Due to their high affinity for the abstraction of hydrogen atoms $^{\bullet}OH$ and $ONOO^-$ are predominantly responsible for cellular membrane oxidation, DNA damage, protein modifications, and the degradation of sugar groups (Di Meo and Venditti, 2020; Juan *et al.,* 2021). This level of oxidative stress is interlinked with a heightened inflammatory response, known to further disrupt cellular integrity. Additionally, improvements in mitochondrial membrane integrity have also been identified as significant contributors to the reduction of dysfunctional energy dynamics that can increase cellular distress and ROS production (Ishihara *et al.,* 2020). Importantly, although H_2 has been demonstrated to be effective in ameliorating harmful free radical species, the direct reducing potential of H_2 is questioned (Penders, Kissner and Koppenol, 2014; Hancock and Russell, 2021; Li *et al.,* 2021), a topic discussed in Chapter 4, Section 4.2.

Research into the influence H_2 has on gene transcription revealed that H_2 exhibits properties that activate nuclear factor erythroid 2-related factor 2 (Nrf2), a protein known to induce genetic transcription by binding to the antioxidant response element (ARE) (Fang *et al.,* 2020). The ARE is a *cis*-acting enhancer sequence responsible for the consequential expression of >200 cytoprotective peptides, proteins and enzymes. Once released from its partner protein Kelch-like ECH-associated protein 1 (KEAP1), Nrf2 can translocate into the nucleus stimulating the transcription and translation of several proteins, many of which enhance antioxidant capacity (Ulasov *et al.,* 2022). These include catalase (CAT) which removes hydrogen peroxide (H_2O_2), superoxide dismutase (SOD) which removes superoxide, and other enzymes and small redox active molecules, such as glutathione (GSH), haem-oxygenase (HO-1) and various peroxidases (-Px) (Liu *et al.,* 2021). Although the molecular target of H_2 interaction has yet to be delineated, further studies have also noted that hydrogen therapy influences apoptosis and has both antioxidant and anti-inflammatory effects in multiple disease models including respiratory, metabolic, and oncological diseases (Ge *et al.,* 2017).

It is now widely accepted that H_2 acts to reduce oxidative and nitrosative stress in biological

systems (Han et al., 2016; Trivic et al., 2017; Chen et al., 2019a; Zhu, Cui and Xu, 2021; Deryugina et al., 2023a) and by doing so can reduce both the apoptotic and inflammatory responses in non-malignant cells, although which mechanism is the cardinal influence here remains unknown. Due to the physical properties of this diatomic molecule (Chapter 1, Section 1.2), it is unlikely to be perceived as a typical signalling molecule, relying on receptor binding mechanisms or electrochemical attraction for modulating cellular responses (discussed in Chapter 4). With such fundamental activities as balancing the reduction/oxidation status of the cell (Shirahata et al., 1997; Ohno et al., 2012; Ishibashi, 2019), influencing genetic transcription (Fang et al., 2020) and mitochondrial functionality (Ishihara et al., 2020) all being influenced by H_2, it is worth exploring whether other diverse pathways may be influenced by H_2-based therapeutics (Chapter 4, Sections 4.3 and 4.4).

1.2.3. H_2 as a Regulator of Apoptosis

Apoptosis is an inherent cellular mechanism responsible for removing cells during development, during infection or disease. This important pathway also eliminates malignant cells, as well as pre-cancerous and virus-infected tissues, in a way that does not initiate an inflammatory response and as such apoptosis can be regarded as a regulated form of cell death (Zamaraev, Zhivotovsky and Kopeina, 2020). This fundamental and protective process has three major triggers known as extrinsic, intrinsic and cytotoxic-T-cell pathways (Gatzka and Walsh, 2007) (Figure 1.2).

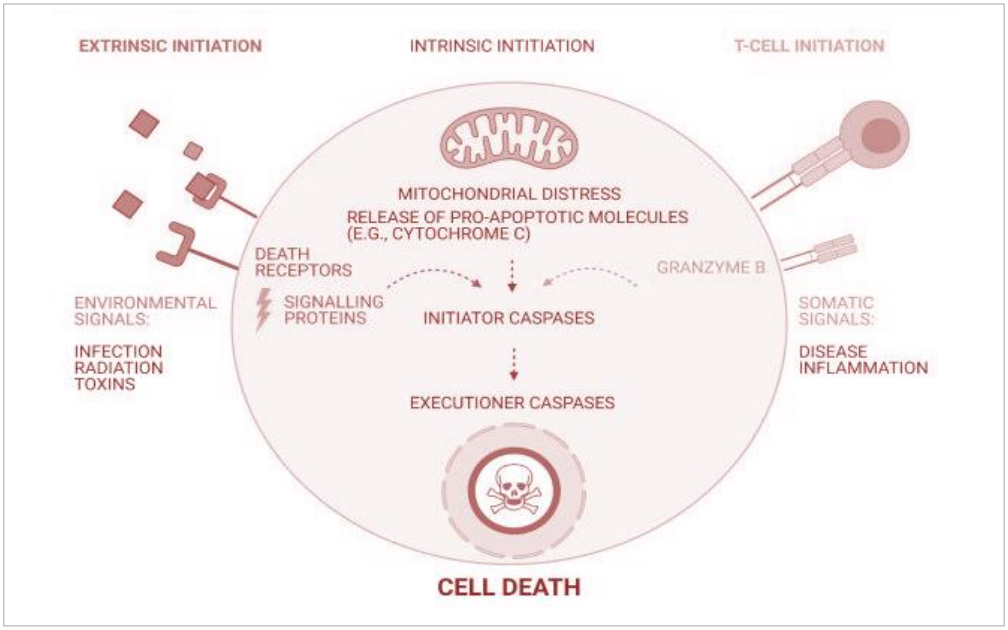

Figure 1.2. Mechanisms of apoptosis initiation. Left: The extrinsic pathway responds to environmental molecular stimulation. Middle: Intrinsic, or mitochondrial activated, pathway. Right: Activation via T-cell ligation. Image created by the author in Biorender.com.

Extrinsic activation of apoptosis involves the aptly named ‘death receptors’ (*e.g.,* TNF-related

apoptosis-inducing ligand receptor 1 (TRAIL-R1/Death Receptor 4 (DR4)) that receive a signal from the surrounding environment, relaying information to the nucleus via intrinsic signalling cascades (Lossie, 2022). This type of activation is often a result of radiation damage (*e.g.,* sunburn), toxicity (*e.g.,* bacterial toxins, or poisons), or an infection that provokes a heightened immune response. In contrast, the intrinsic, or mitochondrial-dependent, pathway is typically activated by the lack of oxygen (hypoxia), or raised levels of ROS/RNS, commonly as a result of metabolic instability and DNA damage, prevalent in such diseases as cancer, cardiovascular disease and type 2 diabetes (Lossie, 2022).

T-cell initiation of apoptosis involves cytotoxic T-cells, lymphatic white blood cells (WBCs), that form part of the immune response, particularly during parasitic and viral infections. These T-cells have particular proteins on their surface ($CD8^+$) that recognise antigenic molecules on the surface of other cells (Zhu, Petit and Van den Eynde, 2019). This particular trait confers selectivity and allows the immune cell to effectively target and destroy infected cells, without damaging uninfected tissues.

Whichever pathway initiates apoptosis, each converges on the execution pathway, the determinative step for cell viability (Wilson, 1998). Research into the inhalation of molecular hydrogen identifies a reduction in the activation of executioner caspases in the cytosol (*e.g.,* caspase 3/7. For example, multiple studies report a reduction in the activity of both initiator (*e.g.,* caspase 12) and executioner caspases (Xie *et al.,* 2012; Liu *et al.,* 2015; Qiu, Liu and Zhang, 2019; Nogueira *et al.,* 2021), as well as abatement of nuclear factor kappa-light-chain-enhancer of activated B cells (NFκB), a transcription factor responsible for upregulating immune responses and pro-inflammatory activities, recognised by Satta *et al.* (2021) when analysing hydrogen enriched haemodialysis fluid. Other models of disease have shown H_2 to protect DNA from oxidative damage, avoiding the initiation of apoptotic cascades. Here, research has identified a reduction in 8-oxo-7,8- dihydro-2'-deoxyguanosine (8-oxo-dG), known to induce mutations during replication. Such oxidative-driven mutations can produce defective proteins that are unable to effectively carry out their designated functions. H_2 helps to alleviate the excessive oxygen radicals involved in the formation of 8-oxo-dG adducts (Hirayama *et al.,* 2018), thereby reducing the likelihood of intrinsically and extrinsically activated apoptosis. Interestingly, as H_2 has also been demonstrated to attenuate excessive inflammatory responses (Gharib *et al.,* 2001; Lu *et al.,* 2022; Lin *et al.,* 2022), it is reasonable to assume that the T-cell initiation of apoptosis is also reduced, although further investment in research is required if we are to fully comprehend the role of H_2 in apoptosis.

1.2.4. H_2 as a Regulator of Inflammation

Inflammation can be triggered by injury, infection or illness and can contribute to the aetiology, symptoms (*e.g.,* pain, temperature, *etc.*) and progression of many health conditions. Herein, pro-inflammatory molecules (e.g., tumour necrosis factor alpha (TNF-α) signal the immune system to produce and release complement proteins, a complex immunoregulatory cascade that has a range of physiological effects including high fever, swelling and loss of function (Belon *et al.,* 2021).

Cellular stress can be caused by a wide range of stimuli including environmental factors such as chemical inhalation, injury or infection, or internal factors including localised and systemic oxidative stress and, or metabolic dysfunction (Chatterjee, Jungraithmayr and Bagchi, 2017). In response to such stimuli, cells begin to produce and release an array of pro-inflammatory cytokines, including chemokines (*e.g.,* monocyte chemoattractant protein-1 (MCP-1)), interferons (*e.g.,* interferon-gamma (Ifγ)) and interleukins (*e.g.,* IL1-β, IL-6). When cytokines are released into the bloodstream, they often damage the cells of the blood vessel walls. This assault on the cellular epithelium increases the permeability of the vessels, which in turn, leads to increased chemical signalling and migration of WBCs, thus perpetuating the inflammatory cascade (Chatterjee, Jungraithmayr and Bagchi, 2017; Hanna and Frangogiannis, 2020) (Figure 1.3).

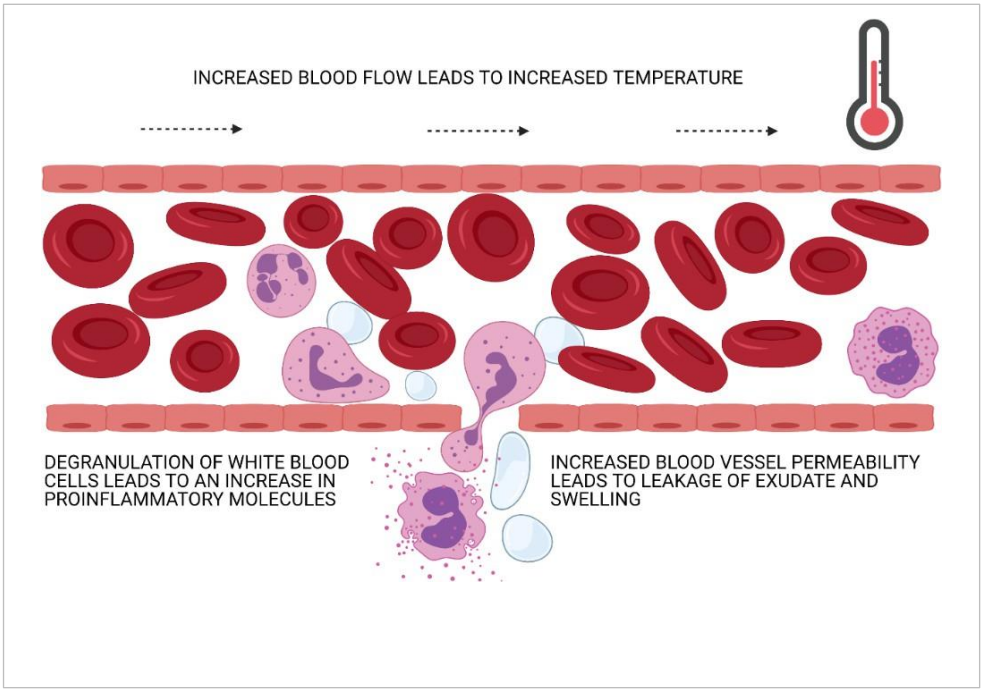

Figure 1.3. The inflammatory process. A graphical interpretation of the inflammatory process. Increased blood flow, blood vessel permeability and the degranulation of white blood cells

lead to the cardinal signs of heat, loss of function, rubor, pain and swelling. Image created by the author in Biorender.com.

During viral or respiratory infection, leukocytes (WBCs), principally monocytes and neutrophils, repeatedly release cytokines (e.g., Il-6, TNF-α) and oxygen radicals that inflict damage on the invading pathogen or dysfunctional cell. Such activity often affects healthy somatic cells in the vicinity, causing further damage to proximal tissues. IgM antibodies, also highly expressed during the innate immune response, triggers the adaptive immunity via lymphocyte (B- and T-cell) immune cell activation.

To illustrate the relevance of inflammation in human disease, clinical research has linked both innate and adaptive immune responses with the initiation and progression of malignant disease (Chen et al., 2020a; Chen et al., 2020b; Rochette et al., 2021), neuropathies (e.g., Parkinson's disease, dementia) (Pajarez et al., 2020; Wang et al., 2020a), metabolic diseases (e.g., diabetes, hyperlipidaemia) (Beverly and Budoff, 2020; Singh et al., 2023), and joint and muscle degeneration (e.g., arthritis, sarcopenia)(Simmonds et al., 2008; Damiano et al., 2019).

Many reports describe the anti-inflammatory effect of molecular hydrogen treatments, and supporting scientific evidence suggests that H_2 suppresses biological markers of oxidative stress and pro-inflammatory peptides(LeBaron et al., 2019a; Ishihara et al., 2020; Nogueira et al., 2021). These protective mechanisms are accomplished not only through interaction with multiple cellular processes, as described above, but also by regulating the activation of p38/ mitogen activated protein kinases (MAPK)/extracellular signal-regulated kinase (ERK) signalling cascades responsible for initiating the biosynthesis of pro-inflammatory cytokines. Furthermore, phosphorylation of MAPKs is known to increase stress-related signalling, whilst H_2 has been demonstrated to inhibit such phosphorylation events in macrophages (Begum et al., 2020).

As yet, however, the primary target(s) for H_2 interactivity in the remediation of inflammation remains unknown, and further sophisticated analysis of H_2 molecular interactions is important to acquire.

1.3. Oxygen

The requirement for oxygen is fundamental to the survival of higher organisms and the average person (73 - 88 kg) consumes approximately 2000 mL of O_2 every minute at standard temperature and pressure (Chapter 8, Table 8.1). To highlight the extensive use of O_2 in emergency care, within the ambulance service in the United Kingdom (UK), O_2 is reported to be administered to ≥2 million patients per annum. This equates to approximately 34% of all attended emergency calls (Dhruve, Davey and Pursell, 2015; O'Driscoll *et al.,* 2017).

Oxygen products are also administered to approximately one in five patients in nosocomial care. In this setting, O_2 inhalation is prescribed for a vast array of life-threatening conditions, including those that cause a rapid onset of depressed breathing, such as anaphylaxis, opioid overdose and pneumonia (Dhruve, Davey and Pursell, 2015). By providing O_2 therapy, clinicians can increase oxygen tension in the alveoli and reduce the burden upon the respiratory system (O'Driscoll *et al*., 2017). Although widely used in emergency medicine, it is important to note that oxygen is also prescribed for the alleviation of chronic respiratory complaints such as asthma, chronic obstructive pulmonary disorder (COPD), cystic fibrosis, and paediatric respiratory disease (Jacobs *et al.,* 2020).

1.4. Oxyhydrogen Gas

In 1977, the Australian/Bulgarian philanthropist, engineer, and inventor, Professor Yull Brown (Ilia Valkov) patented a novel and highly economical electrolytic cell that required no separation diaphragm (reviewed by Rao, Babu, and Rajesh, 2018). This invention was reported to have 90- 95% liquid-to-gas conversion efficiency. In a letter to the Austrian government, in 1979, engineering and development specialist Harald Hanisch calculated that Prof. Brown's electrolyser could produce up to 13.62 cubic feet (ft^3) of gas per kilowatt hour (Kwh), which he considered close to the thermodynamically perfect (a theoretical concept regarded as being realistically impossible to achieve) efficiency of 14.28 ft^3/Kwh (Hanish and Grundel, 1979). When addressing the safety concerns of such an admixture of volatile gases Harald Hanisch suggests that the safety features of the mixture in the hands of Prof. Brown were proved to him 'conclusively', although it is not described how. The letter concludes with a strong recommendation for investment in Prof. Brown's Australian-based company Water Fuel Holdings (Hanish and Grundel, 1979).

Oxyhydrogen generators based on Prof. Yull Brown's original concept are both economically viable and versatile and are commonly used for industrial purposes including as a fuel and fuel additive (Bhave, Gupta and Joshi, 2022), for the generation of gases used within chemical manufacturing and construction industries (Okolie *et al.,* 2021); and potentially, in medical settings.

Few studies have been conducted using oxyhydrogen gas generators, and those that have been undertaken are limited by the modest size of the treatment groups(Guan *et al.,* 2020; Zheng *et al.,* 2021; Kong *et al.,* 2022; Tanaka and Miwa, 2022). Initial human trials with published data have focussed on such respiratory conditions as COPD (Zheng *et al*., 2021) and coronavirus infectious disease, 2019 (COVID-19) (Guan *et al.,* 2020), or on the

treatment of, and rehabilitation from, various forms of cancer (Chen, Lu and Xu, 2020; Kong *et al.,* 2022). Although the use of oxyhydrogen has yet to be widely accepted, the results depicted from respiratory trial data strongly suggest that oxyhydrogen inhalation is an effective adjunct to conventional treatments, and in some instances, may be superior to oxygen treatment alone (Guan *et al.,* 2020). For malignant diseases, oxyhydrogen has been noted to improve quality of life of Stage IV cancer patients by reducing anorexia, nausea and physical malaise (self-reported), with the study further suggesting a reduction in serum markers of disease and contraction of tumour size (Chen *et al.,* 2019b; Chen *et al.,* 2020a Chen *et al.,* 2020b). However, further extensive *in vitro* and *in vivo* modelling will be required if these findings are to be substantiated and accepted in the wider healthcare arena.

1.5 Methods of Administration

Adapted from the publication ' Molecular Hydrogen as Medicine: An Assessment of Administration Methods' (Russell *et al.,* 2021)

Currently, there are a range of delivery methods that can be used for hydrogen administration (Russell *et al.,* 2021), all of which are likely to have distinct effects, depending on the delivery mechanism and somatic route of dispersal. This posits the question, 'which method, or methods, of H_2 administration will be most effective in mitigating certain diseases?'

At present, individual treatments in a medical context can include intravenous application of HRS, ingestion of HRW and inhalation of hydrogen, either alone or in combination with oxygen, i.e., oxyhydrogen. Topical and hyperbaric application of H_2 have also been demonstrated to have salutary effects on such conditions as skin ageing (Tanaka and Miwa, 2022) soft tissue injury (Yoon et al., 2011; Tarnava, 2021), decompression sickness(Bjurstedt and Severin, 1948; Kot, 2014) and cancer (Dole, Wilson and Fife 1975; Chen, Lu and Xu, 2020). Furthermore, as public curiosity into the benefits of H_2 as a lifestyle-enhancing product grows, numerous dietary supplements aim to enhance the production of H_2 through microbial interactions within the gastrointestinal tract. Each method used for increasing the cellular availability of H_2 will deliver different concentrations of molecular hydrogen into the cells and will have unique targets, depending on the administration route. For example, HRW is ingested with many beneficial effects described in the gastrointestinal system (Ostojic, 2021), liver (Xia et al., 2013; Korovljev et al., 2019) and the cerebrum (Mizuno et al., 2017; Todorovic et al., 2021), the latter has been posited to be a result of gut-brain-axis communications and the upregulation of secondary messenger molecules (Ostojic, 2021). In contrast, inhalation of hydrogen targets alternative tissues as H_2 is assimilated through the lung parenchyma into the bloodstream where it is then distributed around the body (Yamamoto et al., 2019). This application method is of great benefit not only for respiratory conditions such as asthma, COVID-19 and COPD (Wang et al., 2020c) but also for dysbiosis as a result of ischemia-reperfusion injury, liver disease or metabolic disease (Ichihara et al., 2015; Ge

et al., 2017).

Further, research into nanoparticle delivery of H_2 that utilizes a biocompatible magnesium micromotor and hyaluronic acid coated in polymeric polylactic-co-glycolic acid (PLGA), offers a novel mechanism for targeted delivery of H_2 (Xu *et al.,* 2021). The following sections (Sections 1.5.1 – 1.5.7) describe and assess the methods used for the delivery of molecular hydrogen in a medical context.

1.5.1 HRW

Research has focused on the effects of HRW on oxidative stress in a wide range of conditions (Yoritaka *et al.,* 2013; Ostojic, 2015; Botek *et al.,* 2019; Kawamura, Higashida and Muraoka, 2020) with largely favourable outcomes. HRW is a versatile option for the treatment of numerous ailments as it is portable and can be produced in several ways. For example, H_2 can be created through the reaction with water and magnesium (Mg), shown below:

Reaction: $Mg\ (s) + 2\ H_2O\ (aq) \rightarrow Mg^{2+}(OH)_2\ (aq) + H_2\ (g)$

This is a single displacement reaction where magnesium displaces hydrogen from water. The produced gas then diffuses into the surrounding waters until a saturation point of ~1.6 ppm is reached (standard air pressure and temperature). The creation of HRW using this method is commercially popular as the portability of either magnesium-containing tablets or hydrogen-generating water flasks provides an accessible form for regular H_2 intake. H_2 can also be infused into an aqueous solution under pressure by utilizing a diffusion stone attached to a hydrogen-generation system (Chapter 2, Section 2.2).

Research into the effect of HRW as a medicament is well established, although, to date, there is limited large-scale, clinical data assessing the effect of ingesting HRW for medical conditions. Providing evidence of the functions of H_2 in a large population would strengthen the assertion that HRW should be regarded as a product that is safe and effective for medical use. Another factor that likely adds to the reticence of regulatory bodies' endorsement of H_2, is that the conversation over the dosing of HRW for numerous conditions is ongoing. Although a minimal dosage of 0.8-0.9 mmol ingested per day has been determined to provide antioxidant effects(Nakayama, Kabayama and Ito, 2016; Settineri *et al.,* 2016; LeBaron *et al.,* 2019a), there is a lack of standardized treatment dosages and protocols. Nevertheless, when analysing the results of contemporary research, the cytoprotective and wider systemic effects of HRW ingestion are intriguing, warranting large-scale and long-term clinical investigations.

Due to the transmission route of H_2 through ingestion of HRW, the most pronounced effects have been described in conditions that affect the gastrointestinal tract and supporting organs such as GERD (Franceschelli *et al.,* 2018), IBD (Chen *et al.,* 2013) and metabolic syndrome

(Nakao *et al.,* 2010). To illustrate the favourable effects HRW imbibition has on the digestive system, an eight-week open-label pilot study reports that ingestion of 1.5L of H_2 (55-65mM) increases endogenous levels of SOD and reduces the excreted levels of MDA in patients with metabolic syndrome (Nakao *et al.,* 2010). During an empirical study assessing the effect of hydrogen on the peristaltic movement of the intestinal tract, a reduction in the strength of muscular contraction was observed, signifying reduced colonic transit (Chen *et al.,* 2011). Additionally, a 12-week clinical study involving 84 patients with GERD, electrolyzed-reduced water (pH >7), containing an unquantified amount of dissolved hydrogen, reduced the levels of biological markers pertaining to oxidative stress (*e.g.,* MDA, 8-oxo-dG (Franceschelli *et al.,* 2018). Although the concentration of hydrogen was not recorded, the authors concluded that symptoms of GERD can be reduced rapidly via ingestion of electrolysed-reduced water (ERW), improving overall quality of life.

In addition to HRW treatment for illness, numerous studies have analysed the post-exercise effects of drinking HRW when it is consumed before physical activity (Nakayama, Kabayama and Ito, 2016; Sha *et al.,* 2018; Botek *et al.,* 2022a), with such studies describing a marked increase in antioxidant activity, reduction in lactic acid accumulation (Aoki *et al.,* 2012; Ostojic, 2015) and improved ventilatory capacity (Kawamura, Higashida and Muraoka, 2020) in athletes. Here, daily intake of HRW is noted to support post-exercise recovery, mitigate ROS-induced inflammation, and aid both recovery and prevention of muscle damage (LeBaron *et al.,* 2019b; Kawamura, Higashida and Muraoka, 2020).

1.5.2 Inhalation

Adapted from the publication 'An Interplay of Gases: Oxygen and Hydrogen in Biological Systems' (Russell, May and Hancock, 2024).

Hydrogen and oxyhydrogen inhalation can be a simple, effective and portable means of administration with several products having been designed to produce H_2-containing gas through the electrolysis of water. Inhalation is a non-evasive mode of hydrogen delivery and can be adapted for use through nebulizers, nasal cannulas, or masks that cover the mouth and nose.

Both H_2 and oxyhydrogen inhalation therapies are evidenced as having positive effects in the respiratory (LeBaron et al., 2019b; Guan et al., 2020; Alharbi et al., 2021) and cardiovascular systems(LeBaron et al., 2019a; Barancik et al., 2020; Singh et al., 2023), likely due to the close correlation between the application method and these particular tissues. The non-invasive inhalation delivery mechanism is an efficient and effective way of providing H_2 systemically and can be used for the treatment of acute and chronic conditions alike.

As yet clinical data involving human research on the absorption and distribution of H_2, specifically

through inhalation, are sparse. Nevertheless, a seminal study of rodent models (Yamamoto et al., 2019) noted that 3% continuous inhalation of H_2 resulted in significant variation in the distribution of hydrogen, (Table 1.1), favouring accumulation in the liver, brain and mesentery adipocytes. Regrettably, the study does not cover the cardiovascular and pulmonary tissues, most likely to be the immediate targets of inhalation therapy.

Table 1.1. Distribution of molecular hydrogen in visceral organs of male Sprague-Dawley rats. Data extracted from (Yamamoto *et al.,* 2019).

Organ	H_2 Concentration - µmol/L	Comments
Brain	26	H_2 can traverse the blood-brain barrier
Kidney	18	Lowest tested tissue concentration of H_2
Liver	29	Glycogen has a high capacity for storing H_2
Mesentery Fat	23	Improved lipid profiling
Thigh Muscle	18	Retained H_2 significantly longer than other tissues

Adding to the information in Table 1.1, data derived from a porcine model noted that H_2 concentration decreased rapidly in arterial blood with a half-life of 92 seconds, but diffusion times were increasingly slower in venous blood (half-life: Portal Vein - 310 seconds; Inferior Vena Cava - 350 seconds) indicating that H_2 is transported throughout the body in a blood-flow dependent manner (Sano *et al.,* 2020). In the liver, noted in Table 1.1 as having the highest concentration of H_2 at 29µmol/L, glycogen may act as a hydrogen storage molecule, retaining high quantities of H_2 *in vivo* (Chapter 4, Section 4.3.4), speculated to be a result of carbohydrate polymers having the structural properties to maintain H_2 within the complex (Zhang, Xu and Yang, 2020). It is possible that due to the capacity of glycogen to retain H_2 in the liver, H_2 activity is prolonged in the hepatic system, which may explain why this distinct tissue is particularly responsive to H_2 administration (Chapter 4, Section 4.3.4). In mammalian models of non-alcoholic fatty liver disease, treatment with 4% and 67% hydrogen inhalation was shown to reduce lipid synthesis and deposition, and serum levels of ALT, aspartate transaminase (AST) and lactate dehydrogenase (LDH) (Kamimura *et al.,* 2011). High doses of H_2 (67%) were defined as having the greatest effect on lipid deposition, whilst low concentration (4%) effects were more prominent in the liver enzyme profiling (Liu *et al.,* 2020a).

It is not only the pulmonary and hepatic systems, however, that are likely to be primary targets

for H_2 delivered through inhalation. In animals, attenuation of LPS-derived sepsis (Fu et al., 2009; Xie et al., 2014; Qi et al., 2021) has also been demonstrated as a result of H_2 inhalation. Here, H2 is demonstrated to subdue the acute inflammatory response that results from blood- borne infection (Qi et al., 2021). Further to systemic infection, there is an emerging body of evidence describing the favourable effects H_2 inhalation has on the wider cardiovascular system (Tamura et al., 2016; Chi et al., 2018; Zhang et al., 2018; LeBaron et al., 2019a; Barancik et al., 2020). Early reports demonstrate that 1.3% hydrogen inhalation for patients with ST- elevation myocardial infarction restored left ventricular modelling 6-months post-administration (Katsumata et al., 2017). Intraoperative inhalation of H_2 was shown to decrease biological markers of lipid peroxidation, diene and tiene conjugates and Schiff bases, an effect most pronounced 1-day post-surgery (Danilova et al., 2021), indicating that H2 could be used in cardiac surgery as an effective and safe antioxidant (Tamura et al., 2016; LeBaron et al., 2019a). In models of chronic heart failure, H_2 inhalation was demonstrated to markedly reduce apoptosis and oxidative damage in peripheral blood cells (Sim et al., 2020) and cardiomyocytes (Chi et al., 2018), whilst H_2 also stimulates cholesterol efflux from foam cells in the cardiovascular system (Song et al., 2012), thereby reducing the mortality risks associated with atherosclerosis and cardiovascular disease.

As cytoprotective and holistic characteristics of hydrogen inhalation have been noted to have systemic effects, interest in this respective H_2-delivery method within the sports industry is developing. Here, clinical studies have revealed that breathing 1% H_2 for 20 minutes whilst exercising amplifies breath-acetate concentrations, a non-invasive marker of lipid metabolism, indicating this method of application promotes favourable lipid metabolism (Hori et al., 2020). Similarly, 4% H_2 inhalation for seven days improved running velocity and reduced levels of insulin-like growth factor-1, a regulator of glucose transportation, in the bloodstream. Significant reductions in the pro-inflammatory marker CRP, and ferritin, an acute phase inflammatory reactant, were also observed (Javorac et al., 2019). Congruent with the hypothesis that H_2 can positively influence the innate immune response. Furthermore, decreases in inflammatory biomarkers (e.g., TNF-α, IL-1β, IL-6); markers of apoptosis (e.g., caspase-3, B-cell lymphoma-2 (Bcl-2), and heat shock proteins (e.g., HSP70)), and increases in SOD activity, were recorded in laboratory models of acute exercise-induced fatigue (Nogueira et al., 2021).

1.5.3 The Differences Between Ingestion and Inhalation

Although direct inhalation of hydrogen-containing gases provides a greater quantity of H_2 into the bloodstream, saturation limits of H_2 into the blood plasma are relatively low at 1.6mg/L (0.8mM), reaching peak concentrations after 5 minutes and returning to baseline levels within 60 minutes. Pharmacokinetic observations in animal models strongly suggest that H_2 is distributed through simple diffusion as H_2 levels diminish rapidly in the arterial bloodstream,

a phenomenon that is not seen in venous blood (Sano *et al.,* 2020). Further investigations have revealed that the brain, heart and skeletal muscle can sequester comparatively large amounts of H_2 when compared with the imbibition of HRW (Liu *et al.,* 2014) (Figure 1.4).

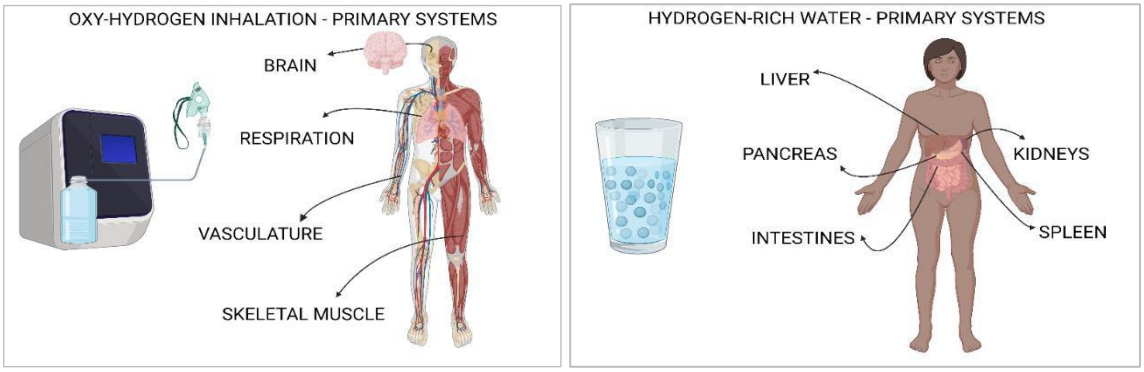

Figure 1.4 Primary target systems of H_2 through inhalation (Left) and ingestion (Right). Images created in Biorender.com

Drinking HRW, in contrast, was demonstrated to primarily affect the liver, pancreas, spleen and intestinal organs (Liu *et al.,* 2014), with both methods of administration resulting in increased levels of H_2 in the liver (Liu et al., 2014; Sano *et al.,* 2020). H_2 inhalation therapy targets alternative tissues to HRW, as H_2 is assimilated through the lung parenchyma into the bloodstream, where it is then distributed around the body. This phenomenon enables the administration of hydrogen through inhalation to be incredibly beneficial for respiratory conditions such as asthma, COVID-19, and COPD, where symptoms were markedly improved with treatment (reviewed by Russell, Nenov and Hancock, 2021). Hydrogen inhalation therapy can also reduce physiological distress caused by injury or disease in the central nervous system where inhalation of H_2 gas is demonstrated to be effective in aiding recovery from both traumatic brain injury (Ono *et al.,* 2017) and degenerative cognitive decline (Nishimaki *et al.,* 2018). In addition, H_2-inhalation is demonstrated to improve cardiac functionality and reduce neurocognitive decline that results from cardiac arrest (Tamura *et al.,* 2020).This suggests that H_2 is absorbed into the pulmonary capillaries and then traverses with the blood flow directly to the heart and is delivered, via the carotid artery, to the brain.

Analysis of tissue samples 30 minutes post-inhalation of H_2, reveals the levels and retention of H_2 in skeletal muscle far surpassed that of any visceral tissue, including the brain and liver. (Nogueira *et al.,* 2018; Shibayama *et al.,* 2020). Clinical evidence supporting this hypothesis has shown that H_2 gas can assist in recovery from physical fatigue, assessed the effects of H_2-inhalation in 27 patients and demonstrated beneficial health effects which included both enhanced physical and respiratory function in the rehabilitation of acute post-COVID-19

patients when compared with patients in the placebo group (Botek *et al.,* 2022c). Therefore, H_2 inhalation therapies can provide benefits during recovery from physical exercise and illness, with evidence suggesting that the anti-inflammatory and antioxidant properties of H_2 can enhance physical performance and mitigate indices of post-exercise and recuperative fatigue (Da Ponte *et al.,* 2018; Botek *et al.,* 2022b).

In contrast to H_2-inhalation therapies, HRW provides a lesser, but calculable dosage of H_2. Commercially available HRW however, can contain variable amounts of H_2, ranging from 0 mg/H_2/L to a supersaturated level of >15mg of H_2/L, with typical saturation levels at 1.6mg/L, H_2 (Singh *et al.,* 2021). Therefore, even with a high consumption of 3L of HRW per day, the maximum dosage would be 45mg/ day, H_2, far below that of inhalation therapies. A clinical study observing the effects of consuming HRW water containing 0.92mg of H_2 per day for two weeks, noted no significant changes in biological markers of physiological stress in exhaustion tests. The peak power output of intensive exercise was maintained only in the HRW cohort (Da Ponte *et al.,* 2018) suggesting that H_2 can enhance skeletal muscle function. Further studies have shown that 5mg of H_2 ingested before exertive exercise can reduce the heart rate during submaximal aerobic exercise, although other parameters such as maximal oxygen uptake (VO_2) and respiratory rate were unaffected (LeBaron *et al.,* 2019b). In contrast, alternative clinical studies have found conflicting evidence, suggesting HRW may improve ventilatory capacity and reduce blood-lactate levels (Drid *et al.,* 2016; Botek *et al.,* 2021). Therefore, whether ingesting HRW is effective in remediating skeletal muscle stress is still a matter of debate, and clinical evidence remains contradictory. It is clear, therefore, that the present information regarding the use of HRW as a supplement for physical performance is inconclusive, and further research in this area is warranted.

In summary, H_2-inhalation therapies are well demonstrated as highly effective anti-inflammatory and antioxidant treatments that are able to provide superior quantities of gas into the body when compared with HRW. Due to the simple mechanism of diffusion of the H_2 molecule, the principal effects of inhalation are typically noticed in the proximal organs of the brain, cardiovascular system and lungs, with skeletal muscle also benefitting from H_2 inhalation. Clinical evidence of the effect of HRW on skeletal musculature is currently inconclusive. However, data in favour of HRW as a therapeutic for gastrointestinal-related disorders is mounting (a factor that has yet to be investigated, in-depth, for H_2-inhalation).

1.5.4 Dietary Supplements

Of late there has been growing interest in products that act as prebiotic substrates for H_2-producing bacteria (Chatterjee, Jungraithmayr and Bagchi, 2017; Yu et al., 2020) in particular Bacteroides and Firmicute species(Hylemon, Harris and Ridlon, 2018). For instance, turmeric, the

root of the *Curcumina Longa* L. perennial has long been utilized as a remedy for gastrointestinal ailments and inflammatory conditions (Soleimani, Sahebkar and Hosseinzadeh, 2018), with many reports now suggesting turmeric modulates the composition of the intestinal microflora for the benefit of the host (Zam, 2018). Initial research suggests the beneficial effect of turmeric may be through microbial efflux of H_2 as a result of turmeric fermentation (Shimouchi *et al.,* 2009). Alongside traditional medical remedies (such as turmeric), increasing the daily intake of dietary fibre and inulin are also shown to positively affect the microbial balance by providing non-absorbable carbohydrate substrates for the metabolic activity of H_2-producing species (Soleimani, Sahebkar and Hosseinzadeh, 2018).

In parallel with prebiotic supplementation, ingestible capsules containing a mixture of calcium (Ca^{2+}), magnesium (Mg^{2+}), plant-based antioxidants and trace minerals that enhance gastrointestinal production of H_2, are commercially available without prescription. However, caution is advised when using such supplements as scientific verification of the concentrations of H_2 produced, molecular effects and long-term efficacy is lacking. Of the data currently available, a double-blind, placebo-controlled cross-over pilot trial (n=10) (Korovljev *et al.,* 2017) showed a 4-week regime of 1 capsule a day containing 46 mg of calcium and 40 mg of magnesium, was effective in reducing both serum triglyceride and fasting insulin levels in a small cohort of middle-aged women (n = 10). Supporting these data, a more recent analysis of the effect of orally administered H_2-inducing calcium-rich powder (n = 18) (Alharbi *et al*., 2021) demonstrated that one 1500 mg capsule per day produced 2.5 µg of H_2, improving pulmonary gas exchange and increasing both haemoglobin and myoglobin saturation of O_2. Although both means provide a calculable dose of H_2, the subject cohorts are small and the conditions investigated unrelated (lipid accumulation – O_2 saturation, respectively).

By encouraging the natural balance of intestinal microflora in favour of hydrogen-producing species this method of H2 ingestion could act as a prophylaxis against such chronic and costly ailments as cardiovascular disease, systemic inflammation and type 2 diabetes. If dietary supplementation should prove to be a cost-effective and sustainable way of enhancing endogenous H_2 production, it could have a major role to play in the future of nutritional education and corresponding healthcare recommendations.

1.5.5 Hydrogen-Rich Saline

As the use of hydrogen generators may be impractical in a nosocomial environment due to the explosivity risk and public safety implications (Chapter 9, Section 9.4), instead HRS is proposed for use in a clinical setting for post-operative care and the treatment of ischemia-reperfusion, liver disease and organ grafting (Yaun and Shen, 2016; Obara *et al.,* 2024). HRS could prove to be a practical method of hydrogen administration as the use of saline solutions

is already commonplace. An early study conducted in Japan suggests that submersion of saline bags into a hydrogen-rich bath for three days can produce a saturated solution (0.8mM) that can then be dispensed in the same way as saline (Fu *et al.,* 2020). Alternatively, direct infusion of H_2 into the media would be more time-effective but would require pressurisation of hydrogen gas to be effective, which could lead to the necessity for enhanced safety protocols and increased costs. Currently, storage at atmospheric pressure of HRS is only recommended for 7 days (Fu *et al.,* 2020), therefore it is likely that investment will be needed for manual training, specialized equipment and storage facilities, whilst the cost-effectiveness of such implementation will also need to be assessed before the use of HRS is widely adopted.

There is limited evidence for the effect of HRS in humans, although a pivotal study has demonstrated efficacy in reducing serum levels of the pro-inflammatory marker IL-6, and the pro-oxidative marker 8-oxo-dG, in patients with rheumatoid arthritis (n=24) (Ishibashi *et al.,* 2014). A supporting body of data orientated around animal studies, describes the infusion of HRS through the peritoneal cavity as reducing the damage caused by surging ROS associated with ischemia-reperfusion, noted to be particularly effective in the liver (Fukuda *et al.,* 2007; Uto *et al.,* 2019). Added to this, reports investigating the effects of H_2 treating pre-transplantation liver segments in an organ bath containing HRS, suggest this distinct method can reduce apoptosis, neutrophil infiltration and oxidative damage, in both the liver and proximal tissues(Uto *et al.,* 2019). Similar findings are found when >1.5ppm (H_2) HRS is infused during post-operative surgical closure of the ileum in rodents (Okamoto *et al.,* 2016). In porcine models, HRS lavage for post-operational peritonitis was shown to ameliorate sepsis-induced organ failure (Sada *et al.,* 2021), a factor attributed to the reduction of the 8-oxo-dG excreted in the urine.

Considering the breadth of molecular hydrogen research and the scope for improved patient outcomes with the widespread use of HRS, future endeavours will have to address the practicalities of creating and storing HRS in the nosocomial environment.

1.5.6 Nanotechnology

The production and storage of hydrogen is a rapidly expanding area of interest for the energy sector as hydrogen is mooted to be an alternative to the burning of fossil fuels. In this regard, nano, or micro, technologies that can retain and store hydrogen whilst mitigating the risk of explosion may significantly reduce the carbon emissions associated with industrial pollution. Having been developed for the retention of H_2 as a fuel source(Guo, 2012) the low weight, low cost and high hydrogen binding capacity of such technologies has now been adopted for medical research.

Nanotechnologies are rapidly becoming of interest for pharmaceutical purposes as they can provide a means of localised delivery for drug administration that is primarily regarded as safe and effective (Sutariya and Pathak, 2014). Here, biologically degradable substances such as magnesium (Mg) and palladium (Pd) are efficacious in producing and storing H_2, respectively. Such metals have been refined to treat such inflammatory-related conditions as cancer (Liu *et al.,* 2020b), rheumatoid arthritis (Xu *et al.,* 2021) and neurodegenerative disease (Bilal *et al.,* 2020). Nano, and micro, technologies can be broadly categorised into two categories; nanodevices and nanoparticles, each with distinct mechanisms that can deliver H_2 within living systems.

1.5.6.1 Nanodevices - Mg/Hyaluronic Acid

Biodegradable magnesium-based micromotors can convert external stimuli into propulsion, as a result of the Mg/H_2O reaction described previously (Section 1.2.1). As Mg is known to degrade rapidly, the addition of hyaluronic acid coated in a PLGA substance has been developed (Guo, 2012), offering the benefit of direct and observable administration of molecular hydrogen when used in parallel with ultrasound visualization. Although promising results have been demonstrated in rodent models (Liu *et al.,* 2014; Murthy, 2017), these devices have yet to be tested in humans and the toxicity of potential bi-products has not been evaluated. However, the potential for this nanotechnology is intriguing and further research in this area could revolutionize the way therapeutic drugs and compounds are introduced into mammalian systems.

1.5.6.2 Nanoparticles – Palladium Hydride (PdH)

Nanoparticles differ from nanodevices in that their crystalline structures contain a large surface area by design, and can therefore adsorb relatively large quantities of substances intended for medical distribution. Research shows that the use of nanoparticles can be an effective strategy for transporting drugs as targeted treatments in models of Alzheimer's Disease (Zhang et al., 2019b) and glioblastoma (Liu et al., 2019). Co-ordinately, for diagnostic purposes, nanoparticles can be designed with specific quantum properties known to improve the quality of both optical and magnetic resonance imaging (Murthy, 2017).

Palladium (Pd) is well-known for its high binding affinity with hydrogen, adsorbing large amounts of hydrogen under environmental conditions. Synthesis of palladium-hydride (PdH) particles utilizes a facile one-step reduction route when forming particles (Zhang *et al.,* 2019b). This chemistry is useful in a medicinal context as it allows for structural lattice formations to either be laden with H_2 for therapeutic use, or as a resource for the detection and purification of H_2, as posited by Zhan *et al.* (2020). Once the nanoparticles have been produced, H_2 can be infused into the aqueous storage solution, imbibing the structures with molecular hydrogen, which can then be stored for future use.

PdH nanoparticles generate bi-products (*e.g.,* palladium crystallites) as they decompose (Cobden *et al.,* 1998), this will need to be considered if such technologies are to be widely used in a clinical context. Nevertheless, PdH particles have been demonstrated to be well tolerated in biological systems and can be loaded with H_2, resulting in the absorption of H_2 at ˜2.46 x 10^{-19} mol per Pd particle (Zhang *et al.,* 2019b). This method effectively stores the H_2 molecules through weak hydrogen bonding until degradation of the complex releases the H_2 load. Another benefit of adopting PdH particles for H_2 delivery is that Pd has alkyne hydrogenation properties that support the prolonged release of hydrogen into the localized tissue (Zhang *et al.,* 2019b). This mechanism of hydrogen therapy has the potential for specific application in neurodegenerative conditions where delivery of H_2 across the blood-brain barrier can reduce oxidative stress in neurons (Wu *et al.,* 2023), thereby affording protection against excessive inflammation and cellular apoptosis. However, such technologies are rarely used as clinical tools and as yet are not produced in sufficient quantities for regular use in a medical context.

1.5.7 Topical Administration – Bath/Gel/Patches

H_2 can be easily administered through the skin, either as an addition to bathing waters, as an absorbable gel or contained within patches designed for the gradual release of H_2 over time. The growing interest in medical H_2 research has inspired a flurry of patented designs for topical products (Safonov, 2019; Perricone, 2021; Satoh, 2021). Innovative gels and patches can overcome the hesitations surrounding accurate dosing by providing both measurable delivery timings and accurate dosages, making them a good candidate for the treatment of wounds. However, as these materials have yet to be widely tested it may be some time before such products can be assessed for efficacy.

Research into the effects of bathing in a hydrogen-rich solution is more established and suggests the antioxidant properties of H_2 can substantially reduce disease severity in skin conditions including age-related degeneration (Tanaka and Miwa, 2022), psoriasis (Zhu *et al.,* 2018) and wound healing (Tarnava, 2021). Early investigations assessing the effect of H_2-infused bathing water on mice purposefully exposed to UVB radiation reported a marked decline in burn severity, coupled with a reduction in pro-inflammatory markers, IL-1β and TNFα, and an increase in the anti-inflammatory cytokine IL-10 (Ignacio *et al.,* 2013). Building on this research, Tanaka and Miwa (2022) assessed the effects of HRW, coupled with H_2-rich poultice application, on various parameters of ageing, and concluded that H_2 reduced rubrous blotches and wrinkles, and rebalanced moisture and oil content, attributed to an enhanced antioxidative capacity in the blood. An eight-week parallel-controlled trial (n=74) involving patients with psoriasis or parapsoriasis *en plaques,* who were treated twice weekly with a 10 to 15-minute hydrogen bath containing 1.0ppm H_2, effected a pronounced reduction in rubor and pruritus in 80% of H_2-treated patients (Tanaka and Miwa, 2022). Furthermore, a seven-day

case study evaluating the effect of H_2 immersion therapy in waters containing 8.0ppm/H_2 on a traumatic injury sustained to the proximal phalanges of the 5th toe (Tarnava, 2021), saw a rapid reduction in pain and inflammation, with improvements to range of motion, and ability to bear weight, were also noted.

The above evidence illustrates the propitious effects of H_2-hydrotherapy for a range of topical inflammatory conditions where conventional synthetic drug treatments have well-known side effects (Lebwohl, 2005; Bajgai *et al.,* 2021). Adopting an H_2 strategy for the treatment of soft and connective tissue injuries could provide a cost-effective and non-invasive alternative to current steroidal management of inflammatory diseases.

1.6 Aims and Objectives

The precise mechanisms of H_2 activity are currently undefined, *i.e.,* the lack of primary target identification, coupled with difficulties regarding administration methods (*e.g.,* dosage and dosage frequencies, and long-term effects of treatments), therefore, there is a requirement for H_2 research to evidence how it can reasonably and effectively be incorporated into global healthcare practices.

By providing novel experimental protocols and innovative theories into the biological activity of H_2, the objective of this thesis is to explore a range of theories incorporating the potential evolutionary requirement of H_2 in living organisms; how H_2 may interact at a molecular level in plants and humans; and the effect of H_2 administration on malignant cells.

Chapter 2: Equipment, Materials and Methods

2.1. Equipment and Reagents

2.1.1 Assessment of Oxyhydrogen Generation with HydroVitality™ Water Electrolysis Device.

- HydroVitality™ oxyhydrogen generator (450 mL/min) (Water Fuel Engineering, Wakefield, UK)
- H_2 Blue™ (Methylene Blue/Platinum nano-particles) (H_2 Sciences Inc., Henderson, USA)
- Clarke-type O_2 electrode (Hannah Instruments Ltd., Bedfordshire, UK, Cat. #Opdo™ HI98198)
- pH Meter Jenway™ 3510 (Camlab, Cambridgeshire, UK. Cat. #SKU - 1140956) + Calibration Standards (pH 4, pH 7 and pH 9.5)

2.1.2 Seed Treatments

- HydroVitality™ oxyhydrogen generator (Water Fuel Engineering, Wakefield, UK)
- *Pisum sativum* seeds (Thompson and Morgan, Suffolk, UK. Cat #24298)
- Centrifuge (Microstar 17, Avantor™/VWR™, Leicestershire, UK.)
- Incubator (LEEC, Nottingham, UK. Precision 190)
- NaCl (Sigma Aldrich, St. Louis, USA. Cat. #S1679)
- Agargel (Sigma Aldrich, St. Louis, USA. Cat. #A3301)
- 70% Ethanol (Sigma Aldrich, St. Louis, USA. Cat. #493546)
- Handheld homogeniser
- Radioimmunoprecipitation (RIPA) Lysis Buffer (Thermo Fisher Scientific, Waltham, USA, Cat. #89900)
- Phosphate Buffer Saline (PBS) Tablets (Thermo Fisher Scientific, Waltham, USA, Cat. #18912014)

2.1.3 Seed Assay – Cupric Reducing Antioxidant Capacity (CUPRAC)

- Spectrophotometer microplate (Spectramax M2, Avantor™/VWR™, Leicestershire, UK.)
- 96-well microtiter plate for microplate assay.
- RIPA lysis buffer (See Section 2.1.2)
- PBS (See Section 2.1.2)
- Cuprac Assay (Bioquochem, Asturias, Spain. Cat. #KF01005)

2.1.4 Seed Assay – Ferric Reducing Antioxidant Potential (FRAP)

- Centrifuge (Microstar 17, Avantor™/VWR™, Leicestershire, UK.)
- Spectrophotometer Jenway™ 6300 (Cole-Parmer, St. Neots, UK. Cat. #WZ-79000-64)
- PBS (See Section 2.1.2)
- Fe^{2+} (Sigma Aldrich, St. Louis, USA. Cat. #215422)
- Fe^{3+} (Sigma Aldrich, St. Louis, USA. Cat. #236489)
- 2,3,5-Triphenyltetrazolium chloride (TPTZ) (Sigma Aldrich, St. Louis, USA. Cat. #1.08380)
- Sodium acetate anhydrous (Sigma Aldrich, St. Louis, USA. Cat. #W302406)
- Acetic acid (Sigma Aldrich, St. Louis, USA. Cat. #A6283)
- Acetate buffer (Sodium acetate anhydrous/Acetic acid) (Sigma Aldrich, St. Louis, USA. Cat. #S7899)
- Iron(III) chloride hexahydrate (FeCl3.6H2O) (Sigma Aldrich, St. Louis, USA. Cat. #F2877)
- RIPA lysis buffer (See Section 2.1.2)

2.1.5 Nematode Treatments

- NaCl (Sigma Aldrich, St. Louis, USA. Cat. #S1679)
- Nematode Growth Medium (NGM): (17 g Bacto agar powder (Sigma Aldrich, St. Louis, USA. Cat #A5306), 3 g NaCl (Sigma Aldrich, St. Louis, USA. Cat #S1679, 2.5 g Bacto peptone (Sigma Aldrich, St. Louis, USA. Cat #P5905), 1 mL cholesterol (Sigma Aldrich, St. Louis, USA. Cat #C3045 - (5 mg/mL in ethanol)), 975mL deionised water, 0.5 mL CaCl2 (1 M) (Sigma Aldrich, St. Louis, USA. Cat #C5670), 1 mL MgSO4 (1 M) (Sigma Aldrich, St. Louis, USA. Cat #83266), 25 mL KPO4 buffer (1 M) (108.3 g KH2PO4 (Sigma Aldrich, St. Louis, USA. Cat #P3786), 35.6 g K2HPO4 (Sigma Aldrich, St. Louis, USA. Cat #P5629), distilled H2O to 1 litre.
- PBS (See Section 2.1.2)
- RIPA lysis buffer (See Section 2.1.2)
- Liquid nitrogen
- Hydrogen peroxide (30% w/w) (Sigma Aldrich, St. Louis, USA. Cat #H1009)
- Incubator (Inculine IL23, VWR™ Leicestershire, UK.)
- Microson XL ultrasonic cell disruptor XL (Misonix, New York, USA.)
- Centrifuge (Microstar 17, Avantor™/VWR™, Leicestershire, UK.)
- UV/Vis Spectrophotometer Jenway™ 6305 (Cole-Parmer, St. Neots, UK. Cat #WZ-99968-68)
- Microscope (Brunel Microscopes, Chippenham, UK. Cat# SP22)
- HydroVitality™ oxyhydrogen generator (Water Fuel Engineering, Wakefield, UK)
- Centrifuge (Microstar 17, Avantor™/VWR™, Leicestershire, UK.)

2.1.6 Cell Culture: Sterilisation

- Roswell Park Medical Institute (RPMI) 1640 media with L-glutamine and sodium bicarbonate (Sigma Aldrich, St. Louis, USA. Cat. #R8758)
- 70% Ethanol (Sigma Aldrich, St. Louis, USA. Cat. #493546)
- Autoclave Priorclave/tactrol 2 (Medline Scientific, Oxfordshire, UK)

2.1.7 Cell Culture and Treatments

- H_2 generator (Aukewel, Guangzhou, China. Cat #ABS-XQ-O2)
- 0.5-micron stainless steel diffusion stone (Filson Filter, Henan, China)
- TK6 cells – cultured from stocks courtesy of Dr. A. Thomas at the University of the West of England
- Foetal Bovine Serum (FBS) (Sigma Aldrich, St. Louis, USA. Cat. #F7524)
- T-75 and T-25 Culture Flasks
- Trypan Blue (Sigma Aldrich, St. Louis, USA. Cat #302643)
- CytoSmart™ cell counting device and software (Axion Biosystems Inc., Atlanta, USA)
- CellDropFL Fluorescence Cell Counter (DeNovix Inc., Wilmington, USA. # CellDrop FL-UNLTD)

2.1.8 Flow Cytometry

- 80% ethanol (Sigma Aldrich, St. Louis, USA. Cat. #493546)
- Accuri™ C6 Flow cytometer (BD Biosciences, Berkshire, UK)
- Vortex (Cole-Parmer, St. Neots, UK. V series Stuart, Cat. #WZ-04729-01)
- PBS (See Section 2.1.2)
- RNase A (Sigma Aldrich, St. Louis, USA. Cat. #10109142001)
- Propidium iodide (Sigma Aldrich, St. Louis, USA. Cat. #P4170)

2.2. Methods

2.2.1 Bioinformatics Methods

Homology between Complex I protein subunits and hydrogenase enzymes was investigated using the Ensembl.com Basic Local Alignment Search Tool - Protein (BLASTP) platform. The amino acid sequences were sourced from www.UniProt.com, whilst sequence alignments were conducted using the Clustal Omega programme, with a sequence identity of > 25% suggesting the potential for similarity of function (Anderson and Brass, 1998). Analysis of protein domains was conducted within Expasy.org, using Dotlet and ScanProtsite programmes.

2.2.2 Assessment of the HydroVitality™ Oxyhydrogen Generator

2.2.2.1 Flow Rate

The volume of gaseous output of the HydroVitality™ device was determined using the water displacement method (Figure 2.1).

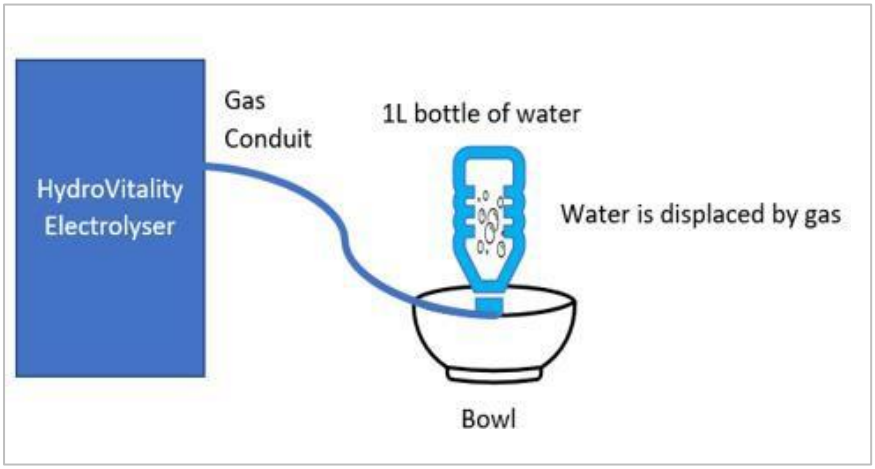

Figure 2.1. Graphical representation of the water displacement method. The graphic depicts oxyhydrogen exiting the generation system through silicon conduit piping into the neck of the upturned bottle containing 1L of water. The bowl below also contains water and consistent pressure and water stabilisation are obtained. The gas produced displaces the water from the bottle into the bowl, and the loss of water from the bottle is measured after one minute, giving a gas output in mL/min.

2.2.2.2 Gas Analysis

Analysis of the gaseous output of the HydroVitality™ device was outsourced to SGS Gas Analysis Services (Bristol, BS15 4PJ, UK). 750mL of gas was collected into a hermetically sealed Tedlar® bag by a field representative of SGS Gas Analysis Services for testing using gas chromatography (22/2/23).

The company (SGS) were asked to test for a variety of contaminants, namely methane (CH_4), carbon monoxide (CO), carbon dioxide (CO_2), sulphides (S) and nitrogen (N_2).

2.2.2.3 Determination of H_2 Content in Aqueous Solutions

Aqueous solutions were infused in glass Duran bottles and the lids were replaced after the sample was removed from the vessel. Bottles were exposed to room temperatures (21 ± 20C) between measurements. Dissolved hydrogen levels were calculated using the titration method, wherein H2 Blue™ is added to 6 mL of water containing an unknown level of H2. H2 Blue™ titration utilises methylene blue and colloidal platinum.

MB is an oxidising agent commonly used as a biological dye, which, in the presence of a platinum catalyst reacts with dissolved molecular hydrogen to produce the reduced (clear) form of methylene blue: leucomethylene blue, shown in reaction 1.

Reaction: MB (Blue) + H_2 → Leucomethylene blue (Clear)

H_2 Blue™ reacts with molecular hydrogen, turning clear in the presence of dissolved hydrogen gas. As additional drops of H_2 Blue™ are added, the dissolved H_2 content is oxidised until totally depleted. This is referred to as the titration endpoint. When the endpoint has been reached, additional drops will no longer turn clear, and the solution will remain blue. The dissolved H_2 content of clear liquids can be calculated with 1 drop (0.025 mL) of cleared H_2 Blue™ representing a concentration of 0.1 mg/mL of H_2. To account for H_2 displacement by O_2, the recordings were multiplied by the saturation point of H_2 in an aqueous solution at 11 m elevation (1.6 mg/L). Results are shown in mg/L which is equivalent to parts per million (ppm). However, many studies in the academic field use various measurements of concentration (Meng et al., 2016; Dobashi, Takeuchi and Koyama, 2020; Cheng et al., 2021; Tanaka and Miwa, 2022). As such discrepancies can be inhibitive to the full comprehension of H2 dosing, a conversion guide is provided in Table 2.1.

Table 2.1. Content of H_2 in aqueous systems conversion table.

HRW Content	Parts per Billion (ppb)	mg/L = Parts per Million (ppm)	Micro-molar (mM)	g/100ml
1 drop of H_2 Blue	100	0.1	0.05	0.01
2 drops of H_2 Blue	200	0.2	0.1	0.02
3 drops of H_2 Blue	300	0.3	0.15	0.03

2.2.2.4 Determination of O_2 Content in Aqueous Solutions

O_2 measurements were obtained using an O_2 electrode (Hannah Instruments Ltd., Bedfordshire, UK, Cat. #Opdo™ HI98198). Recordings were taken every 5 minutes for 15 minutes, post-infusion, and a final recording was taken 30 minutes post-infusion. The samples were subject to the same laboratory conditions as stated in Section 2.2.2.3.

2.2.3 Seeds

2.2.3.1 Storage

Seeds were air-dried on blotting paper for three hours after treatments and stored in a refrigerator (4^0C) overnight.

2.2.3.2 Planting and Incubation

Seeds were weighed and numbered before being planted in agar-filled petri dishes. These plates were sealed with tape and placed in transparent freezer bags, labelled, dated and incubated in chambers with Lux readings equalling 1200. The temperature was set at 23^0C, humidity at 85% and the light cycle was set for 16 hours of light and 8 hours of darkness, for 7 days.

2.2.3.3 Harvest and Cleaning

Seeds were harvested using sterile techniques. The germinated seedlings were then cleaned using ddH_2O to remove any excess agar. Seeds were dried in air and weighed for their biomass with data recorded for later analysis.

2.2.3.4 Processing

Seeds were cleaned, dried and weighed before any incisions were made in the tap root, of which 1 cm was taken for analysis.

2.2.3.5 Determining the Effect of NaCl in Plant Medium.

A common and relatively hardy variety of Mangetout peas (*Pisum sativum* L. 'Oregon sugar pod') was chosen for experimental analysis (Neugschwandtner *et al.,* 2019). To better understand the effects of H_2 upon salinity-challenged germinating seedlings, a preliminary study considering the NaCl content of the growth medium was required. Agargel™ was prepared as per the manufacturer's instructions (7 g Agargel™/L water) for the control group, whilst 50 mM or 100mM of salt (NaCl) was added to assess the comparative growth of seedlings. Seeds were pre-treated (primed) with oxyhydrogen dissolved in distilled water for 10 minutes, dried in air, and placed in a refrigerated unit (4^0C) overnight before planting. The control group seeds were not treated but were refrigerated overnight before planting.

2.2.3.6 a Seed Preparation

Oregon Sugar-pod Mangetout seeds were surface-sterilised as per Oyebanji *et al.* (2009). Briefly, seeds were washed with 80% ethanol for 5 minutes and air-dried for 30 minutes before refrigeration at 4^0C.

The surface-sterilised seeds were randomly extracted from the storage container using the aseptic technique, numbered individually and weighed before treatment. Three seeds were

placed on each plate in small channels, ensuring the seeds would be embedded within the media, each being numbered on the bottom of the plate for identification.

2.2.3.6 b Control

Six seeds, three seeds per dish, were placed in a triangular configuration into two Agargel-filled Petri dishes containing either 0 mM, 50 mM or 100 mM NaCl.

2.2.3.7 H_2O

Six seeds were soaked in individual and lidded Bijou pots (7 mL) containing 4 mL distilled H_2O for 10 minutes, air dried, then placed in Agargel-filled petri dishes containing either 0 mM, 50 mM or 100 mM NaCl.

2.2.3.7 HRW

HRW was prepared using the HydroVitality™ device. Briefly, 300 mL of ddH_2O was placed in a glass container and infused for 30 minutes using 0.5 micron diffusion stone. 4 mL of HRW was aliquoted into Bijou pots (7 mL) before seeds were placed for treatment of 10 minutes, air dried, and then placed in Agargel-filled petri dishes containing either 0 mM, 50 mM or 100 mM NaCl.

2.2.3.8 Antioxidant Assay Preparation

0.05 g (± 0.02 g) of root material from each seed was removed and placed in a 15 mL Falcon tube containing 2 mL of RIPA Lysis Buffer. The contents of each tube were made homogenous. The solution was centrifuged at 600 x g for 6 minutes and 1 mL of the cell lysate material was aliquoted to a 1.5 mL centrifuge tube. Each tube was then flash-frozen in liquid nitrogen before being placed in a freezer (-200C) for storage. For the antioxidant assays, lysate material was collected for immediate analysis. Seven repeats of experimental data were analysed for the FRAP assay, whilst, due to reagent availability, only three repeats of the CUPRAC assay were assessed.

2.2.3.9 a Antioxidant Assay – CUPRAC assay

The data from these experiments was produced by MSc project student Bipana Dewan, under my supervision (Grace Russell). Firstly, a calibration curve with known CUPRAC concentrations was prepared (Supplementary Figure 1). Reagents were used as per manufacturer's instructions (Chapter 2, Section 2.1.3). Antioxidant activity is expressed as µM Trolox Standard). µM Trolox Equivalents = ((OD 450 nm-intercept)/slope)*dilution factor.

The 96-well plate was incubated at room temperature for 30 minutes. The absorbance of the reaction was measured at 450 nm, using a microplate spectrophotometer (Section 2.1.3).

2.2.3.9 b Seeds: Antioxidant Assay - FRAP assay

This data was produced by MSc project student Bipana Dewan under my supervision. Firstly,

a standard curve with known FRAP concentrations was prepared (Supplementary Figure 2). The preparation of seeds was identical to the CUPRAC protocol above. For analysis, the cell lysate was defrosted on ice to prevent excessive enzyme activation. For the assay, 50 µl of extract solution was mixed with 950 µl of FRAP reagent. The mixture was incubated at room temperature for 30 min. The absorbance of the reaction mixture was measured at 593 nm (Benzie and Strain, 1996) using a visible spectrum spectrophotometer (Section 2.1.4).

2.2.4 Determining the Effect of Oxyhydrogen Gas Administration on Salinity- challenged Nematodes.

2.2.4.1 Caenorhabditis elegans: Stock Culture

To analyse the effect of variable NaCl concentrations on the growth and replicative capacity of C*. elegans* nematodes, using aseptic techniques, 1 cm^2 of stock Bristol N2 strain nematodes (Chapter 2, Section 2.1.5) were placed in the center of round Petri dishes containing standard (50 mM NaCl) NGM agar (Section 2.1.5) a process referred to as 'seeding' (Brenner, 1974). The cultures were then incubated for a minimum of five days and a maximum of 10 days, at 22^0C. Four concentrations of NGM agar (NaCl 25 mM/50 mM/100 mM/200 mM) representing suboptimal (25 mM) (Derycke *et al.,* 2007), optimal (50 mM) (Brenner, 1974) and extra-optimal (100 mM/200 mM) (Xie *et al.,* 2012) salinity were prepared, and the newly cultured nematodes were seeded onto five plates of each concentration. These dishes were again placed in the incubator at 22^0C for a minimum of five days.

2.2.4.2 Treatment of Nematodes with Oxyhydrogen gas.

To assess the efficacy of gaseous oxyhydrogen administration on multicellular organisms under duress, nematodes were seeded in corresponding agar plates containing either 25 mM/50 mM/100 mM/200 mM NaCl. The open Petri dishes were then placed in an air-tight, lidded container (15 x 7 x 5 cm/650 mL) which was connected to the HydroVitality™ generation device for 30 minutes (Figure 2.2). After this time, nematodes were returned to the incubator (22^0C) for 48 hours before the morphology and replicative capacity of nematodes were assessed.

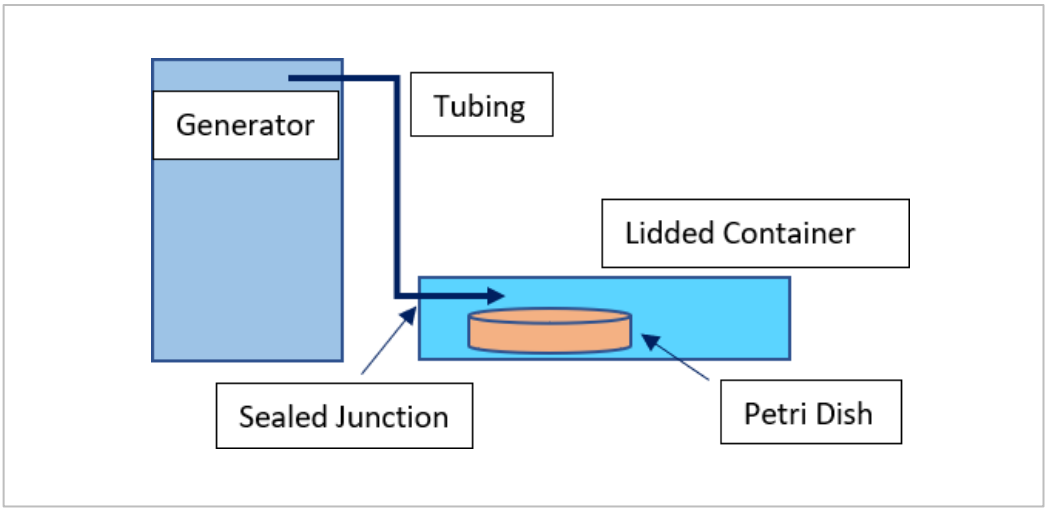

Figure 2.2. Schematic of the oxyhydrogen treatment apparatus depicting the apparatus used to introduce oxyhydrogen into the atmosphere of actively replicating nematodes.

Nematodes were exposed to oxyhydrogen (450 mL/min) for 30 minutes and subsequently incubated for 48 hours before being visually assessed under a microscope at 40 x magnification.

2.2.4.3 Protein Extraction

The protein extraction method used 3 mL of PBS buffer to wash the nematodes from the surface of the agar. 1 mL of liquid was then aliquoted into 1.5 mL centrifuge tubes and centrifuged at 400 x *g* for 3 minutes, forming a pellet of nematodes. The supernatant was removed and disposed of. The nematodes were then washed with 1 mL of PBS, centrifuged at 400 x *g* for 3 minutes and the supernatant removed. Nematodes were treated with either 1 mL of HRW or 1 mL of ddH_2O for 1 hour. The nematode-containing tubes were once again centrifuged at 400 x *g* for 3 minutes. The supernatant was removed and disposed of.

0.5 mL of RIPA buffer with protease inhibitor, was added to the centrifuge tubes, tubes were inverted 5 times and incubated on ice for 5 minutes. The centrifuge tubes were then flash-frozen in liquid nitrogen and partially defrosted before each tube was exposed to three rounds of 10-second sonification using a hand-held cell disruptor inside the tube (Section 2.1.5). The tubes were then thoroughly defrosted and centrifuged at 600 x *g* for 10 minutes.

2.2.4.4 Catalase Assay

The catalase assay is a highly sensitive, simple and direct assay for measuring catalase activity in a variety of biological samples such as cell and tissue lysates or biological fluids The catalase present in the sample reacts with hydrogen peroxide (H_2O_2) to produce water and oxygen. The unconverted H_2O_2 reacts with the catalase enzyme, decreasing the optical density of the solution, which is measured spectrophotometrically at 240 nm, in the ultraviolet spectrum (Hadwan, 2018). Activity is calculated as moles/minutes/mg of cellular suspension

proteins. Molar concentrations are represented by the optical density readings, these values are then divided by time (minutes). The calculated value is again divided by the extinction coefficient of H_2O_2 at 240nm, which is 43.6 M^{-1} cm^{-1} (Zhang *et al.,* 2022).

Using a UV/Vis spectrophotometer, the instrument was blanked using a quartz cuvette (required for the UV wavelength) filled with PBS. To this cuvette, H_2O_2 was added until the absorbance 0.55 - 0.52 was reached. 0.1 mL was extracted from this mixture and discarded. 0.1 mL of nematode lysate was then added to the PBS/H_2O_2 solution and spectrophotometric readings were taken every 10 seconds for 180 seconds.

2.2.5 Cell Culture and Treatment Protocols.

2.2.5.1 Cell Culture Method (Stock Culture).

A 1 mL aliquot of TK6 lymphoblast cells was retrieved from cryogenic storage and defrosted at room temperature for approximately 5 minutes. To 45 mL of RPMI media, 4.5 mL of FBS was added using aseptic techniques. This 'complete' media was placed in a bead bath set at 37^{0}C (5% CO_2). Once heated, 5 mL was transferred into a sterile 50 mL Falcon tube. The 1mL aliquot of cells was transferred into the 50 mL Falcon tube and gently mixed. This solution was then transferred into a T-25 cell culture vial and a further 10 mL of complete media was slowly added. The vial was then placed in the same incubator at 37^{0}C (5% CO_2) for 48 hours.

After 48 hours the culture was removed from incubation and a further 10 mL of complete media was added to the vial, using aseptic techniques. The vial was then replaced in the incubator for a further 72 hours. After this time, an additional 26 mL of warmed complete media was added aseptically to the culture vial. The culture vial was replaced in the incubator for a further 72 hours until experimentation.

2.2.5.1 a Experimental Control

3 x T-25 flasks, each containing 20 mL of complete media were seeded at 1.5 x 10^5 cells per mL. Cells were incubated at 37^{0}C with 5% CO_2.

2.2.5.1 b Acute (single) Treatment

60 mL of non-complete RPMI (- serum) media was infused with oxyhydrogen (300 mL/min of H_2 + 150 mL/min of O_2) gas for 30 minutes H_2. 6 mL of FBS was added post-infusion and 1.5 x 10^5 cells per mL were added to 3 x T-25 flasks (20 mL complete media/flask). Cells were incubated at 37^{0}C with 5% CO_2 and assessed each day at 24, 48 and 72-hour time points. All experiments were performed in triplicate.

2.2.5.1 c Chronic (daily) Treatment

For both control and treatment groups, 20 mL of fresh, respective media *i.e.,* complete media/oxyhydrogen-infused or unadulterated complete media, was added to the culture flask each day. Cells were incubated at 37^0C with 5% CO_2 and assessed at 24 (one infusion), 48 (two infusions) and 72-hour (three infusions) time points.

2.2.5.2 Sterilisation

Aluminium foil-wrapped silicon tubing was autoclaved at 120^0C for 15 minutes and then placed in a drying rack for >1 hour.

The diffusion stone was placed in 100 mL of 70% ethanol inside the biological safety cabinet (Figure 2.3 A-C), ensuring the diffusion stone was fully submersed in ethanol, the HydroVitality™ oxyhydrogen generator was cycled for 2 minutes. With clean, gloved hands, the diffusion stone was removed from the tubing, wrapped with plastic film within the safety cabinet and stored alongside the tubing in an airtight container. All further processes were completed in a sterile environment, using aseptic techniques.

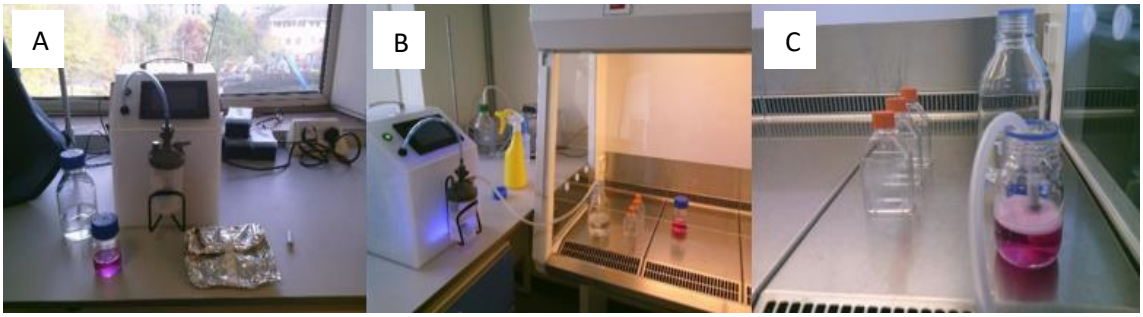

Figure 2.3. Photographs of sterilisation and infusion methods. From left to right: (A) Identifies the equipment needed for sterilisation and infusion (100mL ethanol; 60mL Roswell Park Memorial Institute 1640 (RPMI) cell culture medium; HydroVitality™ oxyhydrogen generator; 6mM silicon tubing (in foil) and 0.5-micron diffusion stone). (B) Shows how the equipment was sterilised. (C) Infusion of cell media.

2.2.5.3 Oxyhydrogen Infusion

All equipment was thoroughly sterilised with 70% ethanol before aqueous infusions. To assess whether the infusion of oxyhydrogen into cell culture media would have any effects on the viability and proliferation of TK6 cells 60 mL of RPMI media was infused in glass 150 mL Duran bottles for 30 minutes using the HydroVitality™ oxyhydrogen generator (450 mL/min of oxyhydrogen). To increase the pressure and improve the infusion of oxyhydrogen into the media the HydroVitality™ device was connected to a 0.5-micron stainless steel diffusion stone via 6 mM silicon tubing (Figure 2.3 (C)). 10% foetal bovine serum (FBS) was added post-infusion. As antibiotics can affect both gene expression and regulation (Ryu *et al.,* 2017), no antibiotic substances were added.

2.2.5.4 H_2 Gas Infusion

Experiments and data generated by MSc student Georgia Mannings under my supervision (Grace Russell). Infusion required bubbling H_2 gas through sterile tubing, without a diffusion stone, for 30 minutes into cell media.

2.2.5.5 Cell Counting: Acute and Chronic Treatments

Cells were gently agitated by hand before 1 mL was removed from the flask and added to a sterile centrifuge tube. The tubes were then centrifuged at 400 x *g* for 5 minutes, forming a pellet of cells in the bottom of the tube. 20 µL of pelleted cells were removed and transferred into a 96- well plate. 20 µL of Trypan Blue was added to the well and mixed well using the motion of the pipette. 10 µL of this mixture was pipetted onto a glass haemocytometer and cell numeration and viability were assessed using automated devices and software (Section 2.1.7).

2.2.5.6 Mitogen Determination

Prior to exposing TK6 cells to mitogens, a comparison between mitogen activity was conducted. To test whether the repressive effect of oxyhydrogen would continue under mitogen stimulation, primary B-cell (Pokeweed (PWM)), T-cell (Concanavalin A (ConA), Phytohemagglutinin (PHA)) and non-specific mitogen, lipopolysaccharide (LPS), were tested for their efficacy in promoting TK6 cell proliferation (Chapter 6, Section 6.5.3).

2.2.5.6 a Concanavalin A

ConA is a standard lymphocyte mitogen used to enhance the proliferation of lymphocytes *in vitro* (Paetkau *et al.,* 1976). Cells were seeded in the same quantities and conditions as the control set. Adapted from Yang *et al*. (2020a), 1 mg of ConA was dissolved in 1 mL of RPMI media. Aliquots of 0.33 mL were added to 20 mL of media in the flasks giving a final concentration of 0.016 mg/mL (16 µg/mL) per flask. Cells were seeded in the same quantities (1.5 x 10^5/mL) and incubated for 24 hours under the same conditions (37^0C/5% CO_2). 2 x repeats were performed.

2.2.5.6 b Lipopolysaccharide

LPS is a bacterial toxin, found in the outer membrane of gram-negative bacteria, which acts as a general, non-specific mitogen (Ziegler-Heitbrock, 1995). Adapted from Alzahrani *et al*. (2022), 5 mg of LPS was dissolved in 1 mL of media. Aliquots of 0.33 mL were added to 20 mL of cell media, giving 80 µg/mL per flask. Cells were seeded in the same quantities (1.5 x 10^5/mL) and incubated for 24 hours under the same conditions (37^0C/5% CO_2). 2 x repeats were performed.

2.2.5.6 c Phytohemagglutinin

PHA is a toxic, sugar-binding, lectin commonly extracted from the red kidney bean (*Phaseolus vulgaris)* and a potent T-cell stimulatory mitogen (Nowell, 1960). Adapted from Maotoana, Burt and Goedhals (2023), 1 mg of PHA was dissolved in 1 mL of media. Aliquots of 0.33 mL were added to 20 mL of cell media, giving 16 µg/mL per flask. Cells were seeded in the same quantities and incubated for 24 hours under the same conditions. 2 x repeats were performed.

2.2.5.6 d Pokeweed Mitogen

PWM is a B-cell-specific mitogen (Mellstedt, 1975). Adapted from experiments conducted by Portugal (2022), 1 mg of PWM was dissolved in 1 mL of media. Aliquots of 0.33 mL were added to 20 mL of cell media, giving 16 µg/mL per flask. Cells were seeded in the same quantities and incubated for 24 hours under the same conditions. 2 x repeats were performed.

2.2.5.7 Flow Cytometry

Flow cytometry was conducted according to the protocol devised by Riccardi and Nicoletti (2006). Briefly, 1 mL cell suspension was removed from each culture flask and transferred into 1.5 mL centrifuge tubes. Cells were centrifuged at 400 x *g* for 5 minutes. Approximately 200,000 cells were counted and the corresponding volume for each culture was subsequently transferred to centrifuge tubes and centrifuged at 400 x *g* for 5 minutes at 4°C. The supernatant was removed and 200 µL of ice-cold PBS was added to each tube. Each cell suspension was transferred to cryovials. 1 mL of ice-cold 80% ethanol was slowly added to each cryovial whilst being vortexed. Samples were left in ice for 10 minutes to fix and stored at -20°C for 24 hours.

On the day of analysis, the samples were warmed to room temperature (20°C ± 2°C) and 1 mL of PBS was added to the cells. Cells were then centrifuged at 600 x *g* for 5 minutes and the supernatant was removed. Each sample was resuspended in 478.5 µl of PBS along with 1.5 µl RNase A. This was incubated at room temperature for one hour. After incubation, 20 µL of propidium iodide stain (50 µg /1 mL (PBS)) was added to each sample and the centrifuge tubes were covered in foil to prevent light access. Flow cytometry was conducted using the BD Accuri™ C6 Plus flow cytometer.

2.2.6 Statistical Analysis

Unless otherwise stated, all data is reported as the mean (n = 3) and the standard error of the mean (mean ± SEM). Statistical analysis was performed using Microsoft Excel™ (2023) software. A paired two-sample t-test assuming equal variance, or analysis of variance (ANOVA) was conducted to determine statistically significant differences between groups.

Post hoc analysis was accomplished using the Tukey-Kramer protocol. Statistically significant data was defined as $p < 0.05$.

Chapter 3: Investigating Hydrogenase Enzymes and Whether Orthologs are found in the Human Proteome.

3.1 Introduction

When considering the volatile chemistry of the Hadean Earth, *circa* 4 billion years ago, it is plausible that the first membrane was formed, not from organic materials, but through the formation of minerals such as mackinawite (Fe[Ni]S) (Lane, 2010; White *et al.,* 2015; Russell and Ponce, 2020). During this period, the Earth's surface was characterised by intense volcanic activity, high temperatures, and a chemically volatile environment. Organic molecules, as we know them today, were not abundant, making it unlikely that the first membranes were composed of organic lipids (Lane 2010). Such semi-permeable, inorganic, proto-membranes can be formed in the vicinity of submarine alkaline hydrothermal vents, where reductive electron-rich volcanic detritus becomes exposed to the acidic, proton-rich oceanic waters, a scenario that potentially provided the chemical disequilibrium and minerals required for organic life (Duval *et al.,* 2021). H_2 and CO_2 are also necessary for the genesis of biological compounds with Preiner *et al*. (2019), suggesting that minerals such as mackinawite and magnetite would perform the role of prebiotic hydrogenases, facilitating organic reactions.

The generation of energy using the chemiosmotic proton gradient ($\Delta\mathfrak{f}$ (protonmotive force) = $\Delta\Psi$ (membrane potential) + ΔpH (proton gradient)) is essential to organic evolution, and is employed across all domains of life (Koch and Schmidt 1991; Lane, 2010; Matreux *et al.,* 2023), with prokaryotes utilising the plasma membrane to create a chemiosmotic gradient. On the other hand, in eukaryotes, the inner membranes of chloroplast and mitochondria provides the selective barrier for a proton gradient to form (Lane, 2010). As biological membranes do not contain the redox reactive minerals necessary for electron transportation in their conformation, accessory proteins that retain metallic clusters are typically embedded in the phospholipid bi-layers. To illustrate, iron-sulphur complexes are found within a multitude of catalytic enzymes, and due to the wide range of redox potential ($^{+}5.0$(2Fe-2S) - $^{-}0.7$(4Fe-4S) V), (Thomson, 1977; Jafari *et al.,* 2022) are frequently utilised in proteins which facilitate electron transportation (*i.e.,* (de)hydrogenases, ferredoxins, *etc*.).

From an evolutionary standpoint, it is highly likely that the dissociation of H_2, ($H_2 \rightarrow 2H^+ + 2e^-$) was a basal function, providing electrons (e^-) and protons (H^+) for such primitive cellular functions as energy production, the formation of reactive signalling molecules, and transportation of inorganic ions across membranes (*e.g.,* K^+, Na^+, Li^+). For example, NADH/ubiquinone oxidoreductase, or Complex I, of the ETC, is the first protein cluster of the

OXPHOS cascade. With each transitional step, the energy of the electrons is utilised until they are transferred to ubiquinone, reducing the substrate to ubiquinol, an endogenous antioxidant (Niki, 1997; Gvozdjáková *et al*., 2020; Cirilli *et al*., 2021), (Figure 3.1).

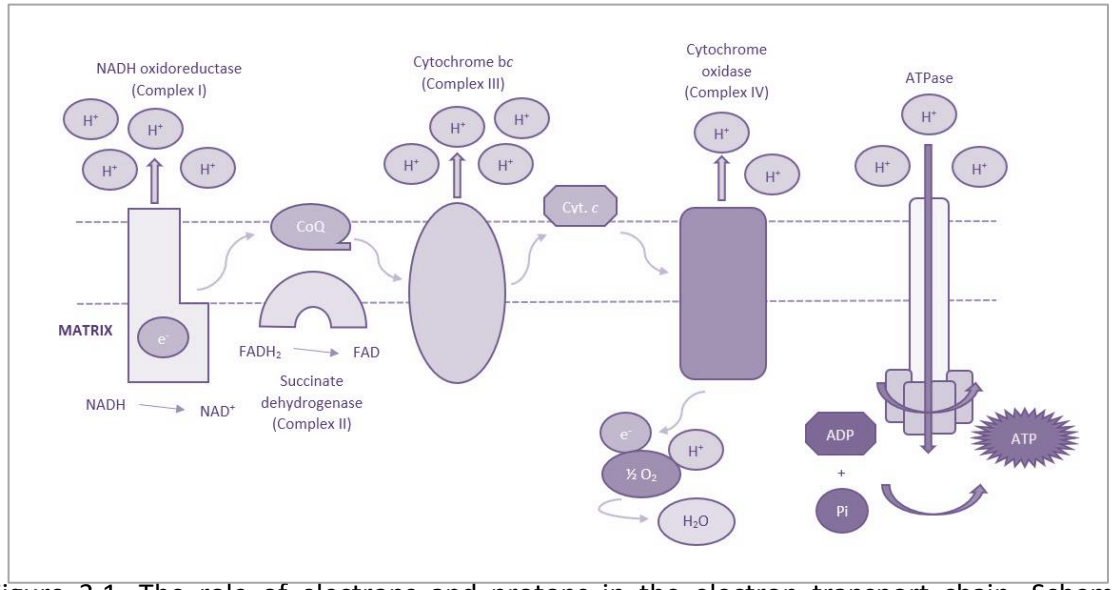

Figure 3.1. The role of electrons and protons in the electron transport chain. Schematic representation of the ETC. Orange: Electrons are abstracted from NADH/FADH and carried through the chain by cofactors ubiquinone (CoQ) and cytochrome *c*. Pale Blue: Protons are pumped across the membrane by Complexes I, III and IV.

3.2 Evolution of the Eukaryotic Cell

The evolution of the eukaryotic lineage is a highly contentious subject that spirits much debate amongst academics (Searcy, 1992; Martin and Müller, 1998; Abhishek *et al.,* 2011; Spang *et al.,* 2019; Imachi *et al.,* 2020). Contemporary thinking reveals five main theories of cellular evolution, i) The H_2 hypothesis, ii) Reverse flow, iii) Engulf, Entangle, Endogenize (E^3), iv) Searcy's model, and v) Syntrophy, detailed in Figure 3.2

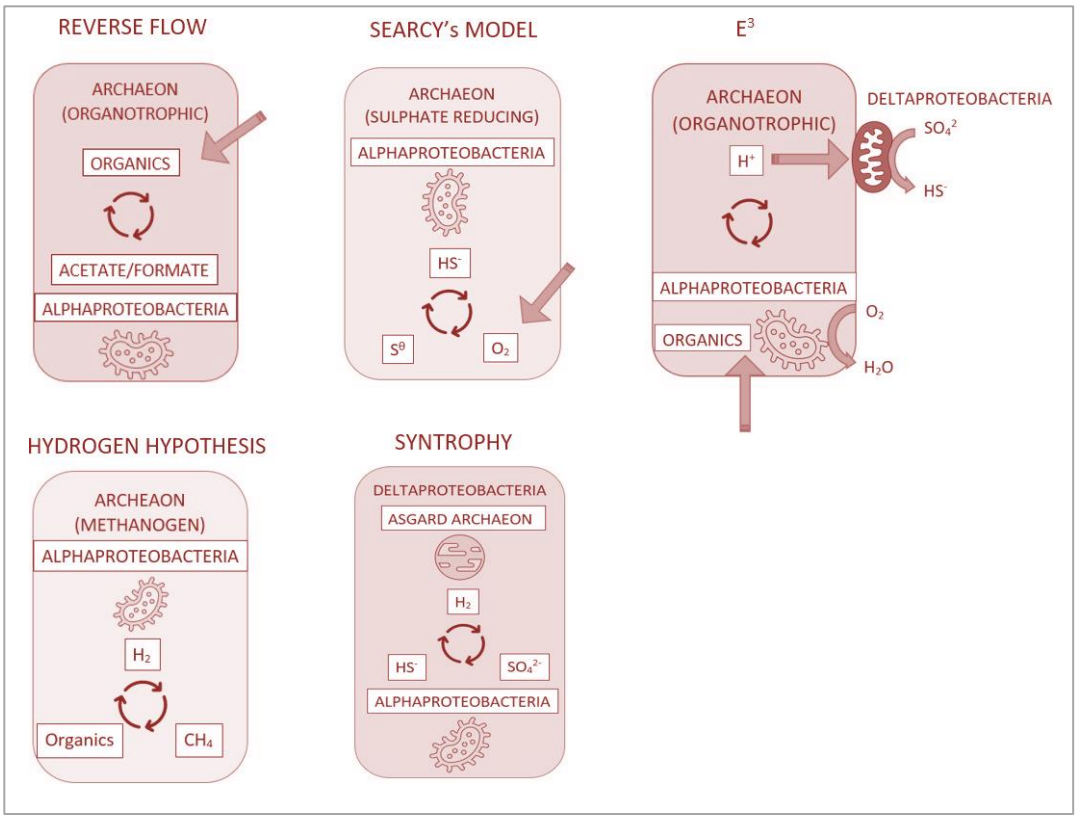

Figure 3.2. Graphical depiction of possible symbiotic relationships giving rise to the eukaryotic cell.

The original H_2 hypothesis suggests that a methane-producing archaeon host engulfed an H_2-producing alphaproteobacterium (class of bacteria in the phylum Pseudomonadota) (Garrity et al., 2004), utilising the supply of H_2 to reduce CO_2, also released by the bacterium as a metabolic by-product (Martin and Müller, 1998). The original H_2 evolution theory has been recently adapted to account for the newly discovered clade of archaeon (named after the mythological domicile of the Norse gods, Asgard), with the authors (Sousa *et al*., 2016) revising the origin of the host from a methanogen to an autotrophic archaeon utilising alphaproteobacterial generated H_2 in the Wood-Ljungdahl carbon fixation pathway. The Reverse Flow model of evolution developed by Spang *et al.* (2019), suggests that a syntrophic affiliation existed between an archaeal host and an alphaproteobacterium, one that relied on reducing equivalents such as H_2, or perhaps acetate or formate, being delivered from an aerobic archaeota to a facultatively aerobic alphaproteobacterium (Spang *et al*., 2019). The E^3 hypothesis describes a metabolic relationship between an Asgard archaeon and two symbionts, an internalised alphaproteobacterium that is likely to have evolved into the mitochondria and a sulphur- reducing deltaproteobacterium whose symbiosis it is postulated was either never completed, transient, or lost in the depths of evolutionary time (Imachi *et al.,* 2020). Searcy's model of eukaryogenesis first postulated in 1992 (Searcy, 1992), advocates for a syntrophic relationship between a wall-less archaeon such as *Thermoplasma spp*. and

a hydrogen sulphide (H_2S) metabolising bacterium. Lastly, the Syntrophy theory proposes an interdependent metabolic mutualism between a sulphate-reducing deltaproteobacterial host, an organotrophic, H_2- releasing Asgard archaeon, and a facultatively aerobic, sulphide oxidising, alphaproteobacterium. Of these pre-eminent theorems, the Syntrophy theorem places the requirement for H_2 at the center of the theory and provides the basis for further discussion (Chapter 3, Section 3.5).

3.2 The Ubiquity of Hydrogenase Enzymes

As the Earth's early atmosphere was likely composed of such reducing gases as CO, H_2 and CH_4, it has been surmised that the ability to utilise iron- (Fe) induced catalysis of H_2, as a means of supplying electrons and protons used for energy production, evolved billions of years ago (Piché-Choquette and Constant, 2019). Therefore, from an evolutionary standpoint, H_2 is likely to be one of the first reducing agents exploited in early forms of energy metabolism.

Hydrogenase enzymes are responsible for catalysing the reversible oxidation/reduction of H_2 (H_2 <--> $2H^+ + e^-$). Such enzymes are found in all single-celled and many multicellular organisms (*e.g.,* plants: *Arabidopsis thaliana* (AtNar1). Accession number: NM_117739) (Russell, Zulfiqar and Hancock, 2020), and can be categorised into specific phylogenic groups, namely iron only, iron-iron and nickel-iron (Fe, Fe-Fe and NiFe, accordingly) (Greening *et al.,* 2016; Piché-Choquette and Constant, 2019). Of these distinct groups, the NiFe hydrogenases are the most commonly occurring, being present in a wide range of bacteria and plants. NiFe hydrogenases can be further divided into four classes, i) the membrane-bound hydrogenases; ii) N_2-fixing cytoplasmic hydrogenases; iii) cytoplasmic hydrogenases that use 8-hydroxy-5-deazaflavin (F420) as a low-potential redox co-factor, and iv) the O_2-sensitive, membrane-bound, energy converting hydrogenases.

Of these subgroups, the membrane-bound, group iv, hydrogenases most resemble the activity of mitochondrial Complex I (Marreiros *et al*., 2013; Read *et al.,* 2021) and as a result, this group is of particular interest here. All characterised NiFe hydrogenases comprise a large subunit containing the NiFe active H_2 deprotonation site and a smaller substructure responsible for housing up to nine FeS clusters (Figure 3.3) (Vaissier and Van Hooris, 2017).

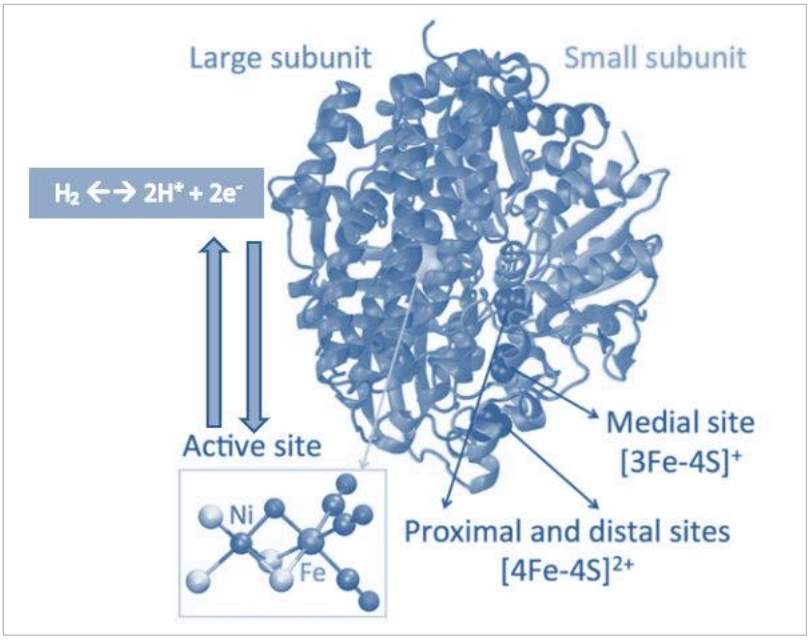

Figure 3.3. The crystalline structure of NiFe Hydrogenase (*Desulfovibrio fructosivorans* - 1YRQ). Image adapted from original by Vaissier and Van Voorhis (2017) (copyright permission given by Van Voorhis (28/12/23)). The NiFe hydrogenase heterodimer with two unique subunits: Blue – Large subunit containing the NiFe active site. Pink – Small subunit with three iron–sulphur clusters channelling electrons to the active site.

3.3 NADH/Ubiquinone Oxidoreductase/Dehydrogenase: Complex I

Complex I (Figure 3.4) is the largest enzyme in the ETC, and has conserved homologues across all domains of life (Friedrich and Scheide, 2000; Vercellino and Sazanov, 2022).

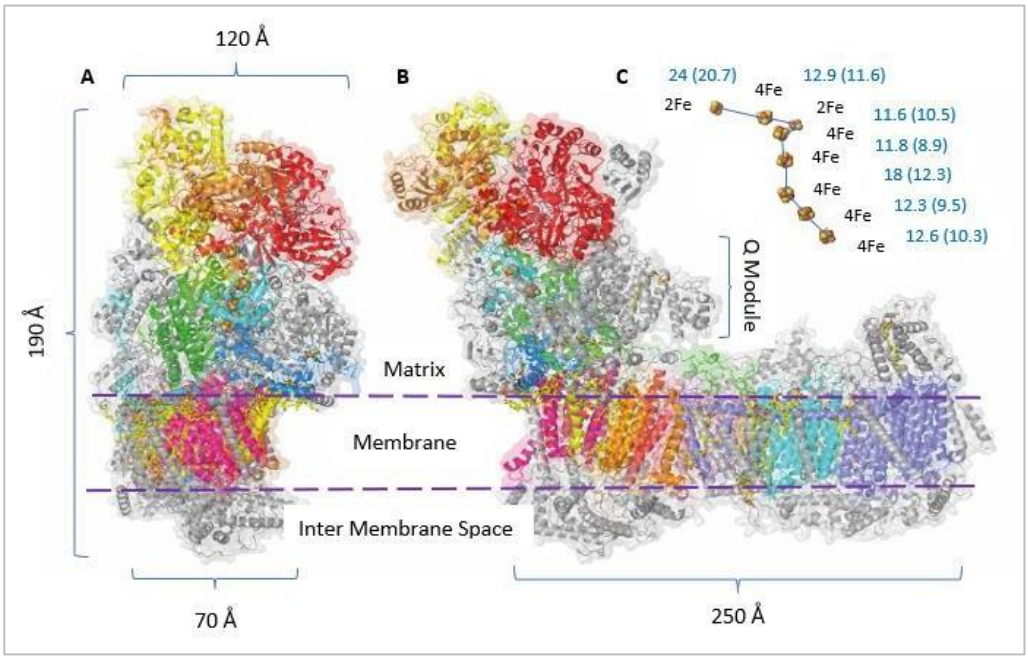

Figure 3.4. Structure and arrangement of mitochondrial Complex I (*Yarrowia lipolytica*). Image Credit – Zickermann *et al.* (2015) (copyright permission given by Zickermann (03/01/2024)). (A) Aspect from the peripheral arm. (B) Aspect rotated 90° to include membrane-bound

subunits. (C) Arrangement of 4Fe-4S(4Fe) and 2Fe-2S(2Fe) clusters in the peripheral arm. Centre-to-centre and edge-to-edge distances (in brackets) are in angstroms.

Due to its near-constant redox activity, and abundant provision of electrons, Complex I is a prominent source of the cardinal reactive oxygen species $O_2^{\bullet-}$ within the mitochondria. There are conceivably two sites where O_2 can access electrons donated by the NADH co-factor, i) at the flavin mononucleotide module, and ii) at the ubiquinone binding site. Bazil *et al.* (2014), identified through *in silico* modelling that the FMN module is the putative site for H_2O_2 production. The authors further adduce that ROS production at the FMN is stimulated by the absence of ubiquinone at the ubiquinone/Complex I interface (Bazil *et al*., 2014). In this configuration, the intraprotein channel through which ubiquinone travels to the docking site (Zickermann *et al.,* 2015), becomes accessible to O_2, exposing O_2 to a region where electrons are concentrated and the potential for reduction to ROS is heightened. Furthermore, the incomplete reduction of ubiquinone at the Q module leads to the production of semiquinone (Gvozdjakova et al., 2020), a negatively charged ion, intermediary, and radical compound. With the redox midpoint potential of the ubiquinone/semiquinone couple (-0.163 V) (Kishi *et al.,* 2017) being similar to the midpoint potential of the oxygen/superoxide couple (-0.16 V) (Wood, 1988), it is reasonable to assume that semiquinones are also able to significantly contribute to $O_2^{\bullet-}$ formation within this domain.

3.4 The Ubiquinone Binding Domain of Complex I

The ubiquinone binding domain of Complex I is predominantly formed of four interdependent protein subunits. In humans, these are mitochondrial-encoded NADH dehydrogenase subunits (*e.g.,* ND1 and ND3), and nuclear-encoded NADH dehydrogenase (ubiquinone) iron-sulphur proteins (*e.g.,* NDUFS2 and NDUFS7). ND1 and ND3 are situated in the membrane section of Complex I, which are homologous with bacterial antiporters (Fiedorczuk and Sazanov, 2018), whilst the nuclear-encoded genes form part of the peripheral arm within the matrix and are reported to have homologues in NiFe hydrogenase enzymes (Friedrich and Scheide, 2000; Vignais and Billoud, 2007; Kampjut and Sazanov, 2022), leading to the continuing theory that the progenitor of Complex I was formed through the ligation of a soluble hydrogenase with proton pumping membrane-bound antiporters (Volbeda and Fontecilla-Camps, 2012; Yu *et al*., 2021).

Using 3.6 Å resolution crystal structuring, Zickermann *et al.* (2015), identified that the matrix-facing α-helices of ND1 are interconnected with NDUFS2, NDUFS7 and ND3, constructing a passage through which ubiquinone travels to the docking site (Zickermann *et al.,* 2015). The ubiquinone/Complex I interface lies within this channel (Kaila, 2018). Further data, collated through various analyses (*e.g.,* biochemical, cryogenic electron microscopy (cryo-EM),

genetic), highlights that ubiquinone reduction occurs at unspecified regions of the NDUFS2 and NDUFS7 units, whilst ND1 and ND3 units form the primary channel structure (Parey *et al.,* 2018). However, other reports infer that ND1 may also have a role in the reduction of ubiquinone (Kurki *et al*., 2000). Therefore, the region of specific enzymatic activity within the ubiquinone module has not been conclusively delineated, although several reports illustrate the likelihood of the nuclear-encoded NDUFS2 and the (N2) Fe-S-containing NDUFS7 subunits as the primary centres for redox activity (Grgic *et al.,* 2004; Kampjut and Sazanov, 2020).

3.5 Bioinformatic Enquiry

To better understand the possible evolutionary relationship between hydrogenases and the functional subunits of Complex I, this enquiry focuses on three microorganisms purportedly involved in the syntrophic hypothesis of evolution, namely a deltaproteobacterium (*Desulfovibrio carbinolicus*), an Asgard archaeon (*Candidatus heimdallarchaeota*) and an alphaproteobacterium (*Rhodobacter sphaeroides*). The membrane-bound hydrogenases (Mbh) included here are i) *C. heimdallarchaeota*, MbhJ (Uniprot# A0A1Q9PFW3) and MbhL (Uniprot# A0A1Q9PFM5), ii) *D. carbinolicus,* unnamed hydrogenase with subunit chains of 494 (Uniprot# A0A4P6HTH3) and 258 (Uniprot# A0A4P61469) amino acids, identified herein as Hyd494 and Hyd258, respectively, and iii) *R. sphaeroides* HupL (Uniprot# Q3J0L7), HupS (Uniprot# 086467), HupU (Uniprot# O86466) and HupV (Uniprot# Q3J0M0).

To assess whether the hydrogenase proteins of interest retained homology within the human proteome an initial basic local alignment search tool (BLAST) of the NiFe hydrogenase enzyme sequences of all three species was applied. This analysis identified >20% sequence homology with NDUFS2 and NDUFS7 of mitochondrial Complex I. A bioinformatic matrix analysis, identifying regions of similarity between Complex I subunits and NiFe hydrogenases, was also conducted (Figures 3.7 and 3.11). Prokaryotic sequences displaying similarities with the human proteins NDUFS2 and NDUFS7 were then aligned and analysed using the Clustal Ω programme, Figures 3.8 - 3.10 and Figures 3.12 - 3.14, accordingly.

3.5.1 The Active Site of NiFe Hydrogenase

A region of interest for the comparison of subunits of Complex I and NiFe hydrogenases is the active site that reduces/oxidises H_2. Although academic debate surrounding the precise mechanism of the NiFe active site is ongoing, the consensus is that two metal ions, or the cofactor methylenetetrahydromethanopterin (for the Fe-only hydrogenase), are needed for effectively catalysing H_2 oxidation/reduction (Tard and Pickett, 2009; Ash, Kendall-Price and Vincent, 2019). Shafaat *et al.* (2013), suggest that as H_2 shares affinity with the low-spin state of the d^6 iron transition metal, the Fe^{2+} ion is responsible for binding H_2, whilst the $Ni^{2+/3+}$ ion

cleaves the molecule, abstracting the protons and leaving metal-bound hydrides (H^-) which may have reductive/antioxidant potential (Figure 3.5).

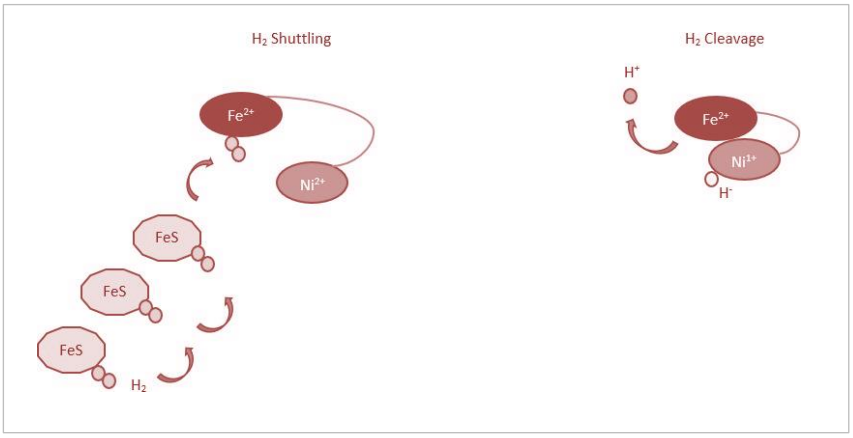

Figure 3.5. The hypothesised activity of the NiFe hydrogenase. Schematic diagram of the proposed mechanism of H_2 cleavage. Left: Shuttling of H_2 via FeS clusters to Fe^{2+}. Right: Cleavage of H_2 and retention of hydride. Note: Ni^{2+} is altered to Ni^{1+}, post cleavage.

BLASTP analysis of NDUFS2 identifies this subunit as being most comparable with the large membrane-bound subunits of NiFe hydrogenases, responsible for H2 catalytic activity. To examine whether these sites are well-conserved in NDUFS2 an alignment between the active sites of the enzymes of interest and NDUFS2 was applied (Figure 3.6)

```
NDUFS2    GLLHRGTEKLIEYKTYLQALPYFDRLDYVSMMCNEQAYSLAVEKLLNIRP--PPRAQWIR    171
HupL(Rs)  GTMWRGLEVILKGRDPRDAWAFTERICGVCTGTHALTSVRAVEDALGISI--PDNANSIR    105
HupV(Rs)  APLYRGFERMLEGRDPRDALTITPRICGICSISQSVAAARALGAAMGLAP--APAGERVA    91
MbhL(Ch)  GFNLRGIEKAMENRTWRQNTMLVPRACGICSAVHQNVYVRVVEKLAGVEDQISERARLIR    117
494 (Dc)  GFQHRGIEARLIGGPDKRTIHFMETLAGDTTIGHSLAHAALVEALT--ETAVPARGRAIA    228

          .   ** *  :                    :  .    :           .. :
```

Figure 3.6. Alignment of the hydrogenase active site sequences with NDUFS2. Sequence alignment of the NiFe hydrogenase active sites with mitochondrial subunit NDUFS2 (human). Coloured section: Yellow represents the non-aligned regions of the active site. Blue indicates conserved redox-active residues. Pink indicates conserved non-redox active residues. Grey indicates non-conserved, yet redox-active, substitute residues. Red highlights tyrosine151. Boxed area identifies the well-conserved region across the species of interest.

The data in Figure 3.6 identifies little homology between the active sites of the hydrogenases considered here and NDUFS2. Nevertheless, key redox active residues within the hydrogenases are conserved, implying retained form and function in this key area of enzyme activity. Perhaps of some pertinence is the -RGXE- motif of the active site which is retained through all of the proteins sequenced and may signify a distant evolutionary relationship between NDUFS2 and the large subunits of NiFe hydrogenases. The conserved glutamic acid residue (glutamic acid 119 –NDUFS2)

is of particular interest as it may be pertinent to proton transference (Ash, Kendall-Price and Vincent, 2019).

The conservation of the amino acid tyrosine 151 between NDUFS2 and MbhL of *C. heimdallarchaeota* (tyrosine 95) is of further intrigue. A crystal structure analysis of NDUFS2, conducted by Kampjut and Sazanov (2020), demonstrates that the ubiquinone molecule docks within 4.5 Å of tyrosine 108 of the ovine NDUFS2 module (corresponding with the human equivalent tyrosine 151), and is therefore of interest as a potential site for H_2 action. The structural analysis also identifies histidine 59 and asparagine 160 (ovine), corresponding to histidine 112 and asparagine 182 (human), as having proton translocation potential. It is suggested that a proton shuttling mechanism between this triad of residues would create a negative charge, enhancing ubiquinone binding potential and lowering the redox potential of the N2 FeS cluster, permitting reverse electron transfer (Kampjut and Sazanov, 2020).

The configuration between the N2-containing NDUFS7 subunit and the proton-transferring NDUFS2 indicates this region of the ubiquinone binding module is likely to be responsible for electron transfer. If the H_2 molecule were to prevent the binding of mitochondrial inhibitors such as rotenone from binding to the Fe-S clusters, or autoxidation of redox-active thiols, this could preserve the form and function, thereby reducing electron leakage and the subsequent formation of ROS which would have significant downstream cellular effects. Should this be the case, and considering it is highly unlikely the subunits of Complex I retain the potential for H_2 catalysis due to loss of the di-metal, redox-active centres; could H_2 have another role in supporting the function of the ubiquinone binding module, protecting the conserved functional sites from oxidation or reducing the formation of ROS?

3.5.2 NDUFS2 (49kDa)

In alignment with previous findings (Read *et al.,* 2021), BLASTP analysis identifies NDUFS2 to be most similar to the large membrane-bound subunits of NiFe hydrogenases, responsible for hydrogenase activity. To gain a better understanding as to whether other regions of NiFe hydrogenases are likely to be replicated in NDUFS2 a similarity matrix, referred to as a dot plot analysis, of sequence homologic similarities was created (Figure 3.7).

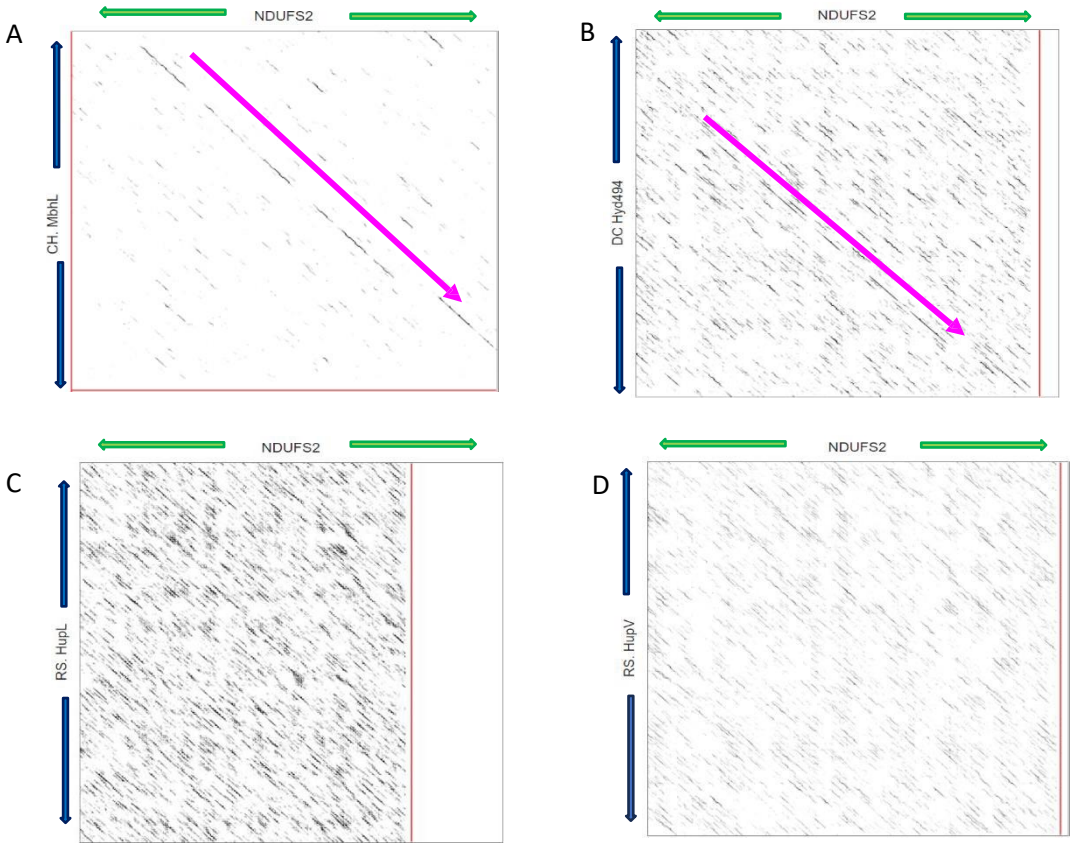

Figure 3.7. Similarity matrix analyses of NDUFS2 and hydrogenases. Dot plot analysis of the NDUFS2 protein (463aa) sequence - X-axis, Green arrows indicate sequence direction. Hydrogenases of interest – Y-axis, Blue arrows indicate sequence direction. Clear alignment indicates areas of homology. (A) *C. heimdallarchaeota* MbhL B (418aa); (B) *D. carbinolicus* Hyd494 (494aa); (C) *R. sphaeroides* HupL (596aa); (D) *R. sphaeroides* HupV (475aa). The horizontal red line indicates a shorter amino acid sequence (NDUFS2). The vertical red line indicates a shorter amino acid sequence of hydrogenases. Regions of interest are marked in Figures 3.7 (A-D) by a pink arrow.

Image 3.7 (A) identifies a closer similarity between NDUFS2 and the MbhL protein of *C. heimdallarchaeota* as described by a clear diagonal pattern. Image 3.7 (B) identifies some similarities between NDUFS2 and the large NiFe hydrogenase subunit of *D. carbinolicus* (Hyd494). Both images 3.7 (C/D), derived from *R. sphaeroides* sequences HupL and HupV, respectively, show little homology with NDUFS2.

Delving into the sequence similarities, Wirth *et al.* (2016), have suggested likely redox functionality within the β1-β2 helices of NDUFS2 at positions 88-96 (human), showing the **-HPXAHXVLR-** arrangement. Histidine 88 and histidine 92 of the short sequence **-HPXAHXVLR-** are noted to be situated in close proximity with both ubiquinol and the terminal 4Fe-4S cluster (N2) of NDUFS7 which may provide the redox sensitivity required for electron translocation to ubiquinone.

Alignment evidence, Figures 3.8, 3.9 and 3.10 also describe conserved homology immediately preceding the **-HPXAHXVLR-** motif. Interestingly, the **-GPQHPXA-** sequence, positions 85-91 (human), not only contains the histidine 88 residue but has two redox-active proline residues, positions 86 and 89 that are in close proximity to histidine 88, a factor that may be significant for redox-specific chemistry and reticent of hydrogenase functionality. Further along the sequence at positions 228-232, lies another conserved motif, **-RPGGV-**, which although it has not been identified as a site for protein modification, is well conserved throughout the hydrogenases considered here and may be integral to the protein structure and therefore function.

An investigation into the predicted sites of post-translational protein modifications including *N*-glycosylation, *N*-myristoylation and phosphorylation sites, using ScanProsite (www.Expasy.org), noted little-to-no homology within regions of interest between NDUFS2 and the NiFe hydrogenases of the prokaryotes studied. However, should H_2 have a role in preventing the oxidation of such functional moieties, it could optimise protein structure and performance, and reduce electron leakage, thereby reducing, or preventing, the reduction of oxygen to superoxide (O_2 → $O_2^{\bullet-}$) and subsequent downstream ROS generation, a factor that would be highly advantageous for maintaining cellular redox homeostasis.

3.5.2.1. *Candidatus heimdallarchaeon* - NDUFS2

With 27% sequence identity, the homology between the human protein NDUFS2 and the large MbhL subunit of *C. heimdallarchaeon* hydrogenase is higher than that between NDUFS2 and Hyd494 of *D. carbinolicus* (23%) and *R. Sphaeroides* (<20%).

```
NDUFS2      WKPPPWNDVDPPKDTIVKNITLNFGPQHPAAHGVLRLVMELSGEMVRKCDPHIGLLHRGT  120
MbhL        YRSRFRTLTDGSDSPPGADHHIFIGPQHPWAEEPAHFIIHLKGERVVEADIRIGFNLRGI  64
            ::    . .*  ..    :  : :***** *.   ::::.*.** * :.* :**:  **


NDUFS2      RLLNHIMAVTTHALDLGAMTPFFWLFEEREKMFEFYERVSGARMHAAYIRPGGVHQDLPL  238
MbhL        RVHSHILWYGILAHDAGFDTMLHISWRDREIIMDIVEDFSGNRVNPALMLPGGVKRDIPK  184
            *.  **.     * * *  * .   . .** .... *  ** *.. * . ****..*.*
```

Figure 3.8. A short section of the Clustal alignment between human NDUFS2 and C. heimdallarchaeon MbhL hydrogenase protein (large subunit). Alignment of human NDUFS2 sections 60-120 and 178-238, and Candidatus heimdallarchaeon hydrogenase (MbhL). Blue/green highlights indicate conserved motifs of interest -GPQHP-. Histidine 88 is bold and underlined. Green/yellow highlights the -HPXAHXVLR- motif. Grey highlights the -RPGGV- motif. Yellow/grey indicates non-conserved moiety.

Of the prominent **-GPQHP-** and **-RPGGV-** motifs shared by NDUFS2 and the MbhL protein, the **-GPQHP-** group is well conserved, which may imply this region has retained redox functionality, and that histidine 88 and/or prolines 86 and 89, could be key amino acids in the partial-to-full reduction of ubiquinone. Contrariwise, the only redox active residue of the **-RPGGV-**, arginine 228, is not conserved, prompting the assumption that this particular region is unlikely to be significant for redox activity, although whether this motif is of structural importance, or could be affected by H_2, has yet to be delineated.

3.5.2.2. *Desulfovibrio carbinolicus* - NDUFS2

The 23% similarity between NDUFS2 and *D. carbinolicus* Hyd494 can be considered to be low and therefore unlikely to have homologues in the human genome (Anderson and Brass, 1998). Although, perhaps importantly, considering the proximity of histidine 88 to the N2 FeS cluster, the histidine residue of the **- GPXHP-** sequence is conserved along with proximal moiety, proline 86 (Figure 3.9). As NDUFS2 is mooted to be a key oxygen-sensing module and a regulator of Complex I activity (Dunham-Snary *et al.,* 2019), these residues may be of pertinence as sites of H_2 activity, with H_2 perhaps protecting such sites from autoxidation and facilitating optimal protein function.

```
NDU2        -------D-PPKDTIVKNI--------TLNFGPQHPAAHGVLRLVMELSGEMVRKCDPHI 113
Hyd494      GCPARPEEPRPAPGVTDHFRLRGEEAHEVAVGPVHAGIIEPGHFRFQCSGEDVYHLEISL 170
                   :  *   :..::         : .** * .     :: :: *** * : :  :


NDUFS2      FGEITRLLNHIMAVTTHALDLGAMTPFFWLFEEREKMFEFYERVSGARMHAAYIRPGGVH 233
Hyd494      ALELERLANHTGDLGAMAGDVGYQPTMAYCGRIRGDFLNLTGLVCGNRFGRGLVRPGGVA 290
              *: ** **   : : * *:*    : :  . * .::::   *.* *:  . :*****
```

Figure 3.9. Alignment of human NDUFS2 section 174-233 and *Desulfovibrio carbinolicus* hydrogenase Hyd494A. Blue highlights indicate conserved motifs of interest. Histidine 88 and proline 86 are bold and underlined. Yellow highlights the - HXXAHXVLR- motif. Grey highlights the -RPGGV- motif.

Further analysis of the **-RPGGV-** motif identifies sequence similarities, with both of the redox active amino acids, arginine 228 and proline 229, being fully conserved. However, whether these residues are significant for electron translocation, or a potential target for H_2, is still unclear and crystallographic analysis of these structures would be beneficial.

3.5.2.3 *Rhodobacter sphaeroides* – NDUFS2

The BLASTP search of comparable sequence identities (Figure 3.10) did not result in a positive match above 20% similarity. Alignment of NDUFS2 with the larger uptake hydrogenases (HupL

and HupV) of alphaproteobacterium *R. sphaeroides* identifies little homology with the **-GPQHP-** motif highlighted in archaeota and deltaproteobacteria, with only proline 86 being preserved in the human protein. Some conservation, however, is observed in the **-RPGGV-** motif, although, the redox-sensitive residues arginine 228 and proline 229 do not appear to be integral to this region in the functional enzyme of *R. sphaeroides*.

```
NDUFS2      WKPPPWNDVDPPKDTI--VKNITLNFGPQHPAAHGVLRLVMELSGEMVRKCDPHIGLLH  117
HupL        -------MVATPNGFNLDNTGRRIVVDPVT-RIEGHMRCEVNVDDQGIIRNAVSTGTMW  51
HupV        --------------------MTRLVVGPFN-RVEGDLEVHLEVAEGA-VTAARVNAPLY  37
                                  : ..*     .   .  :.:           .


NDUFS2    YIRPGGVHQDLPLGLMDD-----------------IYQFSKNFSLRLDELEELLTNNRI   267
HupL      WLV-GGVPCPINIDGVGAVGAINMERLNLVSSIIDQCIQFTNNVYLP-----DVVAIGGF   284
HupV      AVQPGGVTRA--------PG--AAERMRILSSLRSFRRHLERTLFGGPLEAFAALEIEAA   216
           :  ***                                 : ...         .
```

Figure 3.10. Alignment of human NDUFS2 sections 73-133 and 225-260, and *Rhodobacter sphaeroides* hydrogenase large Subunits (HupL and HupU). A short section of the Clustal alignment between human NDUFS2 and *R. sphaeroides* HupL and HupU hydrogenase proteins (large subunit). Histidine 88 is in bold and underlined. Yellow highlights the -HXXAHXVLR- motif and conserved residues. Grey highlights the conserved residues of the -RPGGV- motif.

3.5.3 NDUFS7 (30kDa)

A dot plot analysis of NDUFS7 and the NiFe hydrogenases of interest (Figure 3.11), exposes a strong correlative association between NDUFS7 and the MbhL protein of *C. heimdallarchaeota.*

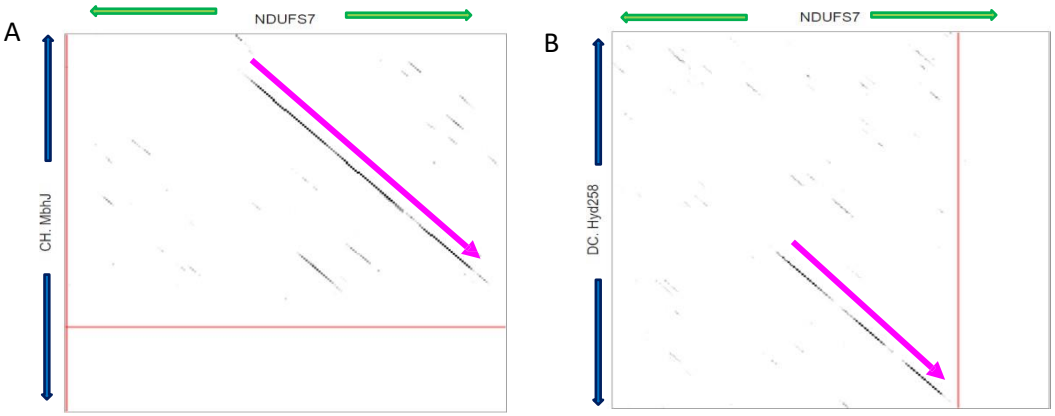

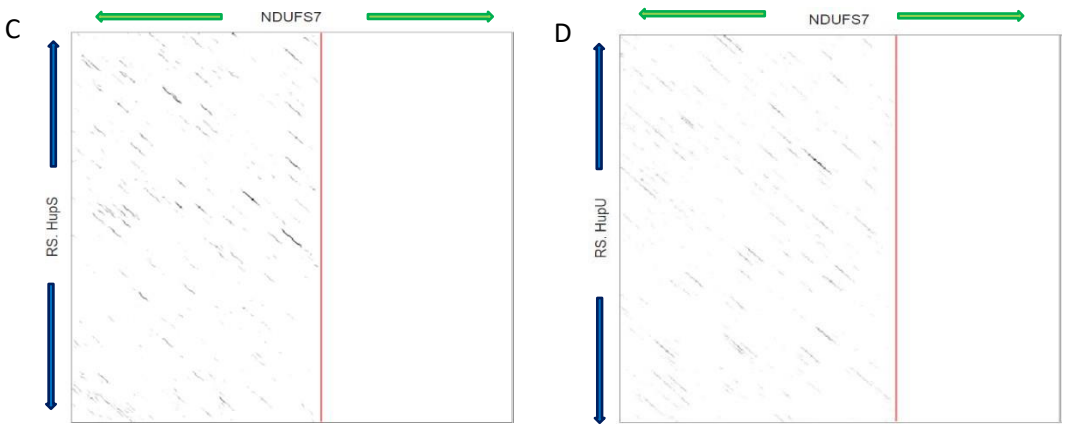

Figure 3.11. Similarity matrix analyses of NDUFS7 and hydrogenases. Dot plot analysis of the NDUFS7 protein (213aa) sequence – X-axis, Green arrows indicate sequence direction. Hydrogenases of interest – Y-axis, Blue arrows indicate sequence direction. Clear alignment indicates areas of homology. (A) *D. carbinolicus* Hyd258 (258aa). (B) *C. heimdallarchaeota* MbhJ (155aa). (C) *R. sphaeroides* HupS (369aa). (D) *R. sphaeroides* HupU (330aa). The horizontal red line indicates the truncation of the amino acid sequence of the hydrogenase. The vertical red line indicates the truncation of the amino acid of NDUFS7. The pink arrow highlights regions of interest due to sequence similarities.

Recent investigations utilising a combination of mass spectroscopy and *in silico* modelling of the NDUFS7 unit identified that bovine arginine 108 and 112 (arginine 111 and 115, in humans) of the highly conserved *C*-terminal **-RASPRQ-** motif were integral to retaining ubiquinone in the hydrophobic cavity (Yoga *et al.,* 2020), although whether direct electron transfer activity occurs at either of these moieties remains unanswered. Downstream of the **-RASPRQ-** motif is another highly conserved sequence **-CCAVEMM-**. The **-CCAVEMM-** motif is of interest as it contains four redox-active residues beginning with double cysteine residues (cysteine 88 and cysteine 89, human) and concluding with double methionine residues (methionine 93 and methionine 94, human), both of which have sulphur groups that are readily oxidised and reduced, and as such are effective redox mediators. The double cysteine residues are of further intrigue as these couplings enable sequential dissociation of protons and electrons, derived from hydrogen, upon N2 cluster reduction (Yu *et al.,* 2020) and therefore may facilitate electron transference to ubiquinone. Should H_2 prevent undue oxidation, or stabilise this region, it is feasible that a steady supply of electrons would be available for the complete reduction of ubiquinone ubiquinol, thereby enhancing the immediate antioxidant potential of the mitochondria which would have significant downstream effects including enhanced membrane potential and increased production of ATP (Kucharská *et al.,* 2018; Zhang *et al.,* 2018).

Further along the sequences detailed in Figures 3.12 - 3.14, there is a well-conserved **-IPGCPP-** motif (180-185, human) rich in redox active proline residues, and containing a cysteine thiol residue at position 183. Having such a concentration of conserved residues known to partake in redox chemistry is intriguing and highly suggestive of conserved function in this region. Interestingly, the **-IPGCPP-** domain is known to undergo *N*-myristoylation, which may be of further importance for signal transduction and innate immune system responses (Wang *et al.,* 2021a). If H_2 were to interact with this particular region, it could influence such cellular signalling cascades as the MAPK pathways, responsible for moderating the expression of proinflammatory factors including NFκB and TNF-α and regulating apoptosis in mammals. This region, therefore, may be relevant to understanding the pleiotropic effects of H_2 bioactivity.

3.5.3.1 *Candidatus heimdallarchaeon* – NDUFS7

Exceeding the 25% threshold for significance, the BLASTP analysis of *C. heimdallarchaeon* shows a 35% similarity with NDUFS7. Of interest here, is that in similarity with the protein of deltaproteobacterium *D. carbinolicus,* only cysteine 86 and glutamic acid 89 are conserved in the **-CCAVEMMH-** short sequence and therefore it is unlikely that this particular arrangement could retain hydrogenase activity. It is more likely that the sequential cysteine residues are involved in securing the Fe cluster. The site for protein kinase C (PKC) phosphorylation (**-RASPRQS-**) shares more sequence identity between species. Should H_2 either inhibit or promote protein phosphorylation (Chapter 4, Section 4.4.2) in this region, this could significantly affect downstream cell signalling events, perhaps accounting for the pleiotropic effects of H_2 application.

The site **-IPGCPP-** noted to be of interest due to *N*-myristoylation, is also reasonably well conserved which may indicate important associations with redox activity and/or cellular signalling (Figure 3.12) in humans as well as in archaea. As a highly redox-sensitive moiety, the centrally located cysteine 182 can be prone to oxidation. Therefore, the question arises, is it possible H_2 could act as a modulator of *N*-myristoylation by preventing cysteine oxidation?

```
NDUFS7      DDLVNWARR-------SSLWPMTF---GLACCAVEMMHMAAPRYDMDRFGVVFRASPRQS  110
MbhJ        ---MGWLKKFGVNCAVRSPWIIHMNAGGCNGCDIEIVDALTPRHDLEQYGITLRGTPRQA  50
               :.* ::        * * : :   *   * :*::.  :**:*::::*:.:*.:***:


NDUFS7      LTNKMAPALRKVYDQMPEPRYVVSMGSCANGGGYYHYSYSVVRGCDRIVPVDIYIPGCPP  185
MbhJ        VTVQVAERVKRVYEQMPLPKFVVAVGNCCTTGGVFQECPFVLGGIDHVLPVDAWVYGCPP  125
            :* ::*  :::**:*** *::**::*.*.. ** :: .  *: * *:::*** :: ****
```

Figure 3.12. Alignment of human NDUFS7 sections 60-110 and 125-185 and *Candidatus heimdallarchaeon* hydrogenase (MbhJ). A short section of the alignment between human NDUFS7 and *C. heimdallarchaeota* MbhJ hydrogenase protein (small subunit). Green highlights indicate conserved motifs of interest. Yellow highlights indicate highly redox-sensitive cysteine thiols.

3.5.3.2 *Desulfovibrio carbinolicus* - NDUFS7

A 35% correlation between the smaller subunit of the NiFe hydrogenase (Hyd258), and NDUFS7 shows retention of the **-RASPRQS-** motif highlighted by Yoga *et al.,* (2020) who identified this region as being integral to retaining ubiquinone in the binding pocket. This suggests that in deltaproteobacteria, this segment may be of importance in maintaining the structure and/or function of the hydrogenase enzyme. Furthermore, the sequence **-RASPRQS-** is identified as containing serine 113 (human), a target for PKC phosphorylation and therefore may be of pertinence for elucidating the influence H_2 may have on protein phosphorylation and cell signalling events (Chapter 4, Sections 4.4.1 and 4.4.2). Interestingly, H_2 is noted to influence other protein kinase pathways (*e.g.,* MAPK) (Han *et al.,* 2016; Begum *et al.,* 2020), therefore understanding whether H_2 has any influence on the molecular activity of this relatively well-conserved region is likely to be of high importance.

```
NDUFS7      EYVVAKLDDLVNWARRSSLWP-MTFGLACCAVEMMHMAAPRYDMDRFGVVFRASPRQSDV  119
Hyd258      KL----------FAKSLRLRQVSAGGCNACEADTNVLTTIVFDLGRFGIDFVASPRHADG  170
            :           :*:   *    : *  .* .:   :::  :*:.***: * ****::*


NDUFS7      CANGGGYYHYSYSVVRGCDRIVPVDIYIPGCPPTAEALLYGILQLQRKIKRERRLQIWYR  212
Hyd258      CAISGGLFDGSPETTGGATPHLPLDLYIPGCPPHPLTILDGLLRLLGQQTPPPTA-----  257
            ** .** :. * ... *.   :*:*:*******   ::* *:*:*  : .
```

Figure 3.13. Alignment of human NDUFS7 sections 61-119 and 180-213 and *Desulfovibrio carbinolicus* hydrogenase Hyd258. A short section of the alignment between human NDUFS7 and *D. carbinolicus* hydrogenase Hyd258. Blue highlights indicate the protein kinase *C* phosphorylation site. Green highlights indicate conserved motifs of interest. Yellow highlights indicate highly redox-sensitive cysteine thiols.

At the downstream **-CCAVEMM-** motif, it is clear this sequence is not homologous in *D. carbinolicus*, although cysteine 86 (human) is conserved and may yet have a functional role in redox and hydrogen biochemistry. The **-IPGCPP-** motif, containing the predicted *N*-myristoylation site **-GCPP-**, is fully conserved, piquing further interest as to whether this region is integral to the location or function of hydrogenase relicts, and therefore relatable to the

electron transference function of NDUFS7, and by extension, the activity of Complex I.

3.5.3.3. *Rhodobacter sphaeroides* – NDUFS7

The BLASTP search indicated <20% homology between the NiFe hydrogenases of *R. sphaeroides* and the NDUFS7 subunit of mitochondrial Complex I. Observations here suggest the HupS protein is marginally more likely to have an evolutionary association with NDUFS7 than HupU as there are indications of conserved redox active moieties in the double cysteine residues 88-89 of the **-CCAVEMM-** sequence along with the alignment of redox-active residues cysteine 283 and prolines 280, 284 and 285 in the **-IPGCPP-** motif, identified as a target for *N*-myristoylation. Interestingly, only alanine 111 of the **-RASPRQS-** PKC phosphorylation site is conserved in both hydrogenase small subunits of *R. sphaeroides.* Crucially, the target for phosphorylation, serine 113, is not present in the alphaproteobacterial hydrogenases (data not shown) suggesting little resemblance of form and function between these particular NiFe hydrogenases and NDUFS7.

```
NDUFS7    -EYVVAKLDDLVNWARRSSLWPMTFGLACCAVEMMHMAAPRYDMDRF-GVVFR------   111
HupS      PSFVPRIAHAMETKPRTPVIWVHGLECTCCSESFIRAAHPLAKDVVLS-MISLDYDDTLM   94
HupU      ----------------MNILWLQASGCGGCTMSLLCAEAPGLFNLLEDAGLRFLWHPSLS   44
                           :*         *: .::     *           : :

NDUFS7    EPRYVVSMGSCANGGGYYHYSYSVVRG-----------------CDRIVPVDIYIPGCPP  185
HupS      HAKAIISWGACASYGCVQAAAPNPTRATPVH-------------KVILDKPIIKVPGCPP  196
HupU      LARHVVAVGSCAAYGGMTIAGGNPSDATGLQYEGTHEGGILPPEFRARDGLPVVNVAGCPT  164
            : ::: *:**  *     . .   .                          : : ***
```

Figure 3.14. Alignment of human NDUFS7 sections 60-112 and 143-185 and Rhodobacter sphaeroides hydrogenase small subunits HupS and HupU. A short section of the alignment between human NDUFS7 and small hydrogenase subunits of R. sphaeroides. Green highlights indicate conserved motifs of interest. Yellow highlights indicate highly redox-sensitive cysteine thiols.

3.6. Summary

The data in Chapter 3 shows that it is unlikely that the closest human homologues of NiFe hydrogenases have retained classical hydrogenase activity due to the lack of a functional Ni-Fe di-metal core (Figure 3.6). Instead, it is possible that redox activity occurs at the N2 FeS cluster within the NDUFS7 module, which is situated in close proximity to the ubiquinone docking site (Zickerman *et al.,* 2015). It can be hypothesised that the protons follow a redox-regulated channel through NDUFS2 and the electrons are transferred to ubiquinone via N2

cluster (NDUFS7)/histidine 88 (NDUFS2) interactions. Similarities above the threshold of significance (Anderson and Brass, 1998), indicative of retained function, are observed between NDUFS7 and the smaller hydrogenase subunits of both the Asgard archaeota (Figure 3.12) and the deltabacterium considered in this study (Figure 3.13). Nevertheless, as this subunit is responsible for the shuttling of electrons and not the ultimate protonation/deprotonation of hydrogen, it is also improbable that NDUFS7 is capable of generating or oxidising H_2. Whether H_2 is able to support the optimal function of such subunits by another mechanism has yet to be elucidated.

CHAPTER 4: A Theoretical Evaluation of the Biological Activity of H_2

4.1 Introduction

H_2 is formed by the amalgamation of two hydrogen (H) atoms with an H-H bonding energy of 107 kcal/mol (4.64 eV) (Kim *et al.,* 2022) and a redox potential ($2H + 2e^- \rightarrow H_2$) of -0.421 eV (pH 7) relative to the standard hydrogen electrode (Karp, 2008). Although the primary modality of action in biological systems has yet to be illuminated, one favoured postulation is that H_2 is able to reduce excessive ROS/RNS through direct interaction with radical and ionic species (*e.g.,* $^{\bullet}OH$, $ONOO^-$). However, whether due to spatial and temporal availability of H_2, the reaction kinetics are favourable in vivo is still a matter of debate (Penders et al., 2014; Hancock, LeBaron and Russell, 2021; Li et al., 2021). Furthermore, although the clinical advantages of H2 therapeutics are now well documented (Korovljev et al., 2017; Guan et al., 2020; Botek et al., 2022; Kura et al., 2022; Tao et al., 2022; Deryugina et al., 2023; Wang et al., 2023a), there are still many questions surrounding the distribution and precise molecular mechanisms relating to the biological activities of H_2. These include, how does H_2 reach target tissues? What are the primary physiological targets of H_2 interactions? And, how does H_2 maintain its influence over time?

With increasing momentum, international research institutions are devoting time and resources to understanding how H_2 affects both cellular and wider somatic physiology. This report assesses the nascent research surrounding H_2 distribution and molecular activity and theorises on the primary aspect(s) of H_2 modality in biological systems.

4.2 Reduction of Reactive Gases

4.2.1 The Hydroxyl Radical

$^{\bullet}OH$ is regarded as the most physiologically detrimental of the suite of ROS, due in part to the expedience with which oxidation of cellular molecules can take place. During cellular stress events the increased production of $O_2^{\bullet-}$, the antecessor molecule to $^{\bullet}OH$ production, occurs either through reductive reactions in such ROS/RNS-producing enzymes as nicotinamide adenine phosphate dinucleotide ($NADP^+$/H) and xanthine oxidases (XOs) (Halliwell, 1978), or via dysfunctional processes within the respiratory ETC (Ratajczak *et al.,* 2019). The latter being the result of the premature reduction of O_2 due to electron leakage at the FMN and Q modules of Complex I (Chapter 3, Section 3.6), and at Complex III (coenzyme *Q*-cytochrome *c* oxidoreductase). Enzymes can also generate $O_2^{\bullet-}$, either as an oxidative burst used as a defence against pathogenic attack or as a consequence of mitochondrial dysfunction (Wang *et al.,* 2018b). Generation of $O_2^{\bullet-}$ under such circumstances utilizes Fe^{2+} or Cu^{2+} metalloproteins when catalysing the monovalent reduction of O_2 with electrons donated by NADH ($2\ O_2 + 2e^-$) or NADPH co-factors, for example. $O_2^{\bullet-}$ has a disproportionation rate constant of $8 \times 10^4\ M^{-1}\ sec^{-1}$ (pH 7.8), albeit, this is a second-order rate reaction (proportional

to the squared concentration of reactants). The first-order rate reaction (the rate of reaction directly proportional to the concentration of a single reactant) is calculated to be 10^6-fold more expedient. In the absence of scavengers, the half-life of $O_2^{\bullet-}$ is noted to range from 0.05 seconds ($O_2^{\bullet-}$ concentration: 1 x 10^{-4} M) to 14 hours ($O_2^{\bullet-}$ concentration: 1 x 10^{-10} M) in biological systems (Fridovich, 1983; Gao *et al.,* 2007), noted in Table 4.1.

Table 4.1. The physical restrictions to ROS/RNS activity in cells. Data extracted and adapted from Zhang *et al.* (2019a). Lifetime: natural log2 divided by the sum of the products of rate constant and concentrations for all molecules that ROS react with. Diffusion distance: calculated with the formula x = (6Dt)1/2 (x, D, t stand for diffusion distance, diffusion coefficients and lifetime, respectively).

Substance	**Chemical Nomenclature**	**Theoretical Distance Travelled (meters)**	**Theoretical Longevity (seconds)**	**Primary Targets**
Hydrogen Peroxide	H_2O_2	10^{-3} m	10^{-3} s	Metal groups and thiols
Hydroxyl Radical	$^{\bullet}OH$	10^{-9} m	10^{-9} s	Indiscriminate – all organic macromolecules
Nitric Oxide Radical	$NO^{\bullet}$	10^{1} m	10^{-1} s	Metal groups and thiols
Peroxynitrite	$ONOO^-$	10^{-6} m	10^{-6} s	CO_2, Cys, Trp, Met and metal groups
Superoxide	$O_2^{\bullet-}$	10^{-9} m	10^{-3} s	Fe–S clusters and $NO^{\bullet}$

$O_2^{\bullet-}$ is regarded as the cardinal ROS as its formation is known to give rise to ROS and RNS, including $^{\bullet}OH$. Here, the dismutation of $O_2^{\bullet-}$ by SOD gives rise to H_2O_2, which can generate $^{\bullet}OH$ through downstream reactions noted below.

$^{\bullet}OH$ is formed through the three-electron reduction of molecular oxygen (Di Meo and Vindetti, 2020), with the biological formation of the hydroxyl radical known to occur in multiple ways. For example, both the Fenton reaction and the Haber-Weiss reaction produce $^{\bullet}OH$ in the presence of H_2O_2.

Fenton Reaction: $O_2^{\bullet-} + H_2O_2 \rightarrow O_2 + {}^{\bullet}OH + OH^-$ (in the presence of Fe ions)

Haber-Weiss Reaction: $Fe^{2+} + H_2O_2 \rightarrow Fe^{3+} + {}^{\bullet}OH + OH^-$

$O_2^{\bullet-}$ reduction can be a result of endogenous SOD activity, or through the Fenton/Haber-Weiss reactions, although the latter is estimated to produce comparatively minor levels of H_2O_2 in cells (Winterbourn, 2020). Reduction of $O_2^{\bullet-}$ is known to be a major source of H_2O_2, a signalling molecule capable of traversing phospholipid membranes, and influencing both cellular and organelle activity (Krohn, Maier and Paschke, 2007; Iglesias-Pedraz and Comai, 2020). Electrostatic attraction of $O_2^{\bullet-}$ to exposed iron-sulphur clusters of enzymes including various ferredoxins, reductases and dehydrogenases, can generate H_2O_2 by releasing a Fe^{2+}/H_2O_2 array (Demidchik, 2017). Releasing the Fe^{2+}/H_2O_2 array can affect post-translational modification to enzyme thiols, activating or deactivating protein activity, an effect that has numerous but less-well-defined downstream signalling effects. The rate of reaction for such protein modifications has been calculated to be $>10^6$ M^{-1} s^{-1} (Winterbourn, 2020).

Seminal calculations on the effect of H_2 is predicted to have within haem proteins, conducted by Kim *et al.* (2022), illustrate the feasibility of antioxidant activity via interactions between H_2 and protohaem. The authors report that the H_2 molecule can bind to the iron (Fe^{2+}) contained within haem, asymmetrically via a dihydrogen bond, and symmetrically through bilateral electron transfer, known as Kubas bonding. Asymmetric binding is noted to be more favourable under physiological conditions due to a moderately lower activation energy (2.04 eV and 2.14 eV, respectively). In reciprocation, Fe^{2+} should reduce the dissociation energy of the H-H bond within the H_2 diatom, forming $Fe^{2+}/H^{\bullet}$ complex, wherein $H^{\bullet}$ would be able to reduce highly reactive ions and radicals. The $Fe^{2+}/H^{\bullet}$ complex was calculated to have a relatively low dissociation energy of 2.78 eV, which would allow the bound $H^{\bullet}$ radical to neutralise another, coterminous, reactive nitrosative or oxidative species (Kim *et al.,* 2022). Accordingly, the authors state that this proposed activity may account for the direct reduction of $^{\bullet}OH$, however the kinetics of this proposed mode of action have yet to be elucidated.

$^{\bullet}OH$ is also produced via homolysis of ONOOH which has a rate constant of decay of 1.2–1.3 M^{-1} s^{-1} at 25 °C, generating both $^{\bullet}OH$ and nitrogen dioxide ($NO2^{\bullet}$) radicals (Merényi and Lind, 1998). $^{\bullet}OH$ is known to react at a diffusion-controlled rate with the reactivity of $^{\bullet}OH$ in biological systems (1 x 109 M-1 s-1) (Halliwell et al., 2022; Lenzen, Lushchak and Scholz, 2022), indicating that this molecule would be unable to travel far before reacting with biological compounds. Li et al. (2019) suggest the action of $^{\bullet}OH$ would be limited to within a 4.5 - 8.6nM range of the site of its generation (Li et al., 2019; Zhang et al., 2019a). As $^{\bullet}OH$ can be produced globally within cells by a range of enzymes (e.g., dehydrogenases, hydratases, reductases, synthases), H_2 would need to be

available at the precise vicinity of •OH production and in significantly large quantities to contribute to the direct scavenging of •OH. This is unlikely when relatively small dosages of H_2 are demonstrated to have therapeutic effects (Alharbi et al., 2022).

Supporting the assumption that H_2 is unlikely to have a significant effect on the direct reduction of •OH, the biomolecular reaction kinetics of •OH with H_2 are calculated to be 4.2 x10^7 M^{-1} s^{-1} (Li et al., 2020), a marked decrease in activity when compared with the oxidative reaction of •OH and macromolecules including lipids and proteins (> 1x 10^9 M^{-1} s^{-1}), which is at least two orders of magnitude higher than any potential reduction initiated by H_2. In addition to the oxidation of macromolecules, •OH also influences amino acid chemistry through oxidative activity, again with kinetics that should outcompete the reductive potential of H_2. Amino acids such as proline and glutamic acid react with •OH with a rate constant of >2.3 x 10^8 M^{-1} s^{-1} (Ishibashi, 2019), whilst reactions with glutathione have been calculated as high as

>1x 10^{10} M^{-1} s^{-1} (Tao, Song and Qin, 2019). This suggests that the reduction of •OH by H_2 would likely be insignificant in biological systems. Therefore, although mooted to be an effective antioxidant, with a potential mode of action being reported by Kim et al. (2022), the ability of H_2 to directly, and effectively, scavenge •OH in the biological milieu of amino acids, gases, lipids etc., comes into question.

In summary, as •OH is a radical species, and as such can react with most organic molecules including lipids, nucleotides, peptides and proteins, it is more likely to interact with localised biological components than with H_2. When the unfavourable dynamics, discussed above, are considered along with the high reactivity, short half-lives and maximal diffusion limits of such reactive species, it is implausible that H_2 would exert such pleiotropic antioxidant effects by primarily acting as a scavenging agent of •OH in biological systems.

4.2.2 The Peroxynitrite Ion

It is now well established that NO•, acting as a secondary signalling molecule, has a multitude of roles in biochemistry. NO• is known to both activate antioxidant transcription pathways, and under aerobic conditions, can react with oxygen-containing radical species, forming more stable nitrate and nitrite products (Hancock and Veal, 2021). The activities of gasotransmitters such as NO• often depend on their cellular concentration, where concentrations above a biological threshold can lead to the induction of cytotoxic processes involving the initiation of free radical cascades, along with oxidative and nitrosative, post-translational modifications to proteins (Del Castello *et al.,* 2019; Hancock and Veal, 2021). NO• toxicity is largely attributed to downstream oxidation products that include paramagnetic nitrogen NO_2• and $ONOO^-$. When NO encounters $O_2^{\bullet-}$, it can spontaneously react, forming $ONOO^-$, with kinetics greater than that of the endogenous antioxidant, SOD (6.75 x 10^9 M^{-1} s^{-1} vs 6.4 x 10^9 M^{-1} s^{-1},

respectively) (Speckmann *et al.,* 2016). Therefore, spontaneous production of $ONOO^-$ can be more rapid than the dismutation of $O_2^{\bullet-}$ into O_2 and H_2O_2.

$ONOO^-$ is a highly reactive and diffusible molecule (Table 4.1). These properties, and the need to avoid oxygen under experimental conditions, mean the rate constant of H_2/$ONOO^-$ interactions have yet to be confirmed. However, of the few studies that have investigated H_2/$ONOO^-$ reactivity, Penders *et al*. (2014) noted no significant increase in the degradation products of peroxynitrous acid (ONOOH), the protonated form of $ONOO^-$, and determined the spontaneous rate of decay, without $ONOO^-$/macromolecule interactions, to be between 1.1 - 1.3 M^{-1} s^{-1} with and without the application of H_2 (Ferrer-Sueta and Radi, 2009; Penders, Kissner and Koppenol, 2014). ONOOH is important to consider here as it is estimated that with a p*K*a of 6.6, denoting a weak acid, a biologically relevant amount of ONOOH could be present in biological systems (Villamena, 2013). This is also likely to be of significance when examining the downstream effects of these redox partners. The products of ONOOH homolysis are $NO_2^{\bullet}$ and $^{\bullet}OH$ (2.5 M^{-1} s^{-1}), whilst the $ONOO^-$ ion is known to produce $O_2^{\bullet-}$ and $NO^{\bullet}$ (0.017 M^{-1} s^{-1}) (Merényi and Lind, 1998). In physiological systems, $ONOO^-$ also reacts with carbon dioxide (CO_2), at a rate constant of 5.8 x 10^4 M^{-1} s^{-1} forming carbon trioxide ($CO_3^{\bullet-}$) and $NO_2^{\bullet}$ as decomposition products (Squadrito and Pryor, 2002), all of which are reactive species known to influence numerous cellular responses.

When studying the reaction kinetics between $ONOO^-$ and H_2 utilizing a selected ion flow tube/mass spectroscopy, no reaction between these species was shown (Viggiano, Midey and Ehlerding, 2006). It can therefore be surmised that the reaction kinetics of H_2 and $ONOO^-$, under physiological parameters such as temperature and pH, have yet to be determined. Nevertheless, the current understanding is that H_2 causes a selective reduction in $ONOO^-$ levels, and, or peroxidative damage in biological systems. Indeed Kiyoi *et al.* (2020) have described a reduction in both $^{\bullet}OH$ and $ONOO^-$ production in murine models when treated by H_2 inhalation. Interestingly, the same study (Kiyoi *et al.,* 2020) noted that the NADPH oxidase (NOX-1) enzyme, responsible for producing the superoxide anion during cellular stress events, was significantly downregulated in the H_2 group. Expression of critical activation components p40-*phox* and p47-*phox* were unaffected, suggesting H_2 may influence the expression or action of other proteins within the NOX-1 complex. NOX enzymes facilitate the conversion of O_2 to $O_2^{\bullet-}$ utilizing $Fe^{+2/3}$ transition metals as catalysts for electron transfer and as such could provide a viable target for H_2 interactions (Hancock, LeBaron and Russell, 2021), although empirical data is required to confirm this.

4.3 Distribution and Retention of H_2

4.3.1 Pharmacokinetics

Pharmacokinetic analysis of H_2 distribution in porcine models (Sano et al., 2020) suggests that, due to the increased half-life of H_2 in venous blood, this diatomic gas likely travels in the plasma and simply diffuses into tissue structures. The physical and chemical characteristics of H_2 (Chapter 1, Section 1.1) should permit the molecule to diffuse through biological fluids, the extra-cellular matrix, cellular membranes and cytosolic compartments. However, it is undetermined whether this mechanism of dispersal would be able to explain the effects seen in distal organs. For example, when hydrogen-rich saline (HRS) is administered via intraperitoneal delivery, substantial amounts of H_2 are recorded in proximal sites such as the pancreas and spleen, whilst stepwise reductions, progressing radially, are shown for the distal organs (Liu et al., 2014). Interestingly, when H_2 is delivered via inhalation, although the primary beneficiary organs are typically in close proximity (e.g., the brain, respiratory system and heart), significant increases in H_2 concentration are also seen in the spleen and skeletal muscle 30 minutes after application. This factor could be explained if H_2 were to transitorily reside within micropores, or pockets, formed within haemoglobin of red blood cells (Diamantis, Unke and Meuwly, 2017; Hancock et al., 2022; Hancock, 2023); or if H_2 could be temporarily retained by molecules suspended in the serum such as carbohydrates or inorganic ions; glycogen and calcium, as examples, discussed in Chapter 4, Sections 4.3.2 – 4.3.4.

One explanation for H_2 distribution is that after imbibition, inhalation or injection, the H_2 molecule diffuses into the bloodstream entering the circulation and allowing for dissemination into all corporal systems. Supporting this theory is early research conducted by Liu *et al.* (2014) on rodent models, where HRW containing 1.25 ppm, 2.5 ppm and 5ppm/H_2 (0.62, 1.25 and 2.5 mM, accordingly) delivered by i) intraperitoneal and intravenous injection of HRS, and ii) inhalation of H_2 at various concentrations (1%,2% and 4%) were studied. The findings show that H_2 concentrations are increased in the blood, brain, intestines, kidney, liver, pancreas, skeletal muscle and spleen following HRW, intravenous HRS, and inhalation of H_2 (Table 4.2). The timing of peak concentrations and retention of H_2 are noted in Table 4.3.

Table 4.2. Concentrations of H_2 in various tissues. Data extracted from Liu *et al.* (2014).

Tissue	**Oral (HRW) - 5ppm Time elapsed: (5 minutes)**	**Intraperitoneal (HRS) - 5ppm Time elapsed: (5 minutes)**	**Intravenous (HRS) - 5ppm Time elapsed: (1 minute)**	**Inhalation (4%) Time elapsed: (30 minutes)**
Blood	5 ppb/g	5 ppb/g	5 ppb/g	5 ppb/g

Liver	170 ppb/g	170 ppb/g	15 ppb/g	25 ppb/g
Kidney	50 ppb/g	75 ppb/g	25 ppb/g	50 ppb/g
Heart	50 ppb/g	0 ppb/g	30 ppb/g	30 ppb/g
Spleen	500 ppb/g	300 ppb/g	40 ppb/g	50 ppb/g
Pancreas	400 ppb/g	250 ppb/g	40 ppb/g	45 ppb/g
Intestine	400 ppb/g	150 ppb/g	20 ppb/g	20 ppb/g
Muscle	20 ppb/g	20 ppb/g	20ppb/g	140 ppb/g
Brain	15 ppb/g	15 ppb/g	20 ppb/g	15 ppb/g

Although this research (Liu *et al.,* 2014) identified that intraperitoneal injection with HRS resulted in H_2 elevation in the majority of tissues analysed, this method was not effective in delivering large amounts of H_2 into the bloodstream, or the wider cardiovascular system, but was highly effective in delivering H_2 to proximal organs including the intestines, liver, pancreas and spleen (Table 4.2). Such results suggest a preference for distribution by simple diffusion, however, this still does not explain the elevated levels of H_2 in distal organs such as the brain and kidneys, when elevated H_2 levels in the blood are not detected (Table 4.3).

Tissue	**Oral (HRW) - 5ppm**		**Intraperitoneal (HRS) - 5ppm**		**Intravenous (HRS) - 5ppm**		**Inhalation (4%)**	
	Peak	Return to baseline	Peak	Return to baseline	Peak	Return to baseline	Peak	Return to baseline
Blood	5 min	> 60 min	5 min	15 min	1 min	3 min	30 min	> 60 min
Liver	5 min	60 min	5 min	15 min	1 min	5 min	30 min	> 60 min
Kidney	5 min	30 min	5 min	15 min	1 min	5 min	30 min	> 60 min
Heart	5 min	15 min	5 min	15 min	1 min	5 min	-	-
Spleen	5 min	30 min	5 min	15 min	1 min	> 5 min	60 min	> 60 min

Pancreas	5 min	60 min	5 min	15 min	1 min	5 min	-	-
Intestine	5 min	60 min	5 min	15 min	1 min	3 min	60 min	> 60 min
Muscle	5 min	30 min	5 min	15 min	1 min	> 5 min	30 min	> 60 min
Brain	5 min	30 min	5 min	15 min	1 min	> 5 min	30 min	> 60 min

One reason for this could be due to experimental protocol recording only H_2 dissolved in the plasma. The saturation point of plasma is in the region of 1.6mg/L/H_2, therefore it is likely that inhalation would provide more H_2 than can be dissolved in the bloodstream. The question then arises, how does enough H_2 travel the blood in order to still be present in detectable levels in the venous bloodstream and often distal organs, up to an hour after treatments?

One study investigating the effects of 100% H_2 insufflation (the act of blowing something into a body cavity) concludes that H_2 likely remains in the plasma (Christ *et al.,* 1994). However, for this to be the case the saturation levels would have to be vastly increased for such wide-ranging effects and distribution patterns to be seen. As physiological pressures are only ~ 120 mm/Hg higher than atmospheric pressure (760 mm/Hg) elevating the saturation levels of H_2 as a result of increased pressure is unlikely. Furthermore, simple diffusion through the plasma cannot explain the gradual increase and retention of H_2 in skeletal muscle, or why H_2 is not only effective in the organs proximal to the delivery site. However, binding of H_2 to glucose molecules or metalloproteins (haemoglobin and myoglobin, as examples), may offer an insight into how H_2 is distributed, retained and/or utilised in somatic systems.

4.3.2 Haem

Haem is an iron-containing prosthetic group present in cytochromes and red blood cells in all vertebrate species, except Antarctic icefish (*Channichthyidae*) (Sidell and O'Brien, 2006). The haemoglobin protein, which has a major role in the transportation and exchange of biological gases (*e.g.,* O_2, NO, CO and CO_2) through direct interactions with haem prosthetic groups, and covalent modifications of thiols and amine moieties (Hancock *et al.,* 2022), is formed of 4 individual subunits, each with the ability to bind a single molecule of O_2. In haemoglobin (and myoglobin) Fe^{2+} is five-coordinated within the N-porphyrin ring, binding oxygen in the sixth position (Figure 4.1).

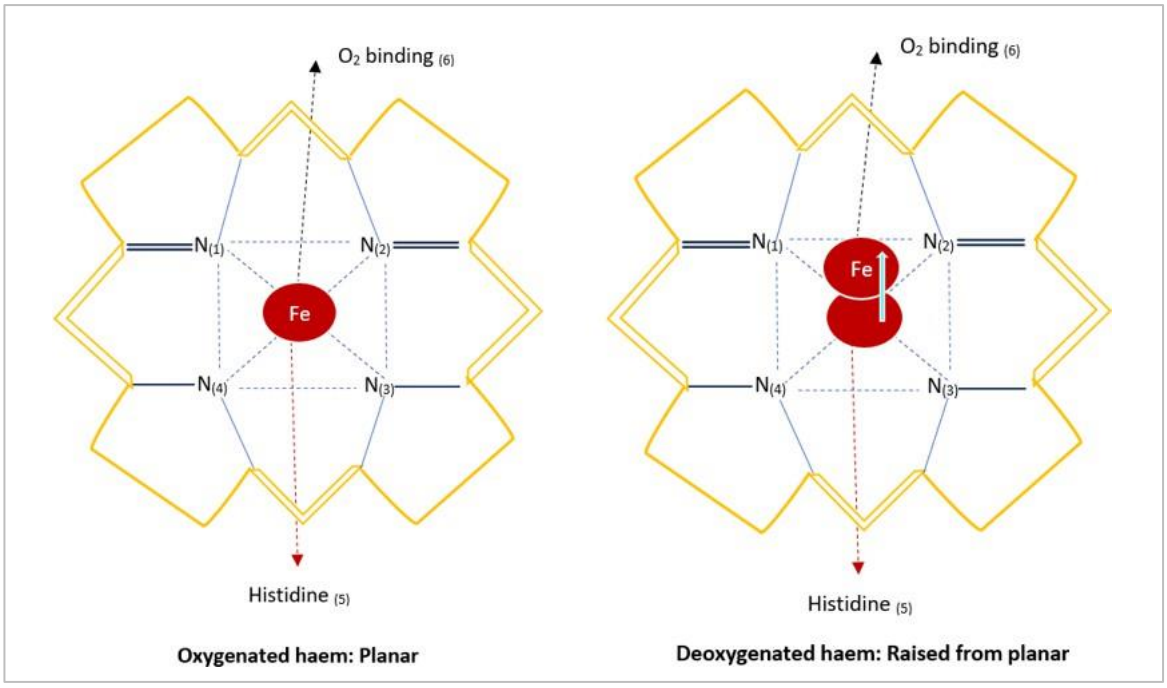

Figure 4.1. Graphical representation of the Fe^{2+} haem prosthetic group. Left – Oxygenated haem (relaxed). Right - Haem in the deoxygenated (tense) form with the distance of Fe from the porphyrin ring increasing by 0.06nm. Brackets indicate binding positions. His – Represents the $Fe^{+2/3}$ binding histidine residue of the protein (*e.g.,* haemoglobin).

The haem is versatile in that it can be present in numerous states, with the levels of each form influencing physiological processes. For example, the ferrous iron (Fe^{2+}) is present in deoxygenated (deoxy-) haem and oxygenated (oxy-) haem, whereas the ferric ion (Fe^{3+}) is present in (met-) haem, a non-oxygen binding configuration. Additionally, there are significant differences in the conformation of haemoglobin related to the ionic status of Fe. To illustrate, deoxygenated haemoglobin is referred to as 'tense' as the globin is shifted 0.06nm distally from the porphyrin ring (Heremans, 1987). On the other hand, oxygenated haemoglobin is defined as being relaxed, with the globin molecule sitting closer to the porphyrin ring (Figure 4.1). The change in oxidation to Fe^{3+} (met-haem) causes a change in the geometry of the haem pocket, favouring the relaxed position, such that oxygen no longer can bind.

The ferromagnetism of haem may also influence the binding characteristics of gases (Hancock and Hancock, 2018). To illustrate, *in silico* analysis of the spin states of ferrous iron identifies that the Fe-N bond distance increases from 2.01 Å in the low-spin state, to 2.1 Å in the high-spin state (Ugalde *et al.,* 2004). Therefore as the high-spin state Fe^{2+} may extend further from the porphyrin ring, high spin state Fe^{2+} may be more effective in attracting O_2 (and H_2) to the haem prosthetic than low-spin Fe^{2+}.

When investigating the effect H_2 may have on haem configuration and utility, daily administration of HRW (8mM/L/day) was noted to improve O_2 saturation in middle-aged

women (Ostojic *et al.,* 2018) and in patients recovering from COVID-19 (Singh *et al.,* 2021). To offer reasoned thought as to how this effect may occur, and accounting for the relaxed and tense states of the haem prosthetic group, there are two ways in which H_2 could affect the oxygenation of haem. Firstly, H_2 may protect Fe^{2+} from becoming oxidised via bilateral Kubas bonding (involving the simultaneous donation of electrons from both hydrogen atoms to the iron center), wherein Fe^{2+}/H_2 arrangements may directly reduce $^{\bullet}OH$ radicals (e.g., $H_2 + 2\ ^{\bullet}OH \rightarrow 2\ H_2O$) and/or other reactive species (Kim *et al.*, 2022) (Figure 4.2). And secondly, if the high-spin state of Fe^{2+} can increase the Fe^{2+}-N bond length then it is possible that H_2 could improve oxygen attachment to the prosthetic haem of low-spin ferrous iron through elongation of the 2.0 Å Fe^{2+}-N bond (Figure 4.3).

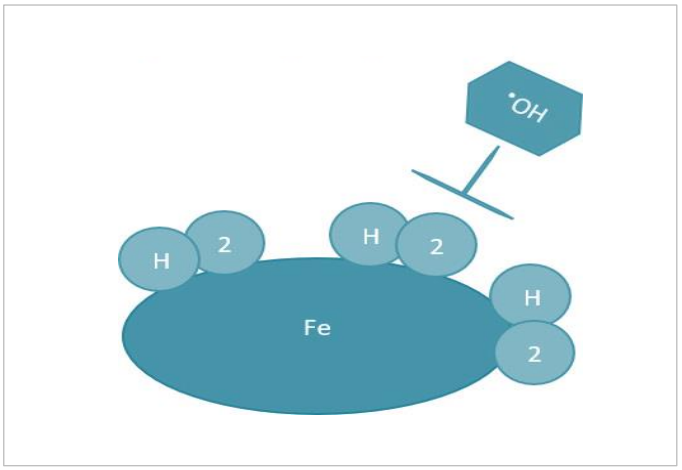

Figure 4.2. A possible mechanism for H_2 prevention of Fe oxidation. A schematic representation of how Kubas binding of H_2 to Fe may protect against oxidation.

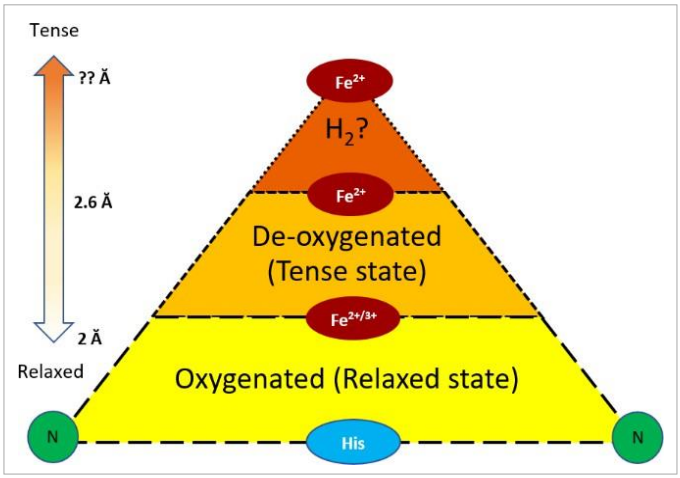

Figure 4.3. The haem trampoline. Single aspect schematic representation of different bond lengths noted between the *N*-porphyrin ring and the iron prosthetic group of haem. Bottom (Yellow): represents the shorter bond of oxygenated haem. Middle (Orange): represents the longer bond length of deoxygenated haem. Top (Umber): represents the theoretical further

elongation through H_2/Fe^{2+} interactions. The arrow (left) demonstrates the increasing/decreasing distance of the Fe prosthetic from the porphyrin ring.

Structural characterisation further identified high- and low-spin Fe-porphyrin derivatives, with research showing that ferric (Fe^{3+}) iron can also be found in the two spin-states (Nihei et al., 2007). These experiments were further expanded when the bond of high-spin Fe^{3+} was found to be increased by 0.4 - 0.5 Å, initiating a bond length of 2.04 Å, away from the nitrogen moieties of porphyrin, compared with low-spin Fe^{3+} which has a bond length of 1.99 Å (Rovira, Ballone and Parrinello, 1997; Bren et al., 2015). Therefore, the question as to whether H_2 interactions could favour high-spin state $Fe^{+2/3}$ arises.

Whether H_2 exerts its effects by extending the length of the $Fe^{+2/3}$ bonds, optimising O_2 adsorption by stabilising the protein structure, through direct interactions with the $Fe^{2+/3+}$ prosthetic moiety, or interactions with histidine 93 of human haemoglobin (and corresponding moieties in other proteins) has yet to be elucidated. H_2 may also impede O_2 dissociation from Fe^{2+} thereby improving O_2 saturation as reported by Singh *et al.* (2021), a topic considered in section 4.3.3.

4.3.3 Protein Pockets and Cavities

Another prevailing theory of H_2 somatic distribution and/or action is one of protein pockets. This hypothesis is based on the identification of discrete hydrophobic channels and surface pockets within protein structures. Such features are typically lined with amino acids of leucine, isoleucine, alanine or valine, characteristically formed in proteins over 100 amino acids in length (Roose, Zemerov and Dmochowski, 2018). Hydrophobic pockets enable non-

covalent/van der Waals interactions with noble gases such as argon (Ar), Krypton (Kr), the much larger atom, Xenon (Xe) (Prangé et al, 1998; Hancock et al., 2022) and perhaps molecular hydrogen.

In similarity with H_2, noble gases are typically deemed inert in biological systems due to having filled electron orbitals, meaning they do not partake in classical electron exchanges. However, numerous studies show that Ar (Ye, Zhang and Sun, 2013; Nespoli et al., 2019), Kr (Perov et al., 2021), Xe (Lawrence et al., 1946; Maze and Laitio, 2020) and helium (He) (Sykes and Lawrence, 1938; Manuilov *et al.,* 2022) can have neurological and cardioprotective effects. Albeit, how these effects are initiated has yet to be fully elucidated. The paragraphs below explore the possibility of indirect, or non-classical, protein/gas interactions.

Studies conducted using X-ray crystallography to assess Xenon-protein interactions report that hydrophobicity and volume of gas delivered are the primary factors in determining gas-protein binding, occurring via weak London dispersion forces (Abraini *et al*., 2014). London

dispersion forces are weak quantum forces involving a temporary intermolecular attraction between atoms which are normally electrically symmetric, resulting in the formation of transitory dipoles in non-polar molecules (Lu, Neese and Bistoni, 2018). As such, London dispersion forces may, in part, explain the biological modality of inert gases. This postulation is purely academic, and extensive modelling and analyses will be required if this speculation is to be refuted or upheld.

Other considerations when assessing the non-chemical effects of protein/molecule interactions should include such physical attributes as the size and weight of atoms and molecules, as these are likely to determine the ability of such molecules to affect protein form and function (Table 4.4).

Table 4.4. The mass and diameter of germane biological substances noting physical properties, atomic mass and kinetic diameters (non-hydrated, non-ionic) of biomolecules.

Substance	**Chemical Nomenclature**	**Molecular Mass (g/mol)**	**Kinetic Diameter**	**Reference(s)**
GASES				
Argon	Ar	40	0.34	Breck, 1974
Carbon dioxide	CO2	44	0.33	Freude, 2004
Carbon monoxide	CO	28	0.37	Matteucci *et al*, 2006
Helium	He	4	0.26	Matteucci *et al.*, 2006
Hydrogen	H_2	2	0.28	Freude, 2004
Krypton	Kr	84	0.36	Breck, 1974
Neon	Ne	20	0.28	Breck, 1974
Nitrogen	N_2	28	0.36	Lewis, 2018
Nitric oxide	NO	30	0.32	Matteucci *et al.*, 2006
Oxygen	O_2	32	0.35	Freude, 2004

Xenon	Xe	131	0.40	Breck, 1974
OTHERS				
Calcium	Ca	40	0.46	Royal Society, 2014a
Glucose	$C_6H_{12}O_6$	180	0.84	Netrabukkana, Lourvanij and Rorrer, 1996
Hydrogen peroxide	H_2O_2	34	0.28	Almasalmeh *et al.,* 2014
Iron	Fe	56	0.41	Royal Society, 2014b
Phosphorous	P	31	0.36	Royal Society, 2014c
Water	H_2O	18	0.20	Almasalmeh *et al.,* 2014

Studies of metmyoglobin, the oxidized form of the haem-containing myoglobin, derived from whale spermatic fluid, observed four discrete ^{129}Xe binding sites within the protein (Tilton, Kuntz and Petsko, 1984). Each ^{129}Xe-binding intra-protein channel was situated antithetically from the O_2 binding site adjacent to the prosthetic iron. In addition, later reports identify two channels by which both O_2 and Xe pass through the protein to reach their respective binding sites have been identified in haemoglobin of *Mycobacterium tuberculosis* (Cazade and Meuwly, 2012). Simulations of dioxygen dynamics recognised Channel 1 as serving as an entry channel for these molecules and NO, whilst Channel 2 was primarily utilised as an exit passage, although this particular channel was noted to be bidirectional. The authors also demonstrate that O_2 utilises Xenon pockets Xe1a and Xe2 as it traverses through the cavity to the haem interface, docking site (DS2/active site). Interestingly, NO was noted to occupy only the Xe2 site which may have further effects, conceivably through inhibiting O_2 release through channel 2 (Figure 4.4). It is therefore plausible that H_2 may utilise such cavities, channels and/or surface pockets to support protein configurations, and extend protein/metal prosthetic bonds (Section 4.3.2), effects that may promote O_2 binding in haem- containing proteins and protect or sustain the catalytic function of metalloenzymes (*e.g.,* CAT,SOD).

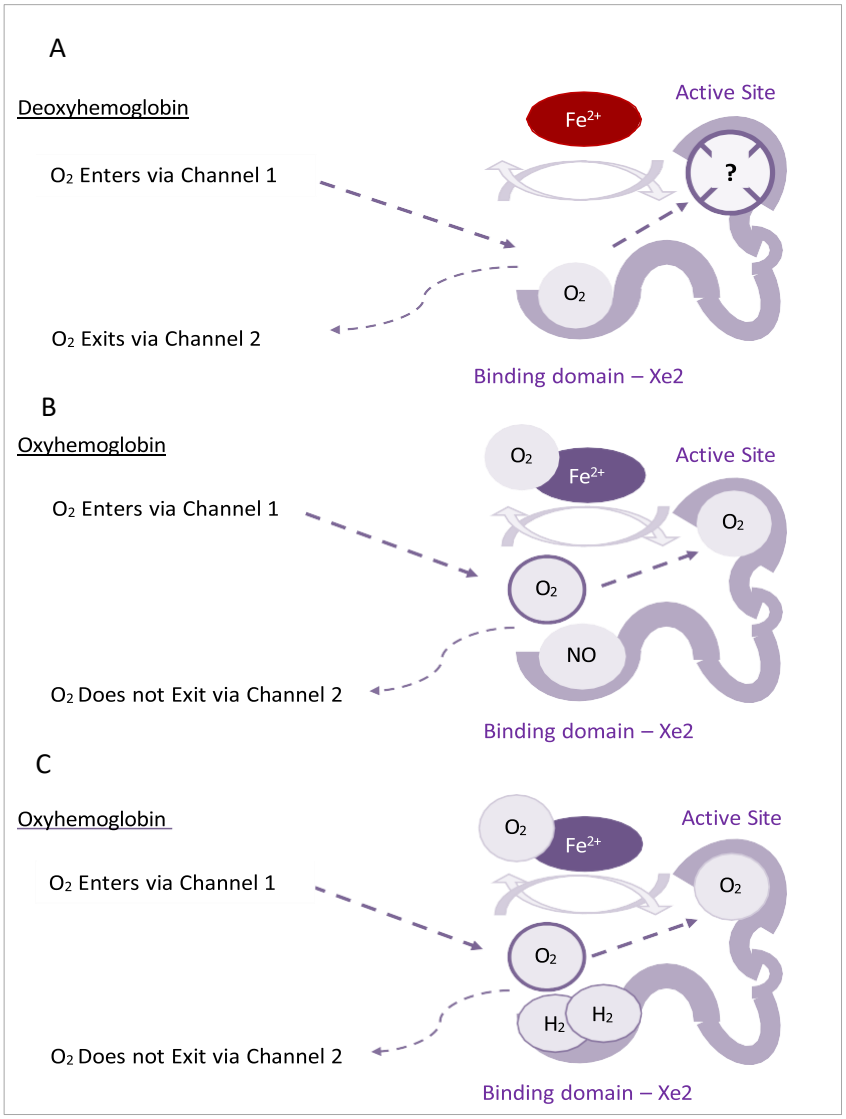

Figure 4.4. Schematic of the potential relevance of 'occupied' Xenon pockets for the oxygenation status of haem. Graphical depiction of how molecules may interact with Xenon pockets, and the possible downstream effects. Active site: DS2 docking domain (Cazade and Meuwley, 2012). (A). Deoxygenated haem with O_2 utilising Xe2 pocket before being expelled into the exit channel. (B). NO binding in Xe2 prevents O_2 binding thereby promoting oxygenation of haem. (C). In similarity with NO, H_2 may occupy Xe2 resulting in haem oxygenation potential.

If such a process is indeed incorporated physiologically, then it can be extrapolated that a similar process may occur in other protein units. Accordingly, should ferromagnetism have a significant role in H_2/protein interactions, it is conceivable that the downstream effects would also be comprehensive (Table 4.5).

Table 4.5. Downstream effects of metalloproteins that may be influenced by H_2, identifying the immediate role and downstream effects of metalloproteins which may be influenced by H_2.

Metalloprotein	Example	Immediate Roles	Downstream Effects	Ref(s)
Dehydrogenases	Complex I (NADH dehydrogenase)	O_2 metabolism	Cellular energy dynamics	Canuto, 2012
Hydratase/Dehydratase	Succinate dehydrogenase/ Fumarate hydratase	Removal of H_2O groups (H + HO)	Cellular energy dynamics	King, Selak and Gottlieb, 2006
Dioxygenases	Indoleamine 2,3-dioxygenase 1	Addition of oxygen	Amino acid metabolism	Tang *et al*., 2021
Dismutases	Superoxide dismutase	Converts oxygen radicals ($2O_2^{\bullet-}$ → $H_2O_2 + O_2$)	Redox status	Mondola *et al.,* 2016
Globins	Haemoglobin	O_2 transportation	Acid/base balance, Hypo/Hyperoxidation status	Pillai *et al*., 2020
Oxidases (Oxidoreductase)	NADH oxidase	O_2 reduction	Redox status, Signalling molecules	Georgiou and Margaritis, 2021.

Proteases	A-disintegrin and metalloprotease 17 (ADAM-17)	Post-translational modification of proteins	Ligand binding, cell signalling	Düsterhöft, Lokau and Garbers, 2019
Synthases	Porphobilinogen synthase	Synthesis of proteins and small molecules	Regulation of cell function	Jaffe, 2020

Supporting the notion that H_2 may be attracted to ferromagnetic moieties, and reside at least temporarily in proteinaceous pockets, it is insightful that for industrial storage purposes, research into H_2-retaining materials has tended to focus on the structural adsorption of H_2 molecules. In fuel cells, carbon nanotubes (Hirscher and Becher, 2003), fullerene nanocages (Shi *et al.,* 2020) and palladium nano-lattice particles (Griessen, Strohfeldt and Giessen, 2016; Narayan *et al.,* 2017) are commonly used for their superior and reversible H_2-retention properties. Metallic ion-containing, organic crystalline structures are noted to have a high capacity for storing H_2. Metalloorganic frameworks are produced using biologically compatible metallic ions (*e.g*., Ca^{2+}, Cu^{2+}, Mn^{2+}, Zn^{2+}) which are connected by organic ligands, forming a microporous structure able to retain H_2 in relatively large quantities up to 5.2% w/w at 1 atm and 196^0C (Rosi *et al.,* 2003; Suh *et al.,* 2012).

The use of such microporous composites is intriguing from a biological stance as the architecture often provides micro-pockets in similarity with the structure of folded proteins. It is therefore feasible that, in accordance with the Xe pocket theory of H_2 activity and distribution (Hancock *et al.,* 2022; Hancock, 2023), H_2 could reside in such cavities, perhaps with metal element interactions. Furthermore, should this phenomenon occur in proteins other than haemoglobin (*e.g*., proteins involved in biomolecule synthesis, DNA repair and replication, and/or metabolism and energy production) (Table 4.5), it could explain the pleiotropic effects of H_2, and account for the movement of H_2 within tissues. Perhaps then, the protein pocket mechanism of H_2 activity may hold some validity. Accordingly, experient data focusing on haem-containing proteins and H_2 interactions, collated using such techniques as nuclear magnetic resonance, and *in silico* modelling, would be highly valued if the questions, i) could metalloproteins be a primary target for H_2 biological effects? And, ii) is a biologically significant level of H_2 retention achieved via metalloprotein absorption at the physiological temperature of 37^0C, are to be addressed.

4.3.4 Glucose and Glycogen

Glucose is a six-carbon monosaccharide with the chemical composition $C_6H_{12}O_6$ which is ubiquitously utilised as an energy source in animals, bacteria, fungi, plants and protozoa. Glucose is the key substrate for both aerobic and anaerobic metabolism in such organisms (Hantzidiamantis and Lappin, 2022). Glycogen, on the other hand, is a large branched-chain polysaccharide storage complex formed of numerous glucose moieties that are connected by two glycosidic bonds, i) an α-1,4-glycosidic bond and ii) an α-1,6-glycosidic bond. In plants, a similar structure known as starch provides the storage capacity for carbohydrates. Unlike the branching-chain structure of glycogen, starch is formed by two polymers, i) amylose, forming linear and coiled chains, and ii) amylopectin that forms branched chains (Wang and White, 1994). Although glycogen and starch structures vary in form, they are chemically identical, with both functioning as energy stores in respective organisms (Brust, Orzechowski and Fettke, 2020). Perhaps then, due to this chemical similarity, both glycogen and starch are likely to have similar H_2-retention capabilities.

In addition to protein structures (Section 4.3.3), glycogen complexes have been identified as effective H_2-retaining molecules, demonstrated in both the liver and skeletal muscle of rodents (Liu *et al.,* 2014; Yamamoto *et al.,* 2019). The liver is the primary source of glycogen production, and concentrations of H_2 in this particular organ (29μmol/L) are noted to exceed that of other systems including the brain (26 μmol/L) and the mesentery (23 μmol/L) (Yamamoto *et al.,* 2019) (Table 1.1). Interestingly, branching glycogen complexes have been identified as effective H_2-retaining molecules (Chapter 4, Section 4.3.4) a factor that may account for protracted activity in the liver (Liu *et al.,* 2014). To illustrate, a study of 3% H_2 inhalation in rodent models identified the cardiopulmonary system and the brain as proximal and primary targets for H_2, however, elevated levels of H_2 were also found in the liver and mesentery (Yamamoto *et al*., 2019). Consuming HRW was demonstrated to reduce glycogen utilisation in the liver in laboratory models of endurance exercise (Kawamura *et al.,* 2019), suggesting H_2 may either inhibit glycogen catalysis or promote glucose transportation into the cells, which would then negate the requirement for glucose release.

In aqueous solutions such as blood plasma or serum, glucose molecules, due to the high hydrogen bond content, become glutinous (i.e., sticky) (Te, Tan and Ichiye, 2010), therefore H_2 may temporarily bind with carbohydrate moieties of glycogen or glycoproteins (Figure 4.5), perhaps also on the surface of red blood cells (Figure 4.6). It can be assumed that weak non-covalent attachments to the glucose components of glycogen (or glucose moieties of proteins) can be made, entrapping the H_2 molecule within the structure which could account for the elevated levels of H_2 in distal sites and in both the hepatic and skeletal muscle systems which are key stores of glycogen. Furthermore, if glutinisation is a mechanism by

which H_2 can adhere, perhaps transiently, to carbohydrate molecules, it would be feasible to assume that in plants the same effects would be seen with starch (Figure 4.5).

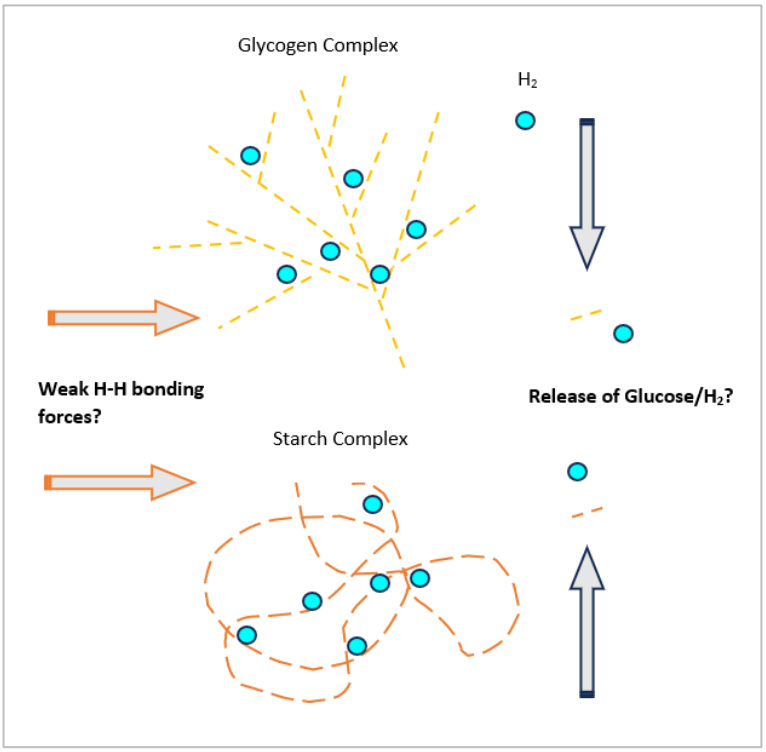

Figure 4.5. A theorised mechanism behind the retention and release of H_2 in glycogen and starch complexes shows a schematic representation of how H_2 may be trapped and released by glucose storage molecules. Above. Glycogen (animals, bacteria, fungi). Below. Starch (plants).

If glucose moieties can retain H2, it would also be reasonable to assume H_2 could bond with free glucose or glycoproteins (e.g., glycophorins A-D on the surface of red blood cells), perhaps preventing glycosylation or other post-translational modifications. Considering dissociation, such weak chemical interactions could be expunged by the velocity of blood flow (Figure 4.6), releasing H2 in the vicinity of distal organs. However, such speculation will need to be empirically assessed if the above theory is to be verified.

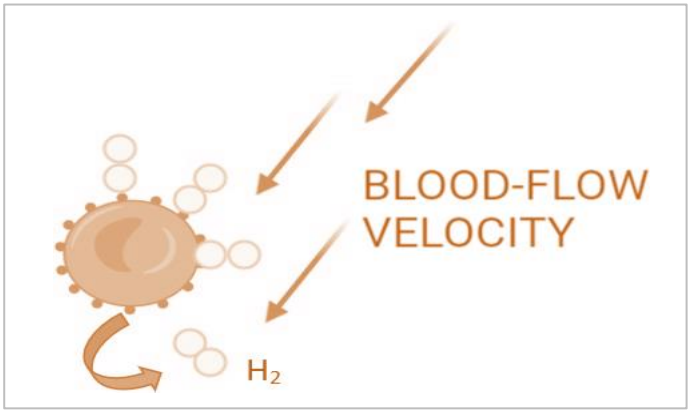

Figure 4.6. A theorised mechanism for H_2 distribution shows a schematic representation of how H_2 may be trapped and released by glycolic moieties of glycolipids/proteins on red blood cells.

4.4 Intracellular Signalling

4.4.1 Calcium Signalling

H_2 is a non-polar, diatomic molecule, a factor that reduces solubility in biological fluids (Roose, Zemerov and Dmochowski, 2018) but enhances the molecules' ability to traverse biological membranes and affect intracellular processes such as signal transduction (Itoh *et al.,* 2011; Begum *et al.,* 2020), gene expression (Morgan *et al*., 1997; Ohta, 2023), and perhaps protein activity and, or conformation as discussed above. When considering cell signalling events, arguably two of the most prominent messengers responsible for regulating cellular activities are the positively charged calcium ion (Ca^{2+}) and the negatively charged phosphate ion (PO_3^{2-}) (Clapham, 2007; Prakriya, 2020). Ca^{2+} regulates a wide range of cellular events including cell contractility and motility, energy metabolism, and neuronal activity, whilst PO_3^{2-} is responsible for the reversible post-translational modifications of proteins (catalysed by kinases for the addition of PO_3^{2-} and phosphatases for the removal of PO_3^{2-}), an action known to alter the polarity of proteins from hydrophobic (apolar) to hydrophilic (polar), enabling protein-protein interactions (Prakriya, 2020).

Ca^{2+} signalling is integral for optimal cellular function and can have wide-ranging influences within the cytoplasm, organelles, and the extracellular milieu. Ca^{2+} signalling is fundamental to canonical stress responses in many cell types including endothelial and epithelial cells which rely, directly and indirectly, on Ca^{2+} influx through membrane-bound ion channels (Filippini, D'Amore and D'Alessio, 2019). Cellular responses to Ca^{2+} signalling are largely dependent on the concentration, spatial orientation and chemo-physical characteristics of Ca^{2+}. Ca^{2+} molecules are highly mobile, travelling through saline solutions rapidly at 40 nm/ms (Einstein, 1905). Therefore, Ca^{2+} signalling is tightly regulated to ensure highly spatially restricted signalling, with cells chelating, compartmentalising, or extruding Ca^{2+} using an array of protein antiporters, ion channels and pumps controlling localised concentrations (Clapham, 2007; Thor, 2019), any, or all, of which may be influenced by H_2.

Interestingly, industrial production of H_2-retaining nanoparticles can involve coating the preformed structures with a layer of Ca^{2+} to augment and reinforce H_2 adsorption (Yoon *et al.,* 2008; Beheshti, Nojeh and Servati, 2011), indicating that H_2 may directly interact with such ions. A*b initio* calculations demonstrate that H_2 can bind with the Ca^{2+} component of calcium oxide (CaO) through weak electron-donation forces, wherein electron transfer occurs from the occupied H_2 σ-orbital to the unoccupied 3δ-orbital of Ca^{2+} (Kim, Sun and Zhang, 2009). If such

binding were to occur under physiological conditions, it would be feasible to assume a strong affinity between Ca^{2+} and H_2 exists, with H_2 perhaps affecting the Ca^{2+}-calmodulin binding potential, an event that would have significant downstream effects on gene transcription, immune responses and muscle contraction (Figure 4.7). Calmodulin (CaM) is a highly conserved sensor of Ca^{2+} which has a fundamental role in cellular signalling (Hussey, Limpitikul and Dick, 2023). The double-lobed CaM molecule can bind up to four Ca^{2+} molecules with each binding region asserting individual effects on protein conformation, thus affecting further Ca^{2+} binding and target recognition (Kawasaki, Soma and Kretsinger, 2019).

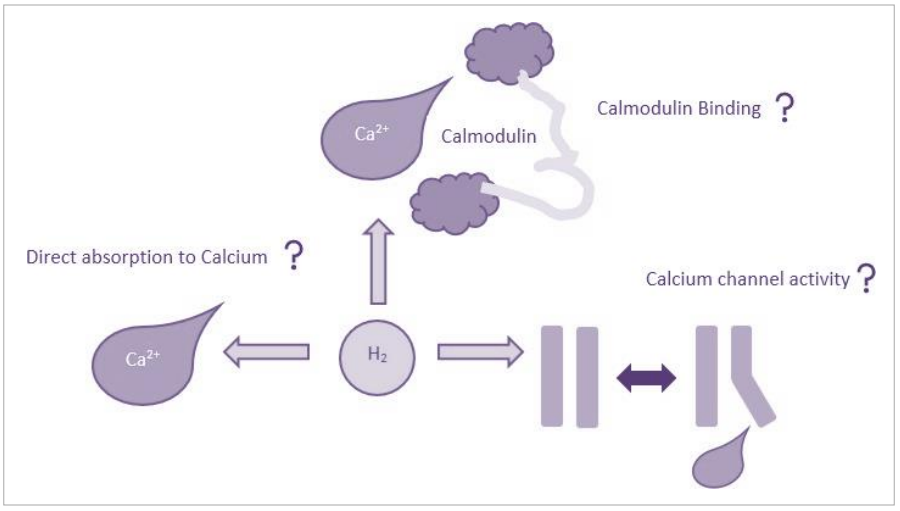

Figure 4.7. Potential effects of H_2 administration on Ca^{2+} signalling. A schematic representation of how H_2 may affect Ca^{2+} signalling

Although evidence is sparse regarding H_2 interactions with Ca^{2+} and Ca^{2+}-derived signalling cascades, Iuchi *et al*. (2016) demonstrated that in a pure chemical system, H_2 can prevent auto-oxidation of unsaturated fatty acids, a factor that reduces Ca^{2+} signal transduction and downstream Ca^{2+}-regulated gene expression. The team theorised that the effects on Ca^{2+} signalling were likely to be a result of a decrease in agonist inducers, or antagonist inhibitors, although did not speculate as to whether H_2 could directly interact with the calcium ion (Iuchi *et al*., 2016). Direct H_2/Ca^{2+} interactions could also affect the production and activity of ROS as Ca^{2+} overload can negatively impact the function of Kreb's cycle enzymes provoking ROS-generating enzyme activation (*e.g.,* α-ketoglutarate dehydrogenase); and via indirect activation of nitric oxide synthases (NOS), a factor that can effectively inhibit the function of cytochrome *c* oxidase (Complex IV), increase electron leakage, and ultimately promote mitochondrial dysfunction (Feno *et al*., 2019).

Alternatively, H_2 may have an indirect influence on calcium signalling, via upstream effects. For example, H_2 could influence ion channel function. If so, would the characteristics of H_2 activity be analogous to the proposed mechanism discussed for metalloproteins and enzymes? For example, Xenon, which utilises protein pockets (Section 4.3.3), is noted to

inhibit calcium signalling (McGuigan *et al.,* 2023), therefore could H_2 utilise similar, or disparate, mechanisms to regulate Ca^{2+} signalling?

In elucidation of this conundrum, Itoh *et al.* (2011) proposed that H_2 treatment suppressed LPS-induced phosphorylation of apoptosis signal-regulating kinase 1 (ASK1) and its downstream effector proteins (*e.g.,* c-Jun N-terminal kinases (JNKs), p38) in macrophage, without affecting NOX-1 production of ROS. Therefore, the potential target(s) for H_2 interactions could be found either at the receptor proteins or immediately downstream of them. These findings are intriguing as they suggest i) Ca^{2+}, either directly or indirectly, could be a target for H_2, with cellular levels being directly affected by the configuration of transmembrane ion channels and antiporters, and/or the size, shape and electrophilic status of Ca^{2+}; and ii) that the primary mechanism of H_2 action may not be related to the direct reducing potential of H_2, but through the regulation of Ca^{2+} influx or activity. Therefore, the question 'does H_2 inhibit ROS/RNS generation by regulating Ca^{2+} influx?' should be considered.

4.4.2 Protein Phosphorylation

Protein phosphorylation is a cardinal mechanism by which intracellular information is communicated in eukaryotic cells. Phosphorylation involves the reversible, post-translational modification of an amino acid (serine, threonine, tyrosine or histidine), through the addition or removal of a PO_3^{2-} phosphoryl group (Newcombe *et al.,* 2022). The addition of the PO_3^{2-} molecule to protein residues alters the conformational structure, and therefore the function, of the modified protein. Kinase enzymes are responsible for facilitating the addition of to the target amino acid, whilst phosphatases catalyse the removal of the molecule.

Kinases are known to form cascades wherein phosphorylation of an antecedent protein leads to sequential phosphorylation of proteins downstream. A good example of this are the MAPK/ERK cascades that mediate between extracellular and intracellular responses to a range of stimuli including cytokines, growth factors, mitogenic substances such as pathogen-associated compounds (*e.g.,* LPS) and oxidative stress (Son *et al.,* 2011). MAPK/ERK is a term for a supergroup of proteins related to signal transduction that are highly conserved throughout eukaryotic species. MAPK pathways utilise numerous, characteristically distinct, proteins (*e.g.,* ERK 1/2, JNK, p38) to relay a signal through the cell to inducible (*e.g.,* Nrf2), or transcriptional elements (*e.g.,* ARE) which further influence cellular activity. To exemplify, activation of serine/threonine MAPK3s through extracellular stimuli or GTP-binding proteins induces the phosphorylation and subsequent activation of MAPK2s. MAPK2s then participate in the dual phosphorylation of the conserved Thr-X-Tyr motif within the activation loop of MAPK (Cargnello and Roux, 2011). MAPKs phosphorylate target substrates on amino acid residues

that are upstream of proline (*e.g.,* Thr-X-Tyr-X-Pro). This mechanism confers specificity of signal transduction, an important factor when considering more than 13000 human proteins are known to be altered through phosphorylation/dephosphorylation events (Vlastaridis *et al.,* 2017). A pro-oxidative cellular environ is known to initiate MAPK pathway signalling which drives the cell towards protection and preservation responses through activating cellular differentiation, motility, proliferation, and of survival pathways (Cargnello and Roux, 2011). Therefore, if H_2 is able to inhibit phosphorylation cascades, through either accumulating in protein pockets (Section 4.3.3) or acting directly on phosphoryl groups, or targets of phosphorylation (*e.g.,* serine, threonine, *etc*.), perhaps via quantum forces (*e.g.,* London dispersion), it could provide a unifying theory to the pleiotropic effects noted in contemporary literature (Itoh *et al.,* 2009; Xia *et al.,* 2013; Zhuang *et al.,* 2020; Slezak *et al.,* 2021; Li *et al.,* 2022).

p38, a highly conserved evolutionary MAPK protein, in particular is associated with heightened inflammatory responses. For instance, increased p38 activity is associated with a higher risk of malignancy, whilst MAPK/p38 inhibitors are demonstrated to reduce inflammation, a hallmark of oncological disease (Naser *et al.,* 2023). H_2 is demonstrated to inhibit MAPK/ERK/JNK/p38 signalling *in vitro* utilising both somatic cell cultures (Begum *et al*., 2020) and gametes (Ma *et al.,* 2022), and also *in vivo,* in rodent models of disease (Liang *et al.,* 2012; Wang *et al.,* 2020b). Although whether the observed effects of H_2 application are due to the increased activity of phosphatases, a reduction of kinase activity, as a result of reduced NFκB/TNF-α activity, or another yet-to-be-defined mechanism (Figure 4.8), is largely unknown.

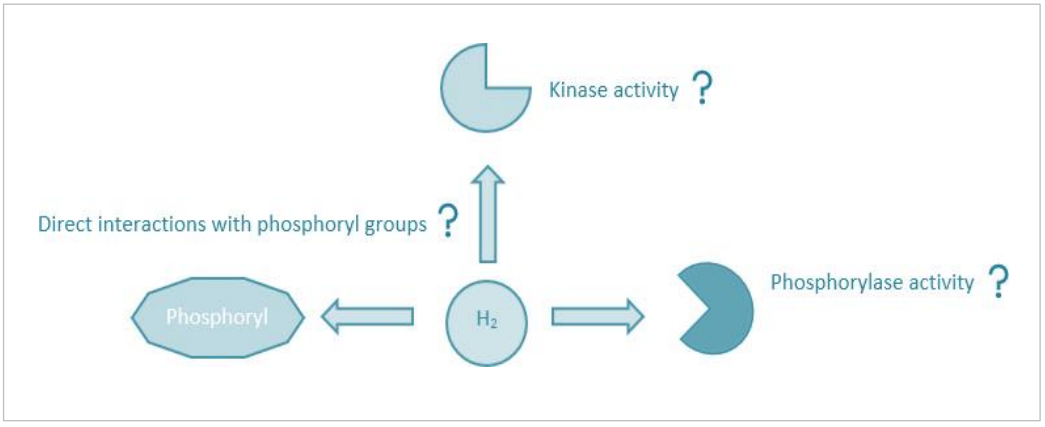

Figure 4.8. Potential effects of H_2 administration on PO_3^{2-} signalling. Schematic representation of how H_2 may affect PO_3^{2-} signalling

4.4.3 Magnetoelectrochemistry

Research into biomagnetism, the magnetic fields produced by living organisms, is well-established with the magnetic field of the heart and brain, magnetocardiogram, and magnetoencephalogram, respectively, being regularly utilised in clinical practice (Roth, 2023).

It is also well-documented that magnetic forces can alter the dynamics of electron spins. Herein, the question as to whether the quantum forces of ferromagnetic prosthetic groups, such as in haem (Fe), or SOD (Mg, Cu), influence the spin-states and therefore the biological activity of H_2, is discussed.

Thermal polarisation of H_2 is known to favour the triplet electron state with most H_2 molecules being observed as in the ortho, or triplet state, at room temperature (~75% ortho/25% para spins) (O'Neill *et al.,* 2023). As the ortho spin of electrons creates a weak diamagnetic, repelling force (Tarzad, 2020), it is unlikely to directly reduce ROS, as one force is likely to repel the other. Nevertheless, it is possible that the triplet spin H_2 molecule could influence such aspects of cell biochemistry as gene expression, protein conformation and/or signal transduction. Although currently a speculative assumption, in depth analyses of the quantum forces driving H_2 biological interactions could provide valuable data.

Although the majority of physiological H_2 may have diamagnetic properties, the impact of the para, or singlet state, H_2 may be of equal importance. The para-spin H_2 molecule, accounting for approximately 25% of physiological H_2 produces a weak paramagnetic, or attractive, force. The singlet state may have redox active potential via magnetoelectrochemical attraction to metalloproteins and prosthetic groups. Radical formation occurs when forward electron translocation is inhibited (e.g., Complex I, mitochondria), and this contributes to ROS formation (Hore, 2012). To illustrate, a flavin- superoxide radical pair ($FH^{\bullet} + O_2^{\bullet-}$) with a singlet spin ($O_2$), will form $F + H_2O_2$, whilst the same pair with the triplet spin state will disassociate, resulting in two free radical molecules, $FH^{\bullet}$ and $O_2^{\bullet-}$ (Ramsey and Kattnig, 2022). Therefore, should H_2 with electrons in the singlet configuration directly interact with transition metal components of proteins, as described by Hancock and Hancock (2018), Kim *et al*. (2022) and (Ohta, 2023), it is possible that the metal group would catalyse the reduction of radicals via reducing the disassociation energy of free H_2 (~4.64 eV - ~2.35 eV) and the formation of an acceptor/$H^{\bullet}$ complex. Logically, the $H^{\bullet}$ radicals could react with oxidants as $O_2^{\bullet-}$ and $^{\bullet}OH$, although as stated in Section 4.2, this would be determined by spatial and temporal availability of the perceived radicals.

Of further consideration for the magnetoelectrochemical effects of H_2 are the metal catalytic centres of such antioxidant enzymes as CAT and SOD, reported to have enhanced activity after exposure to H_2. It can be surmised that singlet spin H_2 may also improve the function of such enzymes by providing additional $H^{\bullet}$ and preserving the reductive capacity of the catalytic metal elements, although this has yet to be empirically verified.

It is therefore plausible, that due to the weak magnetic forces at play, the singlet spin molecule may have antioxidant effects, whilst the triplet state H_2 molecule may influence such cellular

activities as cell signalling, gene regulation and metabolic activity, through stabilising protein structures (Section 4.3.3). When extrapolating the triplet spin state, H_2 could also mediate cell signalling by promoting or inhibiting protein phosphorylation/dephosphorylation events, which is likely to depend on the protein's original function and/or configuration. Should these theoretical concepts be accurate, they could account for the pluripotent effects of H_2 in living systems. Moreover, both the direct antioxidant activity as suggested by Ohsawa *et al.* (2007), Barancik *et al.* (2020), Tian *et al.,* (2021) and Jin *et al*. (2023), and the effects upon cell signalling and gene regulation as described by Itoh *et al*. (2007), Wilson *et al.* (2017), Itoh *et al*. (2019) and Slezak *et al.* (2021), can be reconciled.

Chapter 5: HydroVitality™ Water Electrolysis

5.1 Introduction

First demonstrated in 1789 by Dutch traders Adriaan Paets van Troostwijk and Jan Rudolph Deiman (Chisholm and Cronin, 2016), the electrolysis of water was shown to produce hydrogen and oxygen gases in stiochemical proportions. However, the development of this technology for industrial purposes is credited to both London-based developers Sir Anthony Carlisle and William Nicholson (1800) (Leech and Lam, 2022), and later to the Russian engineer Dmitry Lachenov (1888) (Chisholm and Cronin, 2016).

In the 1970's Professor Yull Brown (Rao, Babu and Rajesh, 2018) patented an oxyhydrogen generator for use as a torch in welding operations (U.S patent – #4014777, 29th March 1977) (Chapter 1, Section 1.4). Latterly, Prof. Brown's technology has been further developed by commercial enterprises to provide a constant flow of oxyhydrogen gas for consumption via inhalation. For instance, devices producing 3L/min of oxyhydrogen have been tested in a clinical capacity in the People's Republic of China (Asclepius) (Guan et al., 2020), whilst other H_2-only and oxyhydrogen-producing devices, with variable flow-rates (450mL – 3L/min), are commercially available.

Most commercially available water electrolysers employ one of two means of hydrogen production involving either an alkaline water electrolysis (AE) which produces oxyhydrogen gas (Figure 5.1), or proton exchange membrane (PEM) (Figure 5.2), which typically produces H_2 gas, with O_2 being ventilated as a byproduct (Wang, Cao and Jiao, 2022).

5.2 Alkaline Water Electrolysis

Alkaline water electrolysis (Figure 5.1) is a process that involves passing a current through an aqueous substance, typically containing a catalyst such as sodium hydroxide (NaOH) or potassium hydroxide (KOH) to instigate the decomposition of the hydrogen-oxygen chemical bond. This electrochemical process produces reactions 1 and 2.

Reaction 1: $2\ H_2O\ (a) + 4\ e^- \rightarrow 2\ OH\text{-}\ (a) + H_2\ (g)$

Reaction 2: $4\ OH^- \rightarrow 2\ H_2O\ (a) + O_2\ (g)$

The gases formed as a result of AE are separated by a porous diaphragm and attracted to either the negative electrode (H^+) or the positive electrode (OH^-), where they recombine, forming H_2 and $O_2 + H_2O$, respectively, and are liberated from the solution. These gases can then be harnessed for multiple purposes, including as a fuel additive for combustion engines or inhalation purposes.

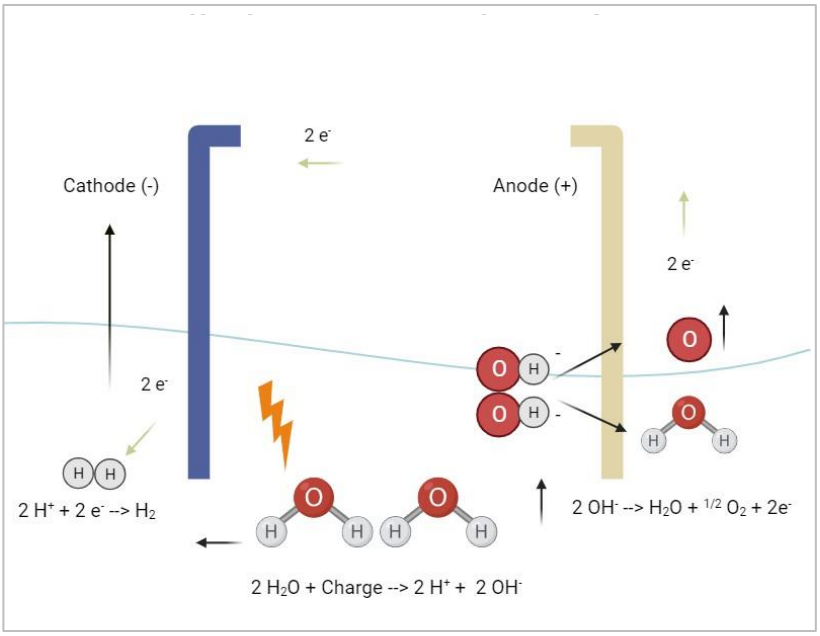

Figure 5.1. AE electrolysis. A schematic representation of the decomposition reactions that take place during alkaline water electrolysis.

5.3 Proton-Exchange Membrane

In contrast, PEM technology (Figure 5.2), developed in 1966 by the General Electric Company, utilises a solid polymer electrolyte membrane (e.g., Nafion) coated in a catalyst (e.g., iridium), along with an applied current, to separate positively charged protons (H^+) from oxygen (Kumar and Himabindu, 2019) (Reaction 3).

Reaction 3: $2\ H_2O \rightarrow 4H^+ + O_2 + 4\ e^- \rightarrow 2\ H_2 + O_2$

The negatively charged electrons (e^-) are transported, via electrical circulation, from the anode to the cathode where the protons and electrons recombine, forming H_2. This technique typically releases O_2 into the surrounding atmosphere and is used in many commercial H_2 infusion and inhalation devices.

To date, there is no upper limit to H_2 dosing as there are no indications of H_2 toxicity (reviewed by Johnsen, Hiorth and Klaveness, 2023), whilst O_2 is a diradical, reactive molecule, required for such essential cellular processes as energy metabolism, and in remedial doses (< 2L/min) is well-tolerated by the body (O'Driscoll *et al.,* 2017). Such is the human requirement for O_2; lack of it for more than a few minutes can be fatal (Parkes, 2012). Therefore, it is logical to assume oxyhydrogen inhalation is likely to be more appropriate for use as a therapeutic agent than H_2-only producing devices as the O_2 content of inhaled breath can be sufficiently reduced with H_2-only machines, increasing the possibility of asphyxiation, light-headedness and unconsciousness.

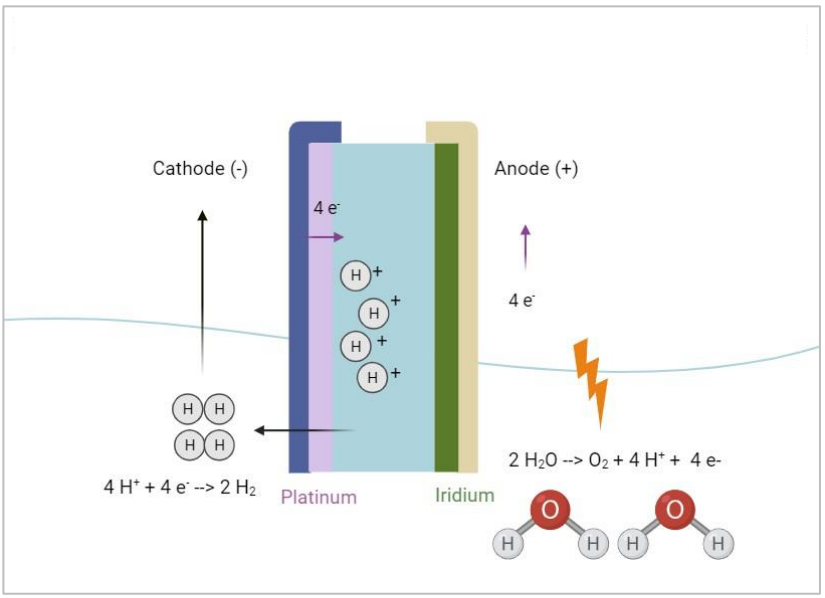

Figure 5.2. PEM electrolysis. A schematic representation of the decomposition reactions that take place during PEM water electrolysis. Central pale green block represents the proton exchange membrane. O_2 is vented from the system into the external atmosphere.

Although the respective technologies vary in ionic exchange potential, materials and reaction specifics, each technology (AE/PEM electrolysis) shares the same basis of core components: an electrolyte responsible for ionic conductivity, an oxygen electrode (anode) for the oxygen evolution reaction and a hydrogen electrode (cathode) responsible for the hydrogen evolution reaction.

Both forms of water electrolysis (AE/PEM) essentially perform the same task, utilising the electrochemical reaction to decompose water molecules (H_2O) into the constituent gases H_2 and O_2. However, as the polymer membrane of PEM devices separates the produced gases, these are more typically used for pure H_2 inhalation, with the produced O_2 being expelled into the surrounding atmosphere as waste. To summarise between AE and PEM electrolysis methods, Table 5.1 highlights the main differences that may be pertinent to the commercialisation of these inhalation devices.

Table 5.1. Comparison between AE and PEM electrolysis devices.

	AE	PEM	References
Purity of Gas	99%	99%	Guo *et al.,* 2019
Ion exchange	OH^- (Alkaline)	H^+ (Acidic)	Kumar and Himabindu, 2019
Catalyst	NaOH/KOH (liquid)	Iridium/Platinum/Rubidium (solid)	van Haersma Buma *et al.,* 2023
Cost of electrode stack production	Inexpensive (£211 – 339)	Expensive (£335 – 935)	Krishnan *et al.,* 2023
Efficiency	62 – 82%	67 – 84%	Nasser *et al*., 2022
Longevity of electrode stacks	~ 90,000 hours	~ 40,000 hours	Järvinen, 2020

5.4 HydroVitality™

As an emerging technology in the field of medical therapeutics, it is important to understand not only the benefits of oxyhydrogen inhalation but also to assess the quality and safety of the devices used to generate the gases consumed. As HydroVitality™ is a commercial product, verification of the device output (flow rate), the purity of gas released and the content of dissolved gas in potable water was assessed (Sections 5.4.1 – 5.4.5). Such safety parameters as operational temperature (< 60^0C), power consumption (< 79 W), pressures (< 0.2 bars) and optimal concentration of the electrocatalyst (20% KOH) had been previously determined by the manufacturers (Water Fuel Engineering, Wakefield, UK).

The HydroVitality™ generator, used for producing oxyhydrogen in the experimental section of this thesis (Chapters 6 and 7), utilises AE technology. HydroVitality™ is a compact (300 x 300 x 250mm), lightweight (8kg) and self-regulating, water electrolysis device that has an integrated electronic control unit (ECU). The ECU regulates the voltage and current passed through the stainless steel electrolysis plates, monitoring such operational parameters as pressure, temperature and electrolyte level. If an electrical surge or operational parameters are superceded, the ECU ensures electrolytic functions are discontinued.

Although either KOH or $NaCHO_3$ can be used as electrolyte catalysts for AE, the HydroVitality™ system employs KOH. If sodium bicarbonate were used this would give 66% hydrogen, 30% CO and 4% CO_2 (Mishra, Khatri and Kumar Jain, 2018) which would be detrimental to health. Furthermore, as both O_2 and H_2 can react with carbon, abundant in the atmosphere and readily dissolvable in aqueous solutions, forming such noxious gases as CH_4, CO_2 and CO. Therefore, it is imperative that the emissions from such devices are assessed (Section 5.4.2).

In addition to producing oxyhydrogen for inhalation, the HydroVitality™ generator can produce

hydrogen-rich water (HRW) when using an accompanying stainless steel diffusion stone (0.5 microns) (Section 5.4.3 and 5.4.4). When the diffusion stone is submerged in aqueous solutions it facilitates gas infusion through pressure, allowing the solution to absorb the hydrogen gas. The HRW produced using this method can then be used for either drinking or bathing in humans and animals, or as a topical treatment for seeds, plants, fungi and fruits.

To assess the flow rate, purity of gas, and the effects of infusing potable water with oxyhydrogen, this chapter focuses on the operational output and infusibility factors of the HydroVitality™ device.

5.4.1 Analysing the Flow Rate of the HydroVitality™ Oxyhydrogen Generator

To assess the flow rate of HydroVitality™, the water displacement method was utilised (Chapter 2, Section 2.2.1.1). The results shown in Figure 5.3 identify that the device produces gas at the rate of 425 (± 26.36) mL/min.

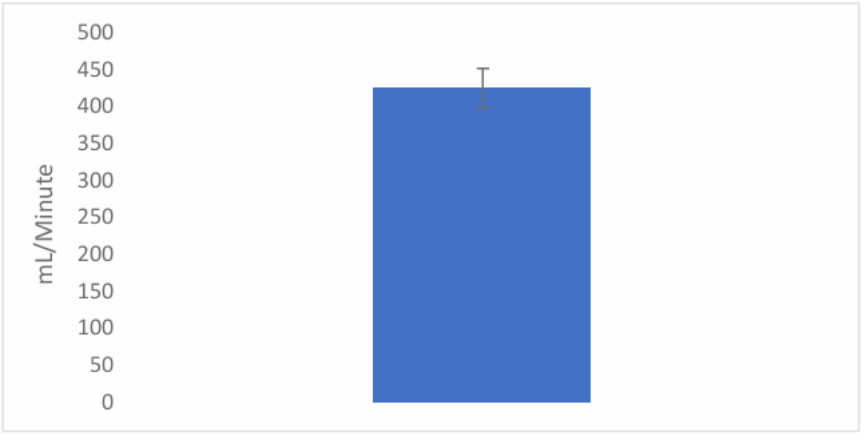

Figure 5.3. Bar chart depicting the mean results of water displacement tests (*n* = 5). Error bars denote ± SEM.

5.4.2 Summary of Gas Analysis

To ensure the gas produced by HydroVitality™ is not contaminated with potentially hazardous or noxious compounds, gas chromatography analysis was outsourced to SGS Gas Analysis Services (Chapter 2, Section 2.2.1.2) (Figure 5.4 (A-D)).

As sulphur is known to combine intrinsically with iron and base metals (Schrama *et al.,* 2017), and inhalation of sulphur-containing compounds can severely irritate the breathing tract (Orellano *et al.,* 2021), to ensure that particulate matter from the stainless steel electrodes (comprised of iron and carbon) does not contaminate the gas, sulphurous compounds methanethiol, ethanethiol, dimethyl sulphide and diethyl sulphide, along with the total sulphur content were also analysed. As negligible amounts of sulphur were detected, it can be assumed with some certainty that potentially harmful hydrogen sulphide (H_2S) or sulphur dioxide (SO_2) gases are not produced by the HydroVitality™ system (Figure 5.4 (D)).

A

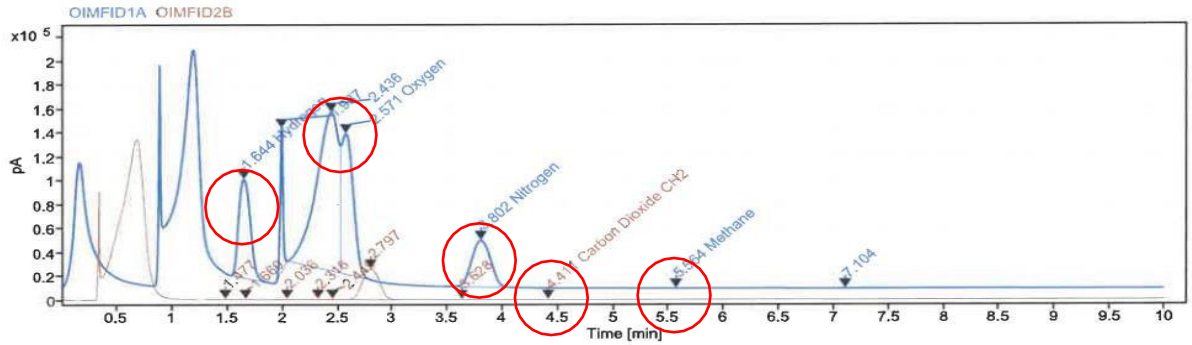

B

Signal: OIMFID1A

Name	RT [min]	RF	Area	Amount [ppm]	Concentration [ppm]	Group
Hydrogen	1.64	359.163	598563.339	1666.550	1666.550	
Oxygen	2.57	1070.871	875227.315	817.304	817.304	
Nitrogen	3.80	1641.822	469222.593	285.794	285.794	
Methane	5.56	3654.439	1498.726	0.410	0.410	
			Sum	2770.058		

Signal: OIMFID2B

Name	RT [min]	RF	Area	Amount [ppm]	Concentration [ppm]	Group
Carbon Dioxide CH2	4.41	324.624	100.872	0.311	0.311	
			Sum	0.311		

C

Tested by	CB	Date	22Feb23
Result	CO_2 = 0.311 ppm, CO NO < 0.1 ppm		
Specification	INFO		
Pass / Fail	N/A		
Approved by:	AEM	Date	23Feb2023
Comment:	N/A		

D

Tested by	AEM	Date	16Feb23
Result	Total Sulphur NO < 0.1 ppm		
Specification	INFO		
Pass / Fail	N/A		
Approved by:	CB	Date	21Feb23
Comment:	N/A		

Figures 5.4 (A-D) Gas chromatography output. (A) The graph depicts the results of the analysis. Circled from left to right: hydrogen, oxygen, nitrogen, carbon dioxide and methane. (B) shows the data translated into parts per million (ppm). (C) CO shows negligible levels of <0.1 ppm, whilst CO_2 is present at 0.311 ppm. (D) Total sulphur content shows ≤0.1 ppm.

The high level of nitrogen in the atmosphere can be difficult to exclude when testing gaseous substances, this is reflected in the analysis (Figure 5.4 (A and B)). Similarly, atmospheric carbon dioxide is readily dissolvable in water, with trace amounts highly likely to have been present in the water used in the bubbler and/or reservoir. The modest CH_4 results given (Figure 5.4 (A)) are likely to be due to traces of dissolved CO_2 in the bubbling or reservoir water reacting with the large amount of H_2 produced by water electrolysis. The results in Figure 5.4 (A-C) identify only trace amounts (< 0.01%) of carbon-based contaminants such as CO, CO_2 and CH_4. With negligible concentrations of carbon-related products reported, it can be confidently assumed that the HydroVitality™ oxyhydrogen generator operates as a closed and pure system. Assessment of sulphur compounds which may form as a result of electrode instability, was also determined to be negligible (Figure 5.4 (D)).

Table 5.2 identifies 10.32% of N_2 present in the analysis. Considering i) atmospheric air contains 78% nitrogen, ii) that evaluation of gases is inherently at risk of atmospheric contamination, and iii) the HydroVitality™ device is a sealed unit. Dissolved gases such as N_2, O_2 and CO_2 in the reservoir are to be expected (applying Henry's Law, the amount of air dissolved in a fluid is proportional to the pressure in the system). It is assumed, therefore, that the nitrogen content is a result of contamination from the environment during collection or testing.

Table 5.2. The gaseous output of HydroVitality™ and inferred output, accounting for atmospheric N_2 contamination.

Compound	**Results (%)**	**Inferred Output Percentage (%)**
Hydrogen	60.16%	66%
Oxygen	29.50%	33%
Nitrous oxide	-	-
Nitrogen	10.32%	-
Methane	0.01%	0.01%
Carbon dioxide	0.01%	0.01%
Carbon monoxide	-	-

5.4.3 Concentration and Retention of H_2 in Oxyhydrogen-infused Water

To identify the concentration of H_2 in HydroVitality™- infused water, quantification of diffused H_2 in distilled water, using the methylene blue-platinum colloidal nanoparticle titration method (Zhu *et al.,* 2023) (Chapter 2, Section 2.2.1.3), is established.

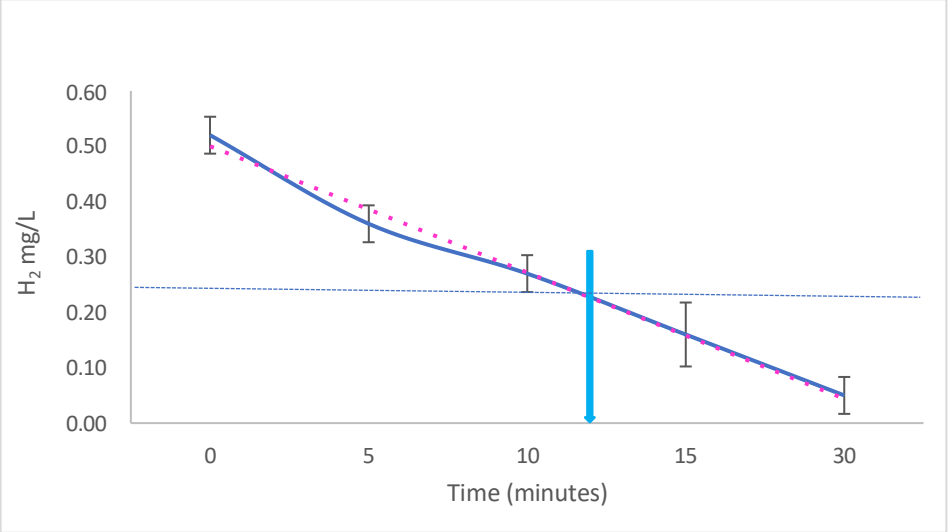

Figure 5.5 Concentration and retention of H_2 in 250 mL of water measured with H_2Blue. The solid blue dots represent the data points. The dotted pink line shows the linear trend of observations. The dotted black line indicates half of the original concentration (H_2). The blue arrow indicates the extrapolated 50% reduction in dissolved H_2. Error bars denote ± SEM. Baseline levels of H_2 were 0 mg/L.

Figure 5.5 identifies that the HydroVitality™ device generates water containing 0.52mg/mL, H_2. The rate of H_2 concentration diminishing by 50% is estimated to be approximately 12 minutes under experimental conditions.

5.4.4 Concentration and Retention of O_2 in Oxyhydrogen-infused Water

Although H_2 may be the active antioxidant component in oxyhydrogen gas, documenting the rise in diffused O_2 levels is of equal interest as O_2 is also a biologically active substance. Levels of O_2 in infused water were determined using dissolved O_2 detection meter (Chapter 2, Section 2.2.1.40). The baseline concentration of O_2 in non-infused water was 8.69 mg/L, this rose above the saturation level of O_2 (12.5 mg/L) to 14.05 mg/mL of O_2 (250 mL) after 30 minutes of infusion (Figure 5.6). The 50% reduction of dissolved O_2 was determined to be approximately 7 hours (420 minutes).

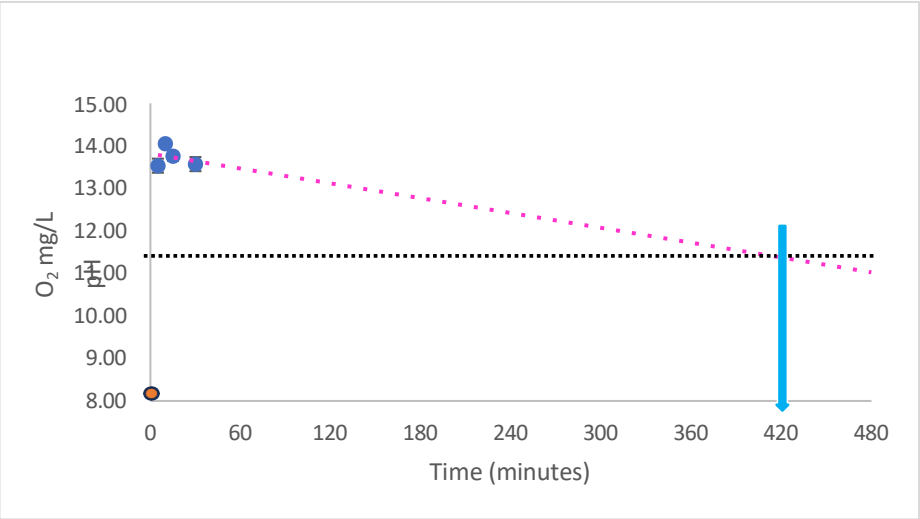

Figure 5.6 Concentration and retention of O_2 in 250 mL of water, measured with Clark-type electrode. The solid blue dots represent the data points. The orange dot indicates the O_2 level before infusion. The dotted pink line shows the linear trend of observations. The dotted black line indicates half of the infused concentration (O_2). The blue arrow indicates the extrapolated 50% reduction in dissolved O_2. Error bars denote ± SEM.

5.4.5 pH Analysis of Oxyhydrogen-infused Water

As the pH of aqueous solutions can directly affect chemical reactions, to better understand the effect of dissolving oxyhydrogen on the pH of potable water, recordings were taken (Chapter 2, Section 2.1.1) 10 and 20 minutes post-infusion (Figure 5.7).

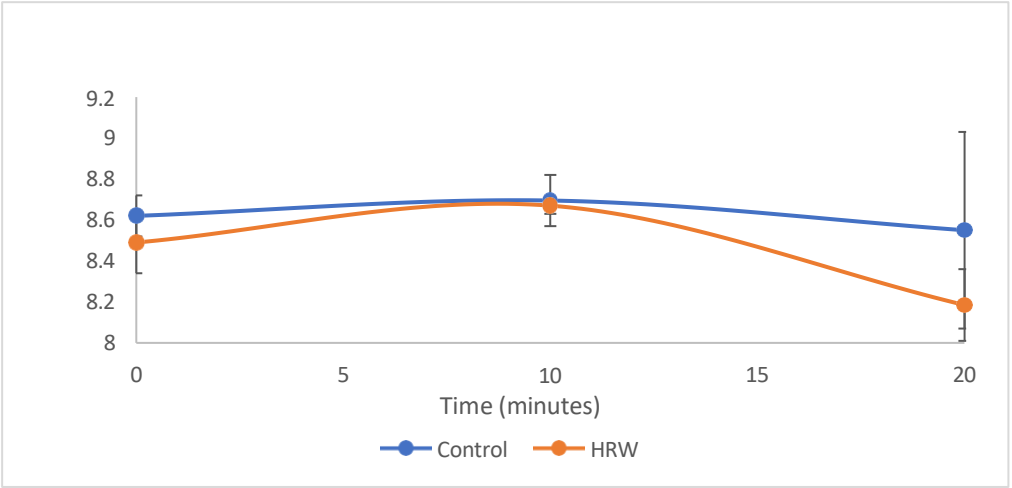

Figure 5.7 The pH of oxyhydrogen-infused water was measured using the Jenway 3510 pH meter. The blue line indicates the control group. The orange line indicates HRW. Error bars denote ± SEM.

5.5 Summary of Findings

To summarise, the commercially available HydroVitality™ alkaline water electrolysis device produces up to 450mL/min of oxyhydrogen gas with the capacity to infuse 250 mL of H_2O with 0.52 mg/L H_2 and 14.05 mg/L O_2 after 30 minutes of infusion. Although the pH of potable water is slightly raised by the infusion process, it remained within the UK government safety

parameters (The Water industry Act, 1991) under experimental conditions. The purity of gas produced by the HydroVitality™ device was deemed to be > 89%, however, when accounting for atmospheric contamination of N_2 within the experimental protocol, it can be inferred that HydroVitality™ creates gas with a purity of 99% (Table 5.2). Furthermore, as HydroVitality™ can be used for inhalation purposes and the infusion of aqueous solutions with both H_2 and O_2, which provides an accessible source of HRW with therapeutic value (0.52 mg/L H_2) (inthlsa.org), it is well placed in the commercial domain.

Chapter 6: Proof of Concept Inquiries

6.1 Introduction

As noted in Chapter 1, Section 1.2, the ability of H_2 to traverse biological membranes is likely to be highly influential, affecting fundamental organelle biochemistry as well as cytosolic reactions, offering a possible explanation as to why the application of H_2 is demonstrated to have positive effects in numerous disease models in both animals, including humans, and plants (Ohsawa et al., 2007; Nishimaki *et al.,* 2018; Johnsen, Hiorth and Klaveness, 2023; Zhu *et al.,* 2023). One of the primary functions of H_2 utilization in both agricultural and clinical settings is as an antioxidant, first demonstrated by Ohsawa *et al.* (2007), in a rodent model of ischemia/reperfusion injury. The highly influential study describes the selective reduction of the highly reactive $^{\bullet}OH$ and $ONOO^-$ molecules, but no reduction in the important signalling molecules H_2O_2 and $NO^{\bullet}$ (Ohsawa *et al.,* 2007). Although the direct antioxidant activities of H_2 are disputed (Chapter 4, Sections 4.2.1 and 4.2.2), by selectively neutralising only the most detrimental ROS/RNS, this mechanism could effectively allow cells to upregulate the expression of antioxidant proteins and peptides, (*e.g.,* CAT; Nrf-2; SOD) (LeBaron *et al.,* 2019a). Upregulation of such endogenous antioxidants is known to enhance tolerance to such environmental stressors as infectious and non-infectious diseases in humans (Ge *et al.,* 2017), and salinity, drought and temperature stress in plants (Hancock and Russell, 2021). Furthermore, H_2 is an ideal candidate as an adjunctive therapy as numerous clinical studies (Supplementary section: Table 1) demonstrate that H_2 is a non-cytotoxic substance which to date, shows no contraindications with other medical interventions including certain drugs (Nakashima- Kamimura *et al.,* 2009), chemotherapeutics (Li *et al.,* 2019b) and immunotherapy treatments (Wu *et al.,* 2019).

6.2 Aims

To better understand the effects of oxyhydrogen administration upon cellular growth and replication in plants, invertebrates, and human-derived cells under physiological stress, these preliminary enquiries assessed whether the diffusion of oxyhydrogen at 450 mL/minute for 30 minutes into the treatment media could affect the germination and growth of salinity challenged legume seeds (*Pisum sativum*) (Methods: Chapter 2, Section 2.2.2). To assess whether oxyhydrogen would have an effect on invertebrates (N2 Bristol *Caenorhabditis elegans*) were also exposed to oxyhydrogen gas (Methods: Chapter 2, Section 2.2.3). Finally, to further adjudge whether oxyhydrogen administration could affect the growth and replicative activity of human-derived Epstein-Barr virus-infected B-lymphocytes (TK6 cells), and the possible consequences this may have for human consumption in malignant disease, oxyhydrogen gas was infused into the cell culture medium (Methods: Chapter 2, Section 2.2.5).

6.3 Plants: Rationale - Germinating Seedlings under Salinity Stress

As the family of Fabaceae incorporate beans, peas and pulses, they are a valuable commodity as a relatively hardy, nutritious and sustainable food source. For agricultural and horticultural purposes, H_2, typically applied as HRW, can be exploited as a seed-priming agent, that can promote α/β-amylase activity (Zulfiqar, Russell and Hancock, 2021) and lead to an increase in accessible and energy-rich solubilised sugars required for the optimal development of germinating seeds, through enhancing antioxidant pathways and stimulating tolerance to such environmental stress factors as i) metallic toxicity from arsenate (As), cadmium (Cd), copper (Cu) and zinc (Zn) (Zulfiqar, Russell and Hancock, 2021), ii) increased levels of salinity (Wu *et al.,* 2020), iii) mitigating plant damage as a result of drought stress (Jin *et al.,* 2013), and iv) enhanced tolerance to herbicides (paraquat) (Russell, Zulfiqar and Hancock, 2020).

6.3.1 Germination, Growth and Antioxidant Capacity of Legume (*Pisum Sativum*) Seeds

6.3.1.1 Determination of the Effect of NaCl in Plant Growth Medium.

The data presented in the results section was generated by MSc student Bipana Dewan under my supervision, using the methods described in Chapter 2, Section 2.2.3. Visual analysis of germinated seedlings strongly suggests the addition of 50mM NaCl (Shrivastava and Kumar, 2015) reduces seedling health and vitality (Figures 6.1b and 6.2b).

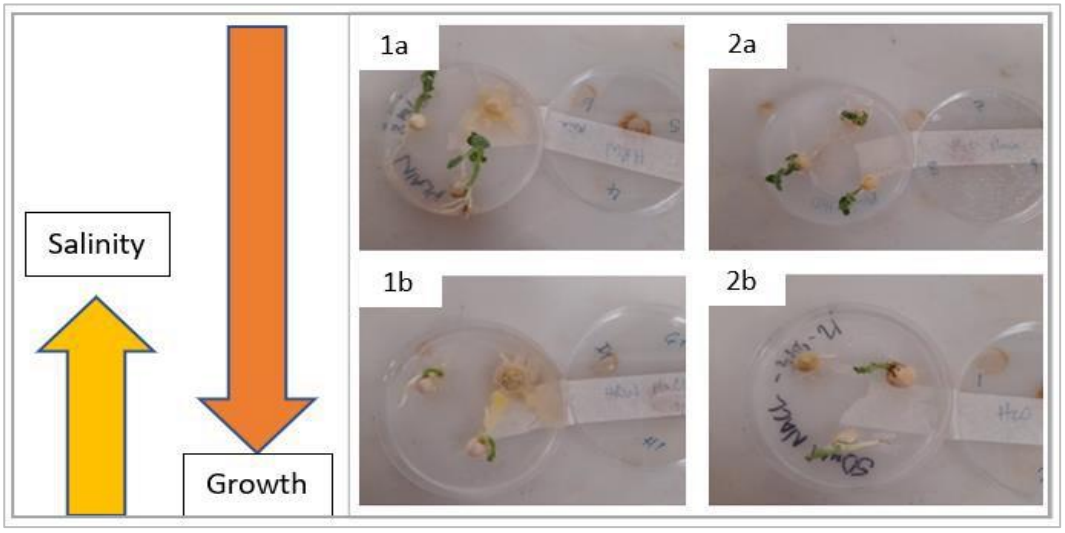

Figures 6.1 (A/B) & 6.2 (A/B) Photographic confirmation of the detrimental effect of increased salinity on legume seed germination (n =3). Top to bottom/Left to Right. Seeds primed with HRW. 1a) 0mM NaCl 1b) 50mM NaCl. Seeds primed with H_2O. 2a) 0mM NaCl 2b) 50mM NaCl.

Image 6.1a shows seeds imbibed with HRW, without salinity challenge, can produce well-germinated seedlings which is noted by the emergence of distinctive leaf and root structures. The lack of these structures in image 6.1b suggests that the addition of 50mM of NaCl into the growth medium actively inhibits germination and subsequent growth of legumes. Image 6.2a suggests that untreated seeds can also produce well-germinated seedlings in the absence of

NaCl. Image 6.2b supports the findings that NaCl does indeed repress the growth of untreated seedlings. However, it is unclear as to whether treatment with oxyhydrogen-infused water can mitigate the effects of salinity stress when compared with hydrated and untreated seeds.

6.3.1.2 Germination and Growth of Salinity Challenged Legume Seeds

To assess the potential of oxyhydrogen-enriched water as a seed priming agent, successful 7-day germination (Figure 6.3), percentage growth (Figure 6.4), CUPRAC (Figure 6.5), FRAP (Figure 6.6), of *Pisum sativum* were analysed.

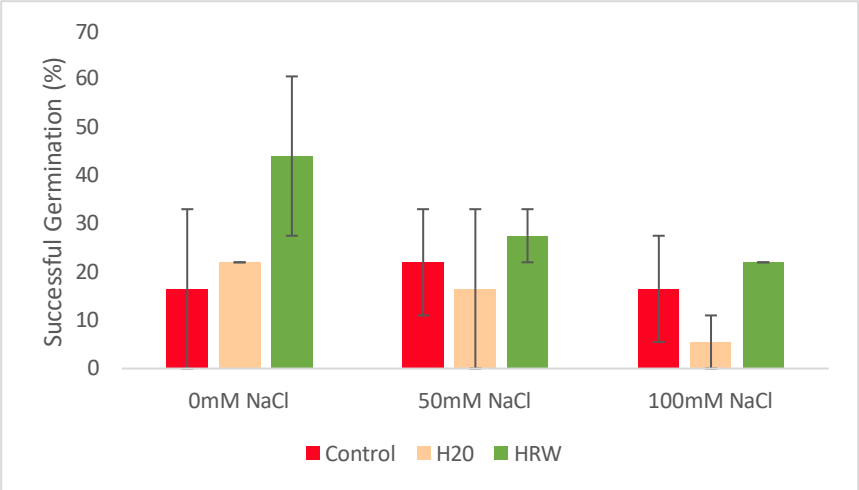

Figure 6.3 Percentage of seeds germinated. 7-day incubation. Data produced by MSc student Bipana Dewan (2022) under my supervision (Grace Russell). Column chart depicting the percentage of successfully germinated seeds (n = 18). Error bars denote ± SEM.

Although no significant results were determined between treatment groups using single-factor ANOVA analysis ($p = 0.078$) there is a trend of improved germination success in HRW-treated seeds. Of further note are the H_2O-treated groups show reduced germination success when compared with both HRW treatment and control. Therefore, to provide more meaningful data on the potential benefits of HRW seed priming, expansion of this protocol to include various seeds, and both field and greenhouse environments, would be highly advantageous.

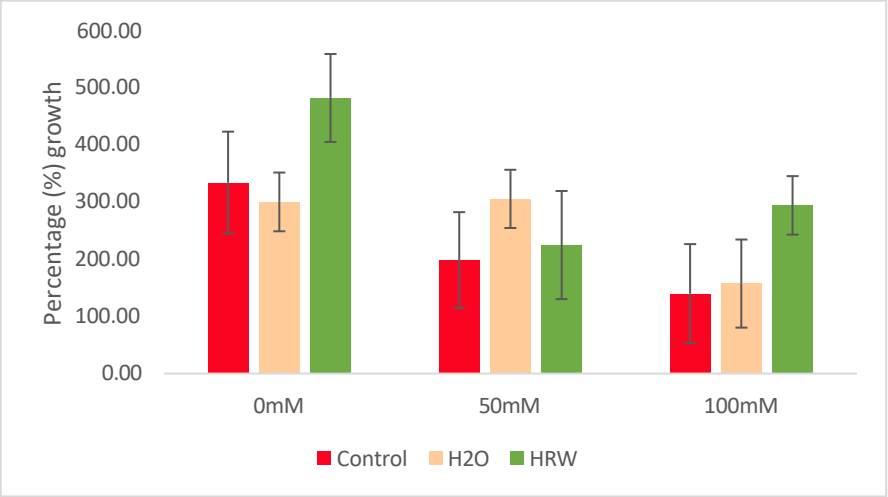

Figure 6.4 Increase in *Pisum sativum* biomass over 7 days. Data produced by MSc student Bipana Dewan (2022) under my supervision (Grace Russell). Column chart depicting the increased biomass of Mangetout seedlings under varying concentrations of salinity (n = 5). Error bars denote ± SEM.

ANOVA analysis does not show any statistical differences between treatment groups ($p = 0.199$). However, as with the germination success protocol (Figure 6.3) there is a trend of enhanced growth with HRW application, particularly when compared with H_2O at 0mM and 100mM NaCl. Accordingly, it may be worthwhile extending future experimentations to include records of hypocotyl elongation, cotyledon expansion and first leaf protrusion, thereby giving a more comprehensive picture of seedling viability.

6.3.1.3 a CUPRAC Assay

The CUPRAC assay enables the total antioxidant capacity (TAC) measurements of hydrophilic as well as hydrophobic samples (Sethi *et al.,* 2020). The main reagent, the copper (II)-neocuproine (2,9-dimethyl1,10-phenanthroline), can oxidize antioxidants generating a coloured product. The chelation with neocuproine enables a faster reaction by elevating the redox potential of the reagent. CUPRAC records the redox reduction between the CUPRAC reagent and the antioxidants of a sample with a leading thiol group (*e.g.,* glutathione) present in the sample. In this process, the reagent reduces itself forming a chelate complex of copper (I)-neocuproine, which provides a colour measurable at 450 nm.

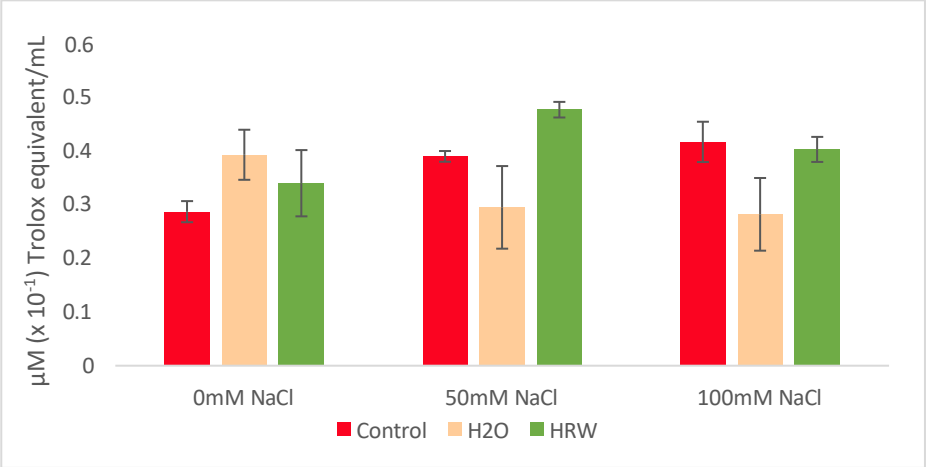

Figure 6.5 CUPRAC antioxidant capacity of germinated-Mangetout seed lysate. Data produced by MSc student Bipana Dewan (2022) under my supervision (Grace Russell). Column chart depicting the cupric antioxidant capacity of seed-primed Mangetout seed lysate (n =3). Error bars denote ± SEM.

Determination of significance using ANOVA analysis shows no marked differences in antioxidant capacity between seed priming treatments ($p = 0.115$). The experimental protocol, however, identifies a slight increase in antioxidant activity when compared with the control and H_2O groups at 50mM NaCl, and the H_2O groups at 100mM NaCl. Therefore, it may be beneficial for these experiments to be further developed to include numerous repeats, along with a variety of seed types and soils, before a conclusion as to whether H_2 has a major effect on the reduction of Cu^{2+} in biological systems can be firmly established.

6.3.1.3 b FRAP Assay

The FRAP assay is a method that measures the reduction of ferric ion (Fe^{3+})-ligand complex to the intensely blue-coloured ferrous (Fe^{2+}) +TPTZ complex (Benzie and Strain, 1996). Antioxidant activity is determined as the increase of absorbance at 593 nm through spectrophotometric analysis.

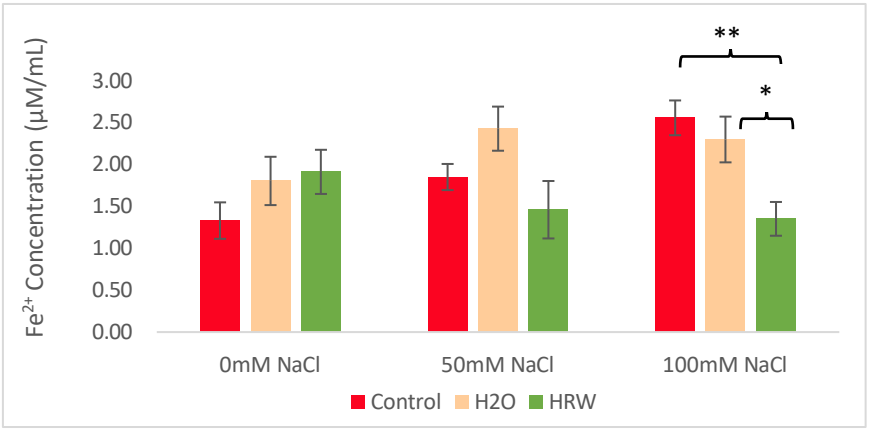

Figure 6.6 Ferric reducing potential of germinated-Mangetout seed lysate. Data produced by MSc student Bipana Dewan (2022) under my supervision (Grace Russell). Column chart graphical representation of the ferric reducing potential of Mangetout seed lysate (n = 7). Error bars denote ± SEM. * Indicates p </= 0.05. ** Indicates p </= 0.01

ANOVA analysis of data shows significant differences between treatments (p = 0.03). The result from Tukey-Kramer post hoc analysis shows a trend of decreased FRAP activity in HRW-primed mangetout seeds planted in 100mM NaCl when compared with the control (p = 0.002) and H_2O-primed seeds (p = 0.023). Although a non-significant decrease in FRAP activity is also observed with 50mM, as this trend does not occur in 0mM NaCl groups, it is thought this may be a result of heightened antioxidant activity during the initial stages (imbibition and respiration) of germination, although further and more sophisticated experimentations will be required if this is to be confirmed.

Considering the antioxidant analyses on germinating legume seeds do not show any definitive antioxidant activity (Figures 6.5 and 6.6), it may be valuable to not only assess the effects on plants, as above; but analysis of the microbial and invertebrate content of the surrounding earth is also appropriate.

6.4 Invertebrates: Rationale - Determining the Effect of Oxyhydrogen Gas Administration on Salinity-challenged Nematodes.

Caenorhabditis elegans nematodes are bilaterally symmetrical invertebrates (Brenner, 1974; Baxter *et al.,* 2013), with a lifespan of approximately 2-3 weeks under optimal conditions. The N2 Bristol strain of *C. elegans* utilised in the following experiments also benefits from this organism being non-infectious, non-pathogenic, non-parasitic, inexpensive and relatively easy to cultivate. Furthermore, *C. elegans* are known to have homologues with approximately 100 genes associated with human disease (The and Wilson, 1999), implying purposeful conservation of protein function throughout evolution (Corsi, 2006), making *C. elegans* an ideal choice for cross-translational laboratory investigations. Using the methods described in Chapter 2, Section 2.2.4, oxyhydrogen gas was administered and the growth and replicative capacity, along with the antioxidant activity of CAT were assessed.

6.4.1 Microscopic Evaluation of Nematodes.

Observations of nematode morphology reveal that a reduction in the optimal concentration (from 50mM to 25mM) of NaCl, in both the control and oxyhydrogen-treated groups, markedly reduced the overall size and numbers of nematodes. There were no noticeable differences between nematode numbers and no morphological differences seen between populations utilising 50mM and 100mM concentrations of NaCl, with or without oxyhydrogen treatment. For both treatment and control groups, nematodes grown on agar containing 200mM NaCl

were typically larger than the standard group (50mM NaCl), although observations of nematode numbers suggest there was no detriment to reproductive capacity.

6.4.2 Antioxidant Assay – Catalase.

The decomposition of the reactive oxygen species H_2O_2 by CAT can be followed directly by the decrease in extinction per unit time at 240 nm. Catalase-specific activity is calculated as moles/minutes/mg of cellular suspension proteins. Molar concentrations are represented by the optical density readings, these values are then divided by time (in minutes), and this given value is divided by the extinction coefficient (43.6 M^{-1} cm^{-1}) (Hadwan, 2018). These calculated values, alongside data time points, were used to create the results (Figure 6.7) (n = 3).

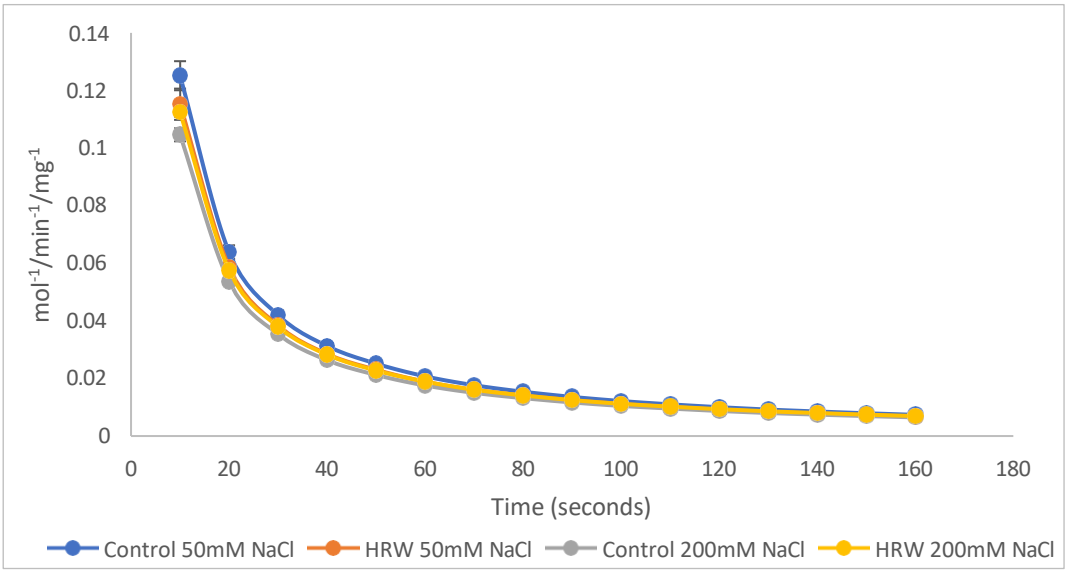

Figure 6.7. Spectrophotometric analysis of catalase enzymatic activity in nematode populations. Line graph interpretation of catalase activity in nematodes cultivated in 50mM and 200mM concentrations of NaCl. Control groups were assigned to each category of NaCl concentration. Blue = Control 50mM/ Orange = 50mM + HRW/ Grey = Control 200mM/ Yellow = 200mM + HRW. Error bars denote ± SEM.

A one-way ANOVA was employed to assess whether there were any statistical differences between groups. No significant differences ($p = 0.98$) were seen using these tests and no further post-hoc analysis was required. Although these data produced negative results, it is possible that the application protocol developed here (Chapter 2, Section 2.2.4.2) did not expose the nematodes to sufficient amounts of oxyhydrogen gas.

6.5 Human Derived TK6 Cells: Rationale - Acute (Single) and Chronic (Daily) Treatments.

Regarding the effect(s) oxyhydrogen may have on mammalian physiology, immortalised, Epstein-Barr virus-infected B-cell lymphoblastoid cells (TK6 cells) provide a valuable model

for investigating whether there are any toxic, or other detrimental effects, of oxyhydrogen administration in immune cells. B-cells are a keystone of the adaptive humoral immune system, being responsible for regulating the production of antigen-specific immunoglobulin (Ig) antibodies. However, when infected with Epstein-Barr Virus (EBV), these cells can become non-functional, devoting cellular mechanisms to immortalisation which has been associated with the initiation and development of certain cancers (Farrell, 2019). Furthermore, it is estimated that approximately 1.5% of global cancer cases are linked to EBV infection (Farrell, 2019). TK6 cells replicate expediently, doubling in approximately 24 hours and are simple to maintain in the laboratory environment. As a non-adherent cell-line, cultivated in a suspension media, it is assumed the proposed methods (Chapter 2, Section 2.2.5) will also permit the cells to readily access the dissolved oxyhydrogen gas.

6.5.1 Acute Treatment

The results of a single treatment (Chapter 2, Section 2.2.5.1b) indicate that oxyhydrogen infusion significantly reduces the proliferation of TK6 cells in culture (Figure 6.8 (A)) without negatively affecting the survival rate (Figure 6.8 (B)), demonstrating that treatment is not cytotoxic. Initial results describe a marked reduction in cell proliferation (Figure 6.8 (A)) with the acute oxyhydrogen treatment in comparison to the control group, at all time points (24 hours, $p = < 0.01$; 48 hours, $p = 0.03$; and 72 hours, $p = 0.01$). Cell viability (Figure 6.8 (B)) was largely unaffected by oxyhydrogen treatment when compared with data from the control group ($p = 0.55$) and statistically relevant differences were only noted between the 48- and 72-hour points ($p = <0.01$), which may be indicative of cellular stress in response to the physical manipulations of testing, and not the treatment *per se*.

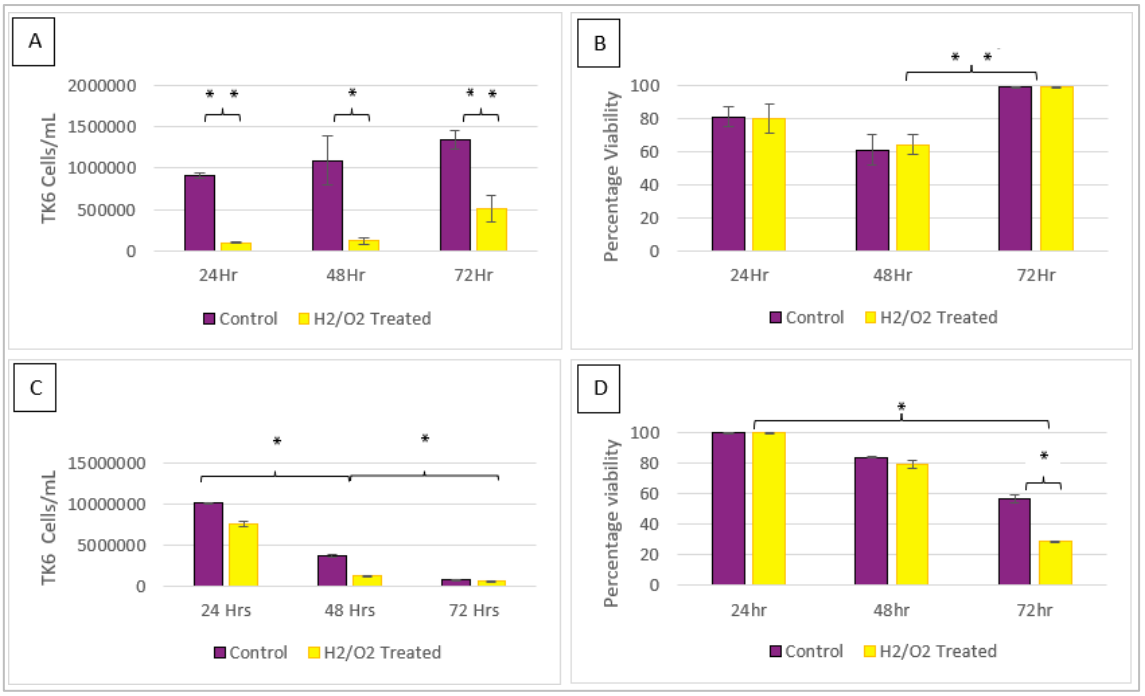

Figure 6.8 (A-D). Column charts representing proliferation and viability of TK6 Cells after exposure to oxyhydrogen (n = 3). Purple bars represent control groups. Yellow bars represent oxyhydrogen-treated groups. (A) Single oxyhydrogen application, count of the cell population. (B) Single oxyhydrogen application, cell viability. (C) Daily oxyhydrogen treatment, count of the cell population. (D) Daily oxyhydrogen treatment, cell viability. Error bars denote ± SEM. * (p = <0.05).

6.5.2 Chronic Treatment

Analysis of the daily treatment protocol (Chapter 2, Section 2.2.5.5c) reveals a significant decline in cell numbers at each timepoint within both control and treated groups (Figure 6.8 (C)), although no statistically relevant differences are noted between treatments (p = 0.64). Statistically significant reductions in the cell count were observed between 24- and 48 hours (p = 0.05) and 48-72 hours (p = 0.03). Cell viability (Figure 6.8 (D)) for daily treated groups was markedly reduced at 72 hours (p = 0.03). A substantial decrease in oxyhydrogen-treated cell viability, when compared with the control group, was also noted at the 72-hour timepoint (p = < 0.01). Collating this data strongly suggests the physical treatment of cells was not well tolerated, causing physiological and reproductive stress, therefore the repeated method of oxyhydrogen administration was deemed ineffective and adaptations to the protocol were applied (Section 6.6.3.3).

6.5.3 Determination of Mitogen Efficacy.

To assess whether oxyhydrogen administration would impact the proliferation of TK6 cells under growth stimulation, it was necessary to assess which mitogenic compound would be most effective in stimulating TK6 cell proliferation (Chapter 2, Section 2.2.5.8), thus the

cultured cells were exposed to four distinct mitogens: 16µg/mL ConA, 80 µg/mL LPS, 16µg/mL PHA and 16µg/mL of PWM. Figure 6.9 details the replicative response to stimulation.

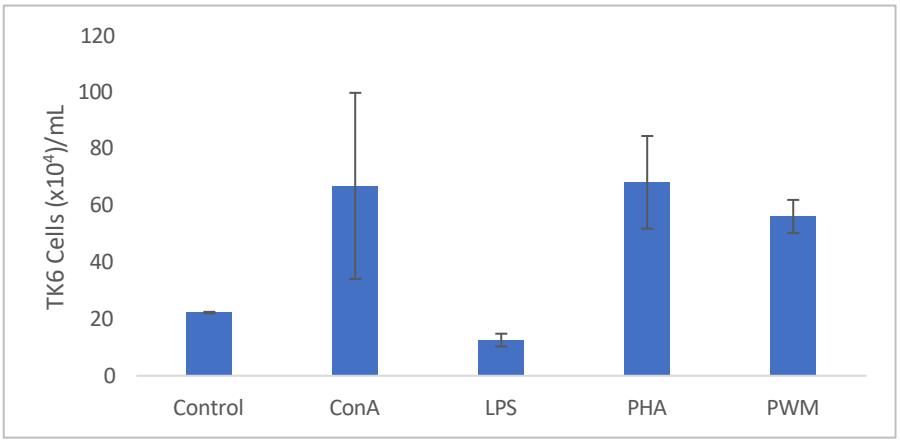

Figure 6.9. Determination of mitogen efficacy in TK6 cells (24-hours). Left to Right. Cellular proliferation of the control group, Con A, LPS, PHA and PWM. Error bars denote ± SEM. (n =2).

The data shows prominent effects with the addition of ConA, PHA and PWM. However, a single-factor ANOVA statistical analysis suggests no significant differences between mitogenic compounds ($p = 0.18$), assumed to be a result of biological variability. Although not a B-cell-specific mitogen, ConA mitogen enhanced the proliferation of TK6 cells in line with PHA and PWM. Because ConA was readily available in the supply chain, easy to handle and relatively inexpensive, this mitogen was chosen for further experiments.

6.6 Recommendations

6.6.1 Determination of the Effect of Hydrogen-Rich Water Administration on Plant Growth.

Observations shown in Figures 6.2 – 6.6 reveal that incorporating 50mM and 100mM of NaCl into the growth medium diminished the growth of germinating seedlings in both the control and HRW groups. The data generated through seed priming with oxyhydrogenated water (Section 6.3) in the manner described (Chapter 2, Section 2.2.3.10) was deemed inconclusive, and as a result, recommendations are that the doctoral thesis limits its scope, focussing on data retrieved from human sources.

6.6.2 Determining the Effect of Oxyhydrogen Gas and Hydrogen-Rich Water Administration on Salinity-Challenged Nematodes.

Analysis of the antioxidant effect of HRW application on salinity-stressed nematodes provided inconclusive data (Figure 6.7). This is likely due to difficulties in assuring the nematodes were sufficiently exposed to oxyhydrogen gas. Treating cultured nematodes with oxyhydrogen in the manner described (Section 2.2.4.2) was deemed to be ineffective and as a result, recommendations are that the doctoral thesis limits its scope, focusing on data retrieved from human sources.

6.6.3 Cell Culture and Treatment Protocols

6.6.3.1 Acute Treatment

No parameters of the acute treatment, with the exception of cell media and culture quantities, are to be altered.

6.6.3.2 Chronic Treatment

As the initial chronic treatment was unsuccessful, likely to be a result of daily handling and manipulation of cells, a novel method involving the daily addition of 10 mL of oxyhydrogen-infused media, an action that reduces the aforementioned physical interventions, was implicated in the ongoing academic study (Chapter 7). The control group was to receive 10 mL of non-infused media daily.

6.7 Summary and Conclusion

Table 6.1 summarises the findings of these collective experiments and highlights the appropriateness of developing these proof-of-concept investigations. The decisions as to whether the above protocols were to be included in, adapted to fit, or excluded from the central treatise were primarily based on four criteria affordability, experimental reproducibility, relevance of data produced and sustainability of procedures. Each topic received a grade from 1-5 (low to high) on suitability for inclusion into the doctoral thesis. A mid-point score of 10 or above was regarded as suitable for continued investigations.

Table 6.1 Assessment of the suitability of the proof of concept experiments for inclusion in the doctoral thesis. Grades are marked from low to high suitability (1-5).

Organism	Affordability	Reproducibility	Relevance of Data	Sustainability	**Total**	Outcome
Nematode (N2 Bristol)	4	1	1	3	**9**	Excluded from study
Pisum sativum	4	2	1	2	**9**	Excluded from study
TK6 Cells	3	5	5	3	**16**	Included

In conclusion, although not all of the experiments in this chapter yielded conclusive results, the data retrieved has uncovered some potentially interesting aspects of the application of oxyhydrogen as a novel antioxidant and cytoprotective compound. These initial experiments underpin the doctoral research documented in the following chapters. It is accepted that due to the constraints of independent research, not all of the interesting or relevant data created here can be further investigated. However, future research into the effects of hydrogen and oxyhydrogen treatments may wish to adapt or expand upon the work presented, whilst others may benefit from the infusion methods developed here.

Chapter 7: The Therapeutic Potential of Oxyhydrogen Gas in Oncology: A Study on Epstein–Barr Virus-Immortalized B-Lymphoblastoid (TK6) Cells

Adapted from the publication 'The Therapeutic Potential of Oxyhydrogen Gas in Oncology: A Study on Epstein–Barr Virus-immortalised B-Lymphoblastoid (TK6) cells' (Russell *et al.,* 2023)

7.1. Introduction

There is an increasing body of evidence highlighting that both H_2 and oxyhydrogen therapies are emerging as effective anti-inflammatory and antioxidant gases (Ohta, 2015; Kura et al., 2019; Nogueira and Branco, 2021; Deryugina et al., 2023a), which are physiologically well tolerated, as demonstrated in a comprehensive range of clinical studies (Kajiyama et al., 2008; Nishimaki et al., 2018; Akagi and Baba, 2019; Chen et al., 2019a; Chen et al., 2020a). As a potential revolutionary anti-inflammatory, antioxidant and anti-tumorigenic substance, interest in hydrogen therapies is rapidly gaining momentum from academic and commercial perspectives, particularly as an adjunctive to classical cancer treatments (Yang, Zhu and Xi, 2018; Chen et al., 2019b; Yang et al., 2020b).

Research into the biological effects of oxyhydrogen is sparse and there are few comparative studies that delineate how the corresponding increase in O_2 affects cellular activities. There are, however, a broad spectrum of both clinical and empirical studies that attest to H_2 as having anti-inflammatory (Itoh *et al.,* 2009; Niu *et al*., 2020; Rochette *et al.,* 2021; Yang *et al.,* 2023) and antioxidant (Slezak *et al.,* 2021; You *et al.,* 2021) properties which may be beneficial for oncological disease.

Research into the effects of H_2 on malignant cell lines indicate that H_2 likely has a dualistic role in redox signalling by (i) inhibiting oxidative activity and supporting metabolic homeostasis (Delos Reyes *et al.,* 2021; Asgharzadeh *et al.,* 2022) and (ii) by promoting apoptosis via upregulating redox-induced signalling cascades (Tsai *et al.,* 2009; Al Zahrani *et al.,* 2019; Russell *et al.,* 2023). Recent investigations into the effects of H_2 and oxyhydrogen treatments have demonstrated significant reductions in the physiological damage that results from oxidative stress and inflammation (Kura *et al.,* 2019; LeBaron *et al.,* 2019a; Fang *et al.,* 2020). For example, in mammary tumour models *in vitro*, HRW was shown to inhibit breast cancer cell viability by remediating oxidative distress and vascular endothelial growth factor-induced (VEGF) angiogenesis via inflammatory response inhibition (Frajese *et al*., 2018). The same study also noted that consumption of HRW delayed the development of human epidermal growth factor receptor-2 (HER2) mammary tumours in BALB-neuT mice, concluding that HRW can suppress breast cancer cell survival in human cells and mammalian hosts. The effects of oxyhydrogen gas inhalation were further studied in a `Real World' survey of 82 Stage III and Stage IV cancer patients where patients inhaled oxyhydrogen for a minimum of 3 hours a day,

for 3 months or longer (Chen *et al.,* 2019b). The evidence collated suggests there were substantial improvements in appetite, cognition, fatigue, pain and sleeplessness after four weeks of daily inhalation, although whether the results from these studies were due to increased apoptosis of malignant cells has yet to be fully elucidated.

7.2 Rationale

EBV belongs to the Herpesviridae Family of viruses (Table 7.1) and is known to cause mononucleosis, idiomatically referred to as glandular fever or the kissing disease. EBV is passed through such bodily fluids as blood, saliva and semen (Zhao et al., 2019), with the symptoms of primary viral infection including dyspnoea, fatigue, fever and light sensitivity, lasting in the region of 2-3 weeks. Moreover, the severity of primary disease being correlated with viral load (Kimura et al., 2008). EBV, in similarity with such viral infections as COVID-19, can progress into post-viral syndrome (myalgic encephalomyelitis/chronic fatigue syndrome (ME/CFS)), where the severity of the primary infection, again being an indicator for developing ME/CFS. Further to this, ME/CFS is reported as a risk factor for carcinogenesis (de Oliveira, Müller-Coan and Pagano, 2016), with previous EBV infection being associated with Burkitt's, Hodgkin's and non-Hodgkin's lymphomas, as well as breast, gastric and nasopharyngeal carcinogenesis (Gequelin et al., 2011).

Table 7.1. Classification table denoting the Epstein-Barr virus taxonomy. Data retrieved from https://ictv.global/taxonomy [Accessed 09/08/2022].

Family	**Herpesviridae**
Species	*Human gamma herpesvirus 4*
Order	*Herpesvirales*
Class	*Herviviricetes*
Phylum	*Peploviricota*
Genus	*Lymphocryptovirus*
Kingdom	*Heunggongvirae*
Realm	*Duplodnaviria*

To date, the pro-apoptotic, anti-tumour effects of hydrogen therapies on solid tissue cancers have been relatively well-studied (Dole, Wilson and Fife, 1975; Runtuwene *et al.,* 2015; Akagi and Baba, 2019; Chen *et al.,* 2019a; Liu *et al.,* 2019; Wang *et al*., 2019; Wu *et al.,* 2019; Meng *et al.,* 2020; Chu *et al*., 2021; Zhu, Cui and Xu, 2021). Nevertheless, investigations into

leukaemic and lymphoma cell lines remain largely unexplored. As approximately 1.5% of global cancer cases are linked with prior EBV infection (Wong *et al.,* 2022), EBV-immortalised immune cells (B-lymphocytes (TK6 cells)) were selected. Furthermore, TK6 cells are easy to culture, chromosomally stable, of the human lineage, and retain expression of the tumour suppressor protein, p53 (Schwartz and Jordan, 1997). These properties make such cells ideal models for understanding the effect of oxyhydrogen gas on the processes that contribute to dysfunctional cell cycling.

7.3 Aims

Treatment of long-term diseases such as malignancies (*e.g.,* breast cancer, Hodgkin's and non-Hodgkin's lymphomas) can be challenging and costly with current pharmaceutical interventions (Hsu, Chang and Chen, 2022; McCloskey *et al.,* 2023). To achieve a better understanding of whether H_2 and/or oxyhydrogen could provide an alternative and sustainable therapy for oncological disease, a series of tests were implemented. Firstly, cell enumeration, to observe whether a single treatment or multiple treatments with H_2 and oxyhydrogen had any noticeable effects on cellular behaviour, was assessed. Secondly, to evaluate whether the initial observations were repeated with the addition of growth stimulus (ConA), further observations of replicative capacity were recorded (oxyhydrogen only). Finally, to elucidate how cell cycling was affected by H_2 and/or oxyhydrogen administration, flow cytometry analysis was applied.

7.4 Results

7.4.1 a pH: Oxyhydrogen

To assess the effects of oxyhydrogen infusion on the pH of the RPMI media, the pH was measured 5 min post-infusion (19 °C ± 2 °C). The results increased from 7.25 (manufacturer's standard) to 8.3 after 30 min of infusion with the oxyhydrogen generator.

7.4.1 b pH: Hydrogen

Assessment of pH in H_2-only infused media at 19 °C (±2 °C) also indicated a rise in pH from 7.25 to 8.3 directly after 30 minutes of infusion.

7.4.2 Retention of Infused H_2 in Cell Media

To confirm that H_2 was dissolved into the media, Figure 7.1 illustrates the levels and retention of H_2. Before infusion, there were no detectable levels of dissolved H_2 in the media. Infusion increased the H_2 content of RPMI media to 0.69 mg/L/H_2, and this gradually decreased over 30 minutes demonstrating the 50% drop of H_2 concentration in RPMI media to be approximately 36 min (extrapolated data). Notably, when compared with a 12 minute retention time (H_2O) (Chapter 5, Section 5.4.3), the depletion of H_2 in media is less rapid in RPMI media, reaching

negligible levels after 30 minutes. For experimental purposes, this period of exposure was deemed sufficient.

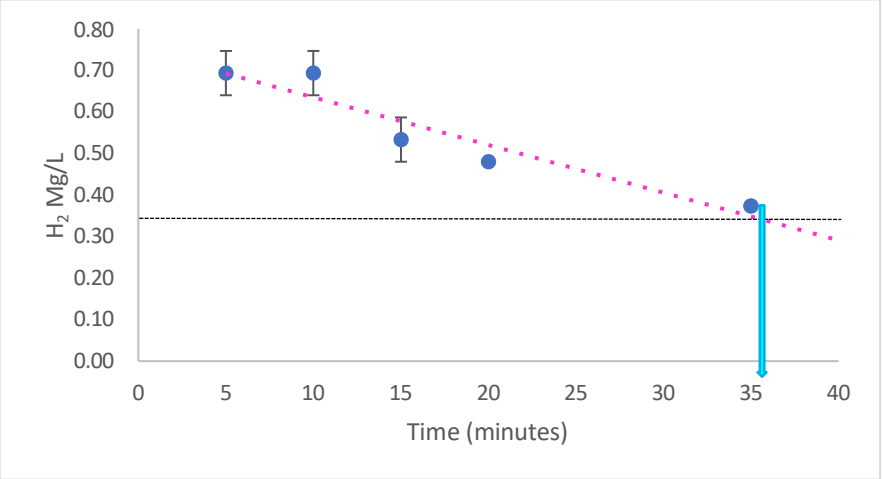

Figure 7.1. The concentration and retention of H_2 in RPMI media, measured with H_2Blue. The dotted pink line shows the trendline for dissolved levels of H_2 in RPMI media following a 30-minute infusion using the HydroVitality™ oxyhydrogen generator (300 mL/min of H_2 + 150 mL/min of O_2). n = 3 for all samples. The horizontal black dotted line indicates a 50% drop in H_2. The intersection between the two, shown with the pale blue arrow, highlights the time it takes for 50% of H_2 to dissipate in RPMI. Error bars denote ± SEM.

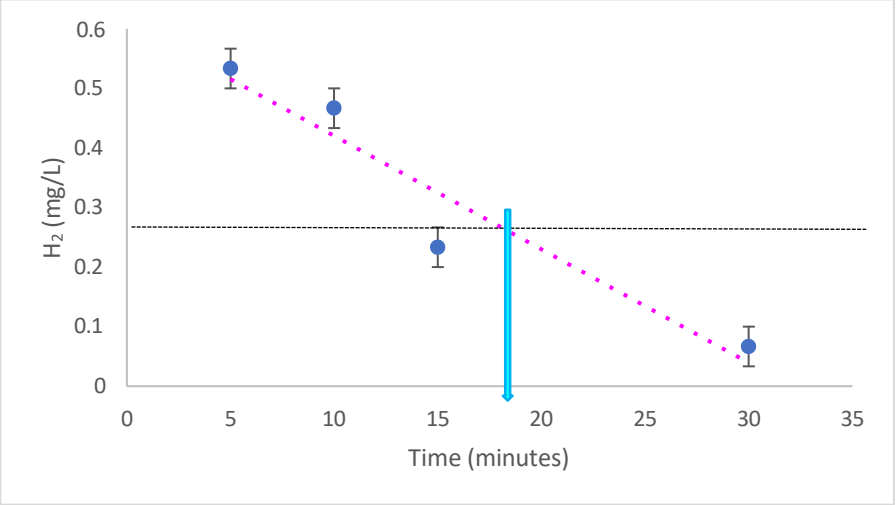

Figure 7.2. The concentration and retention of H_2 in RPMI media, measured with H_2Blue. Data produced by MSc student G. Mannings (2023) under my supervision (Grace Russell). The dotted pink line shows the trendline for dissolved levels of H_2 in RPMI media following a 30-minute infusion using the ABS-XQ-O2 pure hydrogen generator (300 mL/min of H_2). n = 3 for all samples. The horizontal black dotted line indicates a 50% drop in H_2. The intersection between the two, shown with the pale blue arrow, highlights the time it takes for 50% of H_2 to dissipate in RPMI. Error bars denote ± SEM.

7.4.3 Retention of Infused O_2 in Cell Media

To assess the dissolved oxygen content of the RPMI media, Figure 7.3 illustrates the levels and

retention of O_2 in the RPMI media. Prior to infusion, the dissolved O_2 content was recorded at 6.99 mg/L/O_2. Infusion increased the O_2 content to 9.79 mg/L. This gradually depleted, indicating a 50% dissipation rate of approximately 45 minutes.

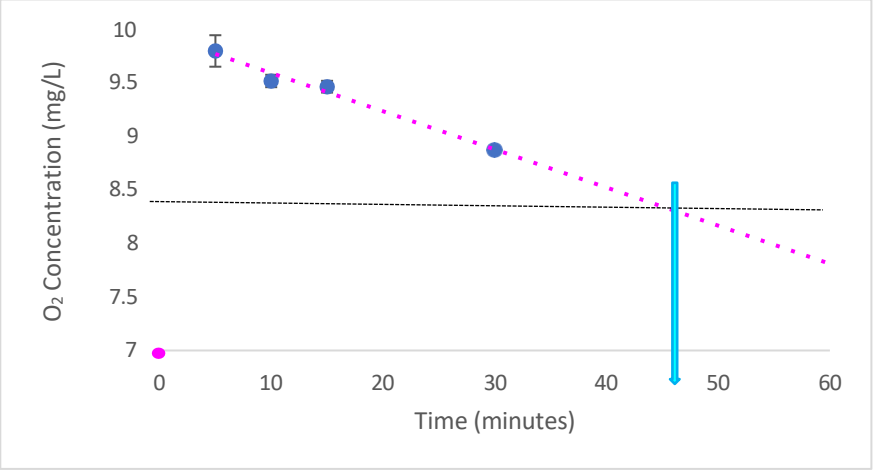

Figure 7.3. The concentration and retention of O_2 in RPMI media. The dotted pink line shows the trendline of dissolved levels of O_2 in RPMI media following a 30-minute infusion using the HydroVitality™ oxyhydrogen generator (300 mL/min/H_2 + 150 mL/min/O_2). n = 3 for all samples. The error bars denote ± SEM. The horizontal black dotted line indicates a 50% drop in O_2. The intersection between the two, shown with the pale blue arrow, highlights the time it takes for 50% of O_2 to dissipate in RPMI. The pink dot represents the levels of O_2 before infusion.

7.4.4 Cell Proliferation Assays

7.4.4.1 Oxyhydrogen

To analyse whether oxyhydrogen gas would affect the replicative capacity of TK6 cells, cell enumeration was initially assessed. Notably, the mean concentration of cells in the control groups approximately doubled from the seeding quantities at 24 h, with the same pattern of events noted at the 48 h and 72 h time points in accordance with expectations (Zhan *et al.,* 2004). However, this initial period of growth and replication is not seen with the oxyhydrogen single treatment groups (Figure 7.3 A). T-test statistical analysis describes no discernible differences in cell density between the acute oxyhydrogen group and the control group at 24 h ($p = 0.061$, 95% CI [5.06, 15.44]), 48 h ($p = 0.135$, 95% CI [−0.22, 22.56]) and 72 h ($p = 0.268$, 95% CI [37.12, 72.74]) (Figure 7.4 A). Instead, there is a non-statistical trend of growth inhibition at all the time points (24, 48 and 72 hours). The cell growth rate is typically recovered 72 h after acute oxyhydrogen exposure.

The same pattern of replication is noted with repeated applications (Figure 7.4 B) in the control group. The daily addition of oxyhydrogen (chronic protocol) did produce significant data at both 24 and 48 h but not at 72 h. Statistical analysis of the daily treatment with oxyhydrogen-infused media (Figure 9.4 B) reveals significant differences between cell population numbers

at 24 (p = 0.029, 95% CI [1.66, 2.32]) and 48 (p = 0.005, 95% CI [3.95, 4.57]) hours but not at 72 h (p = 0.257, 95% CI [4.15, 12.92]).

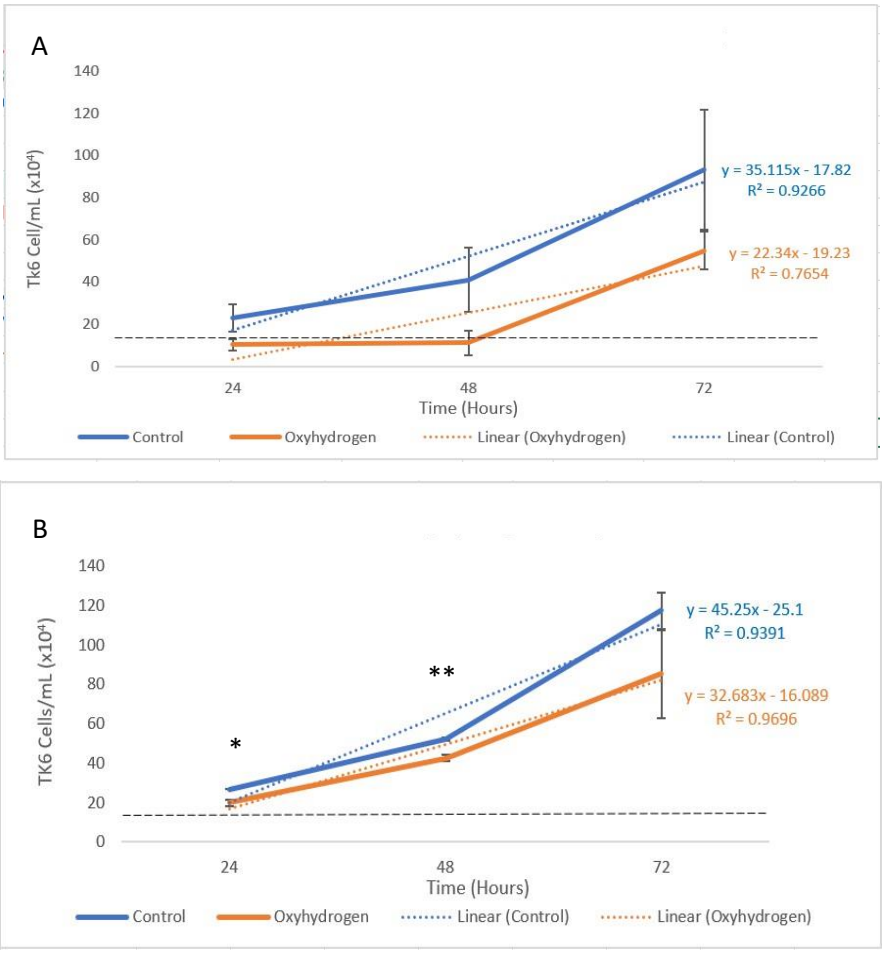

Figure 7.4 (A/B) shows the measure of cell populations in the groups with a single oxyhydrogen treatment (A). Figure 7.4 (B) identifies the cell populations of the daily oxyhydrogen-treated groups. n = 3 for all samples. The error bars denote ± SEM. The blue lines indicate the control groups (A/B). The orange lines depict oxyhydrogen infusion (A/B) * ($p \leq 0.05$), ** ($p \leq 0.01$). The dashed Black lines represent the initial cell-seeding numeration. The blue and orange text (y=) indicate the rate of change. The coefficient of determination (R^2) explains the proportion of variance incorporated in the experimental outcomes, a statistical measure of how well the trend line approximates the data (N.B. R^2 of 1 indicates the data fits the linear model perfectly).

To assess whether the inhibitory effects on cell replication seen in Figure 7.4 (A/B) are repeated in mitogen-stimulated cells, thus giving an indication as to whether oxyhydrogen treatments can suppress the excessive proliferation of malignant cells, 16 µg/mL of ConA was added to

the cell media. Due to time constraints, however, this protocol was not repeated for the H_2-only set of experiments.

Figure 7.5 shows statistically meaningful reductions in the cell populations between the oxyhydrogen group and both the control and mitogen-spiked groups; oxyhydrogen vs. control ($p = 0.017$, 95% CI [17.42, 19.51]) and oxyhydrogen vs. ConA ($p = 0.029$, 95% CI [28.24, 56.23])

at 24 h show that oxyhydrogen alone was most effective at reducing cell proliferation, but no statistical difference between any groups was determined at any other time point ($p \geq 0.05$). However, a non-significant trend of replicative inhibition between the mitogen and the oxyhydrogen/mitogen groups is observed at all time points: 24 h ($p = 0.06$, 95% CI [22.11, 26.08]), 48 h ($p = 0.12$, 95% CI [35.17, 76.97]) and 72 h ($p = 0.15$, 95% CI [58.19, 131.48]).

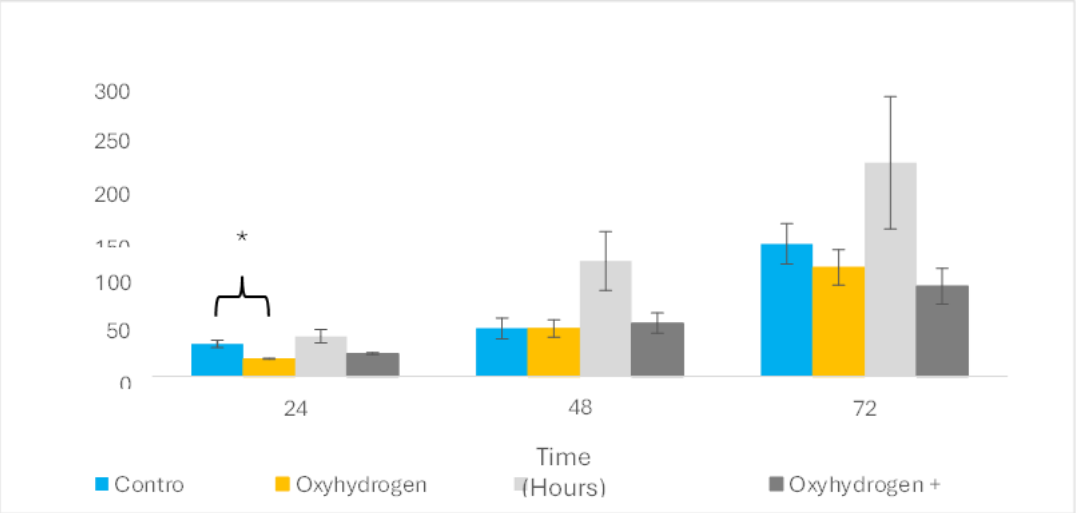

Figure 7.5 The effects of oxyhydrogen gas on mitogen-stimulated TK6 cells. The growth of the cell populations after mitogen stimulation (16 µg/ConA). Blue: Control group (−ve control). Orange: Oxyhydrogen-treated group (+ve control). Pale grey: Concanavalin A group. Dark grey: Oxyhydrogen and Concanavalin A. n = 3 for all samples. The error bars denote ± SEM. * $p \leq 0.05$.

Although no statistically meaningful data were produced when analysing the differences between the ConA-treated and the oxyhydrogen/ConA-treated groups, again there is a clear trend of growth inhibition in the oxyhydrogen/ConA-treated groups across each of the time points, making these groups worthy of further investigation.

7.4.4.2 Hydrogen

H_2-only infusion exhibited a statistically significant reduction in TK6 cell proliferation at 24 ($p = 0.02$, 95% CI [-0.15,1.77]) and 48 hours ($p = 0.04$, 95% CI [3.02, 6.54]) (Figure 7.5). However, this effect was not statistically significant at 72 hours ($p = 0.76$, 95% CI [-1.82, 9.13]). The mean concentration of cells in the control groups approximately doubled from the seeding quantities at 24 h, with a similar pattern of replication noted at the 48 h and 72 h time points.

However, the same pattern is not observed with the hydrogen single treatment groups where the replicative capacity is significantly reduced at 24 (p = 0.02) and 48 hours (p = 0.04) (Figure 7.6).

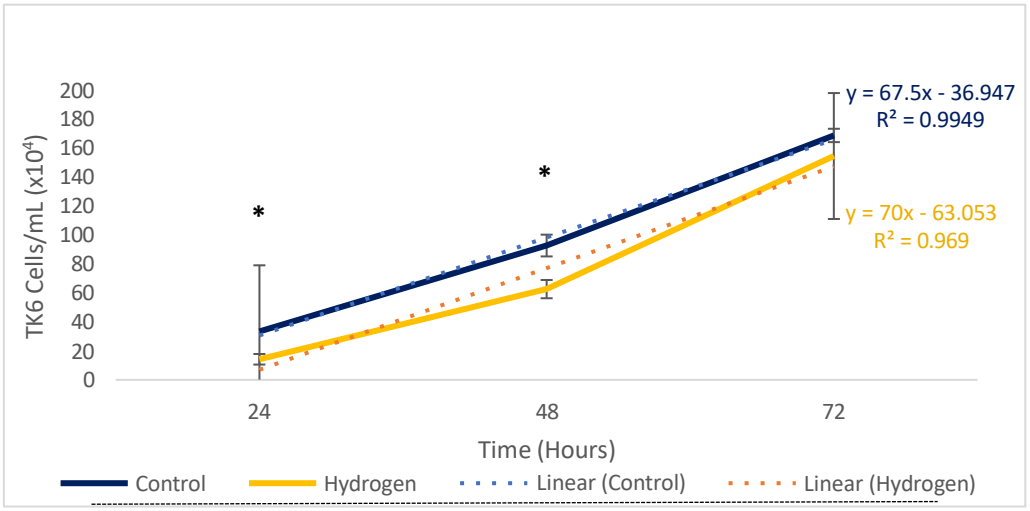

Figure 7.6 shows the measure of cell populations in the groups with a single (acute) hydrogen treatment. Data produced by MSc student G. Mannings (2023) under my supervision (Grace Russell). n = 3 for all samples. The error bars denote ± SEM. The dark blue lines indicate the control groups. The orange lines depict hydrogen infusion * ($p \leq 0.05$). The dashed black lines represent the initial cell-seeding numeration. The blue and orange text (y=) indicate the rate of change. The coefficient of determination (R^2) explains the proportion of variance incorporated in the experimental outcomes, a statistical measure of how well the trend line approximates the data (N.B. R^2 of 1 indicates the data fits the linear model perfectly).

7.4.5 Flow Cytometry

7.4.5.1 Oxyhydrogen

To identify the effects of oxyhydrogen gas on cell cycling, and to gain a better understanding of the mechanisms behind the reduction in cell numbers observed in Figures 7.4 (A/B), 7.5 and 7.6, flow cytometry analysis was performed. Figure 7.7 describes an average of the percentage of cells in each of the cell cycle phases (Growth phases 1 and 2 (G1 and G2, respectively and Stationary phase (S/P)), 24 and 48 hours after a single oxyhydrogen infusion.

The sub growth phase (Sub G1) does not form part of the cell cycle, as staining with propidium iodide (PI) shows degraded or fragmented DNA (Darzynkiewicz, Huang and Zhao, 2017). The cells in the Sub G1 phase have lower DNA content than in the recognised cell cycle phases (G1, G2 and S/P), a factor associated with cellular apoptosis (Darzynkiewicz, Huang and Zhao, 2017; Manohar, Shah and Nair, 2021). Figure 7.7 evinces a distinct increase in cells in the Sub G1 phase at 24 (Control: 9% vs. 46%) and 48 h (Control: 18% vs. 40%) after oxyhydrogen treatment, concomitant with marked decreases in G1 (24 h: Control: 39% vs. 25%; 48 h: Control: 37% vs. 31%) and G2 (24 h: Control: 28% vs. 10%; 48 h: Control: 19% vs. 10%).

The oxyhydrogen treatment group showed statistically relevant differences from the control group at 24 h in the Sub G1 phase (p = < 0.001, 95% CI [37.68, 52.65]), G1 phase (p = 0.001, 95% CI [23.80, 24.66]) and G2 phase (p = 0.002, 95% CI [5.42, 11.58]). Analysis of the cells in S/P identifies no significant differences (p = 0.108, 95 CI [16.57, 20.76]). At 48 h, the significant differences in the oxyhydrogen-treated groups are noted in all phases, Sub G1 (p = 0.004, 95% CI [35.03, 47.51]), G1 (p = 0.002, 95% CI [32.18, 33.89]), S phase (p = 0.004, 95% CI [20.13, 23.41]) and G2 (p = 0.012, 95% CI [6.85, 14.21]). Oxyhydrogen administration clearly reduces the abundance of cells in a population, significantly reducing cell numbers in both growth phases (G1 and G2) and markedly increasing the volume of DNA in the Sub G1 phase, it is reasonable to assume that oxyhydrogen effectively promotes apoptosis in malignant B-cells.

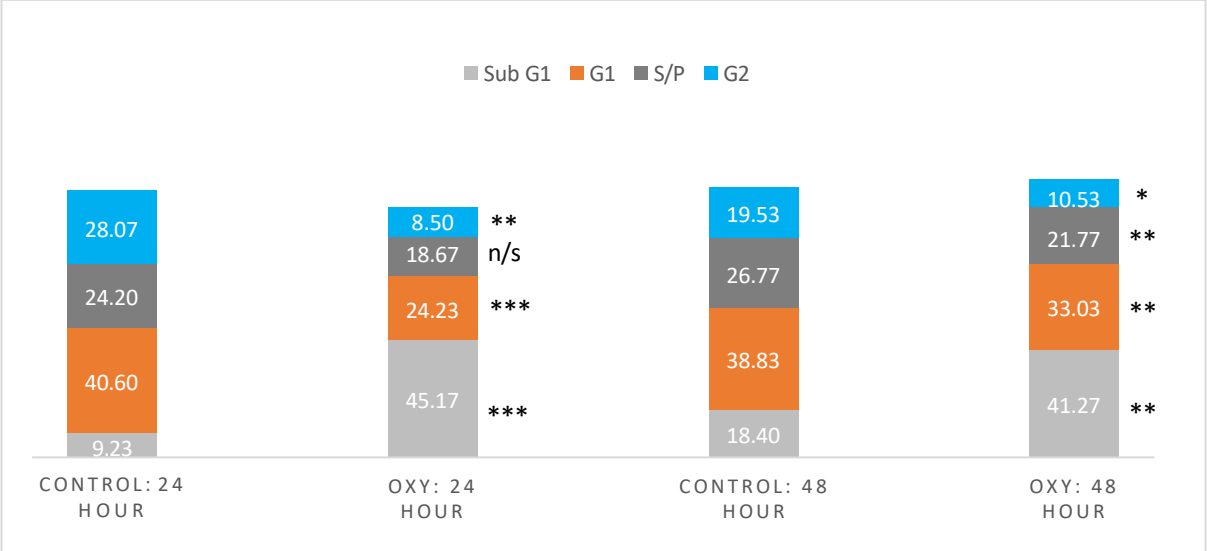

Figure 7.7 shows the percentage of 3000 (± 500 cells) TK6 cells in each phase of the cell cycle. From left to right: Results from the control group 24 h. Results from oxyhydrogen group 24 h. Results from the control group 48 h. Results from oxyhydrogen group 48 h. From top to bottom: Pale Blue, Growth phase 2. Dark Grey, Synthesis phase. Orange, Growth phase 1. Pale Grey, Sub G1. * ($p \leq 0.05$) ** ($p \leq 0.01$) *** ($p \leq 0.001$) n/s = no significance.

7.4.5.2 Hydrogen

Notably, due to an experimental error during the preparation stages wherein the cells were subjected to a centrifugal force of 4000 xg instead of 400 xg, the initial population of cells in the Sub G1 phase is much greater than expected (50.4% (Figure 7.8) vs. 9.23% (Figure 7.7). However, flow cytometry analysis of pure H_2 infusion, in accordance with the oxyhydrogen data, revealed that hydrogen arrests most cells within the Sub G1 phase at both 24 (89.2%) and 48 hours (66.4%) (p = 0.02, 95% CI [85.1, 93.3]; p = 0.39, 95%CI [44.1, 88.7], respectively) (Figure 7.8), indicating that H_2 is effective in promoting apoptosis in these cells. A statistically significant difference between control and hydrogen-infused groups was observed for all other analysed stages of the cell cycle: G1 (p = 0.02, 95% CI [4.91, 5.74]), Synthesis phase (p = 0.04,

95% CI [-4.15, -1.17]) and (p = 0.03, 95% CI [-1.25, 1.14]) at 24 but not 48 hours, G1 (p = 0.16, 95% CI [5.0, 23.9]), synthesis phase (p = 0.30, 95% CI [5.1, 23.2]) and G2 (p = 0.9, 95% CI [2.0, 11.4]).

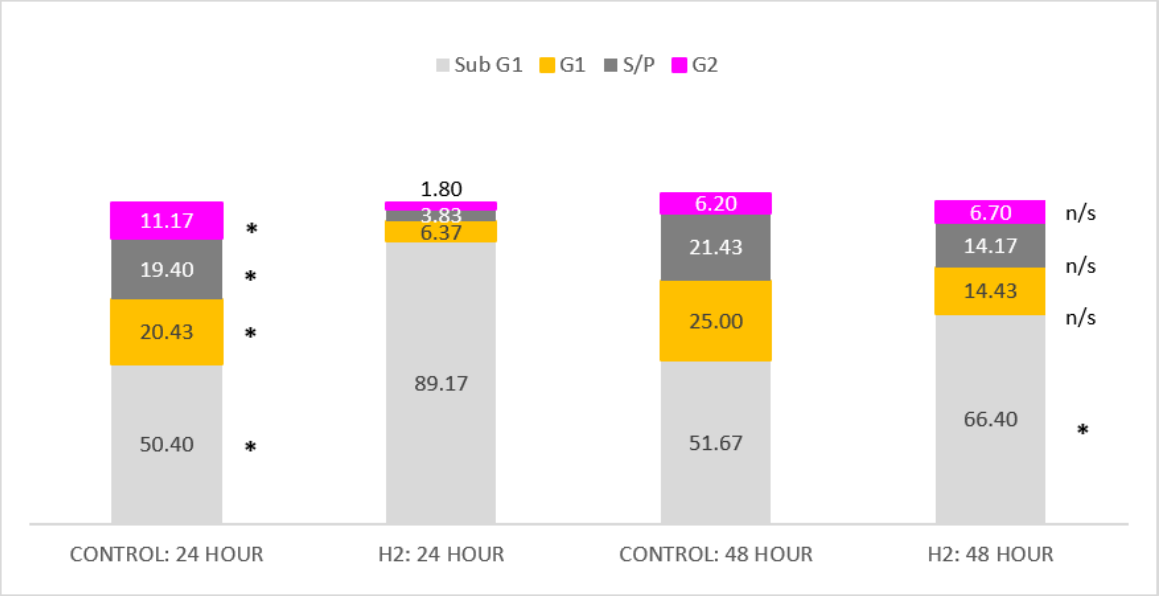

Figure 7.8 shows the percentage of 3000 (± 500 cells) TK6 cells in each phase of the cell cycle. Data produced by MSc student G. Mannings (2023). From left to right: Results from the control group 24 h. Results from hydrogen-infused group 24 h. Results from the control group 48 h. Results from hydrogen-infused group 48 h. From top to bottom: Pink, Growth phase 2. Dark grey, Synthesis phase. Orange, Growth phase 1. Pale grey, Sub G1. * ($p \leq 0.05$) n/s = no significance.

7.5 Summary of Findings

To assess whether oxyhydrogen and/or pure H_2 gas would affect the cell proliferation capacity of TK6 cells, this novel enquiry focused on the effects of infusing each gas into cell culture media in an attempt to simulate the most likely dispersal and retention patterns of the aforementioned gases in the blood or serous fluids. The main findings of this report identify that dissolving H_2 or oxyhydrogen into the cell media has an inhibitory effect on TK6 cell proliferation (Figures 7.3 A/B and 7.4) by upregulating apoptosis (Figures 7.7 and 7.8). These factors may be pertinent in the clinical treatment of numerous malignant conditions and perhaps more so with those associated with previous EBV infection (*e.g.,* breast cancer, Hodgkin's and non-Hodgkin's lymphomas) (Wong *et al*., 2022). However, further comparative research will be required if the questions as to which gas is more effective for treating oncological disease is to be resolved.

Chapter 8: Discussion

8.1 Hydrogen and Eukaryote Evolution

Hydrogen is the most ubiquitous element in the universe which is, today, being explored for its potential use in the agri-food (Russell, Zulfiqar and Hancock 2020; Hancock, Russell and Stratakos, 2022), biomedical (Ohsawa et al., 2007; Slezak et al., 2016; Russell et al., 2021; Russell, Nenov and Hancock, 2021) and energy sectors (Okolie et al., 2021; Capurso et al., 2022), wherein it is used for its antioxidant, anti-inflammatory and high capacity to provide a clean and sustainable fuel. Although the precise mechanisms of biological action has yet to be elucidated (Chapter 4), research into H_2 as a medical treatment for acute, chronic and infectious conditions is now gaining traction, with numerous studies attesting to the safety and efficacy of this novel compound (Chinese Coptionnical Trial Register (ChiCTR); Clinicaltrials.gov; UMIN Clinical Trials Registry).

One explanation as to why H_2 may be an effective nutraceutical is that hydrogen is thought to have a role in life's origin by providing a source of energy for early metabolic processes, with many organisms including archaea, bacteria, plants and protozoa having hydrogenase enzymes that catalyse the reversible oxidation/reduction of H_2 (Chapter 3). Certainly, early chemolithotrophs evolved to utilise such compounds as energy sources, a process termed chemosynthesis, which involves the oxidation/reduction of H_2, or H_2-containing compounds, during metabolism (Dunham *et al.,* 2021).

Over time, as life evolved and atmospheric conditions changed, H_2 became less abundant in relation to other gases. O_2, for example, began to accumulate due to the emergence of photosynthesising organisms, leading to the development of aerobic respiration. This metabolic advancement is predominant in higher organisms including animals and humans. Could it be then, that certain organisms have retained a method of generating H_2 to mitigate the risk of, and potential harm caused by, oxidative stress?

Although there is academic speculation as to whether the membrane-bound subunits of Complex I (*e.g.,* ND1, ND6) may have evolved from hydrogenase enzymes (Yano and Onishi, 2001; Mühlbauer, Gamiz-Hernandez and Kaila, 2021), the analyses conducted in this enquiry (Figures 3.6 – 3.14) do not indicate a clear relationship between such proteins. Instead, cogent similarities are identified between non-membrane bound subunits (NDUFS2 and NDUFS7. Figures 3.6 – 3.10 and 3.11 – 3.14, accordingly) of the ubiquinone binding module of Complex I. In support of the hypothesis that the symbiotic partnership began the evolution of the mitochondrial organelle, and therefore the eukaryotic cell, is the incorporation of numerous α-proteobacterial functional genes within the host's genome (López-García and Moreira, 2006; Roger, Muñoz-Gómez *et al.,* 2017; Muñoz-Gómez *et al.,* 2022). The data presented in

Chapter 3, however, contradicts these findings, indicating that of the hydrogenases analysed, the NiFe hydrogenase subunits of *C. heimdallarchaeota*, and not an alphabacterium, most closely resemble the NDUFS2 and NDUFS7 units of the ubiquinone binding site (Q module), giving further credence to both the E^3 and Syntrophic theories of eukaryotic evolution (Chapter 3, Section 3.2).

Although, the mechanism behind proton abstraction/electron transference in Complex I is a matter of ongoing debate, this report highlights that a conserved -**RGXE-** motif of NDUFS2 (Figure 3.6) may be required for such action (Ash, Kendall-Price and Vincent, 2019). Further analysis of the NDUFS2 subunit (Figures 3.6 – 3.10), shows little corresponding sequence identity with the catalytic subunit of NiFe hydrogenases. However, the non-catalytic, or uptake, hydrogenase subunits of *C. heimdallarchaeota* (MbhJ) and *D. carbinolicus* (Hyd 258) both share 35% sequence homology with the NDUFS7 subunit of Complex I and may have a role in utilising H_2 to prevent oxidation of redox-sensitive moieties including cysteines, serines, histidines and threonines.

Homology between NDUFS2 and the NiFe hydrogenase enzymes of the bacterial species (*D. carbinolicus; R. sphaeroides*) analysed here (Figures 3.9 and 3.10, respectively), is not deemed to reach the threshold of significance of >25% (Anderson and Brass, 1998) attributed to the retention of protein function. With a sequence identity of 27% between the hydrogenase units of *C. heimdallarchaeota* and NDUFS2 (Figure 3.8), it is unlikely this mitochondrial subunit has retained the ability to create or utilise H_2, and without further sequence similarities it appears unlikely that NDUFS2 would be a utile relict of NiFe hydrogenase enzymes. It is still unclear, however, whether NDUFS2 may be responsible for redox activity regarding the full or partial reduction of ubiquinone, or whether this particular subunit is purely of structural significance to the ubiquinone docking site of Complex I.

Perhaps also of pertinence is the lack of commensurate alignments between the alphabacterium *R. sphaeroides* and the Q module subunits of Complex I (Figures 3.7 (C/D) and 3.11 (C/D)), a strong indication that these non-membrane bound units are unlikely to be of alphabacterial origin. Interestingly, the higher 35% sequence identity of NDUFS7, noted with both *C. heimdallarchaeota* and *D. carbinolicus*, supports the supposition that NiFe hydrogenases are likely to have a role in the evolution of the ubiquinone binding/reducing module of Complex I. Furthermore, having significant sequence similarities in NDUFS2 (27%) and NDUFS7 (35%) indicates that Asgard archaea such as *C. heimdallarchaeota* may have had a conspicuous role in eukaryogenesis.

Similarities above the threshold of significance (Anderson and Brass, 1998), indicative of retained function, are observed between NDUFS7 and the smaller hydrogenase subunits of

both the Asgard archaeota (Figure 3.12) and the deltabacterium considered in this study (Figure 3.13). Nevertheless, as this subunit is responsible for the shuttling of electrons and not the ultimate protonation/deprotonation of hydrogen, it is also improbable that NDUFS7 is capable of generating or oxidising H_2. Whether H_2 is able to support the optimal function of such subunits by another mechanism has yet to be elucidated. For example, whether the N2 FeS cluster, a proposed site for $O_2^{\bullet-}$ production, could be an important target for H_2 activity, with H_2 perhaps being attracted to $Fe^{2+/3+}$ ion depending on its spin-state (Hancock and Hancock, 2018), a theorem further discussed in Chapter 4, Section 4.3.2.

Of the conserved sequences identified in this study, the **-IPGCPP-** motif (NDUFS7) (Figures 3.12 – 3.14), identified as a target for *N*-myristoylation, is best conserved between species. As *N*-myristoylation post-translational modifications can result in cellular signalling, localisation of protein and protein stability, the possibility that the fourth residue of this sequence, cysteine 183 (human), maybe a target for H_2 interactions cannot be ruled out. Equally, the PKC phosphorylation site **-RASPRQS**- of NDUFS7 is of interest as H_2 is noted to affect phosphorylation events in the MAPK, growth and proliferation pathway (Han *et al.,* 2016; Begum *et al.,* 2020). This raises the question as to whether H_2 could also influence phosphorylation, altering both the form and function, of the N2-containing NDUFS7 subunit, a protein integral to ubiquinone docking and electron transference.

It is accepted that of the proteins investigated in this research, MbhL and MbhJ of *C. heimdallarchaeota*, and Hyd494 and Hyd258 of *D. carbinolicus* are predicted sequences and have yet to be confirmed and therefore this study can only indicate possibilities. The sequences analysed here will require confirmation of theory through in-depth analysis of protein isolates before accurate determination of form and function can be attained. In mammals Complex I can incorporate in excess of 40 protein subunits, the precise functions of which are largely unresolved. 14 central subunits are known to provide the bioenergetic functions of the enzyme. Seven of these (ND1-6 and ND4L) are encoded by the mitochondrial genome. However, such membrane-bound subunits of Complex I more closely resemble bacterial, non-enzymatic proton antiporters (Fiedorczuk and Sazanov, 2018) and are unlikely to partake in, or directly influence, distinct H_2 actions (opposed to antiporter H^+ transference), and were therefore excluded from this study.

Also of note for this enquiry is that the subjects analysed may not be the primary candidates for eukaryogenesis and are only representative of the prokaryotic clades highlighted in the various theories of evolution. Utilising the aforementioned techniques (Chapter 2, Section 2.2.1) to assess hydrogenase activity in the microbial species included in this inquiry may provide insights into the possibility of evolutionary relativity, providing insights into the fundamental mechanisms underlying H_2 activity, discussed in Chapter 4.

8.2 Efficacy, Purity and Stability of Oxygen and Hydrogen Gases Produced by the HydroVitality™ Electrolyser

8.2.1 HRW

As market for H_2 supplements is rapidly gaining traction, and many portable and non-portable means of producing HRW are already commercially available, testing the gaseous output and levels of infused gases the HydroVitality™ produces when creating HRW, was included in this study (Chapter 5). Briefly, the results of infusing 250 mL (~9 fl. oz) H_2O (the volume of a widely available portable water bottle), with HydroVitality™ show that after 30 minutes of infusion, dissolved H_2 reaches a concentration of 0.52 mg/L (0.26 mM) immediately after infusion, with a 50% reduction in dissolved H_2 noted to be 12 minutes under laboratory conditions (Chapter 5, Section 5.4.3). When accounting for the International Hydrogen Standards Association guidelines for a minimally effective dosage of H_2 (0.5mg H_2 in one litre of water per day) (International Hydrogen Standards Association, 2018), to achieve a therapeutic dose of H_2, consumers would need to consume ~960mL of oxy/hydrogenated water each day. In contrast to the relatively small increase in dissolved H_2 content, O_2 levels are raised from 8.69 mg/L before infusion to 14.05 mg/L post-infusion (Chapter 5, Section 5.4.4) which may have independent or synergistic physiological effects when taken in conjunction with H_2. Furthermore, the 50% reduction in dissolved O_2, extrapolated from the data obtained, was estimated to be in the region of seven hours, a marked increase in retention when compared with H_2. However, whether O_2 increases the therapeutic antioxidant potential of oxyhydrogen-enriched waters is yet to be determined and would be an interesting avenue of study.

The life-supporting properties of water depend upon many factors including solute content (*e.g.,* salinity), temperature and pH. The relationship between pH and temperature in water is complex (Omer, 2019). For non-mineralised water, the pH tends to decrease as the temperature rises, a result of the self-ionisation and the production of hydronium (H_3O^+) and hydroxide (OH^-) ions (Schmidt, 1991). A factor to be considered when assessing the results at 20 minutes post-infusion (Figure 5.7). The recommended limits of the pH of potable water in the UK, as defined by the Drinking Water Inspectorate Water industry Act (1991), vary from a minimum of pH 6.5 to a maximum pH 9.0. The data in Figure 5.7 (Chapter 5, Section 5.4.5) shows that 10 minutes post-infusion, an initial rise in pH occurs (pH 8.49 – 8.67), returning to below base-level recordings (pH 8.19) at 20 minutes post-infusion. Interestingly, non-infused water also showed a mild rise in pH (pH 8.62 – 8.70) after 10 minutes, however, this also returned to below base-level observations 20 minutes post-infusion (pH 8.55), this is possibly a result of the increase in water temperature over time (Murariu *et al*, 2011). Notably, no significant differences were found between oxyhydrogen and controls, with neither of the data produced exceeding the upper limit of safety.

8.2.2 Inhalation

In the rapidly evolving global market of inhalation devices, consumer confidence in such health-related products is a paramount concern for sustaining business success, growth and longevity. To test the purity of the gas formed by HydroVitality™ a 750mL sample of gas was analysed using gas chromatography (Chapter 5, Section 5.4.2). When introducing a new inhalation product to the consumer and healthcare markets another important factor to consider is that users of the product must be able to calculate the dose of therapeutic gases they absorb (Russell, May and Hancock, 2024). To address this in relation to the HydroVitality™ oxyhydrogen generator a flow rate analysis was applied (Chapter 5, Section 5.4.1). The results allow for calculation assessing the percentage of inhaled gases.

On average each person breathes in 500mL of air with every breath, with inhalation lasting approximately 2 seconds. Taking the maximum flow rate of the device tested HydroVitality™ produces 450mL/min oxyhydrogen and the average volume of air intake with every breath (Female: height 1.64 m, weight 72.7 kg and BMI 27.1. Male: height 1.78 m, weight 86.7 kg and BMI 27.4, UK data) (www.worlddata.info), females will inhale 2.5% H_2 with every breath, whilst males will intake approximately 2%.

Formula *(mL/sec)*: H_2 / (Breath – H_2) x 100

If the same formula, adjusted for the flow rate and percentage increase (33%) in O_2 consumption, is applied to the consumption of O_2 giving values of increased oxygen intake of 1.27% (22.27%, O_2) for females and 1.01% (22.01%, O_2) for males, Table 8.1. This may be relevant, for instance, if the user is experiencing rapid or shallow breathing or has a chronic lung condition. For consumer and patient safety, under such circumstances, it would be beneficial to conduct a simple spirometry ensuring accurate measurement of tidal volume and H_2, and/or O_2 consumption.

Table 8.1. Showing calculated percentages of gases inhaled by the average female and male (www.worlddata.info) when breathing regularly.

	Air (250 mL/sec)		Oxyhydrogen (450 mL/min)		H_2-only (300 mL/min)	
(% inhaled)	O_2	H_2	O_2	H_2	O_2	H_2
Female	21%	< 0.0001%	22.27%	2.5%	~ 19%	2.5%
Male	21%	< 0.0001%	22.01%	2%	~ 19.5%	2%

Ongoing studies (www.clinicaltrials.gov; www.chictr.org.cn; www.umin.ac.jp) are evaluating the responses to oxyhydrogen and H_2 therapies in patients with severe symptoms of COVID-19, with preliminary data reporting subjugation of dyspnoea and easement of respiratory symptoms (Guan *et al.,* 2020). There is also forthcoming evidence suggesting H_2 inhalation could be advantageous in alleviating such long-term inflammatory-related lung conditions as asthma(Zhang *et al.,* 2021a) and COPD(Lu *et al.,* 2018). Consequently, it can be surmised that patients with emphysema, cystic fibrosis and pulmonary adenoma, may prosper from hydrogen inhalation therapy; these diseases having similar aetiologies.

8.3 Hydrogen in Oncology

8.3.1 The Role of Oxidative Stress, Reactive Species, and Hydrogen in Carcinogenesis and Antitumor Mechanisms

Carcinogenic development is influenced by oxidative stress and inflammation, with the consequences of aberrant ROS/RNS known to oxidatively modify DNA (Ríos-Arrabal *et al.,* 2013). Oxidative stress describes the disruption of cellular activity that occurs as a result of an increase in the levels of ROS/RNS which can influence such cellular processes as a mediator of apoptosis, lipid oxidation, metabolic instability, and protein modifications (that either inhibit or over-activate functional processes), or through directly targeting DNA, causing lesions and mutations in the genetic sequence (Ríos-Arrabal *et al.,* 2013). During both carcinogenesis and the recovery process, levels of pro-oxidants are heightened due to an increase in metabolic activity, a hypoxic environment (lacking O_2) and/or, reactions to medications (Perillo *et al.,* 2020). ROS/RNS are relatively unstable physiological molecules that act as intermediaries in both apoptotic and survival-related cell signalling pathways (Chapter 4, Sections 4.2.1 and 4.2.2). ROS-induced pathways (*e.g.,* MAPK and protein tyrosine kinase cascades), are also known to influence and enhance the metastatic potential of neoplastic cells (Wang *et al.,* 2019; Fan *et al.,* 2023). In contrast to the anti-apoptotic effect H_2 has in non-malignant diseases (Chapter 1, Section 1.2.3.1), in oncological disease H_2 gas is noted to have antitumor effects via the regulation of ROS-sensitive MAPK-associated

pathways, known to have a dualistic role, either inhibiting or initiating apoptosis (Wang *et al.,* 2018a; Zan *et al.,* 2022; Hasegawa *et al.,* 2022).

8.3.2 Hydrogen Therapy in Modulating Inflammation and Immune Response in Carcinogenic Microenvironments

The inflammatory process (Figure 1.3) is an innate immune response that includes the infiltration of white blood cells to a targeted area and the upregulated expression of pro-inflammatory messengers (*e.g.,* cytokines and chemokines) alongside atypical tissue remodelling and hyperbolic angiogenesis. Inordinate amounts of inflammatory markers are often present in the microenvironment of neoplastic tissues, including those that cannot be directly related to hyper-inflammatory processes (Mantovani *et al.,* 2007). This is important to consider when assessing carcinogenic microenvironments, as during distinct stages of tumour initiation the immune system either identifies and destroys nascent cells or, alternatively, promotes the development of functional cells into neoplastic cells (Jiang and Shapiro, 2014). In addition to having positive effects on the native immune system, H_2 therapies have also been demonstrated to recover the adaptive immune response by elevating levels of $CD8^+$ cytotoxic T-cells (responsible for the destruction of malignant cells) in colorectal cancer patients (Akagi and Baba, 2019).

Through enhancing regulatory activities on redox chemistry and signalling, and modulating both adaptive and innate immune responses, H_2 therapeutics have been shown to restore homeostatic cellular function in numerous health-related conditions under empirical (Itoh *et al.,* 2009; Jiang *et al.,* 2018; Iuchi *et al.,* 2019; Kura *et al.,* 2019; Begum *et al.,* 2020; Deryugina *et al.,* 2023b) and clinical scrutiny (Kajiyama *et al.,* 2008; Nishimaki *et al.,* 2018; Akagi and Baba, 2019; Chen *et al.,* 2020a; Botek *et al.,* 2019, Akagi and Baba, 2020; Guan *et al.,* 2020). Numerous studies attest to the anti-inflammatory activity of H_2, affirming that the levels of pro-inflammatory mediators, which include chemokines (*e.g.,* MCP-1), cytokines (*e.g.,* TNFα) and transcription factors (*e.g.,* (NFκB), are greatly reduced after H_2 administration (Slezak *et al.,* 2021; Wu *et al.,* 2019; Radyuk, 2021). You *et al*. (2021) demonstrated a significant increase in MAPK protein production in malignant airway epithelial cells (A549 and NCI-H292) after mitogen stimulation, which was attenuated by H_2. The findings of Chu *et al.* (2019), and Zhu, Cui and Xu (2021), support this, identifying that incubating cervical and gastric malignant cell lines (HeLa and MGC-803, respectively) in oxyhydrogen gas markedly increased apoptosis. It can therefore be assumed that H_2 has a pivotal role as a regulator of apoptosis.

8.3.3 Effects of Hydrogen and Oxyhydrogen Gases on B-Lymphocyte Proliferation and Apoptosis in TK6 Cells

In the present study, the influence of H_2 and oxyhydrogen gases on rapidly replicating B-lymphocyte proliferation was investigated (Chapter 7). At the forefront of empirical

conceptualisation, this original research focused on p53-positive immortalised B-cells (TK6 cells) and assessed the effects of dissolved H_2 (300mL/min) and oxyhydrogen (150 mL/min/O_2 + 300 mL/min/H_2) gases in the cell media. The study appraised the differences between treatment groups and controls. The findings show that hydrogen and oxyhydrogen gases both produced an inhibitory effect on TK6 cell populations (Figures 7.4 (A/B) and 7.5), which is consistent with investigations into other malignant cell lines (Liu *et al*., 2019; Meng *et al*., 2020; Chu *et al.,* 2021; Zhu, Cui and Xu, 2021).

Briefly, the pH (Section 7.3.1 a/b), O_2 (Figure 7.2) and H_2 contents (Figures 7.1 and 7.3) were recorded, determining increased levels of both substances in the oxyhydrogen group, concomitant with a slight increase in pH (pH 7.25–8.30) which was observed in both H_2-only and oxyhydrogen groups. TK6 cells were incubated with oxyhydrogen-infused media and cell enumeration was assessed (Figure 7.4 A/B), with the oxyhydrogen groups showing reduced cell density 24 and 48 hours after administration. A similar pattern of replicative inhibition was noted when cells were stimulated with the mitogenic compound ConA and treated with oxyhydrogen (Figure 7.6). Aligning with previous studies (Chu *et al.,* 2021) on flow cytometry analysis of TK6 cells, Figures 7.7 and 7.8 identify reduced cell numbers in growth phases 1 and 2 and a marked increase in apoptosis (Sub G1). The acute protocol (single oxyhydrogen treatment) (Figure 7.4 (A)) recognised a non-significant reduction in cell enumeration, the chronic method (daily addition of media) details statistically relevant inhibition at 24 and 48 h (Figure 7.4 (B)), suggesting, as do Meng *et al*. (2020), that the efficacy of oxyhydrogen and/or H_2 may be dose-dependent.

It is interesting to note that the analysis of the present data corresponds with the findings of Chu et al. (2021), and Zhu, Cui and Xu (2021), who identified that incubating malignant cell lines (HeLa (cervical) and MGC-803 (gastric), respectively) in oxyhydrogen gas inhibited proliferation and oxidative stress, and markedly increased apoptosis. In head-and-neck squamous cell carcinoma (HSC4) and fibrosarcoma (HT1080) cell lines, a neutral pH, H_2- enriched, media suppressed both colony formation and proliferation of HSC4 cells, with HT1080 cells showing inhibited basement membrane invasion. In both cell lines, the accumulation of ROS was repressed, leading the authors (Saitoh et al., 2008) to conclude that H_2 therapies could be used as an effective antioxidant and antitumour therapy.

Although the scope of this research could not ascertain the molecular modality behind the effects seen, one factor that cannot be neglected is that the direct infusion of hydrogen and oxyhydrogen into the cell media altered the pH (Chapter 7, Sections 7.3.1.1 and 7.3.1.2), which may account for some of the effects seen in this study. While it is recognised that an increase in pH may have influenced some aspects of cellular activity, the results of further analyses

(Figures 7.4 – 7.8) are congruent with both early (Saitoh *et al*., 2008; Saitoh *et al*., 2010) and contemporary oncological research (Liu *et al*., 2019; Chu *et al.,* 2021; Zhu, Cui and Xu, 2021). However, as H_2 and oxyhydrogen administration are both demonstrated to impart antioxidant, antiproliferative, antitumor and proapoptotic effects (Liu *et al*., 2019; Chu *et al.,* 2021; Zhu, Cui and Xu, 2021), it is unlikely that the effects observed in the present study are solely the result of the raised pH (7.25–8.30). In similarity with these investigations, Yang *et al*. (2020b) identified H_2-enriched Dulbecco's modified eagle medium (DMEM) (0.7 mg/L/H_2) as upregulating ROS-stimulated pyroptotic pathways (ROS/Nod-like receptor family pyrin domain containing 3 (NLRP3)/caspase-1/Gasdermin D), inducing NFκB-regulated apoptosis (Yang *et al*., 2020b). Such findings are also consistent with investigations into NSCLC, A549 and H1975, where *in vitro* analysis showed that the application of various levels of atmospheric H_2 gas significantly reduced cell viability at 60% and 80% H_2 (Saitoh *et al.,* 2010). Further evidence regarding the therapeutic efficacy of molecular hydrogen, as a saline infusion, suggests H_2 may influence MAPK signalling via inhibition of the PI3K/Akt phosphorylation cascade (Jiang *et al*., 2018). Later enquiries also describe a pro-apoptotic effect of H_2 gas administration (20%, 40% and 60%/H_2 + 5% CO_2), which observed a reduction in the cell surface receptor CD47 and decreased expression of the antiapoptotic (Bcl-2) protein (Meng *et al.,* 2020).

In accordance with other H_2-related oncological studies (Saitoh *et al.,* 2008; Saitoh *et al.,* 2010; Wang *et al.,* 2018b; Yang and Zhu 2018; Liu *et al.,* 2019; Meng *et al.,* 2020; Chu *et al.,* 2021; Hasegawa *et al.,* 2022; Zan *et al.,* 2022; Noor *et al.,* 2023), both hydrogen and oxyhydrogen administration is noted to increase apoptosis in malignant cells. Figures 7.7 and 7.8 identify a marked increase in cells in the Sub G1 phase, an indicator of fragmented DNA attributed to apoptotic cell debris (Manohar, Shah and Nair, 2021) at both the 24 and 48-hour time points (oxyhydrogen) and after 24 hours (hydrogen). These data recognise that growth phases 1 and 2 (G1 and G2, respectively) were significantly restricted, with the effect notably lapsing over time.

Effects on the cells in the synthesis phase at 24 hours were minimal in the oxyhydrogen-exposed groups, although the comparative data for this phase became statistically relevant at 48 hours. The cells exposed to pure H_2 showed significantly reduced numbers in the stationary phase, although this trend was not observed at 48 hours, indicating that oxyhydrogen gas may be more effective in inducing apoptosis in malignant cells than H_2-only treatments. These data notwithstanding, further research is required for these findings to be substantiated.

As the demand for cancer services increases with a globally ageing population (Sabri *et al.,* 2022), healthcare services are under increased pressure to meet operational targets (National

Health Service, 2023a), meaning many patients may not receive optimal care. Therefore, there is an urgent need to prioritise, and invest in, both empirical research and robust large-scale clinical trials, if the efficacy of oxyhydrogen inhalation for the treatment of oncological disease is to benefit the global populace. Further research into the molecular modality of H_2, in particular, is of paramount importance if the antitumour effect of H_2 therapies is to be fully understood and exploited effectively.

Chapter 9: Future Perspectives

9.1 Hydrogen for Health

As stated in Chapter 1, Section 1.2, H_2 is classified as a GRAS product by the Food and Drug Administration (2014) and is regarded as a food supplement (E949) under part C group I of regulation 1129/2011 in the European Union (EU Commission Regulation, 2011) and U.K (Food Standards Agency, 2018). However, for there to be a greater understanding of how H_2 initiates antioxidant and cytoprotective properties at a molecular level, it will be necessary to elucidate the primary target, or targets, of H_2 interactions. Analysis of clinical and laboratory data recognises that scavenging of ROS and RNS alone cannot explain the extent of ROS/RNS mitigation by H_2 in cellular and somatic systems. The evidence presented here indicates that H_2 is unlikely to directly reduce either $^{\bullet}OH$ or $ONOO^-$ in significant quantities (Chapter 4, Sections 4.2.1 and 4.2.2). Nevertheless, it is possible that H_2 can prevent the reduction of O_2 to $O_2^{\bullet-}$, possibly through i) maintaining the structural integrity, perhaps stabilising pocket structures within proteins (Chen *et al.,* 2019c; Hancock *et al.,* 2022), ii) through di-hydrogen or Kubas bonding to Fe^{2+} prosthetic moieties, preventing irreversible oxidation (Kim *et al.,* 2022), or iii) via direct or indirect interactions with signalling molecules such as Ca^{2+} (Chapter 4, Section 4.4.1) and/or PO_3^{2-} (Chapter 4, Section 4.4.2).

Pioneering research strongly suggests that H_2 can reduce oxidative damage caused by surgical intervention, such as ischemia-reperfusion or through injury or disease (Gharib *et al*., 2001; Fukuda *et al.,* 2007; Tarnava, 2021). However, whether this is due to the direct reductive potential of H_2, or upstream of ROS and RNS production, has yet to be characterized *in vivo,* and further molecular research is required.

9.2 Wider Research

In addition to the health benefits of hydrogen gas explored here, a wealth of academic studies also identify that exposing plants to H_2 during the germination, plantation and growth phases can enhance root establishment, increase disease resistance and promote the growth and development of leaves, fruits and seeds (Hancock et al., 2021). Incorporating H_2 into the feedwater of plant crops is a relatively simple process which can be implemented in various ways. For example, as a seed-priming agent (Chapter 6, Section 6.3.), H_2 can be used before planting, alternatively, H_2-enriched water and H_2 gas can be used as a topical application for germinating and maturing plants. HRW and HNW can also be obtained by diffusing H_2 gas (formed through water electrolysis) into nutrient solutions and irrigation systems, and by dissolving Mg or H_2 donors (e.g., AB@hMSN, formic acid) in aqueous solutions. Such methods are already being implemented academically (Felix et al., 2019; Wang et al., 2021b; Wang et al, 2023b). The addition of H2 into soil environments is also noted to improve soil quality through increasing H2-oxidising microbial activity and promoting carbon fixation (Stein *et al.,* 2005, Piché-Choquette and

Constant, 2019; Islam, Greening and Hu, 2023), a term referred to as hydrogen fertilisation, however, the process is somewhat complex which may rule out its application in an agricultural setting and whether this type of application would provide a large-scale, long-term solution to replenishing nutrient-deficient soils has yet to be explored.

Global losses of food productivity as a result of increasing burdens (e.g., climate change, pollution and soil erosion) are estimated to be in the region of $170 billion United States Dollars (USD), annually (Razzaq *et al*., 2021). Ergo, there is a pressing requirement for additional, effective means of preserving the nutritional content, preventing the spoilage of and prolonging the shelf-life of fresh produce. In this regard, there is an extensive body of research attesting to the benefits of adding H_2 into the feedwater of seeds, seedlings and maturing plants, wherein, H_2 supplied as HRW, is demonstrated to improve crop viability and yield (Cheng *et al.,* 2021; Wang *et al.*, 2023b). The antioxidant activity of H_2 is proposed to be the primary mode of action involving the upregulation of glutathione and sulphur metabolism (Cui *et al*., 2020), enhanced antioxidant gene expression (Wang *et al.,* 2023b) and promoting hormone synthesis (Felix *et al*., 2019). Such cytoprotective actions proffer resistance to both biotic and abiotic stressors including drought (Yan *et al*., 2022), heavy metal toxicity (Zhang *et al.,* 2017; Cheng *et al.,* 2021), increased salinity (Wu *et al*., 2020), temperature variation (Guan *et al.,* 2019; Wang *et al.*, 2023b) and viral infection (Shao *et al*., 2023).

In this regard, H_2 could enhance food security by enhancing resistance to stress, improving crop yields and maintaining the nutritional value, although further research and investment into the potential of H_2 as a fertiliser is required.

9.3 Research Requirements

9.3.1 Clinical

In a clinical context, the safety of oxyhydrogen-producing devices (reviewed by Ichikawa et al., 2023) could likely lead to hesitation in implementing such therapies within a public healthcare setting. However, as O_2 is also a hazardous gas, and one that is routinely utilised within healthcare, it is conceivable that oxyhydrogen therapies could be introduced as long as stringent guidelines are adhered to. For instance, when using pure O_2 at home, patients are advised not to place canisters close to sources of heat or potential ignition (such as fires, electrical appliances, etc.) (National Health Service, 2023b). However, as oxyhydrogen-generating devices do not require storage of such flammable substances, the risk is mitigated. Nevertheless, full safety protocols will need to be established before either clinical or at-home use is commonplace.

As evidence regarding the efficacy of inhalation products is lacking, there is a requirement for extended analyses covering the questions of optimal dosage and duration of treatments, and

whether pure H_2, or oxyhydrogen inhalation, has greater antioxidant/anti-inflammatory properties. In addition, from feasibility perspective, it will be important to conduct comparative analyses not only on the purported medical benefits but also on the cost, environmental impact, sustainability and durability of materials used. Research into new methods of hydrogen delivery such as H_2-containing gels, HRW, and nanomaterials may also provide a safe and effective way to clinically administer H_2. However, much more evidence is necessary before such novel means of delivery can be assessed. Therefore, continued research into which hydrogen-delivery mechanisms are best suited for individual circumstances will also be required if the widespread medical use of H_2 is to be realised in the future.

To date, molecular hydrogen treatments have shown no toxicity in animals or humans, whilst it is also suggested that H_2 does not accumulate in blood or tissues and that excesses are liberated in the breath (Shin, 2014). Nevertheless, the positive effects of H_2 administration are noticed long after H_2 has been eliminated and warrant long-term clinical observations. Therefore, clinical data must consider not only the delivery mechanism for treating specific conditions, but the distribution, dosage, and duration of such effective treatments. Standardized measurements of hydrogen content and dosage limits will need to be established, conceivably, before large-scale trials can take place. Lastly, for a full understanding of how H_2 or oxyhydrogen gases may interact with medications and/or health and lifestyle supplements, therefore impacting the health of the global population, it will be necessary to comprehend the modality of H_2 antioxidant/anti-inflammatory activity. For this to be realised it will be important to recognise the primary molecular targets and chemical interactions between H_2 and various cellular components, in healthy and diseased states.

9.3.2 Empirical

It is evident that many aspects need to be considered before H_2 can be considered a prescriptible therapy by global health agencies. Unidentified factors of hydrogen biochemistry such as diffusion and reactivity rates, the interaction with metal-containing groups such as haem, and the magnetic spin state may have effects (Chapter 4). There is also a need to identify the primary target, or targets, of H_2 interactions, so that the molecular mechanisms can be identified (Hancock, LeBaron and Russell, 2021). Such work would support clinical data and could indicate whether there are likely to be any long-term or detrimental effects to hydrogen therapies.

To increase the current understanding of H_2 biochemistry it will be necessary to employ several analytical methods on various eukaryotic cells. For example, electron paramagnetic resonance (EPR) spectroscopy, in association with a protein-specific spin label, can be used

to detect radical or ionic adducts on given traps known to react with specific ROS or RNS. If supported by chemiluminescence analysis, this technique would allow a comparative assessment of H_2 scavenging activity with both $ONOO^-$ and $^{\bullet}OH$ which can be applied to both *ex vivo* and *in vitro* analysis. Additionally, a modified CUPRAC assay using *p*-aminobenzoate, *2,4*- and *3,5*-dimethoxybenzoateas; or hydroxyphenyl fluorescein, can be utilised as probes for identifying and quantifying $^{\bullet}OH$ in biological fluids (Li *et al.,* 2020). Utilising such techniques would be useful in providing further information as to whether H_2 can reduce, or prevent formation of, this particular radical. In addition to fluorescent analysis, Halliwell *et al.* (1987) developed a simple and cost-effective, deoxyribose, test tube assay able to determine the reaction rate constants of antioxidant compounds with $^{\bullet}OH$. Here, when $^{\bullet}OH$-reductive antioxidants are added to the assay they compete with deoxyribose, a major target for $^{\bullet}OH$ oxidation, and inhibit chromogen formation. The rate constant for the reaction of the antioxidant with hydroxyl radical can then be deduced by analysing the reduction of the colour formation when using spectrophotometric analysis (Halliwell, Gutteridge and Aruoma, 1987).

Regarding the theory that H_2 may reside in protein pockets and/or affect haem dynamics (Chapter 4, Section 4.3.2), further X-ray crystallography, *in silico* modelling (*e.g.,* X-PLOR (Brünger *et al*., 1998)), could be applied. Nuclear magnetic resonance (NMR) spectroscopy may also help to define the regions of proteins where surface pockets or intraprotein channels may lead to H_2-protein affinity and interaction. Furthermore, taking a bioinformatics approach to identify whether Xe-binding pockets and, or, channels have analogous configurations, particularly in haem-containing proteins, may provide valuable information as to whether such structures are conserved and whether H_2 is likely to have had an important role in maintaining the redox status of cells and larger organisms. Infrared spectroscopy, protein film electrochemistry and whole-cell biochemical assays, such as the one developed by Lacasse *et al.* (2019), may also be able to identify whether H_2 influences the function of Complex I, whilst further sophisticated investigations using such techniques as X-ray crystalline imaging, gene editing/mutation and mass spectroscopy, all of which can help to identify the molecular regions targeted by H_2,should provide valuable insights into the form and functionality of such proteins exposed to H_2. It may also be beneficial to understand whether H_2 competes with other gases or low molecular weight compounds, although, a notable limitation of the aforementioned techniques is that they require frozen samples for analysis, therefore catalytic turnover and kinetics cannot be assessed.

Finally, to identify whether H_2 directly affects Ca^{2+} signalling events it may be beneficial to employ such techniques as Ca^{2+}-specific fluorescent probes (*e.g.,* green fluorescent protein (GFP)-based genetically encoded calcium indicator sensors) such as those initially developed by Nakai, Ohkura and Imoto (2001). To assess the effect(s) H_2 may have on phosphorylation

events there are a myriad of techniques that can be employed. For example, the enzyme-linked immunosorbent assay (ELISA) can detect antibody conjugation of the phosphorylation site of a protein of interest, providing a semi-quantitative analysis of phosphorylated proteins. Alternatively, the Phos-Tag™/ sodium dodecyl sulphate-polyacrylamide gel electrophoresis assay (SDS-PAGE), which binds phosphoryl groups, can also be used (Kinoshita, Kinoshita-Kikuta and Koike, 2009). Furthermore, phosphorylated proteins can be identified through radiolabelling, mass spectroscopy and western blot analyses, whilst there is a range of kinase activity assays that may also indicate whether H_2 is likely to interact upstream of protein phosphorylation. The application of such analyses should provide a fuller picture as to whether H_2 directly targets such signalling cascades.

9.3.3 Field

To better assess the potential for H_2 to support food growth, distribution and production industries, large-scale, in-field research, along with further empirical investigations into the primary, secondary and, perhaps, tertiary effects of H_2 applications will be advantageous. It may also be prudent to analyse whether heritable traits are affected by long-term H_2 usage. This could involve understanding the epigenetic context, hormone regulation, and resistance to biotic and abiotic stressors.

Recent studies, such as that conducted by Cheng *et al.,* (2021), have identified that HNW is suitable for irrigating crops, therefore, it may be propitious to focus on this aspect of H_2 production when considering pre-harvest administration.

For post-harvest applications, comparative analysis of whether treatment with HRW/HNW or H_2 gas, and at what stage in the distribution chain application is most effective, would be of great benefit.

9.3.4 Financial

It is not only the efficacy of H_2 therapies that must be scrutinised, but also the cost-effectiveness, sustainability, and long-term benefits of treatment should be assessed. A major issue for the widespread use of H_2 in industry and, therefore, healthcare, is to lower the cost of H_2 production. To exemplify, the energy required for water electrolysis reaches between 60% and 80% of the total cost (Blanco *et al.,* 2018). Nevertheless, the energy required for H_2 production can be supplied from numerous sources including onsite generators, including solar and wind, and national power grids. At a rate of ¢5/kWh electricity, the cost of hydrogen production through electrolysis systems is likely to range between $5 (United States Dollar (USD)) and $10 per kg ($H_2$) (Finke *et al.,* 2021). However, scaling up such environmentally responsible sources of power (*e.g.,* wind power and photovoltaic technologies) is expected to lead to a 30-80% reduction in the cost of electrolytic H_2 production by 2050, bringing it closer

to the cost of H_2 production from fossil fuels ($1-2 USD) (Finke *et al.*, 2021). Additionally, the purchase and maintenance costs, along with an assessment of the durability and longevity of commercial units versus conventional treatments and processes, will also need to be considered. Moreover, to give a full view of the financial viability of utilising H_2 in the agricultural and healthcare industries, and considering that large-scale research into the potential of H_2 for either industry has yet to be implemented, both the administration methods, and where the introduction of H_2 therapies in agricultural (*e.g.,* pre/post-harvest) or clinical practices (e.g., emergency/recuperative care) would be most efficacious, will have to be assessed.

9.4 Mitigating the Risks

H_2 gas is flammable at temperatures above 527 °C and is known to explode in a combustive reaction when O_2 is present (Ohta, 2014). According to contemporary reports, H_2 should not exceed 4.6% in air and 4.1% by volume in pure oxygen gas(Huang *et al.,* 2010; Hu *et al.,* 2020). Hydrogen, as a pure gas, is an explosion risk and therefore it is not safe, or practical, to store such a volatile gas in the clinical environment. To reduce the hazards associated with the inhalation of such a combustible material, administrable concentrations of H_2 should not exceed one-third of the lower explosion limit. However, as therapeutic effects are demonstrated with the administration of 2% H_2 (Chen, Zhang and Qin, 2021), providing small volumes of H_2 may reduce the necessity for high-risk containment of such a volatile gas. A recent report into the explosivity of AE and PEM generators found that the primary cause of explosions was due to the leakage of hydrogen gas inside the production devices (Ichikawa *et al.,* 2023). Further, a recent study conducted by Leancat Fuel Cell Technology, presented at the 1st International Conference of the European Academy for Molecular Hydrogen Research in Biomedicine, Slovakia (Matolin, 2022), indicates that the presence of a transient explosive atmosphere is applicable in the inner space of connective conduits, the filter bottle, and for a distance of 10 cm around the end of the inhalation tube. Therefore it is imperative that when using H_2-containing gases it is essential to ensure the safety and well-being of those working within the environment.

Using H_2 safely will require proper handling precautions and procedures due to its flammability and potential for explosive reactions. For example, during storage, H_2 will need to be contained in appropriate cylinders in well-ventilated areas away from heat sources, ignition, and direct sunlight (Abohamzeh *et al.,* 2021) a factor that is likely to pose an issue towards comprehensive clinical use particularly in countries such as the UK and USA which have stringent patient-safety policies. Cylinders should also be regularly checked for damage to reduce the potential of leakage. Additionally, as H_2 is lighter than air, proper airflow and ventilation are also necessary to prevent the accumulation of H_2. Equipment, fittings, and

connections of any apparatus using H_2 will also require detectors/monitors, which can provide early warning of malfunction and H_2 leakage. Pressure regulators and flow meters can detect sudden pressure changes and may well be instrumental in preventing harm from faults in H_2-associated equipment. It will be prudent to ensure individuals working with H_2 are adequately trained in the safe handling, storage and emergency procedures, with training to include recognizing the potential hazards, and how to respond to incidences that may involve H_2 (*e.g.,* evacuation, fires, leaks, *etc.*).

When considering the application of H_2 and oxyhydrogen inhalation therapies that utilise the electrolysis of water, the mixture of gases is consumed upon generation and production discontinues when the system is not in use. This safety feature negates the requirement for precarious storage of gaseous compounds, improving the safety of consumers, patients and healthcare workers. Furthermore, H_2 generating devices are uncomplicated to use, require little training or maintenance, and are a sustainable and ecological means of providing therapeutic hydrogen.

Chapter 10: Conclusion

It can be surmised that due to the undefined mechanisms of action, the lack of primary target identification, coupled with difficulties regarding administration methods, dosage and dosage frequencies, as well as the long-term effects of treatment and the patient's innate antioxidant profile; there is a requirement for H_2 research to evidence how it can reasonably and most effectively be incorporated into healthcare practices. Furthermore, knowledge gained from extensive clinical data (Supplementary section: Table 1) has been slow to translate into global healthcare practices.

Chapter 3 of this thesis explores the evolutionary requirement and role of H_2 by assessing the possibility of an ancestral relationship with redox active, ubiquinone binding, subunits of Complex I, finding that, although the level of homology between the *C. heimdallarchaeota* hydrogenase MbhL and subunit NDUFS2 (27%) is above the threshold of significance (Anderson and Brass, 1998), there is little similarity between protein sequences in the active site. Thus concluding that, if NDUFS subunits were derived from functional hydrogenases, the ability to catalyse the oxidation/reduction of H_2 would have been dependent on retaining Ni in the active site.

Despite the precise molecular mechanisms of H_2 activity having yet to be fully elucidated, it appears that H_2 may act as a rather promiscuous molecule, likely having loose affiliations with numerous biological components such as glycogen complexes, iron prosthetic groups and other metallic ions (e.g., Ca^{2+}), perhaps also supporting a diverse range of protein structures and functions (Chapter 4, Sections 4.2.3 and 4.2.4). It is still unclear, however, as to whether H_2 also acts as a direct antioxidant, reducing such pernicious ROS/RNS as $^{\bullet}OH$ and $ONOO^-$ (Chapter 4, Section 4.2) and further in silico modelling, accounting for wider activities in the physiological environment, are required.

The collection of data presented here demonstrates that H_2 therapies can have a wide range of effects in disparate somatic systems (Chapter 8, Section 8.3), with many of the favourable attributes being associated with modulation of the redox environment and concomitant anti-inflammatory qualities (Chapter 1). An additional benefit of H_2 and oxyhydrogen therapies is that they can be delivered in a myriad of ways (Chapter 8, Section 8.2). Progressive innovations, such as oxyhydrogen inhalation devices, and both dissolvable and ingestible tablets, as well as saline infusions and hydrogen inhalation, are easily administered. Commercially available H_2-only and oxyhydrogen inhalation devices can range in both the quality and volume of gas produced. Chapter 5 of this thesis analyses the gaseous output of the HydroVitality™ alkaline water electrolysis, oxyhydrogen generator and confirms the gas

produced is ~66% H_2 and ~33% O_2 at a flow rate of 450mL/min. This gas can also raise both the H_2 and O_2 content when dissolved into aqueous solutions (Chapters 5, 6 and 7).

At the forefront of empirical conceptualisation, Chapter 7 focuses on p53-positive malignant B-cells (TK6 cells), assessed the effects of dissolved H_2 (300mL/min) and oxyhydrogen (300 mL/min, H_2 + 150 mL/min, O_2) gases cell-culture media. Briefly, TK6 cells were incubated with H_2- or oxyhydrogen-infused media. Both H^2 and oxyhydrogen groups show reduced cell density 24 and 48 hours after administration, and aligning with previous studies (Liu et al., 2019; Chu et al., 2021), Figures 7.7 and 7.8 identify reduced cell numbers in growth phases 1 and 2 and a marked increase in apoptosis (Sub G1), suggesting these gases may be effective therapeutics for oncological disease. Lastly, Chapter 9 explores the gaps in knowledge and provides suggestions to further experimentations that may provide valuable information for integrating H_2 technologies into agricultural and healthcare industries.

In conclusion, this treatise advocates for further research into the clinical usage of hydrogen therapeutics. By utilising bioinformatic, empirical and theoretic analyses, the research presented here supports the current literature, and evidences that H_2 is highly likely to provide auspicious protective effects in cellular, and wider, biological and somatic systems.

References

- Abhishek, A., Bavishi, A., Bavishi, A. and Choudhary, M. (2011) Bacterial genome chimaerism and the origin of mitochondria. *Canadian Journal of Microbiology. 57*(1), pp.49-61.
- Abohamzeh, E., Salehi, F., Sheikholeslami, M., Abbassi, R. and Khan, F. (2021) Review of hydrogen safety during storage, transmission, and applications processes. *Journal of Loss Prevention in the Process Industries*. *72*, pp.1-19.
- Abraini, J.H., Marassio, G., David, H.N., Vallone, B., Prangé, T. and Colloc'h, N. (2014) Crystallographic studies with xenon and nitrous oxide provide evidence for protein- dependent processes in the mechanisms of general anesthesia. *Anesthesiology. 121*(5), pp.1018-1027.
- Ahmad, A., Baig, A.A., Hussain, M., Saeed, M.U., Bilal, M., Ahmed, N., Chopra, H., Hassan, M., Rachamalla, M., Putnala, S.K. and Khaliq, M. (2022) Narrative on hydrogen therapy and its clinical applications: safety and efficacy. *Current Pharmaceutical Design*. *28*(31), pp.2519-2537.
- Akagi, J. and Baba, H. (2019) Hydrogen gas restores exhausted CD8+ T cells in patients with advanced colorectal cancer to improve prognosis. *Oncology Reports*. *41*(1), pp.301- 311.
- Akagi, J. and Baba, H. (2020) Hydrogen gas activates coenzyme Q10 to restore exhausted CD8+ T cells, especially PD-1+ Tim3+ terminal CD8+ T cells, leading to better nivolumab outcomes in patients with lung cancer. *Oncology Letters*. *20*(5), p.1.
- Al Zahrani, S.M., Omar, U.M., Rahimulddin, S.A., Al-Ghafari, A.B., Aldahlawi, A.M. and Al Doghaither, H.A. (2019) Antiproliferative and apoptotic effects of the natural alkaline water (Zamzam) in breast cancer cell line MCF-7. *Journal of Cancer Research and Therapeutics*. *15*(5), pp.1098-1104.
- Albracht, S.P. (1993) Intimate relationships of the large and the small subunits of all nickel hydrogenases with two nuclear-encoded subunits of mitochondrial NADH: ubiquinone oxidoreductase. *Biochimica et Biophysica Acta (BBA)-Bioenergetics*. *1144*(2), pp.221-224.
- Aldon, D., Mbengue, M., Mazars, C. and Galaud, J.P. (2018) Calcium signalling in plant biotic interactions. *International Journal of Molecular Sciences*. *19*(3), p. 665.
- Alharbi, A.A.D., Ebine, N., Nakae, S., Hojo, T. and Fukuoka, Y. (2021) Application of molecular hydrogen as an antioxidant in responses to ventilatory and ergogenic adjustments during incremental exercise in humans. *Nutrients*. *13*(2), p.459.
- Alharbi, A.A.D., Iwamoto, N., Ebine, N., Nakae, S., Hojo, T. and Fukuoka, Y. (2022) The acute effects of a single dose of molecular hydrogen supplements on responses to ergogenic adjustments during high-intensity intermittent exercise in humans. *Nutrients*. *14*(19), p.3974.
- Almasalmeh, A., Krenc, D., Wu, B. and Beitz, E. (2014) Structural determinants of the hydrogen peroxide permeability of aquaporins. *The FEBS Journal*. *281*(3), pp. 647-656.

- Alzahrani, N.A., Bahaidrah, K.A., Mansouri, R.A., Alsufiani, H.M. and Alghamdi, B.S. (2022) Investigation of the optimal dose for experimental lipopolysaccharide-induced recognition memory impairment: behavioral and histological studies. *Journal of Integrative Neuroscience*. *21*(2), p.49.
- Amitani, H., Asakawa, A., Cheng, K., Amitani, M., Kaimoto, K., Nakano, M., Ushikai, M., Li, Y., Tsai, M., Li, J.B. and Terashi, M. (2013) Hydrogen improves glycemic control in type1 diabetic animal model by promoting glucose uptake into skeletal muscle. *PLoS One*. *8*(1), p.53913.
- Anderson, I. and Brass, A. (1998) Searching DNA databases for similarities to DNA sequences: when is a match significant? *Bioinformatics*. *14*(4), pp.349-356.
- Aoki, K., Nakao, A., Adachi, T., Matsui, Y. and Miyakawa, S. (2012) Pilot study: Effects of drinking hydrogen-rich water on muscle fatigue caused by acute exercise in elite athletes. *Medical Gas Research*. *2*(1), pp.1-6.
- Asgharzadeh, F., Tarnava, A., Mostafapour, A., Khazaei, M. and LeBaron, T.W. (2022) Hydrogen-rich water exerts anti-tumor effects comparable to 5-fluorouracil in a colorectal cancer xenograft model. *World Journal of Gastrointestinal Oncology*. *14*(1), p.242.
- Ash, P.A., Kendall-Price, S.E. and Vincent, K.A. (2019) Unifying activity, structure, and spectroscopy of [NiFe] hydrogenases: combining techniques to clarify mechanistic understanding. *Accounts of Chemical Research*. *52*(11), pp.3120-3131.
- Bajgai, J., Lee, K.J., Rahman, M.H., Fadriquela, A. and Kim, C.S. (2021) Role of molecular hydrogen in skin diseases and its impact in beauty. *Current Pharmaceutical Design*, *27*(5), pp.737-746.
- Barancik, M., Kura, B., LeBaron, T.W., Bolli, R., Buday, J. and Slezak, J. (2020) Molecular and cellular mechanisms associated with effects of molecular hydrogen in cardiovascular and central nervous systems. *Antioxidants*. *9*(12), p.1281.
- Baxter, C., Rowan, J.S., McKenzie, B.M. and Neilson, R. (2013) Understanding soil erosion impacts in temperate agroecosystems: bridging the gap between geomorphology and soil ecology using nematodes as a model organism. *Biogeosciences*. *10*(11), pp.7133-7145.
- Bazil, J.N., Pannala, V.R., Dash, R.K. and Beard, D.A. (2014) Determining the origins of superoxide and hydrogen peroxide in the mammalian NADH: ubiquinone oxidoreductase. *Free Radical Biology and Medicine*. *77*, pp. 21-129.
- Begum, R., Kim, C.S., Fadriquela, A., Bajgai, J., Jing, X., Kim, D.H., Kim, S.K. and Lee, K.J. (2020) Molecular hydrogen protects against oxidative stress-induced RAW 264.7 macrophage cells through the activation of Nrf2 and inhibition of MAPK signaling pathway. *Molecular & Cellular Toxicology*. *16*, pp.103-118.
- Beheshti, E., Nojeh, A. and Servati, P. (2011) A first-principles study of calcium-decorated, boron-doped graphene for high capacity hydrogen storage. *Carbon*. *49*(5), pp.1561-1567.
- Belon, L., Skidmore, P., Mehra, R. and Walter, E. (2021) Effect of a fever in viral infections— the 'Goldilocks' phenomenon? *World Journal of Clinical Cases*. *9*(2), p. 296.

- Benzie, I.F. and Strain, J.J. (1996) The ferric reducing ability of plasma (FRAP) as a measure
- of "antioxidant power": the FRAP assay. *Analytical Biochemistry*. *239*(1), pp.70-76.
- Beverly, J.K. and Budoff, M.J. (2020) Atherosclerosis: Pathophysiology of insulin resistance, hyperglycemia, hyperlipidemia, and inflammation. *Journal of Diabetes*. *12*(2), pp.102-104.
- Bhave, N.A., Gupta, M.M. and Joshi, S.S. (2023) Combustion, performance, and emission characteristics of diesel engine using oxyhydrogen gas as a fuel additive. *Environmental Science & Pollution Research*. *30*(10), pp.1-14.
- Bilal, M.; Barani, M.; Sabir, F.; Rahdar, A.; Kyzas, G.Z. (2020) Nanomaterials for the treatment and diagnosis of Alzheimer's disease: An overview. *NanoImpact*. *20*, p.100251
- Bjurstedt, H. and Severin, G., 1948. The prevention of decompression sickness and nitrogen narcosis by the use of hydrogen as a substitute for nitrogen (The Arne ZetterstrÖm Method for deep-sea diving). *The Military Surgeon (United States)*. *103*(2), pp.107-116.
- Blanco, H., Nijs, W., Ruf, J. and Faaij, A. (2018) Potential for hydrogen and Power-to-Liquid in a low-carbon EU energy system using cost optimization. *Applied Energy*. *232*, pp.617- 639.
- Blaxter, M. (2011) Nematodes: the worm and its relatives. *PLoS Biology*. *9*(4), p.1001050.
- Botek, M., Krejčí, J., McKune, A.J., Sládečková, B. and Naumovski, N. (2019) Hydrogen rich water improved ventilatory, perceptual and lactate responses to exercise. *International Journal of Sports Medicine*. 40(14), pp.879-885.
- Botek, M., Khanna, D., Krejčí, J., Valenta, M., McKune, A., Sládečková, B. and Klimešová, I. (2022a) Molecular hydrogen mitigates performance decrement during repeated sprints in professional soccer players. *Nutrients.* 14(3), p.508.
- Botek, M., Krejčí, J., McKune, A., Valenta, M. and Sládečková, B. (2022b) Hydrogen rich water consumption positively affects muscle performance, lactate response, and alleviates delayed onset of muscle soreness after resistance training. *Journal of Strength and Conditioning Research*. *36*(10), pp.2792-2799.
- Botek, M., Krejčí, J., Valenta, M., McKune, A., Sládečková, B., Konečný, P., Klimešová, I. and Pastucha, D. (2022c). Molecular hydrogen positively affects physical and respiratory function in acute post-COVID-19 patients: A new perspective in rehabilitation. *International Journal of Environmental Research and Public Health*. *19*(4), p.1992.
- Breck, D.W. and Smith, J.V. (1959) Molecular Sieves. *Scientific American*. *200*(1), pp.85- 94.
- Bren, K.L., Eisenberg, R. and Gray, H.B. (2015) Discovery of the magnetic behavior of hemoglobin: A beginning of bioinorganic chemistry. *Proceedings of the National Academy of Sciences of the United States of America*. *112*(43), pp.13123-13127.
- Brenner, S. (1974) The genetics of Caenorhabditis elegans. *Genetics.* 77 (1), pp.71-94.

- Brünger, A.T., Adams, P.D., Clore, G.M., DeLano, W.L., Gros, P., Grosse-Kunstleve, R.W., Jiang, J.S., Kuszewski, J., Nilges, M., Pannu, N.S. and Read, R.J. (1998) Crystallography & NMR system: A new software suite for macromolecular structure determination. *Acta Crystallographica Section D: Biological Crystallography*. *54*(5), pp.905-921.
- Brust, H., Orzechowski, S. and Fettke, J. (2020) Starch and glycogen analyses: Methods and techniques. *Biomolecules*. *10*(7), p.1020.
- Canuto R.A. (ed.) (2012) Dehydrogenases. *InTech.* Available from: http://dx.doi.org/10.5772/2903. [Accessed 29 January 2022].
- Capurso, T., Stefanizzi, M., Torresi, M. and Camporeale, S.M. (2022) Perspective of the role of hydrogen in the 21st century energy transition. *Energy Conversion and Management*. *251*, p.114898.
- Cargnello, M. and Roux, P.P. (2011) Activation and function of the MAPKs and their substrates, the MAPK-activated protein kinases. *Microbiology and Molecular Biology Reviews*. *75*(1), pp.50-83.
- Chatterjee, S., Jungraithmayr, W. and Bagchi, D. (eds.) (2017). *Immunity and inflammation in health and disease: emerging roles of nutraceuticals and functional foods in immune support*. Academic Press. Cambridge, MA, USA.
- Chen, H., Sun, Y.P., Hu, P.F., Liu, W.W., Xiang, H.G., Li, Y., Yan, R.L., Su, N., Ruan, C.P.,
- Sun, X.J. and Wang, Q. (2011) The effects of hydrogen-rich saline on the contractile and structural changes of intestine induced by ischemia-reperfusion in rats. *Journal of Surgical Research*. *167*(2), pp.316-322.
- Chen, X., Zhai, X., Shi, J., Liu, W.W., Tao, H., Sun, X. and Kang, Z. (2013) Lactulose mediates suppression of dextran sodium sulfate-induced colon inflammation by increasing hydrogen production. *Digestive Diseases and Sciences. 58*,1560–1568.
- Chen, J., Kong, X., Mu, F., Lu, T., Du, D. and Xu, K. (2019a). Hydrogen–oxygen therapy can alleviate radiotherapy-induced hearing loss in patients with nasopharyngeal cancer. *Annals of Palliative Medicine*. *8*(5), p.74651.
- Chen, J.B., Kong, X.F., Lv, Y.Y., Qin, S.C., Sun, X.J., Mu, F., Lu, T.Y. and Xu, K.C. (2019b)
- "Real world survey" of hydrogen-controlled cancer: a follow-up report of 82 advanced cancer patients. *Medical Gas Research*. *9*(3), p.115.
- Chen, Z., Zhang, X., Peng, C., Wang, J., Xu, Z., Chen, K., Shi, J. and Zhu, W. (2019c) D3Pockets: a method and web server for systematic analysis of protein pocket dynamics. *Journal of Chemical Information and Modeling*. *59*(8),3353-3358.
- Chen, J.B., Kong, X.F., Mu, F., Lu, T.Y., Lu, Y.Y. and Xu, K.C. (2020a) Hydrogen therapy can be used to control tumor progression and alleviate the adverse events of medications in patients with advanced non-small cell lung cancer. *Medical Gas Research*. *10*(2),75.
- Chen, J.B., Kong, X.F., Qian, W., Mu, F., Lu, T.Y., Lu, Y.Y. and Xu, K.C. (2020b) Two weeks of hydrogen inhalation can significantly reverse adaptive and innate immune system senescence patients with advanced non-small cell lung cancer: a self-controlled study. *Medical Gas Research*. *10*(4), p.149.

- Chen, W., Zhang, H.T., Qin, S.C. (2021) Neuroprotective effects of molecular hydrogen: A critical review. *Neuroscience Bulletin. 37*, pp.389–404.

- Cheng, P., Wang, J., Zhao, Z., Kong, L., Lou, W., Zhang, T., Jing, D., Yu, J., Shu, Z., Huang, L. and Zhu, W. (2021) Molecular hydrogen increases quantitative and qualitative traits of rice grain in field trials. *Plants*. *10*(11), p.2331.
- Chi, J., Li, Z., Hong, X., Zhao, T., Bie, Y., Zhang, W., Yang, J., Feng, Z., Yu, Z., Xu, Q. and Zhao,
- L. (2018) Inhalation of Hydrogen Attenuates Progression of Chronic Heart Failure via Suppression of Oxidative Stress and P53 Related to Apoptosis Pathway in Rats. *Frontiers in Physiology*. *9*, p.1026.
- Chinese Coptionnical Trial Register (ChiCTR). Keyword: '*Hydrogen*'. Available from: https://www.chictr.org.cn/searchprojEN.html?title=hydrogen&officialname=&subjectid= &regstatus=&regno=&secondaryid=&applier=&studyleader=&createyear=&sponsor=&secsponsor=&sourceofspends=&studyailment=&studyailmentcode=&studytype=&studystage=&studydesign=&recruitmentstatus=&gender=&agreetosign=&measure=&country=&province=&city=&institution=&institutionlevel=&intercode=&ethicalcommitteesanction=&whetherpublic=&minstudyexecutetime=&maxstudyexecutetime=&btngo=btn [Accessed 12/08/2023].
- Chisholm, G. and Cronin, L. (2016) Hydrogen From Water Electrolysis. *Storing Energy: with Special Reference to Renewable Energy Sources*. p.315.
- Christ, A.D., Sarker, S., Bauerfeind, P., Drewe, J., Meier, R. and Gyr, K. (1994) Assessment of gastric acid output by H2 breath test. *Scandinavian Journal of Gastroenterology*. *29*(11), pp.973-978.
- Chu, J., Gao, J., Wang, J., Li, L., Chen, G., Dang, J., Wang, Z., Jin, Z. and Liu, X. (2021) Mechanism of hydrogen on cervical cancer suppression revealed by high-throughput RNA sequencing. *Oncology Reports*. *46*(1), pp.1-11.
- Cirilli, I., Damiani, E., Dludla, P.V., Hargreaves, I., Marcheggiani, F., Millichap, L.E., Orlando, P., Silvestri, S. and Tiano, L. (2021) Role of coenzyme Q10 in health and disease: An update on the last 10 years (2010–2020). *Antioxidants*. *10*(8), p.1325.
- Clapham, D.E. (2007) Calcium signaling. *Cell*. *131*(6), pp.1047-1058.
- ClinicalTrials.gov. Keyword: '*Hydrogen*' Available from: https://clinicaltrials.gov/ct2/results?cond=&term=molecular+hydrogen&cntry=&state=&city=&dist= [Accessed 12/12/2022].
- Cobden, P.D., Nieuwenhuys, B.E., Gorodetskii, V.V. and Parmon, V.N. (1998) Formation and decomposition of palladium hydride particles. *Platinum Metals Review*. *42*(4), pp.141- 144.
- Coppola, C.M., Longo, S., Capitelli, M., Palla, F. and Galli, D. (2011) Vibrational level population of H2 and $H^{+}2$ in the early universe. *The Astrophysical Journal Supplement Series*. *193*(1), p.7.
- Corsi, A.K. (2006) A biochemist's guide to Caenorhabditis elegans. *Analytical Biochemistry. 359*(1), pp.1-17.

- Cui, W., Yao, P., Pan, J., Dai, C., Cao, H., Chen, Z., Zhang, S., Xu, S. and Shen, W. (2020) Transcriptome analysis reveals insight into molecular hydrogen-induced cadmium tolerance in alfalfa: the prominent role of sulfur and (homo) glutathione metabolism. *BMC Plant Biology*. *20*(1), pp.1-19.
- Da Ponte, A., Giovanelli, N., Nigris, D. and Lazzer, S. (2018) Effects of hydrogen rich water on prolonged intermittent exercise. *The Journal of Sports Medicine and Physical Fitness*. *58*(5), pp.612-621.
- Damiano, S., Muscariello, E., La Rosa, G., Di Maro, M., Mondola, P. and Santillo, M. (2019) Dual role of reactive oxygen species in muscle function: can antioxidant dietary supplements counteract age-related sarcopenia? *International Journal of Molecular Sciences*. *20*(15), p.3815.
- Danilova, D.A., Brichkin, Y.D., Medvedev, A.P., Pichugin, V.V., Fedorov, S.A., Taranov, E.V., Nazarov, E.I., Ryazanov, M.V., Bolshukhin, G.V. and Deryugina, A.V. (2021) Application of Molecular Hydrogen in Heart Surgery under Cardiopulmonary Bypass. *Sovremennye Tekhnologii v Meditsine*. *13*(1), pp.71-75.
- Darzynkiewicz, Z., Huang, X. and Zhao, H. (2017) Analysis of cellular DNA content by flow cytometry. *Current Protocols in Immunology*. *119*(1), pp.5-7.
- de Oliveira, D.E., Müller-Coan, B.G. and Pagano, J.S. (2016) Viral carcinogenesis beyond malignant transformation: EBV in the progression of human cancers. *Trends in Microbiology*. *24*(8), pp.649-664.
- Del Castello, F., Nejamkin, A., Cassia, R., Correa-Aragunde, N., Fernández, B., Foresi, N., Lombardo, C., Ramirez, L. and Lamattina, L. (2019) The era of nitric oxide in plant biology: Twenty years tying up loose ends. *Nitric Oxide*. *85*, pp.17-27.
- Delos Reyes, F.S.L.G., Mamaril, A.C.C., Matias, T.J.P., Tronco, M.K.V., Samson, G.R., Javier, N.D., Fadriquela, A., Antonio, J.M. and Sajo, M.E.J.V. (2021) The search for the elixir of life: On the therapeutic potential of alkaline reduced water in metabolic syndromes. *Processes*. *9*(11), p.1876.
- Demidchik, V. (2017) Reactive oxygen species and their role in plant oxidative stress. *Plant Stress Physiology*. (2), pp.64-96.
- Derycke, S., Hendrickx, F., Backeljau, T., D'Hondt, S., Camphijn, L., Vincx, M. and Moens,
- T. (2007) Effects of sublethal abiotic stressors on population growth and genetic diversity of Pellioditis marina (Nematoda) from the Westerschelde estuary. *Aquatic Toxicology*. *82*(2), pp.110-119.
- Deryugina, A.V., Danilova, D.A., Brichkin, Y.D., Taranov, E.V., Nazarov, E.I., Pichugin, V.V., Medvedev, A.P., Riazanov, M.V., Fedorov, S.A., Smorkalov, A.Y. and Makarov, E.V. (2023a) Molecular hydrogen exposure improves functional state of red blood cells in the early postoperative period: A randomized clinical study. *Medical Gas Research*. *13*(2), p.59.
- Deryugina, A.V., Danilova, D.A., Pichugin, V.V. and Brichkin, Y.D. (2023b) The effect of molecular hydrogen on functional states of erythrocytes in rats with simulated chronic heart failure. *Life*. *13*(2), p.418.

- Dhruve, H., Davey, C. and Pursell, J. (2015) Oxygen therapy: emergency use and long term treatment. *Lung Cancer*. *15*(05), p.14.
- Di Lullo, G., Oni, A.O. and Kumar, A. (2021) Blending blue hydrogen with natural gas for direct consumption: Examining the effect of hydrogen concentration on transportation and well-to-combustion greenhouse gas emissions. *International Journal of Hydrogen Energy*. *46*(36), pp.19202-19216.
- Di Meo, S. and Venditti, P. (2020) Evolution of the knowledge of free radicals and other oxidants. *Oxidative Medicine and Cellular Longevity*. p. 9829176
- Diamantis, P., Unke, O.T. and Meuwly, M. (2017) Migration of small ligands in globins: Xe diffusion in truncated hemoglobin N. *PLoS Computational Biology*. *13*(3), p.1005450.
- Dobashi, S., Takeuchi, K. and Koyama, K. (2020) Hydrogen-rich water suppresses the reduction in blood total antioxidant capacity induced by 3 consecutive days of severe exercise in physically active males. *Medical Gas Research*. *10*(1), p.21.
- Dole, M., Wilson, F.R. and Fife, W.P. (1975) Hyperbaric hydrogen therapy: a possible treatment for cancer. *Science*. *190*(4210), pp.152-154.
- Doseděl, M., Jirkovský, E., Macáková, K., Krčmová, L.K., Javorská, L., Pourová, J., Mercolini, L., Remião, F., Nováková, L., Mladěnka, P. and Iacone, R. (2021) Vitamin C—Sources, physiological role, kinetics, deficiency, use, toxicity, and determination. *Nutrients*. *13*(2), p.615.
- Drid, P., Trivic, T., Casals, C., Trivic, S., Stojanovic, M. and Ostojic, S.M. (2016) Is molecular hydrogen beneficial to enhance post-exercise recovery in female athletes? *Science & Sports*. *31*(4), pp.207-213.
- Dunham, E.C., Dore, J.E., Skidmore, M.L., Roden, E.E. and Boyd, E.S. (2021) Lithogenic hydrogen supports microbial primary production in subglacial and proglacial environments. *Proceedings of the National Academy of Sciences of the United States of America*. *118*(2), p.2007051117.
- Dunham-Snary, K.J., Wu, D., Potus, F., Sykes, E.A., Mewburn, J.D., Charles, R.L., Eaton, P., Sultanian, R.A. and Archer, S.L. (2019) Ndufs2, a core subunit of mitochondrial complex I, is essential for acute oxygen-sensing and hypoxic pulmonary vasoconstriction. *Circulation Research*. *124*(12), pp.1727-1746.
- Düsterhöft, S., Lokau, J. and Garbers, C. (2019) The metalloprotease ADAM17 in inflammation and cancer. *Pathology-Research and Practice*. *215*(6), p.152410.
- Duval, S., Zuchan, K., Baymann, F., Schoepp-Cothenet, B., Branscomb, E., Russell, M.J. and Nitschke, W. (2021) Minerals and the emergence of life. *Metals in Life Sciences; Kroneck, P., Sosa Torres, ME, Eds*, pp.135-157.
- Einstein, A. (1905) On the motion of small particles suspended in liquids at rest required by the molecular-kinetic theory of heat. *Annalen der Physik*. *17*(549-560), p.208.
- EU Commission Regulation. *No 1129/2011 of 11 November 2011 amending Annex II to Regulation (EC) No 1333/2008 of the European Parliament and of the Council by establishing a Union list of food additives Text with EEA relevance. Document number:*

- *32011R1129*. Available from: https://eur-lex.europa.eu/legalcontent/EN/ALL/?uri=CELEX%3A32011R1129 [Accessed 14/07/2022]
- Fan, Q., Liang, X., Xu, Z., Li, S., Han, S., Xiao, Y., Xu, Q., Yuan, R., Yang, S. and Gao, H. (2023) Pedunculoside inhibits epithelial-mesenchymal transition and overcomes Gefitinib-resistant non-small cell lung cancer through regulating MAPK and Nrf2 pathways. *Phytomedicine*. *116*, p.154884.
- Fang, W., Tang, L., Wang, G., Lin, J., Liao, W., Pan, W. and Xu, J. (2020) Molecular hydrogen protects human melanocytes from oxidative stress by activating Nrf2 signaling. *Journal of Investigative Dermatology*. *140*(11), pp.2230-2241.
- Farrell, P.J. (2019) Epstein–Barr Virus and Cancer. *Annual Review of Pathology: Mechanisms of Disease. 14*(1), pp.29-53.
- Fassone, E. and Rahman, S. (2012) Complex I deficiency: clinical features, biochemistry and molecular genetics. *Journal of Medical Genetics*. *49*(9), pp.578-590.
- Felix, K., Su, J., Lu, R., Zhao, G., Cui, W., Wang, R., Mu, H., Cui, J. and Shen, W. (2019) Hydrogen-induced tolerance against osmotic stress in alfalfa seedlings involves ABA signaling. *Plant and Soil*. *445*(1/2), pp.409-423.
- Feno, S., Butera, G., Vecellio Reane, D., Rizzuto, R. and Raffaello, A. (2019) Crosstalk between calcium and ROS in pathophysiological conditions. *Oxidative Medicine and Cellular Longevity. 2019*. pp.1-18.
- Ferrer-Sueta, G. and Radi, R. (2009) Chemical biology of peroxynitrite: kinetics, diffusion, and radicals. *ACS Chemical Biology*. *4*(3), pp.161-177.
- Fiedorczuk, K. and Sazanov, L.A. (2018) Mammalian mitochondrial complex I structure and disease-causing mutations. *Trends in Cell Biology*. *28*(10), pp.835-867.
- Filippini, A., D'Amore, A. and D'Alessio, A. (2019) Calcium mobilization in endothelial cell
- functions. *International Journal of Molecular Sciences*. *20*(18), p.4525.
- Finke, C.E., Leandri, H.F., Karumb, E.T., Zheng, D., Hoffmann, M.R. and Fromer, N.A. (2021) Economically advantageous pathways for reducing greenhouse gas emissions from industrial hydrogen under common, current economic conditions. *Energy & Environmental Science*. *14*(3), pp.1517-1529.
- Food and Drug Administration (2014). *GRASNotices.* Available from: https://www.cfsanappsexternal.fda.gov/scripts/fdcc/?set=GRASNotices&id=520&sort=GRN_No&order=DESC&startrow=1&type=basic&search=hydrogen. [Accessed 14 July 2022].
- Food Standards Agency (2018) *Approved additives and E numbers*. Available from: https://www.food.gov.uk/businessguidance/approved-additives-and-e-numbers [Accessed 14 July 2022].
- Frajese, G.V., Benvenuto, M., Mattera, R., Giampaoli, S., Ambrosin, E., Bernardini, R., Giganti, M.G., Albonici, L., Dus, I., Manzari, V. and Modesti, A. (2018) Electrochemically reduced water delays mammary tumors growth in mice and inhibits breast cancer cells survival in vitro. *Evidence-based Complementary and Alternative Medicine: eCAM*. *2018*, p.4753507.

- Franceschelli, S., Gatta, D.M.P., Pesce, M., Ferrone, A., Di Martino, G., Di Nicola, M., De Lutiis, M.A., Vitacolonna, E., Patruno, A., Grilli, A. and Felaco, M. (2018) Modulation of the oxidative plasmatic state in gastroesophageal reflux disease with the addition of rich water molecular hydrogen: A new biological vision. *Journal of Cellular and Molecular Medicine*. *22*(5), pp.2750-2759.
- Freude, D. (2004) Size, mass and kinetics of molecules. *Molecular Physics* [online]. Available from: https://home.uni-leipzig.de/energy/pdf/freume2.pdf [Accessed 29/01/2024].
- Fridovich, I. (1983) Superoxide radical: an endogenous toxicant. *Annual Review of Pharmacology and Toxicology*. *23*(1), pp.239-257.
- Friedrich, T. and Scheide, D. (2000) The respiratory complex I of bacteria, archaea and eukarya and its module common with membrane-bound multisubunit hydrogenases. *FEBS Letters*. *479*(1-2), pp.1-5.
- Fu, Y., Ito, M., Fujita, Y., Ito, M., Ichihara, M., Masuda, A., Suzuki, Y., Maesawa, S., Kajita, Y., Hirayama, M. and Ohsawa, I. (2009) Molecular hydrogen is protective against 6-hydroxydopamine-induced nigrostriatal degeneration in a rat model of Parkinson's disease. *Neuroscience Letters*. *453*(2), pp.81-85.
- Fu, Z., Zhang, Z., Wu, X. and Zhang, J. (2020) Hydrogen-rich saline inhibits lipopolysaccharide-induced acute lung injury and endothelial dysfunction by regulating autophagy through mTOR/TFEB signaling pathway. *BioMed Research International*. p.9121894.
- Fukuda, K.I., Asoh, S., Ishikawa, M., Yamamoto, Y., Ohsawa, I. and Ohta, S. (2007) Inhalation of hydrogen gas suppresses hepatic injury caused by ischemia/reperfusion through reducing oxidative stress. *Biochemical and Biophysical Research Communications*. *361*(3), pp.670-674.
- Gao, J.J., Xu, K.H., Tang, B., Yin, L.L., Yang, G.W. and An, L.G. (2007) Selective detection of superoxide anion radicals generated from macrophages by using a novel fluorescent probe. *The FEBS Journal*. *274*(7), pp.1725-1733.
- Garrity, G.M., Bell, J.A. and Lilburn, T.G., 2004. *Taxonomic outline of the prokaryotes*. Bergey's manual of systematic bacteriology. Volume 2 (2nd ed.) New York: Springer. p. 1388.
- Gatzka, M. and Walsh, C.M. (2007) Apoptotic signal transduction and T cell tolerance.
- *Autoimmunity.* 40(6), pp.442-452.
- Ge, L., Yang, M., Yang, N.N., Yin, X.X. and Song, W.G. (2017) Molecular hydrogen: a preventive and therapeutic medical gas for various diseases. *Oncotarget*. *8*(60), p.102653.
- Georgiou, C.D. and Margaritis, L.H. (2021) Oxidative stress and NADPH oxidase: connecting electromagnetic fields, cation channels and biological effects. *International Journal of Molecular Sciences*. *22*(18), p.10041.
- Gequelin, L.C.F., Riediger, I.N., Nakatani, S.M., Biondo, A.W. and Bonfim, C.M. (2011) Epstein-Barr virus: general factors, virus-related diseases and measurement of viral load after transplant. *Revista Brasileira de Hematologia e Hemoterapia*. *33*(5), pp.383-388.

- Gharib, B., Hanna, S., Abdallahi, O.M., Lepidi, H., Gardette, B. and De Reggi, M. (2001) Anti-inflammatory properties of molecular hydrogen: investigation on parasite-induced liver inflammation. *Comptes Rendus de l'Académie des Sciences-Series III-Sciences de la Vie*. *324*(8), pp.719-724.
- Glass, J.B., Elbon, C.E. and Williams, L.D. (2022) Something old, something new, something borrowed, something blue: the anaerobic microbial ancestry of aerobic respiration. *Trends in Microbiology*. 31(2), pp.135-141.
- Greening, C., Biswas, A., Carere, C.R., Jackson, C.J., Taylor, M.C., Stott, M.B., Cook, G.M. and Morales, S.E. (2016) Genomic and metagenomic surveys of hydrogenase distribution indicate H2 is a widely utilised energy source for microbial growth and survival. The ISME Journal. 10(3), pp.761-777.
- Grgic, L., Zwicker, K., Kashani-Poor, N., Kerscher, S. and Brandt, U. (2004) Functional significance of conserved histidines and arginines in the 49-kDa subunit of mitochondrial complex I. *Journal of Biological Chemistry*. *279*(20), pp.21193-21199.
- Griessen, R., Strohfeldt, N. and Giessen, H. (2016) Thermodynamics of the hybrid interaction of hydrogen with palladium nanoparticles. *Nature Materials*. *15*(3), pp.311- 317.
- Guan, Q., Ding, X.W., Jiang, R., Ouyang, P.L., Gui, J., Feng, L., Yang, L. and Song, L.H. (2019) Effects of hydrogen-rich water on the nutrient composition and antioxidative characteristics of sprouted black barley. *Food Chemistry*. *299*, p.125095.
- Guan, W.J., Wei, C.H., Chen, A.L., Sun, X.C., Guo, G.Y., Zou, X., Shi, J.D., Lai, P.Z., Zheng,
- Z.G. and Zhong, N.S. (2020) Hydrogen/oxygen mixed gas inhalation improves disease severity and dyspnea in patients with Coronavirus disease 2019 in a recent multicenter, open-label clinical trial. *Journal of Thoracic Disease*. *12*(6), p.3448.
- Guo, Q., Yue, Q., Zhao, J., Wang, L., Wang, H., Wei, X., Liu, J. and Jia, J. (2011) How far can hydroxyl radicals travel? An electrochemical study based on a DNA mediated electron transfer process. *Chemical Communications*. *47*(43), pp.11906-11908.
- Guo, K.W. (2012) Green nanotechnology of trends in future energy: a review. *International Journal of Energy Research*, *36*(1), pp.1-17.
- Guo, Y., Li, G., Zhou, J. and Liu, Y. (2019) December. Comparison between hydrogen production by alkaline water electrolysis and hydrogen production by PEM electrolysis. *IOP Conference Series: Earth and Environmental Science*. *371*(4), p. 042022.
- Gvozdjáková, A., Kucharská, J., Kura, B., Vančová, O.G., Rausová, Z., Sumbalová, Z., Uličná, O.G. and Slezák, J. (2020) A new insight into the molecular hydrogen effect on coenzyme Q and mitochondrial function of rats. *Canadian Journal of Physiology and Pharmacology*. *98*(1), pp.29-34.
- Hadwan, M.H. (2018) Simple spectrophotometric assay for measuring catalase activity in biological tissues. *BMC Biochemistry*. *19*(1), pp.1-8.

- Halliwell, B. (1978) Superoxide-dependent formation of hydroxyl radicals in the presence of iron chelates: Is it a mechanism for hydroxyl radical production in biochemical systems? *FEBS Letters*. *92*(2), pp.321-326.
- Halliwell, B., Gutteridge, J.M. and Aruoma, O.I. (1987) The deoxyribose method: a simple "test-tube" assay for determination of rate constants for reactions of hydroxyl radicals. *Analytical Biochemistry*. *165*(1), pp.215-219.
- Halliwell, B. (2022) Commentary for "Oxygen free radicals and iron in relation to biology and medicine: Some problems and concepts". *Archives of Biochemistry and Biophysics*. *718*, p.109151.
- Hammer, H.F., Fox, M.R., Keller, J., Salvatore, S., Basilisco, G., Hammer, J., Lopetuso, L., Benninga, M., Borrelli, O., Dumitrascu, D. and Hauser, B. (2022) European guideline on indications, performance, and clinical impact of hydrogen and methane breath tests in adult and pediatric patients: European Association for Gastroenterology, Endoscopy and Nutrition, European Society of Neurogastroenterology and Motility, and European Society for Paediatric Gastroenterology Hepatology and Nutrition consensus. *United European Gastroenterology Journal*. *10*(1), pp.15-40.
- Han, B., Zhou, H., Jia, G., Wang, Y., Song, Z., Wang, G., Pan, S., Bai, X., Lv, J. and Sun, B. (2016) MAPK s and Hsc70 are critical to the protective effect of molecular hydrogen during the early phase of acute pancreatitis. *The FEBS Journal*. *283*(4), pp.738-756.
- Hanaoka, T., Kamimura, N., Yokota, T., Takai, S. and Ohta, S. (2011) Molecular hydrogen protects chondrocytes from oxidative stress and indirectly alters gene expressions through reducing peroxynitrite derived from nitric oxide. *Medical Gas Research*. *1*(1), pp.1- 9.
- Hancock, J.T. and Hancock, T.H. (2018) Hydrogen gas, ROS metabolism and cell signaling: are hydrogen spin states important? *Reactive Oxygen Species*. *6*(18), pp.389-395.
- Hancock, J.T. and Russell, G. (2021) Downstream signalling from molecular hydrogen. *Plants*. *10*(2), p.367.
- Hancock, J.T., LeBaron, T.W., May, J., Thomas, A. and Russell, G. (2021) Molecular hydrogen: is this a viable new treatment for plants in the UK? *Plants*. *10*(11), p.2270.
- Hancock, J. T., LeBaron, T. W., & Russell, G. (2021) Molecular hydrogen: redox reactions and possible biological interactions. *Reactive Oxygen Species*. *11*, pp.17-25.
- Hancock, J.T. and Veal, D. (2021) Nitric oxide, other reactive signalling compounds, redox, and reductive stress. *Journal of Experimental Botany*. *72*(3), pp.819-829.
- Hancock, J.T., Russell, G., Craig, T.J., May, J., Morse, H.R. and Stamler, J.S. (2022) Understanding hydrogen: Lessons to be learned from physical interactions between the inert gases and the globin superfamily. *Oxygen*. *2*(4), pp.578-590.
- Hancock, J.T., Russell, G. and Stratakos, A.C. (2022) Molecular hydrogen: The postharvest use in fruits, vegetables and the floriculture industry. *Applied Sciences*. *12*(20), p.10448.
- Hancock, J.T. (2023) Are protein cavities and pockets commonly used by redox active signalling molecules? *Plants. 12*(14), p.2594.

- Hancock, J.T. and LeBaron, T.W. (2023) The early history of hydrogen and other gases in respiration and biological systems: Revisiting Beddoes, Cavallo, and Davy. *Oxygen*. *3*(1), pp.102-119.
- Hanisch, H. and Grundel., J, 1979. Engineering testimonial. Yull Brown: Brown's Gas (Hyfuel); US Patent # 4,014,777. Available from: http://www.rexresearch.com/hyfuel/ybrown/4014777.htm.
- Hanna, A. and Frangogiannis, N.G. (2020) Inflammatory cytokines and chemokines as therapeutic targets in heart failure. *Cardiovascular Drugs and Therapy*. *34*(6), pp.849-863.
- Hantzidiamantis, P.J. and Lappin, S.L. (2022) Physiology, Glucose. In *StatPearls* [online]. StatPearls Publishing. [Accessed 23/08/2023].
- Hasegawa, T., Ito, M., Hasegawa, S., Teranishi, M., Takeda, K., Negishi, S., Nishiwaki, H., Takeda, J.I., LeBaron, T.W. and Ohno, K. (2022) Molecular hydrogen enhances proliferation of cancer cells that exhibit potent mitochondrial unfolded protein response. *International Journal of Molecular Sciences*. *23*(5), p.2888.
- Heremans, K. (1987) Pressure effects on the reactions of heme proteins. NATO ASI series. Series C, Mathematical and Physical Sciences. 197, pp.421-445.
- Hirayama, M., Ito, M., Minato, T., Yoritaka, A., LeBaron, T.W. and Ohno, K. (2018) Inhalation of hydrogen gas elevates urinary 8-hydroxy-2'-deoxyguanine in Parkinson's disease. *Medical Gas Research*. *8*(4), p.144.
- Hirscher, M. and Becher, M. (2003) Hydrogen storage in carbon nanotubes. *Journal of Nanoscience and Nanotechnology. 3*(1-2), pp.3-17.
- Hore, P.J. (2012) Are biochemical reactions affected by weak magnetic fields? *Proceedings of the National Academy of Sciences of the United States of America*. *109*(5), pp.1357-1358.
- Hori, A., Ichihara, M., Kimura, H., Ogata, H., Kondo, T. and Hotta, N. (2020) Inhalation of molecular hydrogen increases breath acetone excretion during submaximal exercise: A randomized, single-blinded, placebo-controlled study. *Medical Gas Research*. *10*(3), p.96.
- Hsu, J.Y., Chang, C.J. and Cheng, J.S. (2022) Survival, treatment regimens and medical costs of women newly diagnosed with metastatic triple-negative breast cancer. *Scientific Reports*. *12*(1), p.729.
- Hu, X., Xie, Q., Zhang, J., Yu, Q., Liu, H. and Sun, Y. (2020) Experimental study of the lower flammability limits of H2/O2/CO2 mixture. *International Journal of Hydrogen Energy*. *45*(51), pp.27837-27845.
- Huang, L. (2016) Molecular hydrogen: a therapeutic antioxidant and beyond. *Medical Gas Research*. *6*(4), p.219.
- Hussey, J.W., Limpitikul, W.B. and Dick, I.E. (2023) Calmodulin mutations in human disease. *Channels*. *17*(1), p.2165278.

- Huster, D., Härtel, F., Nuding, S., Schroeder, J., Zhang, Y., Werdan, K. and Ebelt, H. (2019) Prognostic relevance of tissue oxygen saturation in patients in the early stage of multiple organ dysfunction syndrome. *Medizinische Klinik-Intensivmedizin und Notfallmedizin*. *114*, pp.146-153.

- Hylemon, P.B., Harris, S.C. and Ridlon, J.M. (2018) Metabolism of hydrogen gases and bile acids in the gut microbiome. *FEBS Letters*. *592*(12), pp.2070-2082.
- Ichihara, M., Sobue, S., Ito, M., Ito, M., Hirayama, M. and Ohno, K. (2015) Beneficial biological effects and the underlying mechanisms of molecular hydrogen-comprehensive review of 321 original articles. *Medical Gas Research*. *5*(1), pp.1-21.
- Ichikawa, Y., Hirano, S.I., Sato, B., Yamamoto, H., Takefuji, Y. and Satoh, F. (2023) Guidelines for the selection of hydrogen gas inhalers based on hydrogen explosion accidents. *Medical Gas Research*. *13*(2), pp.43-48.
- Ierardi, E., Rosania, R., Zotti, M., Principe, S., Laonigro, G., Giorgio, F., de Francesco, V. and Panella, C. (2010) Metabolic syndrome and gastro-esophageal reflux: A link towards a growing interest in developed countries. *World Journal of Gastrointestinal Pathophysiology*. *1*(3), p.91.
- Iglesias-Pedraz, J.M. and Comai, L. (2020) Measurements of Hydrogen Peroxide and Oxidative DNA Damage in a Cell Model of Premature Aging. *Methods in Molecular Biology. 2144*, pp.245-257.

- Ignacio, R.M., Yoon, Y.S., Sajo, M.E.J., Kim, C.S., Kim, D.H., Kim, S.K. and Lee, K.J. (2013)
- The balneotherapy effect of hydrogen reduced water on UVB-mediated skin injury in hairless mice. *Molecular & Cellular Toxicology*. *9*, pp.15-21.

- Imachi, H., Nobu, M.K., Nakahara, N., Morono, Y., Ogawara, M., Takaki, Y., Takano, Y., Uematsu, K., Ikuta, T., Ito, M. and Matsui, Y. (2020) Isolation of an archaeon at the prokaryote–eukaryote interface. *Nature*. *577*(7791), pp.519-525.

- International Hydrogen Standards Association. (2018) *Concentration/Dose*. Available from: https://www.intlhsa.org/concentration-dose/ [Accessed 12/02/2024].
- Ishibashi, T. (2013) Molecular hydrogen: new antioxidant and anti-inflammatory therapy for rheumatoid arthritis and related diseases. *Current Pharmaceutical Design*. *19*(35), pp.6375-6381.

- Ishibashi, T. (2019) Therapeutic efficacy of molecular hydrogen: a new mechanistic insight. *Current Pharmaceutical Design*. *25*(9), pp.946-955.
- Ishihara, G., Kawamoto, K., Komori, N. and Ishibashi, T. (2020) Molecular hydrogen suppresses superoxide generation in the mitochondrial complex I and reduced mitochondrial membrane potential. *Biochemical and Biophysical Research Communications*. *522*(4), pp.965-970.
- Islam, Z.F., Greening, C. and Hu, H.W., 2023. Microbial hydrogen cycling in agricultural systems–plant beneficial or detrimental? *Microbial Biotechnology* [online]. *16*(8) [Accessed 29/01/2024].

- Itoh, T., Fujita, Y., Ito, M., Masuda, A., Ohno, K., Ichihara, M., Kojima, T., Nozawa, Y. and Ito, M. (2009) Molecular hydrogen suppresses FcεRI-mediated signal transduction and prevents degranulation of mast cells. *Biochemical and Biophysical Research Communications*. *389*(4), pp.651-656.
- Itoh, T., Hamada, N., Terazawa, R., Ito, M., Ohno, K., Ichihara, M., Nozawa, Y. and Ito, M. (2011) Molecular hydrogen inhibits lipopolysaccharide/interferon γ-induced nitric oxide production through modulation of signal transduction in macrophages. *Biochemical and Biophysical Research Communications*. *411*(1), pp.143-149.
- Iuchi, K., Imoto, A., Kamimura, N., Nishimaki, K., Ichimiya, H., Yokota, T. and Ohta, S. (2016) Molecular hydrogen regulates gene expression by modifying the free radical chain reaction-dependent generation of oxidized phospholipid mediators. *Scientific Reports*. *6*(1), p.18971.
- Iuchi, K., Nishimaki, K., Kamimura, N. and Ohta, S. (2019) Molecular hydrogen suppresses free-radical-induced cell death by mitigating fatty acid peroxidation and mitochondrial dysfunction. *Canadian Journal of Physiology and Pharmacology*. *97*(10), pp.999-1005.
- Jacobs, S.S., Krishnan, J.A., Lederer, D.J., Ghazipura, M., Hossain, T., Tan, A.Y.M., Carlin, B., Drummond, M.B., Ekström, M., Garvey, C. and Graney, B.A. (2020) Home oxygen therapy for adults with chronic lung disease. An official American Thoracic Society clinical practice guideline. *American Journal of Respiratory and Critical Care Medicine*. *202*(10), pp.121-141.
- Jafari, S., Tavares Santos, Y.A., Bergmann, J., Irani, M. and Ryde, U. (2022) Benchmark study of redox potential calculations for Iron–Sulfur clusters in proteins. *Inorganic Chemistry*. *61*(16), pp.5991-6007.
- Jaffe, E.K. (2020) Porphobilinogen synthase: An equilibrium of different assemblies in human health. *Progress in Molecular Biology and Translational Science*. *169*, pp.85-104.
- Järvinen, L. (2020) *Design of a PEM electrolyzer test station for experimentation on power quality induced efficiency loss and cell degradation*. Master's theses, Lappeenranta-Lahti University of Technology (LUT).
- Javorac, D., Stajer, V., Ratgeber, L., Betlehem, J. and Ostojic, S. (2019) Short-term H2 inhalation improves running performance and torso strength in healthy adults. *Biology of Sport*. *36*(4), pp.333-339.
- Ji, X., Zheng, W. and Yao, W. (2019) Protective role of hydrogen gas on oxidative damage and apoptosis in intestinal porcine epithelial cells (IPEC-J2) induced by deoxynivalenol: A preliminary study. *Toxins*. *12*(1), p.5.
- Jiang, X. and Shapiro, D.J. (2014) The immune system and inflammation in breast cancer. *Molecular and Cellular Endocrinology*. *382*(1), pp.673-682.
- Jiang, Y., Liu, G., Zhang, L., Cheng, S., Luo, C., Liao, Y. and Guo, S. (2018) Therapeutic efficacy of hydrogen-rich saline alone and in combination with PI3K inhibitor in non-small cell lung cancer. *Molecular Medicine Reports*. *18*(2), pp.2182-2190.
- Jin, Q., Zhu, K., Cui, W., Xie, Y., Han, B.I.N. and Shen, W. (2013) Hydrogen gas acts as a novel bioactive molecule in enhancing plant tolerance to paraquat-induced oxidative

- stress via the modulation of heme oxygenase-1 signalling system. *Plant, Cell & Environment*. *36*(5), pp.956-969.
- Jin, Z., Zhao, P., Gong, W., Ding, W. and He, Q. (2023) Fe-porphyrin: A redox-related biosensor of hydrogen molecule. *Nano Research*. *16*(2), pp.2020-2025.
- Johnsen, H.M., Hiorth, M. and Klaveness, J. (2023) Molecular hydrogen therapy—A review on clinical studies and outcomes. *Molecules*. *28*(23), p.7785.
- Juan, C.A., Pérez de la Lastra, J.M., Plou, F.J. and Pérez-Lebeña, E. (2021) The chemistry of reactive oxygen species (ROS) revisited: outlining their role in biological macromolecules (DNA, lipids and proteins) and induced pathologies. *International Journal of Molecular Sciences*. *22*(9), p.4642.
- Kaila, V.R. (2018) Long-range proton-coupled electron transfer in biological energy conversion: Towards mechanistic understanding of respiratory complex I. *Journal of The Royal Society Interface*. *15*(141), p.20170916.
- Kajiyama, S., Hasegawa, G., Asano, M., Hosoda, H., Fukui, M., Nakamura, N., Kitawaki, J., Imai, S., Nakano, K., Ohta, M. and Adachi, T. (2008) Supplementation of hydrogen-rich water improves lipid and glucose metabolism in patients with type 2 diabetes or impaired glucose tolerance. *Nutrition Research*. *28*(3), pp.137-143.
- Kamimura, N., Nishimaki, K., Ohsawa, I. and Ohta, S. (2011) Molecular hydrogen improves obesity and diabetes by inducing hepatic FGF21 and stimulating energy metabolism in db/db mice. *Obesity*. *19*(7), pp.1396-1403.
- Kampjut, D. and Sazanov, L.A. (2020). The coupling mechanism of mammalian respiratory complex I. *Science*. *370*(6516), p.4209.
- Kampjut, D. and Sazanov, L.A. (2022) Structure of respiratory complex I–an emerging blueprint for the mechanism. *Current Opinion in Structural Biology*. *74*, p.102350.
- Karp, G. (2008) Cell and molecular biology: concepts and experiments. *Cell and Molecular Biology: Concepts and Experiments*. John Wiley & Sons. p.776.
- Katsumata, Y., Sano, F., Abe, T., Tamura, T., Fujisawa, T., Shiraishi, Y., Kohsaka, S., Ueda, I., Homma, K., Suzuki, M. and Okuda, S. (2017) The effects of hydrogen gas inhalation on adverse left ventricular remodeling after percutaneous coronary intervention for ST- Elevated Myocardial Infarction—First Pilot Study in Humans. *Circulation Journal*. *81*(7), pp.940-947.
- Kawamura, T., Fujii, R., Higashida, K. and Muraoka, I. (2019) Hydrogen water intake may suppress liver glycogen utilization without affecting redox biomarkers during exercise in rats. *Gazzetta Medica Italiana-Archivio per le Scienze Mediche*. *178*(9), pp.611-617.
- Kawamura, T., Higashida, K. and Muraoka, I. (2020) Application of molecular hydrogen as a novel antioxidant in sports science. *Oxidative Medicine and Cellular Longevity*. *2020*, p.2328768.

- Kawasaki, H., Soma, N. and Kretsinger, R.H. (2019) Molecular dynamics study of the changes in conformation of calmodulin with calcium binding and/or target recognition. *Scientific Reports*. *9*(1), p.10688.
- Khoo, J., Hagemeyer, C.E., Henstridge, D.C., Kumble, S., Wang, T.Y., Xu, R., Gani, L., King, T., Soh, S.B., Puar, T. and Au, V. (2021) Effects of water stably-enriched with oxygen as a novel method of tissue oxygenation on mitochondrial function, and as adjuvant therapy for type 2 diabetes in a randomized placebo-controlled trial. *Plos One*. *16*(7), p.0254619.
- Kim, Y.H., Sun, Y.Y. and Zhang, S.B. (2009) Ab initio calculations predicting the existence of an oxidized calcium dihydrogen complex to store molecular hydrogen in densities up to 100 g/L. *Physical Review B*. *79*(11), p.115424.
- Kim, S.A., Jong, Y.C., Kang, M.S. and Yu, C.J. (2022) Antioxidation activity of molecular hydrogen via protoheme catalysis in vivo: an insight from ab initio calculations. *Journal of Molecular Modeling*. *28*(10), p.287.
- Kimura, H., Ito, Y., Suzuki, R. and Nishiyama, Y. (2008) Measuring Epstein–Barr virus (EBV) load: the significance and application for each EBV-associated disease. *Reviews in Medical Virology*. *18*(5), pp.305-319.
- King, A., Selak, M.A. and Gottlieb, E. (2006) Succinate dehydrogenase and fumarate hydratase: linking mitochondrial dysfunction and cancer. *Oncogene*. *25*(34), pp.4675- 4682.
- Kinoshita, E., Kinoshita-Kikuta, E. and Koike, T. (2009) Separation and detection of large phosphoproteins using Phos-tag SDS-PAGE. *Nature Protocols*. *4*(10), pp.1513-1521.
- Kishi, S., Saito, K., Kato, Y. and Ishikita, H. (2017) Redox potentials of ubiquinone, menaquinone, phylloquinone, and plastoquinone in aqueous solution. *Photosynthesis Research*. *134*(2), pp.193-200.
- Kiyoi, T., Liu, S., Takemasa, E., Nakaoka, H., Hato, N. and Mogi, M. (2020) Constitutive hydrogen inhalation prevents vascular remodeling via reduction of oxidative stress. *PloS One*. *15*(4), p.0227582.
- Koch, A.L. and Schmidt, T.M. (1991) The first cellular bioenergetic process: primitive generation of a proton-motive force. *Journal of Molecular Evolution*. *33*(4), pp.297-304.
- Kong, X., Lu, T., Lu, Y.Y., Yin, Z. and Xu, K. (2022) Effect of hydrogen inhalation therapy on hearing loss of patients with nasopharyngeal carcinoma after radiotherapy. *Frontiers in Medicine*. *9*, p.828370.
- Korovljev, D., Trivic, T., Drid, P. and Ostojic, S.M. (2017) Molecular hydrogen affects body composition, metabolic profiles, and mitochondrial function in middle-aged overweight women. *Irish Journal of Medical Science*. *187*(1), pp.85-89.
- Korovljev, D., Stajer, V., Ostojic, J., LeBaron, T.W. and Ostojic, S.M. (2019) Hydrogen-rich water reduces liver fat accumulation and improves liver enzyme profiles in patients with non-alcoholic fatty liver disease: a randomized controlled pilot trial. *Clinics and Research in Hepatology and Gastroenterology*. *43*(6), pp.688-693.

- Kot, J. (2014) Medical devices and procedures in the hyperbaric chamber. *Diving and hyperbaric medicine.* 44(4), pp.223-227.
- Krishnan, S., Koning, V., de Groot, M.T., de Groot, A., Mendoza, P.G., Junginger, M. and Kramer, G.J. (2023) Present and future cost of alkaline and PEM electrolyser stacks. *International Journal of Hydrogen Energy*. *48*(83), pp.32313-32330.
- Krohn, K., Maier, J. and Paschke, R. (2007) Mechanisms of disease: hydrogen peroxide, DNA damage and mutagenesis in the development of thyroid tumors. *Nature Clinical Practice Endocrinology & Metabolism*. *3*(10), pp.713-720.
- Kucharská, J., Gvozdjáková, A., Kura, B., Rausová, Z. and Slezák, J. (2018) Effect of molecular hydrogen on coenzyme Q in plasma, myocardial tissue and mitochondria of rats. *Journal of Nutritional Health & Food Engineering*. *8*(5), pp.362-364.
- Kumar, S.S. and Himabindu, V. (2019) Hydrogen production by PEM water electrolysis–A review. *Materials Science for Energy Technologies*. *2*(3), pp.442-454.
- Kura, B., Bagchi, A.K., Singal, P.K., Barancik, M., LeBaron, T.W., Valachova, K., Šoltés, L. and Slezák, J. (2019) Molecular hydrogen: Potential in mitigating oxidative-stress-induced radiation injury. *Canadian Journal of Physiology and Pharmacology*. *97*(4), pp.287-292.
- Kura, B., Szantova, M., LeBaron, T.W., Mojto, V., Barancik, M., Szeiffova Bacova, B., Kalocayova, B., Sykora, M., Okruhlicova, L., Tribulova, N. and Gvozdjakova, A. (2022) Biological effects of hydrogen water on subjects with NAFLD: A randomized, placebo- controlled trial. *Antioxidants*. *11*(10), p.1935.
- Kurki, S., Zickermann, V., Kervinen, M., Hassinen, I. and Finel, M. (2000) Mutagenesis of three conserved Glu residues in a bacterial homologue of the ND1 subunit of Complex I affects ubiquinone reduction kinetics but not inhibition by dicyclohexylcarbodiimide. *Biochemistry*. *39*(44), pp.13496-13502.
- Lacasse, M.J., Sebastiampillai, S., Côté, J.P., Hodkinson, N., Brown, E.D. and Zamble, D.B. (2019) A whole-cell, high-throughput hydrogenase assay to identify factors that modulate [NiFe]-hydrogenase activity. *Journal of Biological Chemistry*. *294*(42), pp.15373-15385.
- Lane, N. (2010) Why are cells powered by proton gradients? *Nature Education. 3(9)*, p.2.
- Lawrence, J.H., Loomis, W.F., Tobias, C.A. and Turpin, F.H. (1946) Preliminary observations on the narcotic effect of xenon with a review of values for solubilities of gases in water and oils. *The Journal of Physiology*. *105*(3), p.197.
- LeBaron, T.W., Kura, B., Kalocayova, B., Tribulova, N. and Slezak, J. (2019a) A new approach for the prevention and treatment of cardiovascular disorders. Molecular hydrogen significantly reduces the effects of oxidative stress. *Molecules*. *24*(11), p.2076.
- LeBaron, T.W., Larson, A.J., Ohta, S., Mikami, T., Barlow, J., Bulloch, J. and DeBeliso, M. (2019b) Acute supplementation with molecular hydrogen benefits submaximal exercise indices. Randomized, double-blinded, placebo-controlled crossover pilot study. *Journal of Lifestyle Medicine. 9*(1), p.36.
- Lebwohl, M. (2005) A clinician's paradigm in the treatment of psoriasis. *Journal of the American Academy of Dermatology*. *53*(1), pp.59-69.

- Leech, M.C. and Lam, K. (2022) A practical guide to electrosynthesis. *Nature Reviews Chemistry*. *6*(4), pp.275-286.
- Lenzen, S., Lushchak, V.I. and Scholz, F. (2022) The pro-radical hydrogen peroxide as a stable hydroxyl radical distributor: Lessons from pancreatic beta cells. *Archives of Toxicology*. *96*(7), pp.1915-1920.
- Lewis, J. (2018) Gas separation membranes: polymeric and inorganic. *Chemical Engineering Education*. *52*(3), pp.223-223.
- Li, Q., Tanaka, Y. and Miwa, N. (2017) Influence of hydrogen-occluding-silica on migration and apoptosis in human esophageal cells in vitro. *Medical Gas Research*. *7*(2), p.76.
- Li, H., Shi, W., Li, X., Hu, Y., Fang, Y. and Ma, H. (2019a) Ferroptosis accompanied by •OH generation and cytoplasmic viscosity increase revealed via dual-functional fluorescence probe. *Journal of the American Chemical Society*. *141*(45), pp.18301-18307.
- Li, S., Liao, R., Sheng, X., Luo, X., Zhang, X., Wen, X., Zhou, J. and Peng, K. (2019b) Hydrogen gas in cancer treatment. *Frontiers in Oncology*. *9*, p.696.
- Li, Q., Xie, F., Yi, Y., Zhao, P., Zhang, X., Zhang, X., Zhang, X. and Ma, X. (2021) Hydroxyl- radical scavenging activity of hydrogen does not significantly contribute to its biological function. *BioRxiv* [online]. pp. 2021-03 [Accessed 29/01/2024].
- Li, T.T., Sun, T., Wang, Y.Z., Wan, Q., Li, W.Z. and Yang, W.C. (2022) Molecular hydrogen alleviates lung injury after traumatic brain injury: Pyroptosis and apoptosis. *European Journal of Pharmacology*. *914*, p.174664.
- Liang, C., Liu, X., Liu, L. and Dongwei, H.E. (2012) Effect of hydrogen inhalation on p38 MAPK activation in rats with lipopolysaccharide-induced acute lung injury. *Journal of Southern Medical University*. *32*(8), pp.1211-1213.
- Liu, C., Kurokawa, R., Fujino, M., Hirano, S., Sato, B. and Li, X.K. (2014) Estimation of the hydrogen concentration in rat tissue using an airtight tube following the administration of hydrogen via various routes. *Scientific Reports*. *4*(1), pp.1-11.
- Liu, H., Liang, X., Wang, D., Zhang, H., Liu, L., Chen, H., Li, Y., Duan, Q. and Xie, K. (2015) Combination therapy with nitric oxide and molecular hydrogen in a murine model of acute lung injury. *Shock*. *43*(5). pp.504-511
- Liu, M.Y., Xie, F., Zhang, Y., Wang, T.T., Ma, S.N., Zhao, P.X., Zhang, X., Lebaron, T.W., Yan,
- X.L. and Ma, X.M. (2019) Molecular hydrogen suppresses glioblastoma growth via inducing the glioma stem-like cell differentiation. *Stem Cell Research & Therapy*, *10*(1), p.145.
- Liu, B., Xue, J., Zhang, M., Wang, M., Ma, T., Zhao, M., Gu, Q. and Qin, S. (2020a) Hydrogen inhalation alleviates nonalcoholic fatty liver disease in metabolic syndrome rats. *Molecular Medicine Reports*. *22*(4), pp.2860-2868.
- Liu, Y., Li, J., Chen, M., Chen, X. and Zheng, N. (2020b) Palladium-based nanomaterials for cancer imaging and therapy. *Theranostics*. *10*(22), p.10057.
- Liu, Y., Yang, X., Liu, Y., Jiang, T., Ren, S., Chen, J., Xiong, H., Yuan, M., Li, W., Machens,
- H.G. and Chen, Z. (2021) NRF2 signalling pathway: new insights and progress in the field of wound healing. *Journal of Cellular and Molecular Medicine*. *25*(13), pp.5857-5868.

- Loer, S.A., Scheeren, T.W. and Tarnow, J. (1997) How much oxygen does the human lung consume? *The Journal of the American Society of Anesthesiologists*. *86*(3), pp.532-537.
- López-García, P. and Moreira, D. (2006) Selective forces for the origin of the eukaryotic nucleus. *Bioessays*. *28*(5), pp.525-533.
- Lossi, L. (2022) The concept of intrinsic versus extrinsic apoptosis. *Biochemical Journal.*
- 479(3), pp.357-384.
- Lu, Q., Neese, F. and Bistoni, G. (2018) Formation of agostic structures driven by London dispersion. *Angewandte Chemie International Edition*. *57*(17), pp.4760-4764.
- Lu, W., Li, D., Hu, J., Mei, H., Shu, J., Long, Z., Yuan, L., Li, D., Guan, R., Li, Y. and Xu, J.
- (2018) Hydrogen gas inhalation protects against cigarette smoke-induced COPD development in mice. *Journal of Thoracic Disease*. *10*(6), p.3232.
- Ma, L., Hao, W., Feng, W.B., Cao, L.C., Qin, L.N., Wang, Y., Liu, M.H., Wang, N.Z., Gao, F.,
- Guo, J.M. and Du, H. (2022) Molecular hydrogen reduces electromagnetic pulse-induced male rat reproductive system damage in a rodent model. *Oxidative Medicine and Cellular Longevity*. *2022*, p.3469474.
- Manohar, S.M., Shah, P. and Nair, A. (2021) Flow cytometry: principles, applications and recent advances. *Bioanalysis*. *13*(3), pp.181-198.
- Mantovani, A., Marchesi, F., Porta, C., Sica, A. and Allavena, P. (2007) Inflammation and cancer: breast cancer as a prototype. *The Breast*. *16*(2), pp.27-33.
- Manuilov, V.M., Suvorov, A.V., Kurkin, S.V., Olenev, Y.O., Pavlov, N.B., Logunov, A.T., Anikeev, D.A. and Orlov, O.I. (2022) Evaluation of the efficiency of oxygen–helium therapy for patients with Covid-19-associated pneumonia. *Human Physiology*. *48*(7), pp.863-870.
- Maotoana, M.G., Burt, F.J. and Goedhals, D. (2023) Identification of T cell responses to the nonstructural glycoproteins in survivors of Crimean-Congo hemorrhagic fever in South Africa. *Journal of Medical Virology*. *95*(10), p.29154.
- Marla, S.S., Lee, J. and Groves, J.T. (1997) Peroxynitrite rapidly permeates phospholipid membranes. *Proceedings of the National Academy of Sciences of the United States of America*. *94*(26), pp.14243-14248.
- Marreiros, B.C., Batista, A.P., Duarte, A.M. and Pereira, M.M. (2013) A missing link between complex I and group 4 membrane-bound [NiFe] hydrogenases. *Biochimica et Biophysica Acta (BBA)-Bioenergetics*. *1827*(2), pp.198-209.
- Martin, W. and Müller, M. (1998) The hydrogen hypothesis for the first eukaryote. *Nature*. *392*(6671), pp.37-41.
- Matolin, V. (2022) Hydrogen inhalers: Principles, Design and Safety features. *1st EUH2 Academy Conference, 2022*. Congress Centre of Slovak Academy of Science, Smolenice Castle, Slovakia.
- Matreux, T., Altaner, B., Raith, J., Braun, D., Mast, C.B. and Gerland, U. (2023) Formation mechanism of thermally controlled pH gradients. *Communications Physics*. *6*(1), p.14.

- Matteucci, S., Yampolskii, Y., Freeman, B.D. and Pinnau, I., 2006. Transport of gases and vapors in glassy and rubbery polymers. *Materials science of membranes for gas and vapor separation*. pp.1-47.
- Maze, M. and Laitio, T. (2020) Neuroprotective properties of Xenon. *Molecular Neurobiology*. *57*(1), pp.118-124.
- McCloskey, C., Ortega, M.T., Nair, S., Garcia, M.J. and Manevy, F. (2023) A systematic review of time and resource use costs of subcutaneous versus intravenous administration of oncology biologics in a hospital setting. *PharmacoEconomics-Open*. *7*(1), pp.3-36.
- McGuigan, S., Marie, D.J., O'Bryan, L.J., Flores, F.J., Evered, L. and Silbert, B. (2023) The cellular mechanisms associated with the anesthetic and neuroprotective properties of xenon: a systematic review of the preclinical literature. *Frontiers in Neuroscience*. *17*, p.1225191.
- McKay, L.F., Holbrook, W.P. and Eastwood, M.A. (1982) Methane and hydrogen production by human intestinal anaerobic bacteria. *Acta Pathologica Microbiologica Scandinavica Series B: Microbiology*. *90*(1-6), pp.257-260.
- Mellstedt, H. (1975) In vitro activation of human T and B lymphocytes by pokeweed mitogen. *Clinical and Experimental Immunology*. *19*(1), p.75.
- Meng, J., Yu, P., Jiang, H., Yuan, T., Liu, N., Tong, J., Chen, H., Bao, N. and Zhao, J. (2016) Molecular hydrogen decelerates rheumatoid arthritis progression through inhibition of oxidative stress. *American Journal of Translational Research*. *8*(10), p.4472.
- Meng, J., Liu, L., Wang, D., Yan, Z. and Chen, G. (2020) Hydrogen gas represses the progression of lung cancer via down-regulating CD47. *Bioscience Reports*. *40*(4), p.20192761.
- Merényi, G., & Lind, J. (1998) Free radical formation in the peroxynitrous acid (ONOOH)/peroxynitrite (ONOO-) system. *Chemical Research in Toxicology*. *11*(4), pp.243- 246.
- Mishra, N., Khatri, D. and Kumar Jain, I. (2018) The Brown's gas application and limitation:
- A review. *International Journal of Emerging Technologies and Innovative Research*. *5*(9),
- pp. 39-43.
- Mizuno, K., Sasaki, A.T., Ebisu, K., Tajima, K., Kajimoto, O., Nojima, J., Kuratsune, H., Hori,
- H. and Watanabe, Y. (2017) Hydrogen-rich water for improvements of mood, anxiety, and autonomic nerve function in daily life. *Medical Gas Research*. *7*(4), p.247.
- Mondola, P., Damiano, S., Sasso, A. and Santillo, M. (2016) The Cu, Zn superoxide dismutase: not only a dismutase enzyme. *Frontiers in Physiology*. *7*, p.594.
- Morgan, R.M., Pihl, T.D., Nölling, J. and Reeve, J.N. (1997) Hydrogen regulation of growth, growth yields, and methane gene transcription in Methanobacterium thermoautotrophicum deltaH. *Journal of Bacteriology*. *179*(3), pp.889-898.
- Mühlbauer, M.E., Gamiz-Hernandez, A.P. and Kaila, V.R. (2021) Functional dynamics of an ancient membrane-bound hydrogenase. *Journal of the American Chemical Society*. *143*(49), pp.20873-20883.

- Müller, H. (2015) *Medical Gases: Production, Applications, and Safety*. John Wiley & Sons.
- Muñoz-Gómez, S.A., Wideman, J.G., Roger, A.J. and Slamovits, C.H. (2017) The origin of mitochondrial cristae from alphaproteobacteria. *Molecular Biology and Evolution*. *34*(4), pp.943-956.
- Muñoz-Gómez, S.A., Susko, E., Williamson, K., Eme, L., Slamovits, C.H., Moreira, D., López-García, P. and Roger, A.J. (2022) Site-and-branch-heterogeneous analyses of an expanded dataset favour mitochondria as sister to known Alphaproteobacteria. *Nature Ecology & Evolution*. *6*(3), pp.253-262.
- Murariu, G., Caldararu, A., Georgescu, L., Voiculescu, M., Puscasu, G. and Basset, A. (2011) Investigation of water parameters in a river system with a two-dimensional regression analysis model. *AIP Conference Proceedings*. *1387*(1), pp. 259-264. American Institute of Physics.
- Murthy, S.K. (2007) Nanoparticles in modern medicine: state of the art and future challenges. *International Journal of Nanomedicine*. *2*(2), pp.129-141.
- Nakai, J., Ohkura, M. and Imoto, K. (2001) A high signal-to-noise Ca2+ probe composed of a single green fluorescent protein. *Nature Biotechnology*. *19*(2), pp.137-141.
- Nakao, A., Toyoda, Y., Sharma, P., Evans, M. and Guthrie, N. (2010) Effectiveness of hydrogen rich water on antioxidant status of subjects with potential metabolic syndrome— an open label pilot study. *Journal of Clinical Biochemistry and Nutrition*. *46*(2), pp.140-149.
- Nakashima-Kamimura, N., Mori, T., Ohsawa, I., Asoh, S. and Ohta, S. (2009) Molecular hydrogen alleviates nephrotoxicity induced by an anti-cancer drug cisplatin without compromising anti-tumor activity in mice. *Cancer Chemotherapy and Pharmacology*. *64*(4), pp.753-761.
- Nakayama, M., Kabayama, S. and Ito, S. (2016) The hydrogen molecule as antioxidant therapy: clinical application in hemodialysis and perspectives. *Renal Replacement Therapy*. *1*(2), pp.1-10.
- Narayan, T.C., Hayee, F., Baldi, A., Leen Koh, A., Sinclair, R. and Dionne, J.A. (2017) Direct visualization of hydrogen absorption dynamics in individual palladium nanoparticles. *Nature Communications*. *8*(1), pp.1-8.
- Naser, R., Fakhoury, I., El-Fouani, A., Abi-Habib, R. and El-Sibai, M. (2023) Role of the tumor microenvironment in cancer hallmarks and targeted therapy. *International Journal of Oncology*. *62*(2), pp.1-28.
- Nasser, M., Megahed, T.F., Ookawara, S. and Hassan, H. (2022) Techno-economic assessment of clean hydrogen production and storage using hybrid renewable energy system of PV/Wind under different climatic conditions. *Sustainable Energy Technologies and Assessments*. *52*, p.102195.
- National Health Service (2023a) Changes to cancer waiting times standards from 1 October 2023. Available from: https://www.england.nhs.uk/long-read/changes-to- cancer-waiting-times-standards-from-1-october-2023/ [Accessed 12/02/2024].

- National Health Service (2023b) *Home oxygen therapy.* Available from: https://www.nhs.uk/conditions/home-oxygen-treatment/ [Accessed 12/02/2024].
- Nespoli, F., Redaelli, S., Ruggeri, L., Fumagalli, F., Olivari, D. and Ristagno, G. (2019) A complete review of preclinical and clinical uses of the noble gas argon: evidence of safety and protection. *Annals of Cardiac Anaesthesia*. *22*(2), p.122.
- Netrabukkana, R., Lourvanij, K. and Rorrer, G.L. (1996) Diffusion of glucose and glucitol in microporous and mesoporous silicate/aluminosilicate catalysts. *Industrial & Engineering Chemistry Research*. *35*(2), pp.458-464.
- Neugschwandtner, R.W., Bernhuber, A., Kammlander, S., Wagentristl, H., Klimek-Kopyra,
- and Kaul, H.P. (2019) Agronomic potential of winter grain legumes for Central Europe: Development, soil coverage and yields. *Field Crops Research*. *241*, p.107576.
- Newcombe, E.A., Delaforge, E., Hartmann-Petersen, R., Skriver, K. and Kragelund, B.B. (2022) How phosphorylation impacts intrinsically disordered proteins and their function. *Essays in Biochemistry*. *66*(7), pp.901-913.
- Nihei, M., Shiga, T., Maeda, Y. and Oshio, H. (2007) Spin crossover iron (III) complexes. *Coordination Chemistry Reviews*. *251*(21-24), pp.2606-2621.
- Niki, E., 1997. Mechanisms and dynamics of antioxidant action of ubiquinol. *Molecular Aspects of Medicine*. *1001*(18), pp.63-70.
- Nishimaki, K., Asada, T., Ohsawa, I., Nakajima, E., Ikejima, C., Yokota, T., Kamimura, N. and Ohta, S. (2018) Effects of molecular hydrogen assessed by an animal model and a randomized clinical study on mild cognitive impairment. *Current Alzheimer Research*. *15*(5), pp.482-492.
- Niu, Y., Nie, Q., Dong, L., Zhang, J., Liu, S.F., Song, W., Wang, X., Wu, G. and Song, D. (2020) Hydrogen attenuates allergic inflammation by reversing energy metabolic pathway switch. *Scientific Reports*. *10*(1), p.1962.
- Nogueira, J.E., Passaglia, P., Mota, C.M., Santos, B.M., Batalhão, M.E., Carnio, E.C. and Branco, L.G. (2018) Molecular hydrogen reduces acute exercise-induced inflammatory and oxidative stress status. *Free Radical Biology and Medicine*. *129*, pp.186-193.
- Nogueira, J.E. and Branco, L.G. (2021) Recent advances in molecular hydrogen research reducing exercise-induced oxidative stress and inflammation. *Current Pharmaceutical Design*. *27*(5), pp.731-736.
- Nogueira, J.E., Amorim, M.R., Pinto, A.P., da Rocha, A.L., da Silva, A.S. and Branco, L.G. (2021) Molecular hydrogen downregulates acute exhaustive exercise-induced skeletal muscle damage. *Canadian Journal of Physiology and Pharmacology*. *99*(8), pp.812-820.
- Noor, M.N.Z.M., Alauddin, A.S., Wong, Y.H., Looi, C.Y., Wong, E.H., Madhavan, P. and Yeong, C.H. (2023) A systematic review of molecular hydrogen therapy in cancer management. *Asian Pacific Journal of Cancer Prevention*. *24*(1), p.37.

- Nowell, P.C. (1960) Phytohemagglutinin: an initiator of mitosis in cultures of normal human leukocytes. *Cancer Research*. *20*(4), pp.462-466.
- Obara, T., Naito, H., Nojima, T., Hirayama, T., Hongo, T., Ageta, K., Aokage, T., Hisamura, M., Yumoto, T. and Nakao, A. (2024) Hydrogen in transplantation: Potential applications and therapeutic implications. *Biomedicines*. *12*(1), p.118.
- O'Driscoll, B.R., Howard, L.S., Earis, J. and Mak, V. (2017) BTS guideline for oxygen use in adults in healthcare and emergency settings. *Thorax*. *72*(Suppl 1), pp.1-90.
- Ohno, K., Ito, M., Ichihara, M. and Ito, M. (2012) Molecular hydrogen as an emerging therapeutic medical gas for neurodegenerative and other diseases. *Oxidative Medicine and Cellular Longevity*. *2012*. pp.1-11.
- Ohsawa, I., Ishikawa, M., Takahashi, K., Watanabe, M., Nishimaki, K., Yamagata, K., Katsura, K.I., Katayama, Y., Asoh, S. and Ohta, S. (2007) Hydrogen acts as a therapeutic antioxidant by selectively reducing cytotoxic oxygen radicals. *Nature Medicine*. *13*(6), pp.688-694.
- Ohta, S. (2012) Molecular hydrogen is a novel antioxidant to efficiently reduce oxidative stress with potential for the improvement of mitochondrial diseases. *Biochimica et Biophysica Acta (BBA)-General Subjects*. *1820*(5), pp.586-594.
- Ohta, S. (2014) Molecular hydrogen as a preventive and therapeutic medical gas: initiation, development and potential of hydrogen medicine. *Pharmacology & Therapeutics*. 144(1), pp.1-11.
- Ohta, S. (2015) Molecular hydrogen as a novel antioxidant: overview of the advantages of hydrogen for medical applications. *Methods in Enzymology*. *555*, pp.289-317.
- Ohta, S. (2021) Direct targets and subsequent pathways for molecular hydrogen to exert multiple functions: Focusing on interventions in radical reactions. *Current Pharmaceutical Design*. *27*(5), pp.595-609.
- Ohta, S. (2023) Molecular hydrogen may activate the transcription factor Nrf2 to alleviate oxidative stress through the hydrogen-targeted porphyrin. *Aging Pathobiology and Therapeutics*. pp.25-32.
- Okamoto, A., Kohama, K., Aoyama-Ishikawa, M., Yamashita, H., Fujisaki, N., Yamada, T., Yumoto, T., Nosaka, N., Naito, H., Tsukahara, K. and Iida, A. (2016) Intraperitoneally administered, hydrogen-rich physiologic solution protects against postoperative ileus and is associated with reduced nitric oxide production. *Surgery*. *160*(3), pp.623-631.
- Okolie, J.A., Patra, B.R., Mukherjee, A., Nanda, S., Dalai, A.K. and Kozinski, J.A. (2021) Futuristic applications of hydrogen in energy, biorefining, aerospace, pharmaceuticals and metallurgy. *International Journal of Hydrogen Energy*. *46*(13), pp.8885-8905.
- Omer, N.H. (2019) Water quality parameters. *Water Quality-Science, Assessments and Policy*. *18*, pp.1-34.
- O'Neill, K.T., Al Ghafri, S., da Silva Falcão, B., Tang, L., Kozielski, K. and Johns, M.L. (2023) Hydrogen ortho-para conversion: process sensitivities and optimisation. *Chemical Engineering and Processing-Process Intensification*. *184*, p.109272.

- Ono, H., Nishijima, Y., Ohta, S., Sakamoto, M., Kinone, K., Horikosi, T., Tamaki, M., Takeshita, H., Futatuki, T., Ohishi, W. and Ishiguro, T. (2017) Hydrogen gas inhalation treatment in acute cerebral infarction: a randomized controlled clinical study on safety and neuroprotection. *Journal of Stroke and Cerebrovascular Diseases*. *26*(11), pp.2587- 2594.
- Orellano, P., Reynoso, J. and Quaranta, N. (2021) Short-term exposure to sulphur dioxide (SO2) and all-cause and respiratory mortality: A systematic review and meta- analysis. *Environment International. 150*, p.106434.
- Ostojic, S.M. (2015) Molecular hydrogen in sports medicine: new therapeutic perspectives. *International Journal of Sports Medicine*. *36*(4), pp.273-279.
- Ostojic, S.M. (2021) Hydrogen-rich water as a modulator of gut microbiota? *Journal of Functional Foods*. *78*, p.104360.
- Ostojic, S.M., Korovljev, D., Stajer, V. and Javorac, D. (2018) 28-Days hydrogen-rich water supplementation affects exercise capacity in mid-age overweight women. *Medicine & Science in Sports & Exercise*. *50*(5), pp.728-729.
- Oyebanji, O.B., Nweke, O., Odebunmi, O., Galadima, N.B., Idris, M.S., Nnodi, U.N., Afolabi, A.S. and Ogbadu, G.H. (2009) Simple, effective and economical explant-surface sterilization protocol for cowpea, rice and sorghum seeds. *African Journal of Biotechnology*. *8*(20), pp. 5395-5399.
- Paetkau, V., Mills, G., Gerhart, S. and Monticone, V. (1976) Proliferation of murine thymic lymphocytes in vitro is mediated by the concanavalin A-induced release of a lymphokine (costimulator). *The Journal of Immunology*. *117*(4), pp.1320-1324.
- Pajares, M., I. Rojo, A., Manda, G., Boscá, L. and Cuadrado, A. (2020) Inflammation in
- Parkinson's disease: mechanisms and therapeutic implications. *Cells*. *9*(7), p.1687.
- Parey, K., Brandt, U., Xie, H., Mills, D.J., Siegmund, K., Vonck, J., Kühlbrandt, W. and Zickermann, V., 2018. Cryo-EM structure of respiratory complex I at work. *Elife* [online]. *7*, p.39213 [Accessed 29/01/2024].
- Parkes, M.J. (2012) The limits of breath holding. *Scientific American*. *306*(4), pp.74-79.
- Penders, J., Kissner, R. and Koppenol, W.H. (2014) ONOOH does not react with H2: Potential beneficial effects of H2 as an antioxidant by selective reaction with hydroxyl radicals and peroxynitrite. *Free Radical Biology and Medicine*. *75*, pp.191-194.
- Perillo, B., Di Donato, M., Pezone, A., Di Zazzo, E., Giovannelli, P., Galasso, G., Castoria,
- G. and Migliaccio, A. (2020) ROS in cancer therapy: The bright side of the moon. *Experimental & Molecular Medicine*. *52*(2), pp.192-203.
- Perov, A.Y., Ovchinnikov, B.M., Parusov, V.V., Bobrovnikov, A.V., Safronova, V.G. and Holodilin, Y.D. (2021) The method of inhalation therapy with micro-doses of mixtures noble gases with oxygen. *ArXiv preprint* [online] *2111.10231* [Accessed 29/01/2024].
- Perricone, N.V. (2021) Perricone Hydrogen Water Co LLC. *Medication enhancement using hydrogen*. U.S. Patent 11,129,848. *Application granted*. Available from: https://www.freepatentsonline.com/10076540.html [Accessed 14/08/2023].

- Pham, C. V., Escalera-López, D., Mayrhofer, K., Cherevko, S., & Thiele, S. (2021) Essentials of high performance water electrolyzers – from catalyst layer materials to electrode engineering. *Advanced Energy Materials*. *11*(44), p.2101998.

- Piché-Choquette, S. and Constant, P. (2019) Molecular hydrogen, a neglected key driver of soil biogeochemical processes. *Applied and Environmental Microbiology*. *85*(6), p. 2418.
- Pillai, A.S., Chandler, S.A., Liu, Y., Signore, A.V., Cortez-Romero, C.R., Benesch, J.L., Laganowsky, A., Storz, J.F., Hochberg, G.K. and Thornton, J.W. (2020) Origin of complexity in haemoglobin evolution. *Nature*. *581*(7809), pp.480-485.

- Portugal, R. (2022) ELISpot assay for the detection of ASFV-specific interferon-gamma (IFN-γ)-producing cells. *Methods in Molecular Biology. 2503*, pp.169-178.
- Prakriya, M. (2020) Calcium and cell function. *The Journal of Physiology*. *598*(9), p.1647.
- Prangé, T., Schiltz, M., Pernot, L., Colloc'h, N., Longhi, S., Bourguet, W. and Fourme, R. (1998) Exploring hydrophobic sites in proteins with xenon or krypton. *Proteins: Structure, Function, and Bioinformatics*. *30*(1), pp.61-73.
- Preiner, M., Xavier, J.C., Vieira, A.D.N., Kleinermanns, K., Allen, J.F. and Martin, W.F. (2019) Catalysts, autocatalysis and the origin of metabolism. *Interface Focus* [online]. *9*(6), p.20190072 [Accessed 29/01/2024].
- Qi, B., Yu, Y., Wang, Y., Wang, Y., Yu, Y. and Xie, K. (2021) Perspective of molecular hydrogen in the treatment of sepsis. *Current Pharmaceutical Design*. *27*(5), pp.667-678.
- Qiu, P., Liu, Y. and Zhang, J. (2019) Recent advances in studies of molecular hydrogen against sepsis. *International Journal of Biological Sciences. 15*(6), p.1261.
- Radi, R. (2018) Oxygen radicals, nitric oxide, and peroxynitrite: Redox pathways in molecular medicine. *Proceedings of the National Academy of Sciences of the United states of America*. *115*(23), pp.5839-5848.
- Radyuk, S.N. (2021) Mechanisms underlying the biological effects of molecular hydrogen. *Current Pharmaceutical Design*. *27*(5), pp.626-735.
- Ramsay, J. and Kattnig, D.R. (2022) Radical triads, not pairs, may explain effects of hypomagnetic fields on neurogenesis. *PLOS Computational Biology*. *18*(9), p.1010519.
- Ransy, C., Vaz, C., Lombès, A. and Bouillaud, F. (2020) Use of H2O2 to cause oxidative stress, the catalase issue. *International Journal of Molecular Sciences*. *21*(23), p.9149.
- Rao, K.S., Babu, G.S. and Rajesh, M. (2018) Analysis and reduction of fuel consumption and emissions in internal combustion engines. *International Research Journal of Engineering and Technology*. *5*(5), pp.4110-4117.
- Ratajczak, E., Małecka, A., Ciereszko, I., & Staszak, A. M. (2019) Mitochondria are important determinants of the aging of seeds. *International Journal of Molecular Sciences*. *20*(7), p.1568.

- Razzaq, A., Wani, S.H., Saleem, F., Yu, M., Zhou, M. and Shabala, S. (2021) Rewilding crops for climate resilience: economic analysis and de novo domestication strategies. *Journal of Experimental Botany. 72*(18), pp.6123-6139.
- Read, A.D., Bentley, R.E., Archer, S.L. and Dunham-Snary, K.J. (2021) Mitochondrial iron– sulfur clusters: Structure, function, and an emerging role in vascular biology. *Redox Biology*. *47*, p.102164.
- Riccardi, C. and Nicoletti, I. (2006) Analysis of apoptosis by propidium iodide staining and flow cytometry. *Nature Protocols*. *1*(3), pp.1458-1461.
- Ríos-Arrabal, S., Artacho-Cordón, F., León, J., Román-Marinetto, E., del Mar Salinas- Asensio, M., Calvente, I. and Núñez, M.I. (2013) Involvement of free radicals in breast cancer. *Springerplus*. *2*, pp.1-12.
- Rochette, L., Zeller, M., Cottin, Y. and Vergely, C. (2021) Antitumor activity of protons and molecular hydrogen: underlying mechanisms. *Cancers*. *13*(4), p.893.
- Roger, A.J., Muñoz-Gómez, S.A. and Kamikawa, R. (2017) The origin and diversification of mitochondria. *Current Biology*. *27*(21), pp.1177-1192.
- Roose, B.W., Zemerov, S.D. and Dmochowski, I.J. (2018) Xenon-protein interactions: Characterization by X-ray crystallography and hyper-CEST NMR. *Methods in Enzymology*. *602*, pp.249-272.
- Rosewarne, F., 2005. Medical gases-their properties and uses. *Anaesthesia and Intensive Care*. *33*(5), p.697.
- Rosi, N.L., Eckert, J., Eddaoudi, M., Vodak, D.T., Kim, J., O'Keeffe, M. and Yaghi, O.M. (2003) Hydrogen storage in microporous metal-organic frameworks. *Science*. *300*(5622), pp.1127-1129.
- Roth, B.J. (2023) Biomagnetism: The first sixty years. *Sensors*. *23*(9), p.4218.
- Rovira, C., Ballone, P. and Parrinello, M. (1997) A density functional study of iron-porphyrin complexes. *Chemical Physics Letters*. *271*(4-6), pp.247-250.
- Royal Society (2014a) *Calcium - Element information, properties and uses.* Available from: https://www.rsc.org/periodic-table/element/20/Calcium [Accessed 13/07/2023].
- Royal Society (2014b) *Iron - Element information, properties and uses.* Available from: https://www.rsc.org/periodic-table/element/26/iron [Accessed 13/07/2023].
- Royal Society (2014c) *Phosphorus - Element information, properties and uses.* Available from: https://www.rsc.org/periodic-table/element/15/phosphorus [Accessed 13/07/2023].
- Runtuwene, J., Amitani, H., Amitani, M., Asakawa, A., Cheng, K.C. and Inui, A. (2015) Hydrogen–water enhances 5-fluorouracil-induced inhibition of colon cancer. *PeerJ*. *3*, p.859.
- Russell, M.J. and Ponce, A. (2020) Six ‘must-have’minerals for life’s emergence: Olivine,
- pyrrhotite, bridgmanite, serpentine, fougerite and mackinawite. *Life*. *10*(11), p.291.

- Russell, G., Veal, D. and Hancock, J.T. (2020) Is glyceraldehyde-3-phosphate dehydrogenase a central redox mediator? *Reactive Oxygen Species*. *9*(26), pp.48-69.
- Russell, G., Zulfiqar, F. and Hancock, J.T. (2020) Hydrogenases and the role of molecular hydrogen in plants. *Plants*. *9*(9), p.1136.
- Russell, G., Nenov, A. and Hancock, J. (2021) Oxy-hydrogen gas: The rationale behind its use as a novel and sustainable treatment for COVID-19 and other respiratory diseases. *European Medical Journal.* pp.21-27.
- Russell, G., Nenov, A., Kisher, H. and Hancock, J.T. (2021) Molecular hydrogen as medicine: An assessment of administration methods. *Hydrogen*. *2*(4), pp.444-460.
- Russell, G., Thomas, A.D., Nenov, A., Mannings, G. and Hancock, J.T. (2023) The therapeutic potential of oxyhydrogen gas in oncology: A study on Epstein–Barr Virus- immortalised B-Lymphoblastoid (TK6) cells. *Hydrogen*. *4*(4), pp.746-759.
- Russell, G., May, J. and Hancock, J.T. (2024) An interplay of gases: Oxygen and hydrogen in biological systems. *Oxygen*. *4*(1), pp.37-52.
- Ryter, S.W. (2020) Therapeutic potential of heme oxygenase-1 and carbon monoxide in acute organ injury, critical illness, and inflammatory disorders. *Antioxidants*. *9*(11), p.1153.
- Ryu, A.H., Eckalbar, W.L., Kreimer, A., Yosef, N. and Ahituv, N. (2017) Use antibiotics in cell culture with caution: genome-wide identification of antibiotic-induced changes in gene expression and regulation. *Scientific Reports*. *7*(1), p.7533.
- Sabri, S.M., Annuar, N., Rahman, N.L.A., Musairah, S.K., Abd Mutalib, H. and Subagja, I.K. (2022) Major trends in ageing population research: A bibliometric analysis from 2001 to 2021. *International Academic Symposium of Social Science. 2022*, p. 311.
- Sada, H., Egi, H., Ide, K., Sawada, H., Sumi, Y., Hattori, M., Sentani, K., Oue, N., Yasui, W. and Ohdan, H. (2021) Peritoneal lavage with hydrogen-rich saline can be an effective and practical procedure for acute peritonitis. *Surgery Today. 51*(11), pp.1860-1871.
- Safonov, V.L. (2019) H2 Universe LLC. *Systems and methods for topical application of molecular hydrogen.* U.S. Patent Application No. 16/376,894. Status: *pending*. Available from: https://patents.google.com/patent/US20190308001A1/en [Accessed 14/08/2023].
- Saitoh, Y., Okayasu, H., Xiao, L., Harata, Y. and Miwa, N. (2008) Neutral pH hydrogen- enriched electrolyzed water achieves tumor-preferential clonal growth inhibition over normal cells and tumor invasion inhibition concurrently with intracellular oxidant repression. *Oncology Research Featuring Preclinical and Clinical Cancer Therapeutics*. *17*(6), pp.247-255.
- Saitoh, Y., Harata, Y., Mizuhashi, F., Nakajima, M. and Miwa, N. (2010) Biological safety of neutral-pH hydrogen-enriched electrolyzed water upon mutagenicity, genotoxicity and subchronic oral toxicity. *Toxicology and Industrial Health*. *26*(4), pp.203-216.

- Salah, M., Osman, H. and Hosny, O. (2018) Performance-based reliability-centered maintenance planning for hospital facilities. *Journal of Performance of Constructed Facilities*. *32*(1), p.4017113.
- Saleem, F., Am Hur, S., Cahalan, M., Stewart, C., Sljivic, I., Bhuiyan, I., Aulakh, A., Fleetham, J., Guenette, J. and Ryerson, C. (2023) International guideline recommendations and eligibility criteria for home oxygen therapy. *The Lancet Respiratory Medicine*. *11*(5), pp.402-405.
- Sánchez, M., Sabio, L., Gálvez, N., Capdevila, M. and Dominguez-Vera, J.M. (2017) Iron chemistry at the service of life. *IUBMB Life*. *69*(6), pp.382-388.
- Sano, M., Ichihara, G., Katsumata, Y., Hiraide, T., Hirai, A., Momoi, M., Tamura, T., Ohata,
- S. and Kobayashi, E. (2020) Pharmacokinetics of a single inhalation of hydrogen gas in pigs. *PLoS One*. *15*(6), p.234626.

- Satoh, F., Sasaki, H., Kurokawa, R., Hirano, S. and Ichikawa, Y., Miz Co Ltd (2021) *Method and molecular hydrogen-containing composition for promotion of postoperative recovery*.
- U.S. Patent Application 17/147,692. Status: *pending*. Available from: https://patents.google.com/patent/US20210213049A1/en [Accessed 14/08/2023].

- Satta, H., Iwamoto, T., Kawai, Y., Koguchi, N., Shibata, K., Kobayashi, N., Yoshida, M. and Nakayama, M. (2021) Amelioration of hemodialysis-induced oxidative stress and fatigue with a hemodialysis system employing electrolyzed water containing molecular hydrogen. *Renal Replacement Therapy*. *7*(1), pp.1-9.
- Schmidt, H.J. (1991) A label as a hidden persuader: chemists' neutralization
- concept. *International Journal of Science Education*. *13*(4), pp.459-471.
- Schrama, F.N.H., Beunder, E.M., Van den Berg, B., Yang, Y. and Boom, R. (2017) Sulphur removal in ironmaking and oxygen steelmaking. *Ironmaking & Steelmaking*. *44*(5), pp.333- 343.
- Schwartz, J.L. and Jordan, R. (1997) Selective elimination of human lymphoid cells with unstable chromosome aberrations by p53-dependent apoptosis. *Carcinogenesis*. *18*(1), pp.201-205.
- Searcy, D. (1992) Origins of mitochondria and chloroplasts from sulfur-based symbioses. *The Origin and Evolution of the Cell*. pp. 47-78.
- Senn, N. (1888) Rectal insufflation of hydrogen gas an infallible test in the diagnosis of visceral injury of the gastro-intestinal tract in penetrating wounds of the abdomen. *Journal of the American Medical Association. 10*(25), pp.767-777.
- Sethi, S., Joshi, A., Arora, B., Bhowmik, A., Sharma, R.R. and Kumar, P. (2020) Significance of FRAP, DPPH, and CUPRAC assays for antioxidant activity determination in apple fruit extracts. *European Food Research and Technology*. *246*, pp.591-598.
- Settineri, R., Ji, J., Luo, C., Ellithorpe, R.R., de Mattos, G.F., Rosenblatt, S., LaValle, J., Jinenez, A., Ohta, S. and Nicolson, G.L. (2016) Effects of hydrogenized water on intracellular biomarkers for antioxidants, glucose uptake, insulin signaling and SIRT 1 and telomerase activity. *American Journal of Food and Nutrition*. 4(6), pp.161-168.

- Sha, J.B., Zhang, S.S., Lu, Y.M., Gong, W.J., Jiang, X.P., Wang, J.J., Qiao, T.L., Zhang, H.H., Zhao, M.Q., Wang, D.P. and Xia, H. (2018). Effects of the long-term consumption of hydrogen-rich water on the antioxidant activity and the gut flora in female juvenile soccer players from Suzhou, China. *Medical Gas Research*. *8*(4), p.135.

- Shafaat, H.S., Rüdiger, O., Ogata, H. and Lubitz, W. (2013) [NiFe] hydrogenases: a common active site for hydrogen metabolism under diverse conditions. *Biochimica et Biophysica Acta (BBA)-Bioenergetics*. *1827*(8-9), pp.986-1002.

- Shao, Y., Lin, F., Wang, Y., Cheng, P., Lou, W., Wang, Z., Liu, Z., Chen, D., Guo, W., Lan, Y. and Du, L. (2023) Molecular hydrogen confers resistance to rice stripe virus. *Microbiology Spectrum*. *11*(2), pp.4417-4422.

- Sharifi-Rad, M., Anil Kumar, N.V., Zucca, P., Varoni, E.M., Dini, L., Panzarini, E., Rajkovic, J., Tsouh Fokou, P.V., Azzini, E., Peluso, I. and Prakash Mishra, A. (2020) Lifestyle, oxidative stress, and antioxidants: Back and forth in the pathophysiology of chronic diseases. *Frontiers in Physiology*. *11*, p.694.

- Shi, M., Bi, L., Huang, X., Meng, Z., Wang, Y. and Yang, Z. (2020) Design of three- dimensional nanotube-fullerene-interconnected framework for hydrogen storage. *Applied Surface Science*. *534*, p.147606.

- Shibayama, Y., Dobashi, S., Arisawa, T., Fukuoka, T. and Koyama, K. (2020) Impact of hydrogen-rich gas mixture inhalation through nasal cannula during post-exercise recovery period on subsequent oxidative stress, muscle damage, and exercise performances in men. *Medical Gas Research*. *10*(4), p.155.

- Shimouchi, A., Nose, K., Takaoka, M., Hayashi, H. and Kondo, T. (2008) Effect of dietary turmeric on breath hydrogen. *Digestive Diseases and Sciences*. *54*(8), pp.1725-1729.

- Shin, W. (2014) Medical applications of breath hydrogen measurements. *Analytical and Bioanalytical Chemistry*. *406*(16), pp.3931-3939.

- Shin, D., Cho, E.S.R., Bang, H.T. and Shim, K.S. (2016) Effects of oxygenated or hydrogenated water on growth performance, blood parameters, and antioxidant enzyme activity of broiler chickens. *Poultry Science*. *95*(11), pp.2679-2684.

- Shirahata, S., Kabayama, S., Nakano, M., Miura, T., Kusumoto, K., Gotoh, M., Hayashi, H., Otsubo, K., Morisawa, S. and Katakura, Y. (1997) Electrolyzed–reduced water scavenges active oxygen species and protects DNA from oxidative damage. *Biochemical and Biophysical Research Communications*. *234*(1), pp.269-274.

- Shrivastava, P. and Kumar, R. (2015) Soil salinity: A serious environmental issue and plant growth promoting bacteria as one of the tools for its alleviation. *Saudi Journal of Biological Sciences*. *22*(2), pp.123-131.

- Sidell, B.D. and O'Brien, K.M. (2006) When bad things happen to good fish: the loss of hemoglobin and myoglobin expression in Antarctic icefishes. *Journal of Experimental Biology*. *209*(10), pp.1791-1802.

- Sim, M., Kim, C.S., Shon, W.J., Lee, Y.K., Choi, E.Y. and Shin, D.M. (2020) Hydrogen-rich water reduces inflammatory responses and prevents apoptosis of peripheral blood cells

- in healthy adults: a randomized, double-blind, controlled trial. *Scientific Reports*. *10*(1), p.12130.
- Simmonds, R.E. and Foxwell, B.M. (2008) Signalling, inflammation and arthritis: NF-κ B and
- its relevance to arthritis and inflammation. *Rheumatology*. *47*(5), pp.584-590.
- Singh, R.B., Halabi, G., Fatima, G., Rai, R.H., Tarnava, A.T. and LeBaron, T.W. (2021) Molecular hydrogen as an adjuvant therapy may be associated with increased oxygen saturation and improved exercise tolerance in a COVID-19 patient. *Clinical Case Reports*. *9*(11), p.5039.
- Singh, R.B., Fatima, G., Fedacko, J., Mojto, V., Sumbalová, Z., Tarnava, A., Pokotilo, O., Nazarov, E.I., Lee, K.J., Ferenczyova, K. and Vlkovlkova, J. (2023) Effects of molecular hydrogen in the pathophysiology and management of cardiovascular and metabolic diseases.*Preprints* [online]. Available from: https://www.preprints.org/manuscript/202304.1223/v1 [Accessed 30/01/2024].
- Slezák, J., Kura, B., Frimmel, K., Zálešák, M., Ravingerová, T., Viczenczová, C., Okruhlicová, Ľ. and Tribulová, N. (2016) Preventive and therapeutic application of molecular hydrogen in situations with excessive production of free radicals. *Physiological Research. 65*(1), pp.11-28.
- Slezak, J., Kura, B., LeBaron, T.W., Singal, P.K., Buday, J. and Barancik, M. (2021) Oxidative stress and pathways of molecular hydrogen effects in medicine. *Current Pharmaceutical Design*. *27*(5), pp.610-625.
- Sobue, S., Inoue, C., Hori, F., Qiao, S., Murate, T. and Ichihara, M. (2017) Molecular hydrogen modulates gene expression via histone modification and induces the mitochondrial unfolded protein response. *Biochemical and Biophysical Research Communications*. *493*(1), pp.318-324.
- Soleimani, V., Sahebkar, A. and Hosseinzadeh, H. (2018) Turmeric (Curcuma longa) and its major constituent (curcumin) as nontoxic and safe substances. *Phytotherapy Research*. *32*(6), pp.985-995.
- Son, Y., Cheong, Y.K., Kim, N.H., Chung, H.T., Kang, D.G. and Pae, H.O. (2011) Mitogen- activated protein kinases and reactive oxygen species: How can ROS activate MAPK pathways? *Journal of Signal Transduction*, *2011*[online]. p.792639 [Accessed 30/01/2024].
- Song, G., Tian, H., Qin, S., Sun, X., Yao, S., Zong, C., Luo, Y., Liu, J., Yu, Y., Sang, H. and Wang, X. (2012) Hydrogen decreases athero-susceptibility in apolipoprotein B-containing lipoproteins and aorta of apolipoprotein E knockout mice. *Atherosclerosis*. *221*(1), pp.55- 65.
- Sousa, F.L., Neukirchen, S., Allen, J.F., Lane, N. and Martin, W.F. (2016) Lokiarchaeon is hydrogen dependent. *Nature Microbiology*. *1*(5), pp.1-3.
- Spang, A., Stairs, C.W., Dombrowski, N., Eme, L., Lombard, J., Caceres, E.F., Greening, C., Baker, B.J. and Ettema, T.J. (2019) Proposal of the reverse flow model for the origin of the eukaryotic cell based on comparative analyses of Asgard archaeal metabolism. *Nature microbiology*. *4*(7), pp.1138-1148.

- Speckmann, B., Steinbrenner, H., Grune, T. and Klotz, L.O. (2016) Peroxynitrite: From interception to signaling. *Archives of Biochemistry and Biophysics*. *100*(595), pp.153-160.
- Squadrito, G.L. and Pryor, W.A. (2002) Mapping the reaction of peroxynitrite with CO2: Energetics, reactive species, and biological implications. *Chemical Research in Toxicology*. *15*(7), pp. 885-895.
- Stein, S., Selesi, D., Schilling, R., Pattis, I., Schmid, M. and Hartmann, A. (2005) Microbial activity and bacterial composition of H2-treated soils with net CO2 fixation. *Soil Biology and Biochemistry*. *37*(10), pp.1938-1945.
- Storz, J.F., 2018. *Hemoglobin: Insights Into Protein Structure, Function, and Evolution*. Oxford University Press, USA.
- Suh, M.P., Park, H.J., Prasad, T.K. and Lim, D.W. (2012) Hydrogen storage in metal–organic frameworks. *Chemical Reviews*. *112*(2), pp.782-835.
- Sutariya, V.B.; Pathak, Y., 2014. (Eds.) *Biointeractions of Nanomaterials*; CRC Press: Boca Raton, FL, USA.
- Sykes, W.S. and Lawrence, R.C. (1938) Helium in anaesthesia. *British Medical Journal*. *2*(4051), p.448.
- Tamura, T., Hayashida, K., Sano, M., Suzuki, M., Shibusawa, T., Yoshizawa, J., Kobayashi, Y., Suzuki, T., Ohta, S., Morisaki, H. and Fukuda, K. (2016) Feasibility and safety of hydrogen gas inhalation for post-cardiac arrest syndrome–first-in-human pilot study. *Circulation Journal*. *80*(8), pp.1870-1873.
- Tamura, T., Suzuki, M., Hayashida, K., Kobayashi, Y., Yoshizawa, J., Shibusawa, T., Sano, M., Hori, S. and Sasaki, J. (2020) Hydrogen gas inhalation alleviates oxidative stress in patients with post-cardiac arrest syndrome. *Journal of Clinical Biochemistry and Nutrition*. *67*(2), pp.214-221.y
- Tanaka, Y. and Miwa, N. (2022) Repetitive bathing and skin poultice with hydrogen-rich water improve wrinkles and blotches together with modulation of skin oiliness and moisture. *Hydrogen*. *3*(2), pp.161-178.
- Tang, K., Wu, Y.H., Song, Y. and Yu, B. (2021) Indoleamine 2, 3-dioxygenase 1 (IDO1) inhibitors in clinical trials for cancer immunotherapy. *Journal of Hematology & Oncology*. *14*(1), pp.1-21.
- Tao, G., Song, G. and Qin, S. (2019) Molecular hydrogen: current knowledge on mechanism in alleviating free radical damage and diseases. *Acta Biochimica et Biophysica Sinica*. *51*(12), pp.1189-1197.
- Tao, G., Zhang, G., Chen, W., Yang, C., Xue, Y., Song, G. and Qin, S. (2022) A randomized, placebo-controlled clinical trial of hydrogen/oxygen inhalation for non-alcoholic fatty liver disease. *Journal of Cellular and Molecular Medicine*. *26*(14), pp.4113-4123.
- Tard, C. and Pickett, C.J. (2009) Structural and functional analogues of the active sites of the [Fe]-,[NiFe]-, and [FeFe]-hydrogenases. *Chemical Reviews*. *109*(6), pp.2245-2274.

- Tarnava, A. (2021) Supersaturated hydrogen-rich water hydrotherapy for recovery of acute injury to the proximal phalanges on the 5th toe: A case report. *The Journal of Science and Medicine*. *3*(1).
- Tarzad, U. (2020) Supreme theory of everything: Whole universe in a simple formula. *London Journal of Research in Science: Natural and Formal*. 20(5), pp.73-90.
- Te, J.A., Tan, M.L. and Ichiye, T. (2010) Solvation of glucose, trehalose, and sucrose by the soft-sticky dipole–quadrupole–octupole water model. *Chemical Physics Letters*. *491*(4- 6), pp.218-223.
- The Water industry Act (1991) *The physical and chemical properties of water.* Available from: https://www.dwi.gov.uk/the-physical-and-chemical-properties-of-water/ [Accessed 12/02/2024].
- The, C. and Wilson, R.K. (1999) How the worm was won: The *C. elegans* genome sequencing project*. Trends in Genetics. 15*(2), pp.51-58.
- Thomson, A.J. (1977) Redox potentials of iron-sulphur clusters. *Nature*. *266*(5605), pp.771-772.
- Thor, K. (2019) Calcium—nutrient and messenger. *Frontiers in Plant Science*. *10*, p.440.
- Tian, Y., Zhang, Y., Wang, Y., Chen, Y., Fan, W., Zhou, J., Qiao, J. and Wei, Y. (2021) Hydrogen, a novel therapeutic molecule, regulates oxidative stress, inflammation, and apoptosis. *Frontiers in Physiology*. *12*, p.2281.
- Tilton Jr, R.F., Kuntz Jr, I.D. and Petsko, G.A. (1984) Cavities in proteins: structure of a metmyoglobin xenon complex solved to 1.9. ANG. *Biochemistry*. *23*(13), pp.2849-2857.
- Todorovic, N., Zanini, D., Stajer, V., Korovljev, D., Ostojic, J. and Ostojic, S.M. (2021) Hydrogen-rich water and caffeine for alertness and brain metabolism in sleep-deprived habitual coffee drinkers. *Food Science & Nutrition*. *9*(9), pp.5139-5145.
- Trivic, T., Vojnovic, M., Drid, P. and Ostojic, S.M. (2017) Drinking hydrogen-rich water for 4 weeks positively affects serum antioxidant enzymes in healthy men: A pilot study. *Current Topics in Nutraceutical Research*. *15*(1), pp.45-48.
- Tsai, C.F., Hsu, Y.W., Chen, W.K., Ho, Y.C. and Lu, F.J. (2009) Enhanced induction of mitochondrial damage and apoptosis in human leukemia HL-60 cells due to electrolyzed-reduced water and glutathione. *Bioscience, Biotechnology, and Biochemistry*. *73*(2), pp.280-287.
- Tsubone, H., Hanafusa, M., Endo, M., Manabe, N., Hiraga, A., Ohmura, H. and Aida, H. (2013) Effect of treadmill exercise and hydrogen-rich water intake on serum oxidative and anti-oxidative metabolites in serum of thoroughbred horses. *Journal of Equine Science*. *24*(1), pp.1-8.
- Ugalde, J.M., Dunietz, B., Dreuw, A., Head-Gordon, M. and Boyd, R.J. (2004) The spin dependence of the spatial size of Fe (II) and of the structure of Fe (II)-porphyrins. *The Journal of Physical Chemistry A*. *108*(21), pp.4653-4657.
- Ulasov, A.V., Rosenkranz, A.A., Georgiev, G.P. and Sobolev, A.S. (2022) Nrf2/Keap1/ARE signaling: Towards specific regulation. *Life Sciences*. *291*, p.120111.

- UMIN Clinical Trials Registry. Keyword 'Hydrogen'. Available from:
- https://center6.umin.ac.jp/cgi-open-bin/ctr_e/index_fw.cgi [Accessed 11/08/2023].
- Uto, K., Sakamoto, S., Que, W., Shimata, K., Hashimoto, S., Sakisaka, M., Narita, Y., Yoshii, D., Zhong, L., Komohara, Y. and Li, X.K. (2019) Hydrogen-rich solution attenuates cold ischemia-reperfusion injury in rat liver transplantation. *BMC Gastroenterology*. *19*(1), pp.1-9.

- Vaissier, V. and Van Voorhis, T. (2017) Quantum chemical approaches to [NiFe] hydrogenase. *Essays in Biochemistry*. *61*(2), pp.293-303.

- Vallee, Y., Shalayel, I., Ly, K.D., Rao, K.R., De Paëpe, G., Märker, K. and Milet, A. (2017) At the very beginning of life on Earth: the thiol-rich peptide (TRP) world hypothesis. *International Journal of Developmental Biology*. *61*(8-9), pp.471-478.

- van Haersma Buma, B.N., Peretto, M., Matar, Z.M. and van de Kaa, G. (2023) Towards renewable hydrogen-based electrolysis: Alkaline vs Proton Exchange Membrane. *Heliyon*. *9*(7).

- Viggiano, A.A., Midey, A.J. and Ehlerding, A. (2006) Kinetics of the reactions of ONOO− with
- small molecules. *International Journal of Mass Spectrometry*. *255*, pp.65-70.
- Vignais, P.M. and Billoud, B. (2007) Occurrence, classification, and biological function of hydrogenases: an overview. *Chemical Reviews*. *107*(10), pp.4206-4272.

- Villamena, F.A. 2013. *Chemistry of reactive species.* Molecular Basis of Oxidative Stress. pp.1-48. John Wiley & Sons, Inc.
- Vishwakarma, R.K. and Negi, D.S. (2020) The development of COX-1 and COX-2 inhibitors: a review. *International Journal of Pharmaceutical Sciences and Research. 11*(8), p.3544.
- Vlastaridis, P., Kyriakidou, P., Chaliotis, A., Van de Peer, Y., Oliver, S.G. and Amoutzias,
- G.D. (2017) Estimating the total number of phosphoproteins and phosphorylation sites in eukaryotic proteomes. *Gigascience*. *6*(2), p.15.
- Volbeda, A. and Fontecilla-Camps, J.C., 2012. *The evolutionary relationship between complex I and [NiFe]-hydrogenase.* A Structural Perspective on Respiratory Complex I: Structure and Function of NADH: ubiquinone oxidoreductase. pp.109-121. Dordrecht, Springer.

- Wang, L. and White, P. (1994) Structure and properties of amylose, amylopectin. *Cereal Chemistry*. *71*(3), pp.263-268.
- Wang, D., Wang, L., Zhang, Y., Zhao, Y. and Chen, G. (2018a) Hydrogen gas inhibits lung cancer progression through targeting SMC3. *Biomedicine & Pharmacotherapy*. *104*, pp.788-797.

- Wang, W., Chen, D., Zhang, X., Liu, D., Cheng, Y. and Shen, F. (2018b) Role of plant respiratory burst oxidase homologs in stress responses. *Free Radical Research*. *52*(8), pp.826-839.
- Wang, H., Luo, Y.H., Shen, G.N., Piao, X.J., Xu, W.T., Zhang, Y., Wang, J.R., Feng, Y.C., Li,
- J.Q., Zhang, Y. and Zhang, T. (2019) Two novel 1, 4-naphthoquinone derivatives induce human gastric cancer cell apoptosis and cell cycle arrest by regulating reactive oxygen species-mediated MAPK/Akt/STAT3 signaling pathways. *Molecular Medicine Reports*. *20*(3), pp.2571-2582.
- Wang, X.X., Zhang, B., Xia, R. and Jia, Q.Y. (2020a) Inflammation, apoptosis and autophagy as critical players in vascular dementia. *European Review for Medical and Pharmacological Sciences*. *24*(18), pp.9601-9614.
- Wang, P., Zhao, M., Chen, Z., Wu, G., Fujino, M., Zhang, C., Zhou, W., Hirano, S.I., Li, X.K. and Zhao, L. (2020b) Hydrogen gas attenuates hypoxic-ischemic brain injury via regulation of the MAPK/HO-1/PGC-1a pathway in neonatal rats. *Oxidative Medicine and Cellular Longevity*. *20*(3), pp.2571-2582.
- Wang, S.T., Bao, C., He, Y., Tian, X., Yang, Y., Zhang, T. and Xu, K.F. (2020c) Hydrogen gas (XEN) inhalation ameliorates airway inflammation in asthma and COPD patients. *QJM: Monthly Journal of the Association of Physicians*. *113*(12), pp.870-875.
- Wang, B., Dai, T., Sun, W., Wei, Y., Ren, J., Zhang, L., Zhang, M. and Zhou, F. (2021a) Protein N-myristoylation: functions and mechanisms in control of innate immunity. *Cellular & Molecular Immunology*. *18*(4), pp.878-888.
- Wang, Y., Lv, P., Kong, L., Shen, W. and He, Q. (2021b) Nanomaterial-mediated sustainable hydrogen supply induces lateral root formation via nitrate reductase- dependent nitric oxide. *Chemical Engineering Journal*. *405*, p.126905.
- Wang, T., Cao, X. and Jiao, L. (2022) PEM water electrolysis for hydrogen production: fundamentals, advances, and prospects. *Carbon Neutrality*. *1*(1), p.21.
- Wang, Y., Wang, M., Xie, B., Wen, D., Li, W., Zhou, M., Wang, X., Lu, Y., Cong, B., Ni, Z. and Ma, C. (2023a) Effects of molecular hydrogen intervention on the gut microbiome in methamphetamine abusers with mental disorder. *Brain Research Bulletin*. *193*, pp.47-58.
- Wang, X., An, Z., Liao, J., Ran, N., Zhu, Y., Ren, S., Meng, X., Cui, N., Yu, Y. and Fan, H. (2023b) The role and mechanism of hydrogen-rich water in the Cucumis sativus response to chilling stress. *International Journal of Molecular Sciences*. *24*(7), p.6702.
- White, L.M., Bhartia, R., Stucky, G.D., Kanik, I. and Russell, M.J. (2015) Mackinawite and greigite in ancient alkaline hydrothermal chimneys: identifying potential key catalysts for emergent life. *Earth and Planetary Science Letters*. *100*(430), pp,105-114.
- Wilson, M.R. (1998) Apoptosis: unmasking the executioner. *Cell Death & Differentiation*. *5*(8), pp.646-652.
- Wilson, D.F. (2017) Oxidative phosphorylation: regulation and role in cellular and tissue metabolism. *The Journal of Physiology*. *595*(23), pp.7023-7038.

- Wilson, H.R., Veal, D., Whiteman, M. and Hancock, J.T. (2017) Hydrogen gas and its role in cell signalling. *CAB Reviews*. *12*(45), pp.1-3.
- Winterbourn, C.C. (2020) Biological chemistry of superoxide radicals. *ChemTexts*. *6*(1), pp.1-13.
- Wirth, C., Brandt, U., Hunte, C. and Zickermann, V. (2016) Structure and function of mitochondrial complex I. *Biochimica et Biophysica Acta (BBA)-Bioenergetics*. *1857*(7), pp.902-914.
- Wong, Y., Meehan, M.T., Burrows, S.R., Doolan, D.L. and Miles, J.J. (2022) Estimating the global burden of Epstein-Barr virus-related cancers. *Journal of Cancer Research and Clinical Oncology*. *148*(1), pp.31-46.
- Wood, P.M. (1988) The potential diagram for oxygen at pH 7. *Biochemical Journal*. *253*(1), p.287.
- Worlddata.info (2020) *Average height for men and women worldwide*. Available from: https://www.worlddata.info/average-bodyheight.php [Accessed 08/12/2023].
- Wu, Y., Yuan, M., Song, J., Chen, X. and Yang, H. (2019) Hydrogen gas from inflammation treatment to cancer therapy. *ACS Nano*. *13*(8), pp.8505-8511.
- Wu, Q., Su, N., Shabala, L., Huang, L., Yu, M. and Shabala, S. (2020) Understanding the mechanistic basis of ameliorating effects of hydrogen rich water on salinity tolerance in barley. *Environmental and Experimental Botany*. *177*, p.104136.
- Wu, C., Zou, P., Feng, S., Zhu, L., Li, F., Liu, T.C.Y., Duan, R. and Yang, L. (2023) Molecular hydrogen: an emerging therapeutic medical gas for brain disorders. *Molecular Neurobiology*. *60*(4), pp.1749-1765.
- Xia, C., Liu, W., Zeng, D., Zhu, L., Sun, X. and Sun, X. (2013) Effect of hydrogen-rich water on oxidative stress, liver function, and viral load in patients with chronic hepatitis
- *Clinical and Translational Science*. *6*(5), pp.372-375.
- Xie, K., Yu, Y., Huang, Y., Zheng, L., Li, J., Chen, H., Han, H., Hou, L., Gong, G. and Wang,
- G. (2012) Molecular hydrogen ameliorates lipopolysaccharide-induced acute lung injury in mice through reducing inflammation and apoptosis. *Shock*. *37*(5), pp.548-555.
- Xie, K., Liu, L., Yu, Y. and Wang, G. (2014) Hydrogen gas presents a promising therapeutic strategy for sepsis. *BioMed Research International*. *2014*, pp.1-9.
- Xu, C., Wang, S., Wang, H., Liu, K., Zhang, S., Chen, B., Liu, H., Tong, F., Peng, F., Tu, Y. and Li, Y. (2021) Magnesium-based micromotors as hydrogen generators for precise rheumatoid arthritis therapy. *Nano Letters*. *21*(5), pp.1982-1991.
- Yamamoto, R., Homma, K., Suzuki, S., Sano, M. and Sasaki, J. (2019) Hydrogen gas distribution in organs after inhalation: Real-time monitoring of tissue hydrogen concentration in rat. *Scientific Reports*. *9*(1), p.1255.
- Yamazaki, M., Kusano, K., Ishibashi, T., Kiuchi, M. and Koyama, K. (2015) Intravenous infusion of H2-saline suppresses oxidative stress and elevates antioxidant potential in thoroughbred horses after racing exercise. *Scientific Reports*. *5*(1), p.15514.

- Yan, M., Yao, Y., Mou, K., Dan, Y., Li, W., Wang, C. and Liao, W. (2022) The involvement of abscisic acid in hydrogen gas-enhanced drought resistance in tomato seedlings. *Scientia Horticulturae*. *292*, p.110631.
- Yang, Y., Zhu, Y. and Xi, X. (2018) Anti-inflammatory and antitumor action of hydrogen via reactive oxygen species. *Oncology Letters*. *16*(3), pp.2771-2776.
- Yang, L., Ao, Q., Zhong, Q., Li, W. and Li, W. (2020a) SIRT1/IGFBPrP1/TGF β1 axis involved in cucurbitacin B ameliorating concanavalin A-induced mice liver fibrosis. *Basic & Clinical Pharmacology & Toxicology*. *127*(5), pp.371-379.
- Yang, Y., Liu, P.Y., Bao, W., Chen, S.J., Wu, F.S. and Zhu, P.Y. (2020b) Hydrogen inhibits endometrial cancer growth via a ROS/NLRP3/caspase-1/GSDMD-mediated pyroptotic pathway. *BMC Cancer*. *20*(1), p.28.
- Yang, W.C., Li, T.T., Wan, Q., Zhang, X., Sun, L.Y., Zhang, Y.R., Lai, P.C. and Li, W.Z. (2023)
- Molecular hydrogen mediates neurorestorative effects after stroke in diabetic rats: the TLR4/NF-κB inflammatory pathway. *Journal of Neuroimmune Pharmacology*. *18*(1), pp.90- 99.
- Yano, T. and Ohnishi, T. (2001) The origin of cluster N2 of the energy-transducing NADH–quinone oxidoreductase: comparisons of phylogenetically related enzymes. *Journal of Bioenergetics and Biomembranes*. *33*(3), pp.213-222.
- Ye, Z., Zhang, R. and Sun, X. (2013) Bustling argon: biological effect. *Medical Gas Research*. *3*(1), pp.1-4.
- Yoga, E.G., Angerer, H., Parey, K. and Zickermann, V. (2020) Respiratory complex I– mechanistic insights and advances in structure determination. *Biochimica et Biophysica Acta (BBA)-Bioenergetics*. *1861*(3), p.148153.
- Yoon, M., Yang, S., Hicke, C., Wang, E., Geohegan, D. and Zhang, Z. (2008) Calcium as the superior coating metal in functionalization of carbon fullerenes for high-capacity hydrogen storage. *Physical Review Letters*. *100*(20), p.206806.
- Yoon, K.S., Huang, X.Z., Yoon, Y.S., Kim, S.K., Song, S.B., Chang, B.S., Kim, D.H. and Lee,
- K.J. (2011) Histological study on the effect of electrolyzed reduced water-bathing on UVB radiation-induced skin injury in hairless mice. *Biological and Pharmaceutical Bulletin*. *34*(11), pp.1671-1677.
- Yoritaka, A., Takanashi, M., Hirayama, M., Nakahara, T., Ohta, S. and Hattori, N. (2013) Pilot study of H2 therapy in Parkinson's disease: A randomized double-blind placebo- controlled trial. *Movement Disorders. 28*(6), pp.836-839.
- York, A. (2017) Evolutionary insights from the Vikings. *Nature Reviews Microbiology*. *15*(2), pp.65-65.
- You, I.S., Sharma, S., Fadriquela, A., Bajgai, J., Thi, T.T., Rahman, M.H., Sung, J., Kwon, H.U., Lee, S.Y., Kim, C.S. and Lee, K.J. (2021) Antioxidant properties of hydrogen gas attenuates oxidative stress in airway epithelial cells. *Molecules*. *26*(21), p.6375.

- Yu, X., Gurry, T., Nguyen, L.T.T., Richardson, H.S. and Alm, E.J. (2020) Prebiotics and community composition influence gas production of the human gut microbiota. *MBio*. *11*(5), pp.10-1128.
- Yu, H., Schut, G.J., Haja, D.K., Adams, M.W. and Li, H. (2021) Evolution of Complex I-like respiratory complexes. *The Journal of Biological Chemistry*. *296*, p.100740.
- Yuan, L. and Shen, J. (2016) Hydrogen, a potential safeguard for graft-versus-host disease and graft ischemia-reperfusion injury? *Clinics*. *71*, pp.544-549.
- Zam, W. (2018) Gut microbiota as a prospective therapeutic target for curcumin: A review of mutual influence. *Journal of Nutrition and Metabolism*. *2018*, p.1367984.
- Zamaraev, A.V., Zhivotovsky, B. and Kopeina, G.S. (2020) Viral infections: negative regulators of apoptosis and oncogenic factors. *Biochemistry*. *85*(10), pp.1191-1201.
- Zan, R., Wang, H., Cai, W., Ni, J., Luthringer-Feyerabend, B.J.C., Wang, W., Peng, H., Ji, W., Yan, J., Xia, J. and Song, Y. (2021) Controlled release of hydrogen by implantation of magnesium induces P53-mediated tumor cells apoptosis. *Bioactive Materials*. *9*, pp.385- 396.
- Zanini, D., Todorovic, N., Korovljev, D., Stajer, V., Ostojic, J., Purac, J., Kojic, D., Vukasinovic, E., Djordjievski, S., Sopic, M. and Guzonjic, A. (2021) The effects of 6-month hydrogen-rich water intake on molecular and phenotypic biomarkers of aging in older adults aged 70 years and over: A randomized controlled pilot trial. *Experimental Gerontology*. *155*, p.111574.
- ZetterstrÖm, A. (1948) Deep-sea diving with synthetic gas mixtures. *The Military Surgeon (United States)*, *103*(2), pp.104-106.
- Zhan, L., Sakamoto, H., Sakuraba, M., Wu, D.S., Zhang, L.S., Suzuki, T., Hayashi, M. and Honma, M. (2004) Genotoxicity of microcystin-LR in human lymphoblastoid TK6 cells. *Mutation Research/Genetic Toxicology and Environmental Mutagenesis*. *557*(1), pp.1-6.
- Zhan, C., Li, H., Li, X., Jiang, Y. and Xie, Z. (2020) Synthesis of PdH0. 43 nanocrystals with different surface structures and their catalytic activities towards formic acid electro- oxidation. *Science China-Materials*. *63*(3), pp.375-382.
- Zhang, J., Hao, H., Chen, M., Wang, H., Feng, Z. and Chen, H. (2017) Hydrogen-rich water alleviates the toxicities of different stresses to mycelial growth in *Hypsizygus marmoreus*. *AMB Express*. *1*(7), pp.1-11.
- Zhang, Y., Tan, S., Xu, J. and Wang, T. (2018) Hydrogen therapy in cardiovascular and metabolic diseases: from bench to bedside. *Cellular Physiology and Biochemistry*. *47*(1), pp.1-10.
- Zhang, L., Wang, X., Cueto, R., Effi, C., Zhang, Y., Tan, H., Qin, X., Ji, Y., Yang, X. and Wang,
- H. (2019a) Biochemical basis and metabolic interplay of redox regulation. *Redox Biology*. *26*, p.101284.

Zhang, L., Zhao, P., Yue, C., Jin, Z., Liu, Q., Du, X. and He, Q. (2019b) Sustained release of bioactive hydrogen by Pd hydride nanoparticles overcomes Alzheimer's disease. *Biomaterials*. *197*, pp.393-404.

Zhang, Y., Xu, J. and Yang, H. (2020) Hydrogen: An endogenous regulator of liver homeostasis. *Frontiers in Pharmacology*. *11*, p.877.
Zhang, J., Feng, X., Fan, Y., Zhu, G. and Bai, C. (2021a) Molecular hydrogen alleviates asthma through inhibiting IL-33/ILC2 axis. *Inflammation Research*. *70*, pp.569-579.
Zhang, R., Xue, B., Tao, Y., Zhao, H., Zhang, Z., Wang, X., Zhou, X., Jiang, B., Yang, Z., Yan, X. and Fan, K. (2022) Edge-site engineering of defective Fe–N4 nanozymes with boosted catalase-like performance for retinal vasculopathies. *Advanced Materials*. *34*(39), p.2205324.
Zhao, M., Nanbo, A., Sun, L. and Lin, Z. (2019) Extracellular vesicles in Epstein-Barr virus' life cycle and pathogenesis. *Microorganisms. 7*(2), p.48.
Zheng, Z.G., Sun, W.Z., Hu, J.Y., Jie, Z.J., Xu, J.F., Cao, J., Song, Y.L., Wang, C.H., Wang, J., Zhao, H. and Guo, Z.L. (2021) Hydrogen/oxygen therapy for the treatment of an acute exacerbation of chronic obstructive pulmonary disease: results of a multicenter, randomized, double-blind, parallel-group controlled trial. *Respiratory Research*, *22*(1), p.149.
Zhu, Q., Wu, Y., Li, Y., Chen, Z., Wang, L., Xiong, H., Dai, E., Wu, J., Fan, B., Ping, L. and Luo, X. (2018) Positive effects of hydrogen-water bathing in patients of psoriasis and parapsoriasis en plaques. *Scientific Reports*. 8(1), p.8051.
Zhu, J., Petit, P.F. and Van den Eynde, B.J. (2019) Apoptosis of tumor-infiltrating T lymphocytes: a new immune checkpoint mechanism. *Cancer Immunology, Immunotherapy*. *68*(5), pp.835-847.
Zhu, B., Cui, H. and Xu, W. (2021) Hydrogen inhibits the proliferation and migration of gastric cancer cells by modulating lncRNA MALAT1/miR-124-3p/EZH2 axis. *Cancer Cell International*. *21*(1), pp.1-10.
Zhu, C., Wei, F., Jiang, H., Lin, Z., Zhong, L., Wu, Y., Sun, X. and Song, L. (2024) Exploration of the structural mechanism of hydrogen (H2)-promoted horseradish peroxidase (HRP) activity via multiple spectroscopic and molecular dynamics simulation techniques. *International Journal of Biological Macromolecules*. *258*, p.128901.
Zhuang, X., Yu, Y., Jiang, Y., Zhao, S., Wang, Y., Su, L., Xie, K., Yu, Y., Lu, Y. and Lv, G. (2020) Molecular hydrogen attenuates sepsis-induced neuroinflammation through regulation of microglia polarization through an mTOR-autophagy-dependent pathway. *International Immunopharmacology*. *81*, p.106287.
Zickermann, V., Wirth, C., Nasiri, H., Siegmund, K., Schwalbe, H., Hunte, C. and Brandt, U. (2015) Mechanistic insight from the crystal structure of mitochondrial Complex I. *Science*. *347*(6217), pp.44-49.
Zulfiqar, F., Russell, G. and Hancock, J.T. (2021) Molecular hydrogen in agriculture. *Planta*. *254*(3), pp.1-14.

Abbreviation List

8-oxo-dG - 8-Oxo-2'-deoxyguanosine

ADP – Adenosine diphosphate

AE – Alkaline water electrolysis

ALP - Alanine phosphatase

ALT - Alanine aminotransferase

ANOVA – Analysis of variance

ARE – Antioxidant response element

ASK - Apoptosis signal-regulating kinase

AST - Aspartate aminotransferase

ATP – Adenosine triphosphate

Bcl2 - B-cell lymphoma-2

BLASTP - Basic local alignment search tool: protein

cAMP - Cyclic adenosine 3,5-monophosphate

CAT – Catalase

CFS – Chronic fatigue syndrome

CK – Creatinine kinase

CNS – Central nervous system

ConA – Concanavalin A

COPD – Chronic obstructive pulmonary disorder

COVID-19 – Coronavirus infectious disease (2019)

CRP – C-reactive protein

CUPRAC – CUPric reducing antioxidant assay

CVD – Cardiovascular disease

CVS – Cardiovascular system

DMEM - Dulbecco's modified eagle medium

DNA – Deoxyribose nucleic acid

DR4 - Death Receptor 4

DWI - Drinking Water Inspectorate

EBV – Epstein-Barr virus

ECU - Electronic control unit

ELISA - Enzyme-linked immunosorbent assay

EPR - Electron paramagnetic resonance

ERK - Extracellular signal-regulated kinase

ERW – Electrolysed reduced water

ETC – Electron transport chain

FAD - Flavin adenine dinucleotide

FBS - Foetal bovine serum

FMN – Flavin mononucleotide

FOSB - Finkel-Biskis-Jinkins murine osteosarcoma viral oncogene homolog B

FRAP – Ferric reducing antioxidant protocol

FUNDC-1 - FUN14 domain-containing protein 1

GERD - Gastroesophageal reflux disease

GGT - Gamma-glutamyl transferase

GPx – Glutathione peroxidase

GRAS – Generally regarded as safe

GRP78 - 78-kDa glucose-regulated protein

GSH – Glutathione

GTP - Guanosine-5'-triphosphate

HBOT – Hyperbaric oxygen therapy

HBV - Hepatitis B virus

HDL- High density lipoprotein

HER2 - Human epidermal growth factor receptor-2

HNW – Hydrogen nanobubble water

HO-1 – Haem oxygenase 1

HRS – Hydrogen-rich saline

HRW – Hydrogen-rich water

HSC4 - Head-and-neck squamous cell carcinoma cells

HSP – Heat shock protein

IBD - Irritable bowel disease

IBS - Irritable bowel syndrome

ICAM-1 - Intercellular cell adhesion molecule 1

IFγ – Interferon gamma

IL – Interleukin

IVF - *in vitro* fertilisation

JNK - c-Jun N-terminal kinases

KEAP-1 - Kelch-like ECH-associated protein 1

LDH – Lactate dehydrogenase

LDL - Low density lipoprotein

LPS – Lipopolysaccharide

MAPK – Mitogen-associated protein kinase

Mbh – membrane-bound hydrogenase

MCP-1 - Monocyte chemoattractant protein-1

MDA – Malondialdehyde

ME/CFS – Myalgic encephalomyelitis/chronic fatigue syndrome

MMP - Matrix metalloproteinases

MS – Multiple Sclerosis

NAc - Nucleus accumbens

NAD(H) - Nicotinamide adenine dinucleotide

NADP(H) - Nicotinamide adenine dinucleotide phosphate

NAFLD - Non-alcoholic fatty liver disease

NASA - National Aeronautics Space Agency

ND - NADH dehydrogenase subunit

NDUFS - NADH dehydrogenase [ubiquinone] iron-sulphur protein

NDUFV - NADH:ubiquinone oxidoreductase core V subunits

NFκB - Nuclear factor kappa B

NGM – Nematode growth medium

NHS – National Health Service

NLRP3 - Nod-like receptor family pyrin domain containing 3

NMR - Nuclear magnetic resonance

NOS - Nitric oxide synthase

NOX - NADPH oxidase

Nrf2 - Nuclear factor erythroid 2-related factor 2

NSAID - Non-steroidal anti-inflammatory drugs

NSCLC - Non-small cell lung carcinoma

OXPHOS – Oxidative phosphorylation

PBS - Phosphate buffer saline

PEM – Proton exchange membrane

PHA – Phytohemagglutinin

PKC – Protein kinase C

PLGA - Poly (lactic-co-glycolic acid)

PNS – Peripheral nervous system

PWM – Pokeweed mitogen

-Px – Peroxidase

RIPA - Radioimmunoprecipitation

RNS – Reactive nitrogen species

ROS – Reactive oxygen species

RPMI - Roswell Park Medical Institute

SCFA – Short chain fatty acid

SDS/PAGE - Sodium dodecyl sulphate-polyacrylamide gel electrophoresis assay

SEM - Standard error of the mean

SIRT-1 - NAD-dependent deacetylase sirtuin-1

SOD – Superoxide dismutase

TAC – Total antioxidant capacity

TCA – The citric acid (tricarboxylic acid) cycle

TNFα – Tumour necrosis factor alpha

TPTZ - 2,3,5-Triphenyltetrazolium chloride

TRAF - Tumour necrosis factor receptor–associated factor

TRAIL R1 - TNF-related apoptosis-inducing ligand receptor 1

USD – United States dollars

VEGF – Vascular endothelial growth factor

WBC – White blood cells

XO – Xanthine oxidase

ZO-1 - zona occludin 1

Supplementary Section

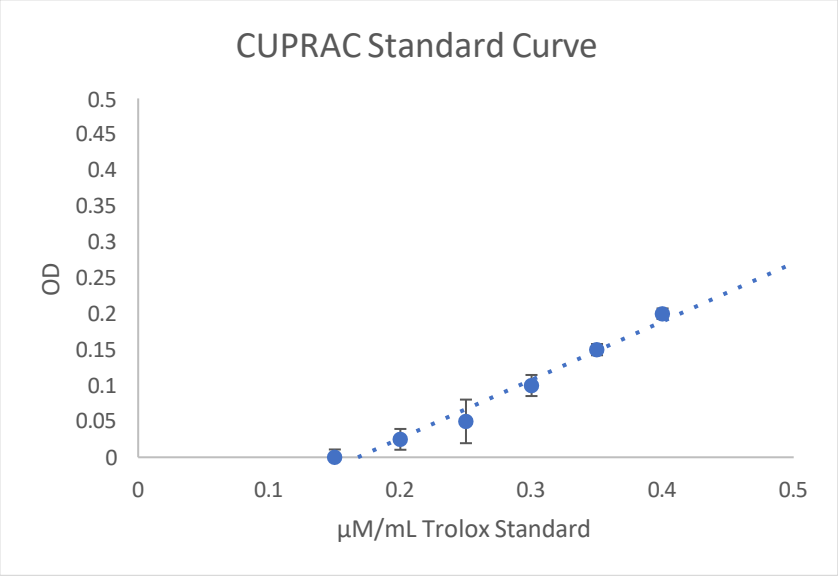

Supplementary Figure 1: Standard curve (CUPRAC) Error bars ± SEM. (n = 3)

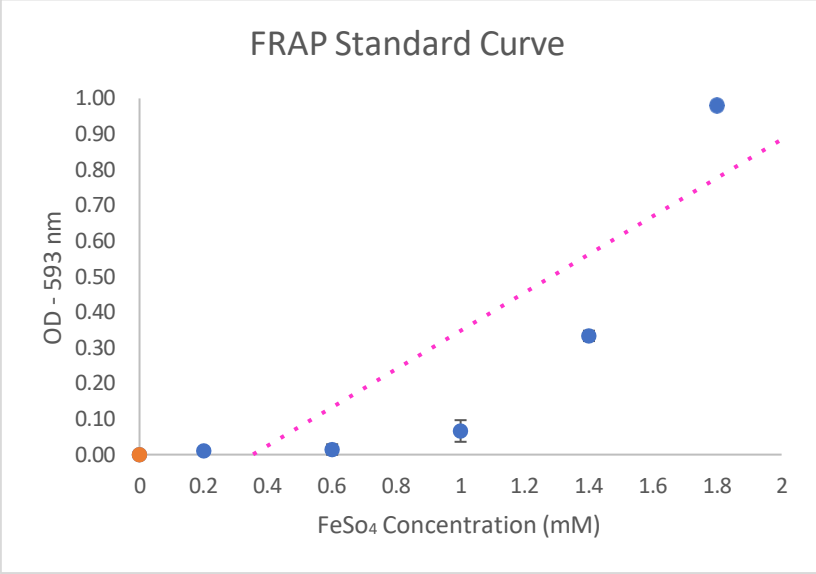

Supplementary Figure 2: Standard curve (FRAP) Error bars denote ± SEM (n = 3)

Alphanumeric Identifier	Condition	Administration Method	Design	No. of Participants	Conclusion	Reference
UMIN000010014	Parkinson's Disease	HRW (1.6ppm) (1L/day/336 days)	Placebo-controlled, Randomized, Double-blind, Parallel assignment	18	The results indicate that drinking HRW was safe and well tolerated, and a significant improvement in total UPDRS	Yoritaka et al., 2013
NCT02832219	Obesity	Tablet (2g/day/28 days)	Randomised, Cross-over assignment	12	A significant reduction of fasting insulin levels and serum triglycerides resulted in a reduced body/fat percentage	Korovljev et al., 2018
UMIN000002218	Cognitive Impairment	HRW (500mL/day/730 days)	Double-blinded, Randomised, Parallel assignment	120	HRW significantly improved Alzheimer's Disease Assessment Scale-cognition sub-scale (ADAS-cog) scores. Particularly in patients with the APOE4 genotype.	Nishimaki et al., 2018
NCT03818347	Solid Tumours	Oxyhydrogen Inhalation (3L/min/3-hrs/day/3 months)	Randomised, Single Group Assignment	30	Remediated radiotherapy-induced hearing loss. Inhalation mitigated tumour progression and alleviated the side effects of medications. Improved indices of immunosenescence in lymphocytes	Chen et al., 2019 Chen et al., 2020a Chen et al., 2020b
NCT03846141	Exhaustive Exercise	H_2 Inhalation (4%/45mL/min/20 min/day/7 days)	Cross-over, Placebo-controlled, Randomised	20	4.2% increase in peak running velocity. Significant reduction in serum ferritin and IGF-1. A moderate reduction in CRP.	Javorac et al., 2019
NCT03625362	NAFLD	HRW (6ppm) (1L/day/28 days)	Randomised, Cross-over assignment	12	Reduced liver-fat accumulation and decreased serum levels of AST.	Korovljev et al., 2019
UMIN000027700	Fatigue	HRW (4 weeks)	Placebo-controlled, Double-blind, Randomized	60	Reduced fatigue and enhanced performance	Mikami et al., 2019
NCT04378712	COVID-19	Oxyhydrogen Inhalation (3L/min/8-hours/day)	Non-randomised, Parallel assignment	90	Inhalation improved disease severity and reduced dyspnoea and chest pain	Guan et al., 2020
UMIN000032523	Cardiovascular Disease	HRW (7ppm)	Randomised, Double-blind,	68	Improved endothelial function of arteries and arterioles	Ishibashi et al., 2020

		(500mL/day/14 days)	Placebo-controlled assignment			
NCT02830854	Cognitive function in >65-year-old women	H_2 Inhalation (3%/20 min/day/28 days)	Open-label, Single group assignment	13	Assessments include Mini-Mental State Exam (MMSE) and ADAS-cog tests - Improved cognitive function in patients with mild dementia was observed.	Korovljev et al., 2020
CTRI/2018/03/012487	Metabolic syndrome	HRW (1.6ppm) (250mL/3 times a day/168 days)	Randomised, Parallel group, Placebo-controlled	60	Improved blood/lipid profile. Reduction of pro-inflammatory markers and blood/glucose	LeBaron et al., 2020
NCT02918188	Graft Vs. Host Disease (GI tract)	HRW (0.8ppm) (500mL/3 times a day for 12 months)	Open-label, Single group assignment	17	Remission (n = 13) Partial remission (n = 1) Progression (n = 3)	Qian et al., 2020
KCT0003763	Antioxidant Profile	HRW (1ppm) (1.5L/day/28 days)	Double blinded, parallel	38	Reduced apoptosis of peripheral blood mononuclear cells. Reduced CD14+ cells. Reduced intracellular NFκB	Sim et al., 2020
UMIN000019820	Post-Cardiac Arrest Syndrome	H_2/O_2 Inhalation (2% H_2)	Randomised, Double-blinded, Parallel assignment	360	Reduced arterial oxidative stress. No alteration to inflammatory cytokine levels.	Tamura et al., 2020
NCT04167202	Acute Ankle Sprain	Topical HRW (30 minute immersion 4 times a day for 1 day)	Pilot study	18	HRW was equivalent to RICE protocol in reducing ankle swelling and improving both range of motion and single-leg balance	Javorac et al., 2021
NCT04046211	Healthy Volunteers	H_2 Inhalation (2.4%)	Open-Label Single group assignment	8	H_2 gas does not appear to cause clinically significant adverse effects in healthy adults.	Kheir et al., 2021
NCT04430803	Ageing	HRW (15ppm) (0.5L/day/182 days)	Blinded, Randomised, Parallel assignment	40	Increased telomere length and DNA methylation. Increased levels of choline, creatine and *N*-Acetylaspartic Acid in the brain. Improved physical function.	Zanini et al., 2021

NCT04000451	COPD	Oxy-hydrogen Nebulised (6-8-hours/7 days)	Randomised, Parallel assignment	108	H_2/O_2 treatment was superior O_2 therapy in relieving cough, dyspnoea and sputum.	Zeng et al., 2021
NCT05013606	Myalgic encephalomyelitis/ Chronic Fatigue	HRW (1.6ppm)	Randomised, Parallel Assignment	23	Therapeutic molecular hydrogen did not yield improvement on any biological or symptom measure in individuals with ME/CFS	Friedberg and Choi, 2022
ChiCTR2200062253	Allergic Rhinitis	HRS	Randomized, Double-blind	120	Improvement of clinical symptoms. Reduction in eosinophilic protein. T-cell and B-cell regulatory cells unaffected	Jin et al., 2022
NCT03818347	Radiotherapy-induced Hearing Loss	Oxyhydrogen Inhalation (3 L/min for 3-67 hours/day for 4-12 weeks)	Interventional	17	Statistically relevant differences noted in hearing capacity at 4 weeks. No statistically relevant differences between groups at 12 weeks. No side effects were observed after the inhalation of H_2	Kong et al., 2022
NCT05325398	NAFLD	HRW (1.6ppm) (0.33L/8-hours/56 days)	Open-label, Non-randomised, Parallel assignment	30	Significantly improved Body Mass Index, lipid profile and non-significant decreases in lactate dehydrogenase and NFkB, HSP70 and MMP9. Mild reduction in blood pressure and weight.	Kura et al., 2022
ChiCTR2100043260	Post-operative Cognitive Function	Oxyhydrogen Inhalation	Randomised, Parallel group, Placebo-controlled	170	Decreased incidence of delirium in noncardiac patients. Reduced CRP levels but increased pain perception.	Lin et al., 2022
ChiCTR2100049865	Hypertension	Oxyhydrogen Inhalation	Parallel	60	Inhalation exerts a favourable effect on blood pressure, reducing plasma levels of angiotensin II, aldosterone, and cortisol, as well as lowering the aldosterone-to-renin ratio in plasma	Liu et al., 2022
ChiCTR2200059988	Alcohol Detoxification	HRW/H_2 Inhalation	Parallel	20	Hydrogen decreases Breath alcohol concentration and relieves the symptoms of hangovers.	Lv et al., 2022
jRCTs06119004	Noise-induced Hearing Loss	H_2 Inhalation (2 L/min for 2 hours/day for 6 days)	Multi-centre, double-blind, randomized clinical trial	65	Inhalation of H_2 gas was effective for treating ISSNHL in diabetic patients and those with severe hearing loss, but not patients with hypertension. No side effects were observed after the inhalation of H_2	Okada et al., 2022

ChiCTR-IIR-16009114	NAFLD	Oxyhydrogen Inhalation (3L/min/1-hour/13 weeks)	Randomized, placebo-controlled	43	Reduced liver-fat accumulation and Improved serum lipid and hepatic enzyme profiles	Tao et al., 2022
ChiCTR2200059060	Subarachnoid Haemorrhage	H_2 Inhalation (3%)	Open label, Randomized, Parallel assignment	30	Hydrogen reduced the accumulation of lactic acid in the nervous system via inhibition of HIF1-α	Peng et al., 2023
jRCTs031180352	Brain Ishemia (Post cardiac arrest)	H_2 Inhalation (2% H_2 for 18 hours)	Multicentre, Randomised, Double-blind, Placebo-controlled trial	73	May improve 90-day survival without neurological sequela	Tamura et al., 2023

Supplementary Table 1. Data retrieved from registered clinical trials with published outcomes (2013 – 2023). Search term 'Hydrogen'. Key: Chinese Clinical Trial Registry (ChiCTR); Clinical Trials Register India (CTRI); Japan Registry for Clinical Trials (jRCT); University Hospital Medical Information Network (UMIN)

Supplementary Table 1. REFERENCES

Chen, J., Kong, X., Mu, F., Lu, T. and Xu, K. (2019) Hydrogen-oxygen therapy can alleviate radiotherapy-induced hearing loss in patients with nasopharyngeal cancer. *Annals of Palliative Medicine*. *8*(5), 746-751.

Chen, J.B., Kong, X.F., Mu, F., Lu, T.Y., Lu, Y.Y. and Xu, K.C. (2020a) Hydrogen therapy can be used to control tumor progression and alleviate the adverse events of medications in patients with advanced non-small cell lung cancer. *Medical Gas Research*. *10*(2), 75.

Chen, J.B., Kong, X.F., Qian, W., Mu, F., Lu, T.Y., Lu, Y.Y. and Xu, K.C. (2020b) Two weeks of hydrogen inhalation can significantly reverse adaptive and innate immune system senescence patients with advanced non-small cell lung cancer: a self-controlled study. *Medical Gas Research*. *10*(4), 149.

Ishibashi, T., Kawamoto, K., Matsuno, K., Ishihara, G., Baba, T. and Komori, N. (2020) Peripheral endothelial function can be improved by daily consumption of water containing over 7 ppm of dissolved hydrogen: A randomized controlled trial. *PloS one*. *15*(5), p.0233484.

Jin, L., Fan, K., Tan, S., Liu, S., Ge, Q., Wang, Y., Ai, Z. and Yu, S. (2022) The beneficial effects of hydrogen-rich saline irrigation on chronic rhinitis: A randomized, double-blind clinical trial. *Journal of Inflammation Research*. *15*, p.3983.

Korovljev, D., Stajer, V., Ostojic, J., LeBaron, T.W. and Ostojic, S.M. (2019) Hydrogen-rich water reduces liver fat accumulation and improves liver enzyme profiles in patients with non-alcoholic fatty liver disease: a randomized controlled pilot trial. *Clinics and Research in Hepatology and Gastroenterology*, *43*(6), 688-693.

Korovljev, D., Trivic, T., Drid, P. and Ostojic, S.M. (2018) Molecular hydrogen affects body composition, metabolic profiles, and mitochondrial function in middle-aged overweight women. *Irish Journal of Medical Science (1971-)*. *187*(1), 85-89.

Korovljev, D., Trivic, T., Òtajer, V., Drid, P., Sato, B. and Ostojic, S. (2020) Short-term H_2 inhalation improves cognitive function in older women: A pilot study. *International Journal of Gerontology*. *14*(2), 149-150.

LeBaron, T.W., Singh, R.B., Fatima, G., Kartikey, K., Sharma, J.P., Ostojic, S.M., Gvozdjakova, A., Kura, B., Noda, M., Mojto, V. and Niaz, M.A. (2020) The effects of 24-week, high-concentration hydrogen-rich water on body composition, blood lipid profiles and inflammation biomarkers in men and women with metabolic syndrome: A randomized controlled trial. *Diabetes, Metabolic Syndrome and Obesity*. pp.889-896.

LeBaron, T.W., Singh, R.B., Fatima, G., Kartikey, K., Sharma, J.P., Ostojic, S.M., Gvozdjakova, A., Kura, B., Noda, M., Mojto, V. and Niaz, M.A. (2020) The effects of 24-week, high-concentration hydrogen-rich water on body composition, blood lipid profiles and inflammation biomarkers in men and women with metabolic syndrome: A randomized controlled trial. *Diabetes, Metabolic Syndrome and Obesity: Targets and Therapy*. *13*, p.889.

Lin, H., Du, J., Tian, Z., Yu, Y., Cui, Y. and Xie, K. (2022) Hydrogen gas treatment improves postoperative delirium and cognitive dysfunction in elderly noncardiac patients. *Journal of Personalized Medicine*. *13*(1), p.67.

Liu, B., Jiang, X., Xie, Y., Jia, X., Zhang, J., Xue, Y. and Qin, S. (2022) The effect of a low dose hydrogen-oxygen mixture inhalation in midlife/older adults with hypertension: A randomized, placebo-controlled trial. *Frontiers in Pharmacology*. *13*, p.1025487.

Lv, X., Lu, Y., Ding, G., Li, X., Xu, X., Zhang, A. and Song, G. (2022) Hydrogen intake relieves alcohol consumption and hangover symptoms in healthy adults: a randomized and placebo-controlled crossover study. *The American Journal of Clinical Nutrition*. *116*(5), pp.1208-1218.

Mikami, T., Tano, K., Lee, H., Lee, H., Park, J., Ohta, F., LeBaron, T.W. and Ohta, S. (2019) Drinking hydrogen water enhances endurance and relieves psychometric fatigue: a randomized, double-blind, placebo-controlled study. *Canadian Journal of Physiology and Pharmacology*. *97*(9), pp.857-862.

Nishimaki, K., Asada, T., Ohsawa, I., Nakajima, E., Ikejima, C., Yokota, T., Kamimura, N. and Ohta, S. (2018) Effects of molecular hydrogen assessed by an animal model and a randomized clinical study on mild cognitive impairment. *Current Alzheimer Research*. *15*(5), 482-492.

Okada, M., Ogawa, H., Takagi, T., Nishihara, E., Yoshida, T., Hyodo, J., Shinomori, Y., Honda, N., Fujiwara, T., Teraoka, M. and Yamada, H. (2022) A double-blinded, randomized controlled clinical trial of hydrogen inhalation therapy for idiopathic sudden sensorineural hearing loss. *Frontiers in Neuroscience*. *16*, p.1024634.

Peng, Z., Li, X.J., Pang, C., Zhang, J.T., Zhu, Q., Sun, J.Q., Wang, J., Cao, B.Q., Zhang, Y.H., Lu, Y. and Li, W. (2023) Hydrogen inhalation therapy regulates lactic acid metabolism following subarachnoid hemorrhage through the HIF-1α pathway. *Biochemical and Biophysical Research Communications*. *663*, pp.192-201.

Sim, M., Kim, C.S., Shon, W.J., Lee, Y.K., Choi, E.Y. and Shin, D.M. (2020) Hydrogen-rich water reduces inflammatory responses and prevents apoptosis of peripheral blood cells in healthy adults: A randomized, double-blind, controlled trial. *Scientific Reports*. *10*(1), pp.1-10.

Tamura, T., Suzuki, M., Hayashida, K., Kobayashi, Y., Yoshizawa, J., Shibusawa, T., Sano, M., Hori, S. and Sasaki, J. (2020) Hydrogen gas inhalation alleviates oxidative stress in patients with post-cardiac arrest syndrome. *Journal of Clinical Biochemistry and Nutrition*. *67*(2), 214-221.

Tamura, T., Suzuki, M., Homma, K., Sano, M., Iizuka, R., Narimiya, H., Tsuruta, R., Kaneda, K., Fujita, M., Sasaki, J. and Akasaka, O. (2023) Efficacy of inhaled hydrogen on neurological outcome following brain ischaemia during post-cardiac arrest care (HYBRID II): a multi-centre, randomised, double-blind, placebo-controlled trial. *EClinicalMedicine*. *58*.

Tao, G., Zhang, G., Chen, W., Yang, C., Xue, Y., Song, G. and Qin, S. (2022) A randomized, placebo-controlled clinical trial of hydrogen/oxygen inhalation for non-alcoholic fatty liver disease. *Journal of Cellular and Molecular Medicine*. *26*(14), pp.4113-4123.

Yoritaka, A., Takanashi, M., Hirayama, M., Nakahara, T., Ohta, S. and Hattori, N. (2013) Pilot study of H_2 therapy in Parkinson's disease: A randomized double-blind placebo-controlled trial. *Movement Disorders*. *28*(6), 836-839.

Zanini, D., Todorovic, N., Korovljev, D., Stajer, V., Ostojic, J., Purac, J., Kojic, D., Vukasinovic, E., Djordjievski, S., Sopic, M. and Guzonjic, A. (2021) The effects of 6-month hydrogen-rich water intake on molecular and phenotypic biomarkers of aging in older adults aged 70 years and over: A randomized controlled pilot trial. *Experimental Gerontology*. *155*, p.111574.

Zheng, Z.G., Sun, W.Z., Hu, J.Y., Jie, Z.J., Xu, J.F., Cao, J., Song, Y.L., Wang, C.H., Wang, J., Zhao, H. and Guo, Z.L. (2021) Hydrogen/oxygen therapy for the treatment of an acute exacerbation of chronic obstructive pulmonary disease: results of a multicenter, randomized, double-blind, parallel-group controlled trial. *Respiratory Research*. 22(1), 1-12.

Ziegler-Heitbrock, H.W.L. (1995) Molecular mechanism in tolerance to lipopolysaccharide. *Journal of Inflammation*. *45*(1), pp.13-26.

Grace Russell List of Publications (2021 – 2024)

Hancock, J.T. and Russell, G. (2021) Downstream signalling from molecular hydrogen. *Plants*. *10*(2), p.367.

Hancock, J.T., LeBaron, T.W. and Russell, G. (2021) Molecular hydrogen: Redox reactions and possible biological interactions. *Reactive Oxygen Species (Apex)*, *11*.

Hancock, J.T., LeBaron, T.W., May, J., Thomas, A. and Russell, G. (2021) Molecular hydrogen: is this a viable new treatment for plants in the UK? *Plants*. *10*(11), p.2270.

Hancock, J.T., Russell, G. and Stratakos, A.C. (2022) Molecular hydrogen: The postharvest use in fruits, vegetables and the floriculture industry. *Applied Sciences*. *12*(20), p.10448.

Hancock, J.T., Russell, G., Craig, T.J., May, J., Morse, H.R. and Stamler, J.S. (2022) Understanding hydrogen: Lessons to be learned from physical interactions between the inert gases and the globin superfamily. *Oxygen*. *2*(4), pp.578-590.

Hancock, J.T., LeBaron, T.W., May, J., Thomas, A. and Russell, G. (2023) Alleviation of plant stress by molecular hydrogen. In *Gasotransmitters Signaling in Plants under Challenging Environment* (pp. 101-120). Cham: Springer International Publishing.

Hancock, J.T., May, J.E., LeBaron, T.W., Punampalam, R. and Russell, G. (2024) An exploration of the direct biological targets of molecular hydrogen. In *Molecular Hydrogen in Health and Disease* (pp. 21-38). Cham: Springer Nature Switzerland.

Hancock, J.T., LeBaron, T.W., May, J., Thomas, A., Zulfiqar, F. and Russell, G. (2024) Molecular hydrogen as a beneficial postharvest treatment. In *Oxygen, Nitrogen and Sulfur Species in Post-Harvest Physiology of Horticultural Crops* (pp. 303-318). Academic Press.

Russell, G., Nenov, A., Kisher, H. and Hancock, J.T. (2021) Molecular hydrogen as medicine: An assessment of administration methods. *Hydrogen*. *2*(4), pp.444-460.

Russell, G. and Nenov, A. (2022) Molecular hydrogen therapies and the benefits for menopausal and perimenopausal women: An aphoristic review. *GSC Biological and Pharmaceutical Sciences*. *21*(2), pp.112-115.

Russell, G., Thomas, A.D., Nenov, A. and Hancock, J.T. (2022) The influence of molecular hydrogen therapies in managing the symptoms of acute and chronic COVID-19. *Medical Research Archives*. *10*(9).

Russell, G., Rolfe, V. and Adukwu, E. (2022) How are turmeric and its derivative products beneficial for intestinal health?. *Modern Journal of Medicine and Biology*. *1*(2).

Russell G, and Nenov A. (2023) The effects of molecular hydrogen therapies on fertility. *SciBase Clinical and Medical Case Reports*. *1*(1), p.1001.

Russell, G., Thomas, A.D., Nenov, A., Mannings, G. and Hancock, J.T. (2023) The therapeutic potential of oxyhydrogen gas in oncology: A study on Epstein–Barr Virus-immortalised B-lymphoblastoid (TK6) cells. *Hydrogen*. *4*(4), pp.746-759.

Russell, G., May, J. and Hancock, J.T. (2024) An interplay of gases: Oxygen and hydrogen in biological systems. *Oxygen*. *4*(1), pp.37-52.

Tran, H.N., Udoh, S., Russell, G., Okeyoyin, O.R., Aftab, S., Rodriguez, I., Tabe, E.S. and Adukwu, E.C. (2022) Recent advances in the application of essential oils as potential therapeutic candidates for candida-related infections. *Applied Microbiology*. *2*(2), pp.397-413.

Zulfiqar, F., Russell, G. and Hancock, J.T. (2021) Molecular hydrogen in agriculture. *Planta*. *254*(3), p.56.